Amino acid racemization dating: Method development using African ostrich (*Struthio camelus*) eggshell

Molly Katherine Crisp

PhD

University of York

Department of Chemistry

June 2013

ABSTRACT

Ostrich eggshell (OES) is ubiquitous in archaeological sites in Africa and is a favoured substrate for amino acid racemisation (AAR) geochronology, yielding consistent results and thought to approximate a closed system with respect to protein diagenesis. It was found that the intra-crystalline fraction in OES can be isolated by oxidative pre-treatment and that these amino acids are resistant to leaching and unaffected by changes in the environmental pH (between pH 5 and 9). The intra-crystalline fraction in OES therefore effectively operates as a closed system with respect to protein diagenesis. This intra-crystalline fraction is likely to be a superior sample compared to whole-shell samples, removing uncertainty introduced through variable leaching rates, different ground water conditions and potentially exogenous contamination.

Kinetic studies on modern OES indicate that high temperature data should be treated with caution when used to extrapolate kinetic parameters at low temperatures. This reinforces previous work that indicates the underlying mechanisms driving protein diagenesis need to be better understood in order to estimate accurate kinetic parameters, as the pathways of diagenesis are different at high and low temperatures. Nonetheless, hydrolysis and racemization have been shown to follow predictable patterns of diagenesis, and are therefore useful for the application of relative dating in AAR geochronology. Therefore, a chronological framework for southern South Africa was built by AAR analysis of a suite of OES samples, with calibration from independent dating methods (optically stimulated luminescence and radiocarbon), up to 151 ka. Through extensive artificial heating studies on modern OES samples, a checklist of 6 markers has been developed to identify sub-fossil samples that have been exposed to high temperatures. Exclusion of these heated samples from AAR age models significantly increases the age resolution. Analysis of several amino acid chiral pairs allowed age resolution over the full time range studied (~0.3 ka – 151 ka), allowing differentiation of MIS 1, 2, 3/4, 5 and 6. It has been shown that OES AAR offers a useful additional relative dating technique for archaeological and palaeontological sites from the same regions as Pinnacle Point and Elands Bay Cave, up to at least 151 ka (MIS 6). Furthermore, as 151 ka samples have racemization for some amino acids (e.g. isoleucine) only half way to equilibrium, there is considerable potential for OES AAR geochronology in South Africa beyond 151 ka.

In addition, a preliminary study has demonstrated the potential of mass spectrometry in helping to unravel the complex nature of protein diagenesis within bio-minerals. Peptides from ~71 ka sub-fossil samples were successfully extracted and sequenced. It is believed this is the first time this has been done for eggshell samples of this age. This kind of study offers interesting insights

into the patterns of protein preservation and degradation, with implications for understanding the role and function of proteins in the bio-minerals.

Finally, a new ultra-high pressure liquid chromatography (UHPLC) method for the chiral separation of amino acids has been developed, with an analysis time (60 min including flush time) approximately half that of the previous HPLC method, allowing a higher throughput of samples. This new method also separates additional analytes, previously unstudied in AAR geochronology, which may offer further insight into protein diagenesis within bio-minerals.

CONTENTS

LIST OF FIGURES

LIST OF TABLES

ACKNOWLEDGMENTS

Foremost, I would like to thank my supervisor, Kirsty Penkman, for her invaluable teaching, patience, guidance and support, both scientific and personal. I feel I have developed as a scientist over the past 4 years, and I have Kirsty to thank for this.

I would like to thank all the people responsible for writing the original grant proposal, supplying samples and for giving me the position! These include Kirsty Penkman, Matthew Collins, Jane Thomas-Oates, Brendan Keely, Julia Lee-Thorp, John Parkington and Curtis Marean.

I had the pleasure of working with an amazing group of people in both Chemistry and BioArCh who created both an enthusiastic and productive working atmosphere. A special thank you goes to Bea Demarchi for all her technical guidance and writing critique, Kirsty High for her help on the XRD and the hours she spent proof reading for me, Jo Simpson for proof reading and Sheila Taylor for technical support and cake breaks. I would also like to thank Rick Allen, Karl Heaton and Matt Pickering for technical support.

I had the pleasure of working with a number of great students including Emily Pilgrim, Seb Green and Michael Morgan-Williams - you definitely livened things up at times… thank you for not ballsing things up! ;-)

I am incredibly lucky to have a close and supportive family, so a special thank you goes out to you guys: especially my siblings Tom and Ann, my nephew Harrybo, my in-laws Joan and Bill, my dog Lochy, my Grandparents, especially my Granddad who helped inspire my love of science and Sue for giving me my first taste for scientific research. My Dad has been a constant source for honest advice, love and support through what has been, at times, a crappy few years for our family.

I would also like to thank my ‘non-science’ friends, who kept me sane by taking me biking, boating, snowboarding and for the occasional drink: The Lillies, Scooby Doo, Karen Dalby and Pete Beverley… love you guys!

My loving husband Darren has been a constant source of support and laughs- you’ve got me through the hardest of times, I thank you with all my heart because I don’t know how I could have done it without you.

Lastly, I have so much to thank my Mum for; I don’t think I can do her justice here. Her enthusiasm and positive outlook will always be an inspiration to me.

Dedicated to Pam Crisp, 13.04.1953 – 18.04.2011

and Rod Barratt, 04.04.1947 – 12.07.2012

DECLARATION

I hereby certify that the work described in this thesis is my own, except where otherwise acknowledged, and has not been submitted previously for a degree at this, or any other, university.

The data presented in Chapters 3 and 4 has been published, in part, in the following publication: Crisp, M., Demarchi, B., Collins, M., Morgan-Williams, M., Pilgrim, E., Penkman, K.E.H. 2013. Isolation of the intra-crystalline proteins and kinetic studies in *Struthio camelus* (ostrich) eggshell for amino acid geochronology. *Quaternary Geochronology* 16: 110-128.

The pH study included in Chapter 3 was performed in collaboration with Michael Morgan-Williams and is included in the afore mentioned publication. The mass spectrometry study in Chapter 7 was performed in collaboration with Beatrice Demarchi.

Molly Crisp

CHAPTER 1: INTRODUCTION

The general consensus is that our genus, *Homo*, evolved in Africa during the Quaternary period (present day – 2.58 Ma) (Cann *et al.*, 1987; Klein, 1995; White *et al.*, 2003; Gibbard *et al.*, 2010; Pontzer, 2012). *Homo* are characterised primarily by their large brain volumes compared with their ancestors, and their ability to use tools (Lewin and Foley, 2003). Arguably the earliest of this genus, *Homo habilis* (literally 'handy man'), is believed to have been present in East Africa from ~2.3 – 1.4 Ma (Leakey *et al*., 1964; Kimble *et al*., 1997). Fossil evidence for their descendants, *H. erectus*, suggests they existed for ~ 1.8 M years from ~ 1.9 Ma, occupying both Africa and Eurasia (Anton, 2003). *H. erectus* has a more 'modern human' physique, with elongated legs and shorter arms, and is the oldest *Homo* species associated with stone hand axes (Blumenschine *et al.*, 2003; Anton, 2003). Although there are several different theories, it is speculated that our species (*H. Sapiens)* descended from *H. heidelbergensis,* which itself had evolved from the African *H. erectus* by approximately 700 ka (see Rightmire, 1998; 2009). The earliest examples found so far of 'anatomically modern humans' (*H. sapiens*), so called because their skeletal remains are indistinguishable from our own, were found in Ethiopia and have been dated to ~ 200 ka (McDougal *et al*., 2005). However, evidence for modern human behaviour has not been observed until later in the fossil record. Arguably, the earliest evidence found so far, exemplified by the exploitation of marine resources, dates to as early as ~164 ka in South Africa (Marean *et al.*, 2007). The criteria used to define modern behaviour vary by author and can be contentious, but tend to include physical manifestations of an increased ability to problem solve, complex planning and/or behaviour associated with culture, for example evidence of the controlled use of fire, language, personal ornamentation, burial of the dead, production of stone tools, technologies to allow sea crossings and extended trade networks (McBrearty and Brooks, 2000; Henshilwood and Marean, 2003; Nowell, 2010; d'Errico and Stringer, 2011; Wynn & Coolidge 2011). The Quaternary period is therefore often thought of as 'The Age of the Humans', and Africa has clearly been pivotal in human development. By the end of the Pleistocene (11.7 ka – present day), modern humans had dispersed from Africa across the globe and were the only hominin species remaining (DeGiorgio *et al.*, 2009; Mellars, 2006). The routes, reasons and timing of the modern human dispersal remain poorly understood. Fluctuating temperatures and variations in sea level define this period in our history; were these climatic shifts a driving force for dispersal, and for the development of modern human behaviour? Despite extensive research, significant questions remain, not least because of the difficulty of linking the sparse fossil record to a robust and defensible dating technique, and hence to the climate record. There are many dating techniques, but none as yet which span the entire Quaternary time period with a high degree of resolution (Millard, 2008). Amino acid racemization (AAR) geochronology has the potential to span a large

portion of the Quaternary period (e.g. Bada, 1984; Brooks *et al.*, 1990; Penkman *et al.*, 2011). OES has been shown to be an excellent substrate for AAR (Brooks *et al.*, 1990; Miller *et al.*, 1992; 1999), and given its ubiquitous nature at archaeological sites in Africa (e.g. Butzer *et al.*, 1979; Kandel and Conrad, 2005; Orton, 2008; Texier *et al.*, 2010), it offers itself as a useful dating tool to gain further insight into the evolution of early humans, and of modern human behaviour in South Africa.

1.1. THE QUATERNARY PERIOD: CLIMATE, EVOLUTION AND DATING TECHNIQUES

1.1.1. Climate

The Quaternary period extends from the present day to 2.58 Ma (Cann *et al.*, 1987; Klein, 1995; White *et al.*, 2003; Gibbard *et al.*, 2010) and is characterised by its fluctuating climate; cold glacial periods interspersed with warmer inter-glacial periods (e.g. Head *et al.,* 2008; Fig. 1.1). The period contains two epochs, the Pleistocene (up to 11.7 ka) and the Holocene (11.7 ka – present) (Walker *et al.*, 2009), the latter being the current inter-glacial stage. The shifts in temperature are believed to be primarily driven by periodical changes in the earth's orbital rhythms; a theory first suggested by Croll in 1875, and later developed by Milankovitch in the early 20th century (e.g. Berger, 1988). Each variable has a different periodicity, the combination of these variables are believed to be the principal cause of the complex temperature patterns observed (Fig. 1.1; Hayes *et al.*, 1976; Imbrie *et al.*, 1992). The three variables are:

- Eccentricity ('E' in Fig. 1.1): The Earth's orbit changes from near circular to elliptical. These changes are driven by the gravitational fields of other plants, e.g. Jupiter and Saturn, with a periodicity of approximately 100 ka (Hays *et al.,* 1976).
- Axial tilt ('T' in Fig. 1.1): The angle of the Earth's tilt changes slightly with respect to the plane of the Earth's orbit, with a periodicity of ~ 41 ka.
- Precession ('P' in Fig. 1.1): This gyroscopic motion has a periodicity of ~ 26 ka.

The changes in orbital rhythms influence the sun's radiation on the planet, changing season lengths and therefore affecting the climate. Evidence for fluctuating past temperatures came from the studies of stable isotopes within marine micro-fossils in deep sea cores (e.g. Shackleton, 1987), and later in water from ice cores (e.g. Stuiver *et al.,* 1995). The premise is that the ratio of stable oxygen isotopes (^{18}O:^{16}O) reflects the sea temperature; a greater proportion of ^{18}O reflects

colder climates, a smaller proportion reflects a warmer climate (Emiliani 1955; 1966; Shackleton, 1987). The ^{18}O:^{16}O ratio is usually expressed as $\delta^{18}O$:

$$\delta^{18}O = ((^{18}O / {}^{16}O)_{sample} / (^{18}O / {}^{16}O)_{standard}) - 1 \qquad \textit{Equation 1.1}$$

where $\delta^{18}O$ is usually expressed in per mil, and the standard ratio ($(^{18}O / {}^{16}O)_{standard}$) can be from either an actual reference material or a hypothetical reference material with an isotopic composition based on an existing reference material, e.g. the Standard Mean Oxygen Water (SMOW; Coplen, 1994).

In marine micro-fossils $\delta^{18}O$ reflects both the isotopic composition of water in which they were formed, and the isotopic fractionation of the mineralization process, which is also a function of temperature (e.g. Grossman and Ku, 1986). The isotopic composition of the sea water reflects the ice volume, the average $\delta^{18}O$ of continental ice and any local hydrological effects (e.g. Jouzel *et al.*, 1997). Nevertheless, these isotopic records give a good indication of marine climate fluctuations over the past 2.6 Ma. Each glacial and inter-glacial stage is usually referred to as a 'Marine Isotope Stage' (MIS). Each stage is differentiated by the preceding number, where even numbers indicate glacial stages and odd numbers indicate inter-glacials; for example, the current inter-glacial (the Holocene) is labelled as 'MIS 1'. The absolute dates for the individual stages have been achieved using paleaomagnetism (Shackleton and Opdyke, 1973; Imbrie *et al.*, 1984; Hilgen, 1991).

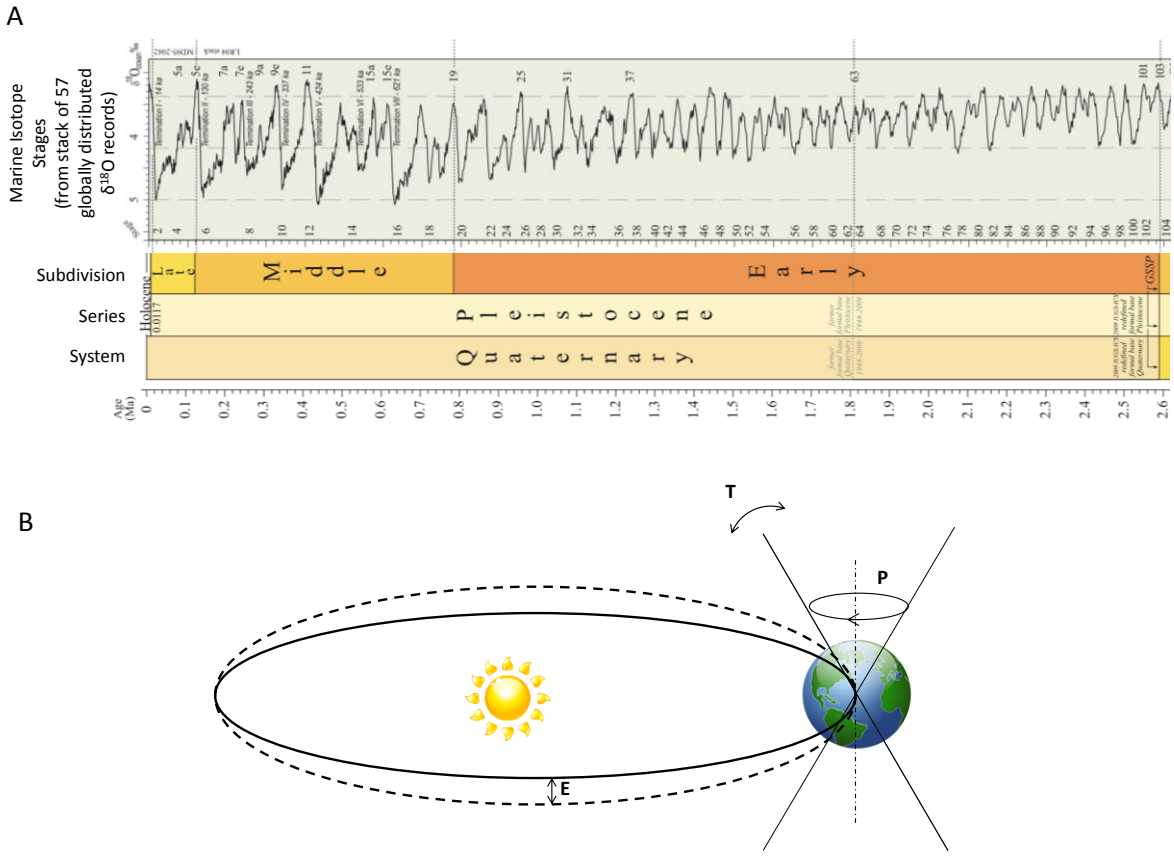

Figure 1.1: A: Climate history of the Quaternary period, inferred by changes in the ratio of oxygen isotopes within marine micro-organisms ($\delta^{18}O$: high indicates a warm period, a low $\delta^{18}O$ indicates a cold period; numbers indicate the MIS; modified from Cohen and Gibbard, 2011). B: The three main changes in the Earth's movements which affect climate: E = eccentricity, T = axial tilt, P = precession

1.1.2. Human evolution in South Africa

The fluctuating climate over the Quaternary period caused expansions and contractions of habitats, due in part to changing sea levels (Adams and Faure, 1997). In South Africa, the changing climate resulted in the south coastal plain (SCP) spending much of the Pleistocene isolated from the rest of Africa by a combination of i) the Cape Fold Belt (CFB), a series of sandstone mountains creating a physical barrier between the coastal planes and the rest of South Africa, and ii) increased sea levels during inter-glacial periods causing submergence of coastal routes of migration from the coastal planes to the rest of Africa (Fig. 1.2; Compton, 2011). During the Pleistocene much of South Africa was an arid and inhospitable environment (Fig. 1.2; Compton, 2011), and it is thought that early humans may have retreated to the coasts where they could exploit marine resources (Marean *et al.*, 2007; Compton, 2011). Indeed, coastal sites on the

west and south of Africa offer some of the best archaeological sites with evidence for the evolution of anatomically and culturally modern humans, e.g. Pinnacle Point (Marean *et al.*, 2004), Nelson Bay Cave (Deacon, 1978), Elands Bay Cave (Parkington, 1992), Howiesons Poort (Lombard, 2005) and Blombos Cave (Henshilwood *et al.*, 2001). These isolated pockets of hominids may have been subject to different selection processes, e.g. higher population density or variable resources (allotropic evolution; Compton, 2011).

The earliest evidence so far for anatomically modern humans (*Homo sapiens*) appears in the fossil record at a site in Ethiopia, dated to ~ 200 ka (McDougall *et al.*, 2005). Arguably, the earliest evidence so far for modern human behaviour appears in the fossil record at ~ 164 ka at Pinnacle Point, South Africa; exemplified in this case by the use and modification of pigments, production of stone bladelets and the exploitation of marine resources (Marean *et al.*, 2007). It is therefore clear that the African fossil record is fundamental to our understanding of the evolution of anatomically and culturally modern humans.

By ~ 60 ka *Homo sapiens* had dispersed from Africa and eventually populated every continent with the exception of Antartica (Mellars, 2006; DeGiorgio *et al.*, 2009; Petraglia *et al.,* 2010). However, the route, reason and exact timing of this dispersal is still largely open to interpretation (e.g. Stringer, 2000; Stringer, 2003; Bailey, 2004). Did the harsh climate drive the cultural evolution of man (Lahr and Foley, 1994; Henshilwood and Marean, 2003), or was this step of our evolution inevitable (Klein, 2009)? In order to answer these questions the global climate record needs to be linked to the terrestrial, and often sparse, fossil record.

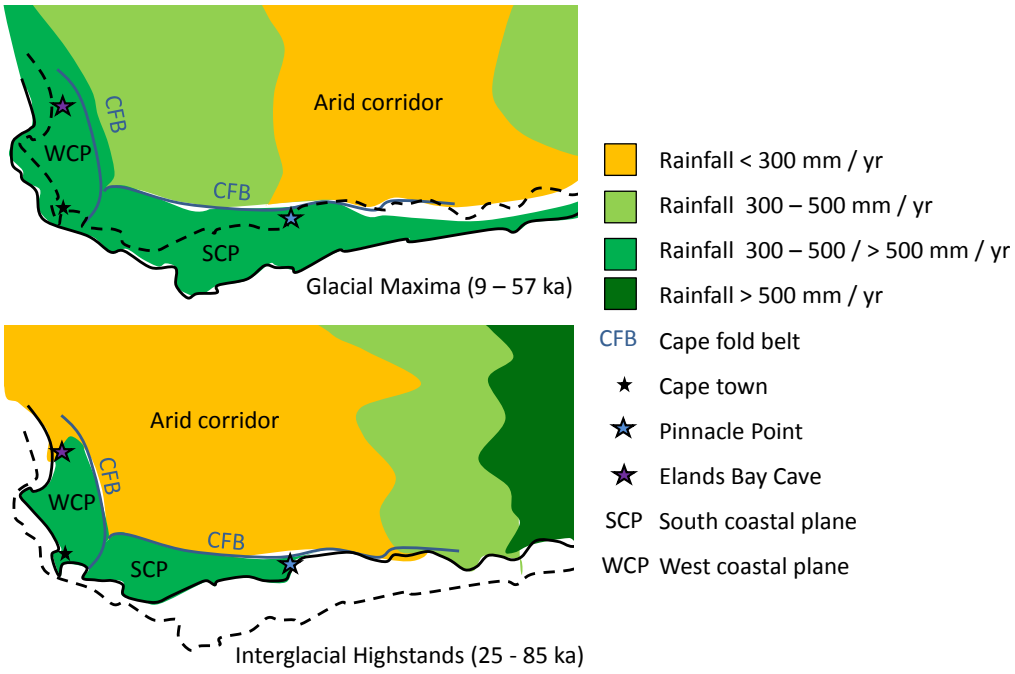

Figure 1.2: Effect of climate change on habitable land in South Africa. Cape fold belt is a series of sandstone mountains creating a physical barrier between the coastal planes and the rest of South Africa (modified after Compton, 2011).

1.1.3. Principal dating techniques

Dating techniques for the Quaternary period not only need to span large time scales, but also require high resolution to be able to put the evidence of anatomical and cultural human evolution in the correct chronological order. It is unlikely that there is one 'perfect' dating technique for the Quaternary period, so interpretation of sites often utilises several dating techniques. The choice of technique is dependent on the restrictions for a specific site, e.g. geographic or environmental restrictions, age range, or relevant sample types. Currently, the most commonly used dating techniques for this period in South Africa are:

- Radiocarbon dating (Sec. 1.1.3.1.),
- U-series (Sec. 1.1.3.2.),
- Potassium / Argon dating (Sec. 1.1.3.3.),
- Luminescence dating (Sec. 1.1.3.4.), and,
- Electron spin resonance (ESR) (Sec. 1.1.3.5.).

These techniques are discussed in more detail below.

1.1.3.1. Radiocarbon dating

Radiocarbon dating is arguably the most well established archaeological dating technique. It is used for the dating of organic materials, e.g. wood, charcoal, shells, antler, bone, peat / organic bearing sediments, carbonate deposits such as calcite, dissolved CO_2 and carbonate in ocean / lake / groundwater sources (Walker, 2005). The method is based on the radioactive β-decay of ^{14}C into the more stable ^{14}N. ^{14}C is produced in the atmosphere, by cosmic rays colliding with ^{14}N (Libby, 1955). Carbon then combines with oxygen to form CO_2, which is later absorbed and photosynthesized by plants, and thus enters the food chain. After an organism stops metabolic turn over, it stops taking on new ^{14}C and the ratio of ^{14}C / ^{12}C will decrease. This decrease can be related to the age of the sample using the following equation (Stuiver and Polach, 1977):

$$t = \tau \, ln(N/N_0) \qquad \textit{Equation 1.2}$$

where N_0 is the amount of ^{14}C at time (t) = 0 and N is the amount of ^{14}C remaining after time, t. The mean-life, τ, is the average time that an atom would survive before undergoing radioactive decay. The mean-life is derived from the half-life, $T_{1/2}$:

$$T_{1/2} = \tau \, ln2 \qquad \textit{Equation 1.3}$$

where the half-life of ^{14}C is 5730 years.

There are two approaches used to calculate the radiocarbon age, i) the β-counting method, where the rate of β-emissions from a sample can be related to the concentration of ^{14}C, and ii) the direct analysis of the concentrations of ^{12}C and ^{14}C using accelerator mass spectrometry (AMS). AMS analysis is more expensive, but benefits from requiring smaller sample sizes (Walker, 2005).

The age limit of radiocarbon dating is controlled by the half-life of ^{14}C, detection methods, and sample quality; this is typically about ~ 45 ka (Libby, 1955; Godwin, 1962; Walker, 2005). More recently, a pre-treatment preparative step for charcoal ('ABOx' method), allows samples as old as 50 – 60 ka to be dated (Bird *et al.*, 2003). Isotopic enrichment, a process which involves the controlled isotopic enrichment of ^{14}C by magnitudes of 6-7, has been used to extend this limit to ~75 ka (Stuiver *et al.*, 1978). However, this procedure is lengthy, expensive and requires a large sample amount (Stuiver *et al.*, 1978).

Radiocarbon dating had originally assumed that the ratio of ^{14}C / ^{12}C in the earth's atmosphere is, and always has been, constant. However, this has since been proven not to be the case (e.g. Renfrew and Clarke, 1974). The ^{14}C / ^{12}C ratio in the atmosphere is, for example, affected by changes in cosmic ray flux, which is affected by changes in the Earth's geomagnetic field and variations in the intensity of solar activity (Stuiver *et al.*, 1991). Furthermore, events such as

volcanic eruptions, the burning of fossil fuels and atomic bomb tests have influenced the concentrations of ^{14}C in the atmosphere (Walker, 2005). Therefore, a calibration is required in order to convert radiocarbon years to calendar years (see review in Blackwell & Bucky 2008). The most recent calibration, INTCAL09, uses a variety of independent dating methods with concomitant radiocarbon analysis to allow calibration back to 24 ka (van der Pilcht, 2002). Dendrochronology is used up to ~12.2 ka (Stuiver *et al.*, 1998; Kromer and Spurk, 1998). U-series on corals and radiocarbon analysis on laminated marine sediments allows extension back to 50 ka (Walker, 2005; Reimer *et al*., 2009).

Radiocarbon dating is further complicated by the natural isotopic fractionation processes which in biological systems favour uptake of lighter isotopes, therefore artificially reducing the concentration of ^{14}C compared to that of the atmosphere (Walker, 2005). The opposite effect is observed for sea water, which preferentially absorbs heavier isotopes. Therefore, marine organisms which utilise the dissolved carbonate may have artificially high concentrations of ^{14}C, although this may be offset by the marine reservoir effect (see below). However, this type of isotopic fractionation affects all isotopes of C, e.g. ^{12}C, ^{13}C and ^{14}C, and therefore it may be accounted for with consideration of the ratio of stable carbon isotopes (e.g. $^{12}C/^{13}C$) (Walker, 2005). This correction is done by calculating the normalised sample activity (A_{SN}) from the sample activity (A_S) and $\delta^{13}C$ using Equation 1.4 (Stuiver and Polach, 1977). By convention samples are normalised to '-25' per mil, which is postulated to be mean value of terrestrial wood (Stuiver and Polach, 1977). $\delta^{13}C$ can be calculated using the ratio of ^{13}C and ^{12}C in the same way that $\delta^{18}O$ is calculated (Eq. 1.1).

$$A_{SN} = A_S\,(1\text{-}2(25 + \delta^{13}C)/1000) \qquad \textit{Equation 1.4}$$

The marine reservoir effect is a process caused by the radioactive decay of ^{14}C in deep water, without it being replenished. This results in modern sea water having an apparent radiocarbon age (e.g. the $^{12}C/^{14}C$ ratio in the ocean is not in equilibrium with the atmosphere). The apparent sea water age can vary greatly globally (e.g. Shackleton *et al.*, 1988; Reimer and Reimer, 2006), and therefore may lead to large errors in radiocarbon dates of marine organisms, which are used to date coastal archaeological sites (Walker, 2005).

Radiocarbon dating has been used extensively in Africa to date Middle and Late Stone Age sites, e.g. various sites up to 60 ka in South Africa (Vogel and Beaumont, 1972; Bird *et al.*, 2003), and Late Stone Age sites in East Africa (Ambrose, 1998). It has also been used to directly date OES (Vogel *et al.*, 2001), which has been used to calibrate AAR ages (Miller *et al.*, 1999).

1.1.3.2. Uranium-Thorium dating

^{238}U, ^{235}U and ^{232}Th are all naturally occurring unstable isotopes, which decay via a complex series of reactions, eventually forming the stable isotopes of ^{206}Pb, ^{207}Pb and ^{208}Pb in turn (Figure 1.3; Lowe and Walker, 1997). Each isotope has a different half-life, and hence is applicable to a different age range; for the Quaternary period the daughter/parent combinations most commonly used are $^{230}Th/^{234}U$ (5 – 350 ka) $^{231}Pa / ^{235}U$ (> 200 ka), $^{231}Pa / ^{230}Th$ (> 250 ka) (Walker, 2005), and $^{234}U / ^{238}U$ (potential to date up to 1.5 Ma; Smart, 1991).

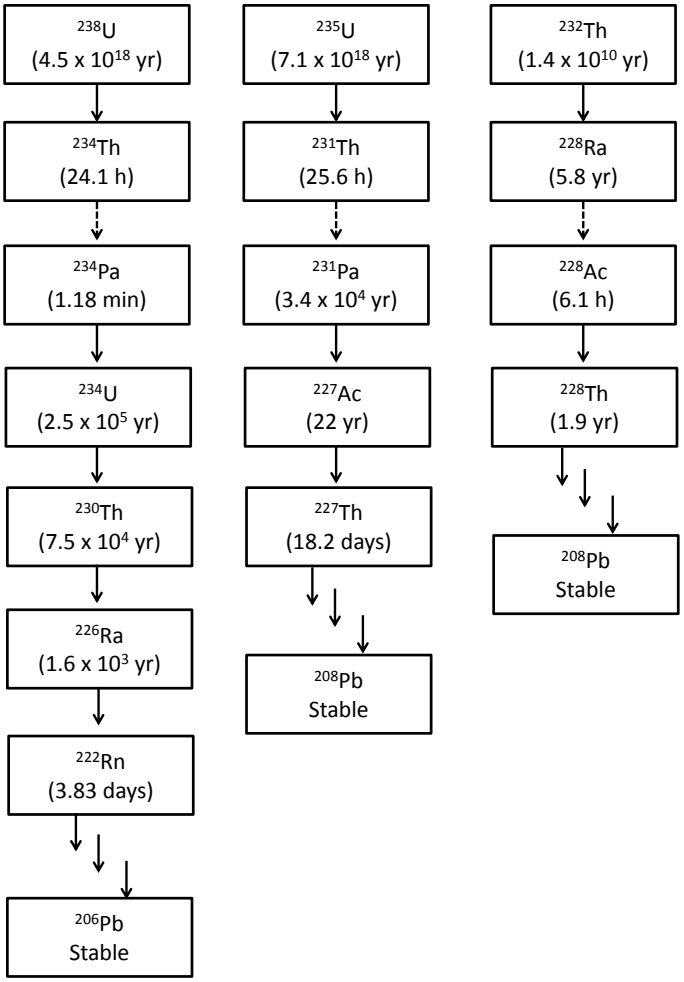

Figure 1.3: Decay pathways used in U-series dating. Solid arrow = α decay. Dotted arrow = β decay. Three arrows = series of degradation steps. Half-lives of unstable atoms are given in parentheses.

Suitable substrates need to demonstrate closed system behaviour in regards to U and Th uptake, which currently limits U-series largely to speleothems and flowstones (Gascoyne *et al.*, 1983; Smart, 1991), and corals (Pickett *et al.*, 1989; Hoang and Taviani 1991). That being said, recent developments in the use of laser-ablation multi-collector inductively coupled plasma mass spectrometry may open up the range of materials which are suitable for U-series dating to bones teeth and possibly mollusc shell (e.g. Eggins *et al.*, 2005).

U-series dating using the $^{230}Th/^{234}U$ decay pathway has been used to date flow stones from between 39 – 92 ka at Pinnacle point, South Africa (Marean *et al.*, 2007).

1.1.3.3. K / Ar and Ar / Ar dating

K/Ar and Ar/Ar are radiometric based dating techniques. Naturally occurring ^{40}K decays via two major pathways: i) β-emission to form ^{40}Ca, and, ii) electron capture to form ^{40}Ar (Lowe and Walker, 1997). β-emission is the major decay pathway; however, as ^{40}Ca is abundant in the natural environment, this decay is not useful for dating.

The ratio of $^{40}K/^{40}Ar$ can be used to date the time elapsed since igneous rocks were last molten. Whilst molten, ^{40}Ar gas trapped within the rock can escape. However, once the rock has cooled ^{40}Ar gas produced from the subsequent decay of ^{40}K becomes trapped within the mineral structure. The half-life of ^{40}K is ~ 1250 Ma, therefore K/Ar dating is appropriate only for samples > 100 ka and is also limited to igneous rocks. In addition the rock samples need to have both a high concentration of K and be able to retain Ar gas over geological time spans; biotite has been found to be the best in both these respects (Walker, 2005).

Both K/Ar and Ar/Ar dating methods use the ratio of $^{40}K/^{40}Ar$ to assign ages, they differ only in the method of analysis of ^{40}K concentration. K/Ar dating requires two samples, of the same size, as ^{40}K and ^{40}Ar need to be measured separately. If the two samples are not homogeneous, or exactly the same size, then errors in age estimation are introduced. Ar/Ar dating has the benefit that only a single sample is required. In Ar/Ar dating the ^{40}Ar concentration is measured directly but the ^{40}K concentration is measured indirectly from the ^{39}Ar concentration, which can be measured simultaneously with the ^{40}Ar. ^{39}K is the most abundant isotope of K, it is also a stable isotope and therefore using the known natural ratio of $^{39}K/^{40}K$, the ^{39}K concentration is therefore proportional to the concentration of ^{40}K at the point of mineralisation. ^{39}K is artificially converted in the lab by neutron irradiation to form ^{39}Ar. The concentration of ^{39}Ar is therefore proportional to that of ^{39}K which is in turn proportional to ^{40}K. Therefore, the $^{40}K/^{40}Ar$ ratio can be inferred from the $^{40}Ar/^{39}Ar$ ratio. The higher concentration of ^{39}K than ^{40}K results in an increased analytical precision for Ar/Ar dating and allows samples as young as 10 ka to be dated. Key assumptions of K/Ar and Ar/Ar dating are that the system remains closed in regards to K and Ar, and that the only source of ^{40}Ar is from the degradation of ^{40}K.

K/Ar and Ar/Ar dating are limited to volcanic rocks, and are therefore not suitable for all sites. This tends to limit the use of K/Ar and Ar/Ar dating to archaeological in Africa to the East African Rift Valley (Deacon and Deacon, 1999), and to early hominid evolution, e.g. > 1 Ma (Brown and Lajoie, 1971; Leakey et al 1978; Boaz, 1979).

1.1.3.4. Luminescence dating

Optically stimulated luminescence (OSL) and thermoluminescence (TL) dating have the same underlying principles as each other, and are collectively called luminescence dating.

Materials containing radioactive isotopes, e.g. ^{238}U, ^{235}U, ^{232}Th or ^{40}K, continuously bombard both themselves, and any surrounding material, with the products of their decay, e.g. α and β particles, and γ radiation. The principal of luminescence dating techniques is that energy from this ionising radiation, and from cosmic rays, may be stored in crystal defects (or 'traps') in common minerals, such as feldspars or quartz, in the form of metastable electrons. The amount of energy stored will increase with the exposure time, and as such the build-up of charge can act as a chronometer.

The traps can be emptied by i) formation of the mineral by crystallisation (e.g. the cooling of magma), ii) intense pressure, iii) exposure to intense heat, and iv) exposure to light (Duller, 2004; Lian and Roberts, 2006); these are known as 'bleaching' events. However, in terms of dating applications, light and heat are the most commonly utilised bleaching events.

To date a sample the amount of stored energy since the last bleaching event (termed the 'equivalent dose', D_e) is divided by the dose rate from the environment (e.g. contribution from radioactive isotopes in the mineral and surrounding material, and the contribution from cosmic rays) (Duller, 2008a):

$$Age\ (ka) = D_e\ (J\ kg^{-1}) / dose\ rate\ (J\ kg^{-1}\ ka^{-1}) \qquad Equation\ 1.5$$

In a laboratory, the stored energy (D_e) can be released in the form of luminescence by stimulation; when an electron is released from a trap it emits energy in the form of a photon. When this light energy is released by controlled heating experiments it is termed thermoluminescence (TL; Aitken, 1985; Duller, 2008a), and when the luminescence is stimulated with light, it is termed 'optically stimulated luminescence' (OSL; Huntley *et al.*, 1985; Aitken, 1998). The amount of stimulated light emitted is related to both the samples age and the level of exposure to radiation over this time period, i.e. the 'dose rate'.

TL tends to be used for the analysis of samples such as brick, flint or pottery to assess the age since the last heating event (Duller, 2008a). OSL is most frequently used to date the time since exposure to light of mineral grains (typically quartz and sometimes feldspar), i.e. to date the deposition of sediments, in particular wind-blown deposits (Duller, 2008a). OSL has been used frequently to date sites in Africa, indeed OSL was used as an independent dating method in this study (Chapter 6). Therefore, the following discussion will focus on OSL.

D_e is generally calculated using the 'regeneration' procedure (Duller, 2008a). In this method the luminescence signal from the sample is measured prior to the sample being bleached by exposure to light. The sample is then irradiated with known doses of increasing intensity and the luminescence signal measured. From these 'regenerated' luminescence measurements a dose response curve can be constructed, from which the D_e can be calculated.

The contribution to the dose rate from the α, β and λ radiation can be calculated using one of two approaches, i) chemical analysis of the burial environment (i.e. measuring the concentrations of K, U and Th), or ii) directly measuring the emission of radiation either *in situ* or from a sample collected from the site (Duller, 2008a). An internal and external dose rate may need to be calculated, depending on the sample; for example, pottery and flint contain radioactive isotopes and are therefore themselves a source of radiation which also needs to be taken into account (Duller, 2008a). The contribution to the dose rate from cosmic rays can be estimated based on the latitude and longitude of the site, and on the burial depth of the sample (Duller, 2008a).

The main constraints on the upper age limit of OSL are set by the saturation limit of the mineral, the stability of the traps, and the magnitude of the environmental dose rate (Duller, 2004; Walker, 2005; Lian and Roberts 2006; Duller, 2008a). The saturation limit of a sample is reached when all of the traps are full, thus further exposure to radiation will not increase the observed luminescence signal. This can be assessed from where the luminescence signal falls onto the dose response curve. The age uncertainties for samples approaching saturation may be high. The saturation limit will vary for different samples, and will be reached faster if the environmental dose rate is high (Duller, 2008a).

A limitation of using feldspar is a fading of the signal (termed 'anomalous fading'), due to the traps leaking their stored energy; at present it is not possible to accurately account for this phenomenon (Duller, 2008a). Fortunately, anomalous fading is not observed for quartz minerals (Duller, 2008a). Grain to grain variability, due to the mineral components or their depositional history, and incomplete bleaching events also pose potential sources of error for OSL. However, incomplete bleaching may be overcome by analysing single grains of sample, i.e. single grains of sand or silt, instead of aliquots of many grains (Duller, 2008a; 2008b; Jacobs *et al.*, 2013). Grains which have been incompletely bleached will have anomalously old ages. Therefore, OSL analysis of aliquots containing a number of grains which have previously undergone incomplete bleaching events will give an average age which is anomalously high.

When sampling sediments for OSL dating it is imperative that samples are not exposed to light during excavation. This is usually done by using an opaque sampling tube which can be driven

into the sediment. Where this is not possible, e.g. when the sediment is too hard packed, sampling should be performed under a dim red light and the exclusion of other light.

The accuracy of OSL of young samples (e.g. < 1000 yrs) can be affected by incomplete bleaching events, low luminescence signals and changing burial conditions which in turn change the dose rate (Madsen and Murray, 2009). Unfortunately, the low luminescence signals in young samples necessitate the analysis of aliquots of many mineral grains, meaning incomplete bleaching events can lead to increased age uncertainties (Madsen and Murray, 2009).

The age range of OSL is hard to quantify, because it varies considerably depending on site specific details and the appropriate age range is expanding as the dating technique advances. For example, recent developments using thermally transferred OSL (TT-OSL) with quartz crystals (see Duller and Wintle, 2012) have reported age limits of ~400 ka (Wang *et al.*, 2006). However, typical age limits for quartz crystals tend to be in the region of 75 – 150 ka (Duller *et al*., 2008a). OSL dating has been used at numerous sites in Africa to date up to ~ 151 ka (e.g. Jacobs *et al.*, 2006; Rector and Reed, 2010; Jacobs *et al.*, 2011; Zink *et al.,* 2012; Jacobs *et al.*, 2013).

1.1.3.5. Electron spin resonance

Electron spin resonance (ESR) is similar to both TL and OSL, as all three are 'trapped charge techniques' (Walker, 2005). ESR dating can be used on many media including tooth enamel, mollusc shell, quartz and coral (Walker, 2005). In ESR, paramagnetic electrons are formed from the radiation released from the decay of naturally occurring radioactive nuclei (e.g. U, Th and/or K) and from cosmic rays (Walker, 2005). These electrons accumulate in defects in the crystal matrix (Henning and Grün, 1983; Grün, 1989). The accumulated dose can be related to the time since mineralisation of the sample.

The accumulated dose of radiation can be measured by resonating the captured electrons using high-frequency electromagnetic radiation in a strong magnetic field (Aitken, 1990). Similarly to TL and OSL, the annual dose (internal and external radiation sources including cosmic radiation), and the accumulated dose need to be calculated in order to calculate the sample's age, e.g. Equation 1.5. The annual dose can be calculated in the same was as in luminescence dating (Sec. 1.1.3.4.).

Many of the errors applicable to luminescence dating are applicable to ESR, e.g. incomplete bleaching events, leaking energy from traps and calculation of the dose rate. Ideally, the dose rate should remain constant throughout the depositional history of the sample. However, the dose rate may change with sample reworking or changing groundwater conditions, both which may change the exposure to radioisotopes and hence the rate of increase of the accumulated dose. In addition, it has been shown that tooth enamel, bone and mollusc shell are all capable of

uranium uptake, which can limit the accuracy of ESR depending on the extent of this uptake, and the model chosen to account for it (Rink, 1998; Grün *et al*., 2001).

The age range of ESR and the accuracy of the ages calculated are highly dependent on the substrate used. For example, the dating range for mollusc shells can be as large as 0 – 2000 ka, but they suffer from poor age accuracy due to open system behaviour (Abeyratne *et al.,* 1997; Schellmann & Radtke, 1999). ESR has been used to date tooth enamel from Africa ranging from 10 ka – 2 Ma (Grün, 1993; Rink, 1997; Grün *et al.*, 2001), however uranium uptake limits the precision (Rink, 1998; Grün *et al*., 2001).

1.2. AN INTRODUCTION TO AAR GEOCHRONOLOGY

Organic compounds are known to be contained within sub-fossil organisms (Abelson, 1954), and the diagenesis of these organics may be used as a premise for dating the material (Abelson, 1955). There are many reactions involved in diagenesis, e.g. decomposition (Sec. 1.3.2.), hydrolysis (Sec. 1.3.3.) and racemization (Sec. 1.3). However, the main focus of AAR geochronology is racemization. AAR geochronology therefore relates the degree of AAR in fossil bio-minerals to the thermal age (Hare and Mitterer, 1969). Quantitation of amino acids is done using chromatographic techniques, such as gas chromatography (GC; Sec. 8.1.1.) or liquid chromatography (LC; Sec. 2.3.2.; Chapter 8).

1.2.1. The nature of amino acids and *racemization*

Amino acids are the building blocks of proteins; their general structure is tetrahedral with an α-carbon at the centre bonded to a hydrogen group, an amine group, a carboxylic acid group and an 'R' group (Fig. 1.4), where the R group defines the identity of the amino acid (Table 1.1). Amino acids join together via condensation reactions to form peptide chains, held together by peptide bonds (Fig. 1.4); hydrolysis is the reverse reaction where the peptide bond is broken.

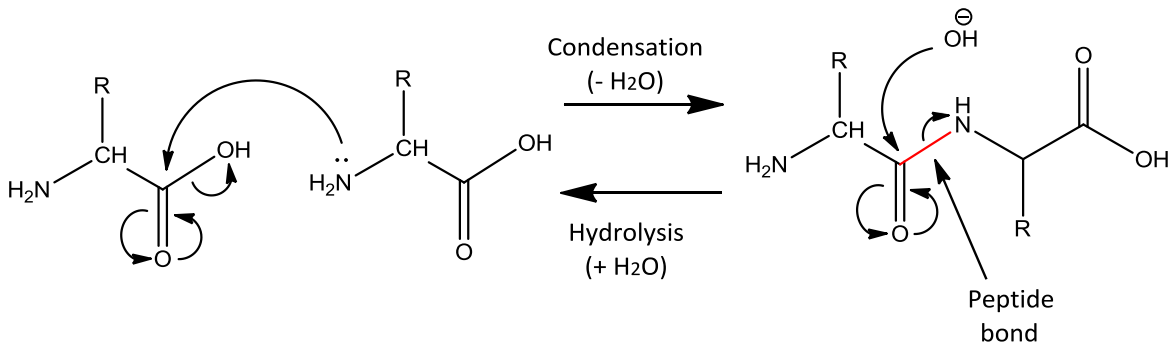

Figure 1.4: Schematic showing peptide bond formation and hydrolysis

All amino acids, with the exception of glycine, have an asymmetric carbon at their centre, resulting in each amino acid having two enantiomeric isomers (Fig. 1.5). The Carl-Ingold-Prelog nomenclature ('R' or 'S') can be applied in order to designate stereo-centres of this type. However, in biology the 'L' and 'D' notation tends to be used instead. The two nomenclatures differ slightly; the R/S denotation gives the absolute stereochemistry of the isomer, whereas the L/D refers to the direction in which a theoretical glyceraldehyde starting material (which retains its stereochemistry during synthesis) rotates the plane of polarised light; L = laevorotary (left), D = dextrorotary (right). Generally, D = R and L = S, however cysteine (with a sulfur in the R group) has D = S and L = R. In nature, organisms use almost exclusively L-amino acids, including L-cysteine (with the exception of some bacterial amino acids which use D-amino acids; Bhattacharyya and Banerjee, 1974); therefore for simplicity, AAR tends to use the L/D notation instead of the R/S notation.

Amino acid	Three letter code	Single letter code	R group
Alanine	Ala	A	– CH_3
Cysteine	Cys	C	– CH_2 S H
Aspartic acid	Asp	D	– CH_2 COOH
Glutamic acid	Glu	E	– $(CH_2)_2$ COOH
Phenylalanine	Phe	F	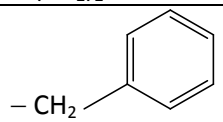
Glycine	Gly	G	– H
Histidine	His	H	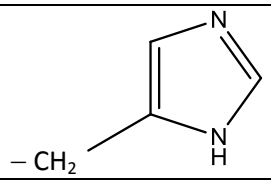
Isoleucine	Ile	I	– CH (CH_3) CH_2 CH_3
Lysine	Lys	K	– $(CH_2)_4$ NH_3
Leucine	Leu	L	– CH_2 CH $(CH_3)_2$
Methionine	Met	M	– $(CH_2)_2$ S CH_3
Asparagine	Asn	N	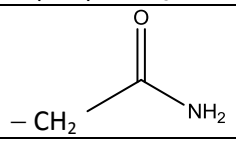
Proline*	Pro	P	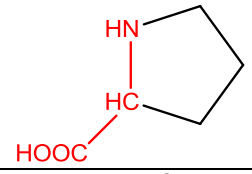
Glutamine	Gln	Q	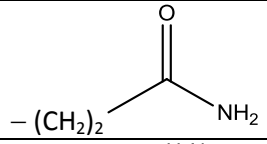
Arginine	Arg	R	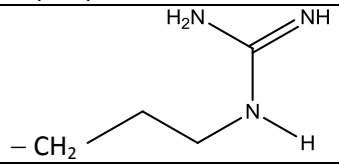
Serine	Ser	S	– CH_2 OH
Threonine	Thr	T	– CH (OH) CH_3
Valine	Val	V	– CH $(CH_3)_2$
Tryptophan	Trp	W	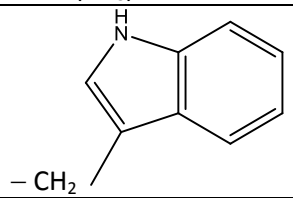
Tyrosine	Tyr	Y	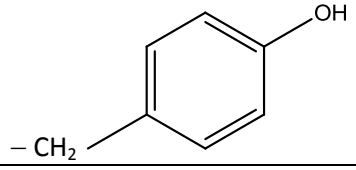

*Table 1.1: Summary of amino acid structures and abbreviations. * Proline has a secondary amine group as the R group (shown in black) is bonded both to the alpha carbon and the nitrogen in the amine group (shown in red).*

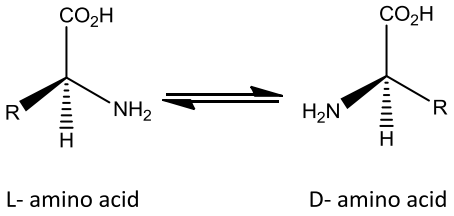

Figure 1.5: Schematic of amino acid racemization

As the L- and D- isomers are chemically identical, neither is thermodynamically favoured; therefore, upon the death of the organism, when biological control ceases, racemization ensues between the two enantiomers (Fig. 1.5).

A small number of amino acids have an additional asymmetric carbon in their side chain, resulting in 4 isomers, e.g. Ile (Fig. 1.6), where L-Ile has an enantiomer (D-Ile) and two diastereomers (D-allo-Ile and L-allo-Ile).

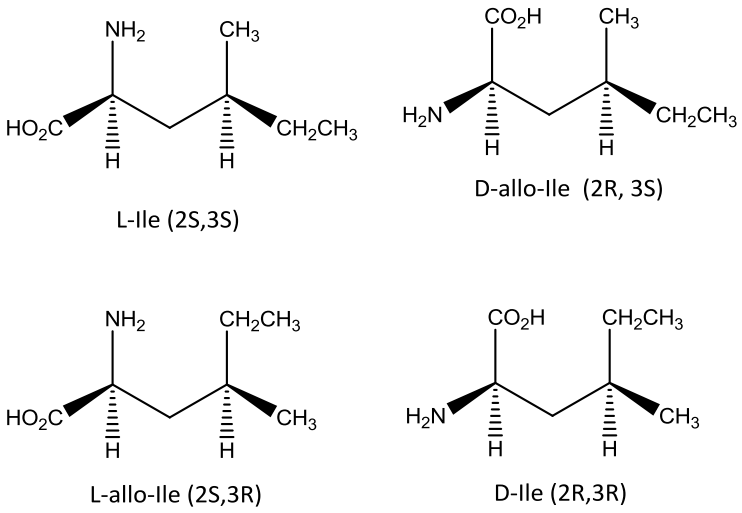

Figure 1.6: The isomers of Ile

In the case of Ile, conversion between L-Ile and its diastereomers is more correctly termed 'epimerization'. Conveniently however, under geological conditions L-Ile almost exclusively epimerizes to form D-allo-Ile, as both L-allo-Ile and D-Ile are unstable (Bada *et al.,* 1986). The extent of Ile epimerization is therefore expressed as the ratio of D-allo-Ile / L-Ile (A/I), instead of 'D/L' as is used for other amino acids. For simplicity, throughout this thesis the term 'racemization' will be used to describe both *true* racemization and Ile epimerization.

The extent of racemization is usually expressed by the D/L value (or A/I for Ile). Eventually a dynamic equilibrium will be reached, for most amino acids this is D/L = 1, for Ile this is A/I ≈ 1.3 (Bada, 1972a; Hare, 1974).

1.2.1.1. Mechanism of racemization

Racemization is a chemical reaction hence according to the Arrhenius Equation its rate increases with an increase in temperature (Laidler, 1984). AAR therefore equates the D/L value to a sample's thermal age (integrated time-temperature), e.g. D/L = 0 at time zero, and a thermally old sample at equilibrium would have a D/L of 1.

The generally accepted mechanism for racemization of free amino acids involves the base catalysed abstraction of the hydrogen from the α-carbon, e.g. with OH^- (Neuberger, 1948; Fig. 1.7). The carbanion intermediate is resonance stabilised by the carboxylic acid group (Fig. 1.7). The carbanion configuration will probably be a sp^2 hybridized carbon, which is a planar. Therefore, re-protonation can occur on either face of the carbanion, resulting in a mix of L and D isomers. Generally, the more electron withdrawing character of the 'R' group, the more stabilised the intermediate and the faster the rate of racemization (Matsuo *et al.,* 1967; Smith *et al.,* 1978). It is believed that the proton abstraction is the rate limiting step (Bada, 1972b). Smith *et al.* (1978) studied the kinetic parameters of free amino acids in heated aqueous solutions and found that the relative rates of racemization were as follows: Ser > Thr > Asp > Glu > Phe > Ala > Leu > Ile > Val. They found that although the electronic effects of the R group play an important role, they do not solely define the rate of racemization, and that both steric effects of the R group and solvent effects are also significant. For example, they studied the rate of Alanine racemization in phosphate buffered solutions and found that the rate increased with an increase of pH from 6.5 to 8.5 and with an increase in phosphate buffer concentration (e.g. an increase in the ionic strength). They also found that the rate of Phe racemization was slower than would be predicted solely on the inductive effects of its R group ($PhCH_2$), this they attributed to the steric effects of the bulky aryl moiety, hindering the rate of racemization.

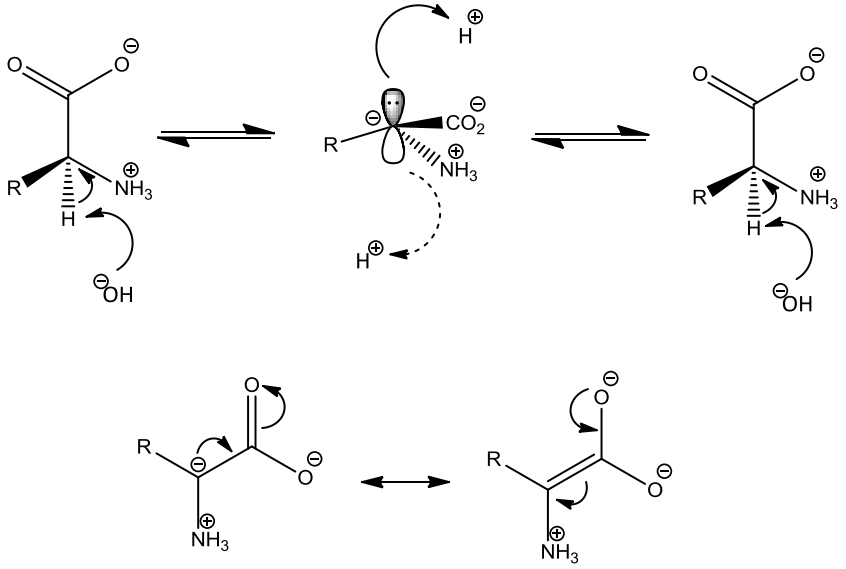

Figure 1.7: Top: Mechanism for the base catalysed racemization of amino acids. Bottom: Resonance stabilisation of the carbanion intermediate

Racemization is also possible under acidic conditions, albeit the rates tend to be slower than under basic conditions (Hare, 1969). Frank *et al.* (1981) observed that the rates of amino acid racemization under acidic conditions were in the following order: Asp > Glu > Phe > Ala > Val > Ile > Ser; racemization is enhanced where the electronic effects of the side chain stabilise the enolized intermediate (Fig. 1.8).

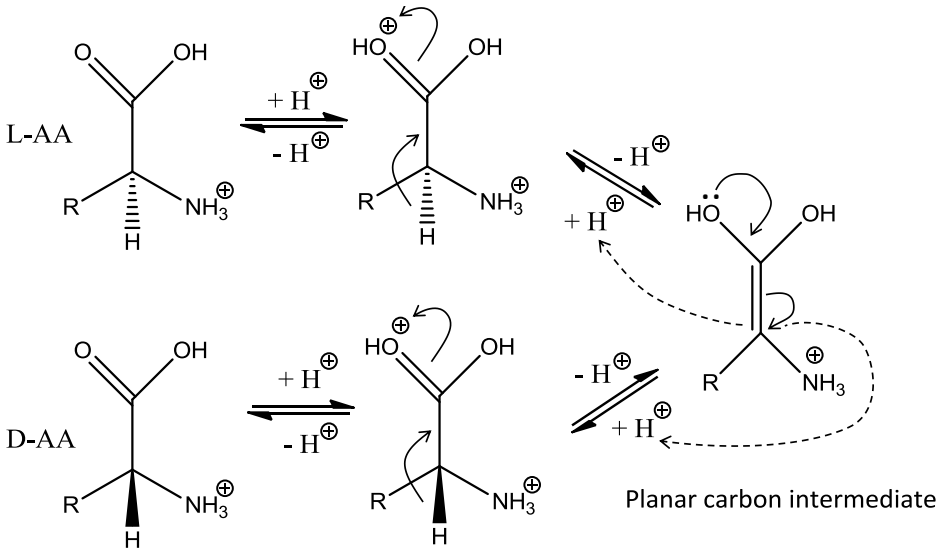

Figure 1.8: Mechanism for racemization for amino acids in acidic conditions (Frank et al., 1981). The planar carbon intermediate can add the H back from either side, resulting in the formation of both D- and L-amino acids.

1.2.1.2. The effect of pH

Amino acids have different ionic forms depending on the pH, e.g. Fig. 1.9. Basic conditions may increase the rates of racemization by: 1) aiding proton abstraction from the α-carbon (Neuberger, 1948); and 2) increasing the rate of peptide hydrolysis, creating an increased number of terminally-bound amino acids (Hill, 1965; Liardon and Ledermann, 1986), where racemization is enhanced (Smith and Evans, 1980; Mitterer and Kriausakul, 1984). Indeed, elevated pH has been shown to affect the rate of AAR, especially at pH > 10, in proteins (Schwass and Finley, 1984; Friedman and Liardon, 1985; Casado *et al.,* 2007) and proteins in some bio-minerals (e.g. Ohtani, 1995; Bright and Kaufman, 2011b; Orem and Kaufman, 2011)

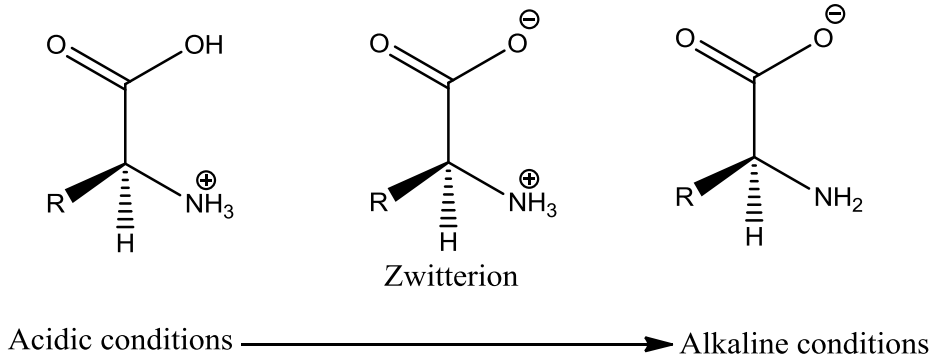

Figure 1.9: Ionic forms of amino acids at different pHs

1.2.2. Analysis of amino acids

Historically, AAR studies have focussed on the epimerization of Ile, primarily because of the ease of separation of its enantiomers (e.g. Hare *et al.,* 1985). However, the developments of chiral gas chromatography (GC) methods (e.g. Frank *et al.*, 1977; Sec. 8.1.1.) and chiral high pressure liquid chromatography (HPLC) methods (Bruckner *et al.*, 1991; Kaufman and Manley, 1998) have made the analysis of several amino acids more routine.

The advantages of analysing several amino acids are three fold:

i) Temporal advantage:

Amino acids have different rates of racemization (Bada, 1984); therefore analysing several amino acids will give resolution over a large age range. For example, free Phe heated at 25 °C in pH 7.6 solution would take an estimated 2000 yrs to reach a D/L value of 0.33, Asp would take ~3500 years and Ile ~ 48,000 years (Bada, 1984). In bio-minerals, the rates of AAR are different to those

of free amino acids in solution, for example Asp racemizes the most rapidly (Sec. 1.3.1.1.) and has therefore been used to date Holocene samples, e.g. land snails as young as 300 yrs (Goodfriend *et al.*, 1992). Ile has a much slower rate of racemization and is therefore better suited to dating Pleistocene samples, e.g. 70 – 100 ka OES from South Africa (Miller *et al.*, 1992). The range of AAR can be extended even further back when considering samples from a colder climate, e.g. AAR studies of mollusc shells from Britain dated samples as old as ~ 1 Ma (Miller *et al.*, 1979), and likewise opercula from Britain dated samples as old as ~2 Ma (Penkman *et al.*, 2011).

ii) Identification of compromised or contaminated samples:

The amino acid rates of racemization, although different, should indicate the same thermal age for a given sample. Therefore, analysis of several amino acids can be used as an internal check for compromised samples (e.g. Chapter 6).

iii) Increasing our understanding of diagenesis within bio-minerals:

The diagenetic environment within bio-minerals is complex (Sec. 1.3.4.); therefore, a better understanding of this complex system may be gained from studying more components from within the system (Sec. 1.3.4.).

1.2.3. In search of a closed system

It is essential that the amino acids used for AAR geochronology are in a closed system, such that contamination is avoided, and factors which influence racemization (Sec. 1.2.2.) are either excluded, or at least consistent for all samples within a study (Towe and Thompson,1972; Sykes *et al.*, 1995). Restricting analysis to closed system amino acids therefore limits variables to species effects (matrix composition, protein sequence and structure), temperature and age. Furthermore in a closed system both amino acids and their degradation products are retained, therefore dating may also be possible utilising other diagenetic reactions. For example, Penkman and colleagues (2011) included the dehydration of Ser to Ala in their analysis of *Bithynia* opercula from the Thames river terraces in Britain.

It has been hypothesised that during the formation of the calcium carbonate bio-mineral of some species, amino acids become trapped in the crystal's interstitial sites (termed 'intra-crystalline'), and therefore potentially form a closed system (Towe and Thompson, 1972; Fig. 1.10). Indeed, calcite crystals grown *in vitro* have been found to incorporate Asp (up to 3 % w/w) into their structure (Demarchi *et al.*, unpublished data). Recent studies have put forward alternative theories of bio-mineralisation mechanisms (e.g. Gebauer *et al.*, 2008; Meldrum and Sear, 2008), and so it is still not clear how the proteins are trapped and exactly where they are located. It is

argued that perfect crystals cannot have inclusions such as proteins (Simkiss, 1986). Therefore, in this study we use the term 'intra-crystalline' according to the operational definition of Sykes *et al.* (1995, pp. 1059), i.e:

"the organic matter within bio-minerals which is resistant to strong chemical oxidation".

If intra-crystalline proteins approximate a closed system, they should be protected from both the external environment (e.g. changes in pH; Sec. 1.2.1.2.), and from diffusive loss (e.g. leaching) of both the amino acids and the products of their degradation. It has long been suggested that focussing on the diagenesis of the intra-crystalline protein fraction alone should improve the reliability of AAR geochronology (Towe, 1980).

Oxidative pre-treatment with NaOCl (sodium hypochlorite, or bleach) has been shown to effectively remove the inter-crystalline and any exogenous proteins, isolating the intra-crystalline proteins (Fig. 1.10) in many bio-minerals, e.g. mollusc shell (Sykes *et al.*, 1995; Penkman *et al.*, 2008; Demarchi *et al.*, 2013a), opercula (Penkman *et al.*, 2011) and coral (Ingalls *et al.*, 2003; Hendy *et al.*, 2012; Tomiak *et al.*, 2013). Studies on mollusc shells have shown that the intra-crystalline protein fraction provides more reliable data for AAR geochronology than the whole-shell proteins (Sykes *et al.*, 1995; Penkman *et al.*, 2007, 2008). Penkman *et al.* (2008) showed that within, and between, sample D/L variability was reduced when using bleach pre-treatment in two taxa of fossil freshwater gastropods, although variability was not reduced for the bivalve *Corbicula*.

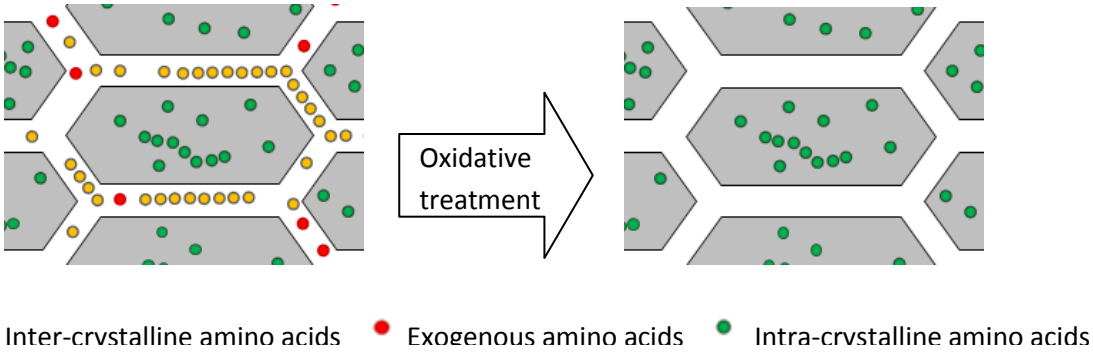

Figure 1.10: Schematic of the possible locations of amino acids within bio-minerals (Figure modified from Sykes et al., 1995). The intra-crystalline amino acids are contained within the mineral crystals whilst the inter-crystalline amino acids are between them, and therefore free to diffuse out of the structure; likewise exogenous amino acids may contaminate the inter-crystalline fraction.

1.2.3.1. Ratite eggshell

A variety of ratite eggshells have been utilised for AAR geochronology, e.g. OES from Africa (Brooks *et al.,* 1990; Miller *et al.,* 1991; 1992; 1999), extinct elephant birds from Australia (Kaufman and Miller, 1995) and Madagascar (Clarke, 2006), and emu shells from Australia (Miller *et al.,* 2000; Magee *et al.,* 2009).

Brooks *et al.* (1990) used heating studies of modern OES and independently dated sub-fossil samples in order to extrapolate age estimates of up to ~77 ka, which were consistent with independent radiocarbon ages. Similar studies using Ile epimerization in OES were performed by Miller *et al.* (1991; 1992; 1999) yielding estimated ages of up to ~ 200 ka at sites in South Africa. Clarke *et al.* (2006) used Ile epimerisation, calibrated using radiocarbon dating, to estimate the ages of elephant bird eggshells from Madagascar, the shells were then analysed for stable isotopes for palaeo-climatic reconstructions (Sec. 1.2.5.).

It has been argued that the success of ratite eggshell for AAR is due to its closed system behaviour with respect to protein diagenesis (e.g. Brooks *et al.*, 1990; Miller *et al.*, 1992; Kaufman and Miller, 1995; Miller *et al.*, 1999, 2000; Clarke *et al.*, 2006). Brooks *et al.* (1990) reported that under conditions of continuous leaching, OES 'retained 99% of its original stable amino acid content', compared to ~60% under similar conditions for mollusc shells (Miller and Hare, 1980). Previous studies using ratite eggshell have therefore not used an oxidative pre-treatment step, instead cleaning the sample by physically removing the outer layers and then removing one-third of the sample with an acid treatment (Miller *et al.*, 1992).

1.2.4. Absolute dating using AAR vs relative dating

Racemization is a chemical reaction and affected by temperature according to the Arrhenius Equation (Laidler, 1984; Sec. 5.1.). However, the observed trends of diagenesis in sub-fossils are complex and often difficult to fully justify (Sec. 1.3.4.).

In order to utilize AAR geochronology as a numerical (rather than a relative) dating method, protein diagenesis needs to be accurately described and calibrated for a given geographic region and, ideally, accurate kinetic parameters derived. A site may be calibrated by analysis of a suite of well stratified samples which have been independently dated. For example, Miller *et al.*, 1999 analysed a suite of OES samples from Boomplaas caves in South Africa, and calibrated the younger of these samples using radiocarbon dating. This allowed the AAR dating of the Howiesons Poort industry to ~ 66 ka +/- 5 ka by extrapolation from the calibrated samples.

Rates of protein diagenesis are too slow at ambient temperatures to be studied in real time, so high-temperature experiments have often been used to simulate reaction kinetics at lower temperatures and estimate kinetic parameters (e.g. Brooks *et al.*, 1990; Miller *et al.*, 1999). Arrhenius parameters (e.g. activation energies and frequency factors) have then been used to extrapolate ages over geological time spans (e.g. Bada and Schroeder, 1972; Brooks *et al.*, 1990; Miller *et al.*, 1999; Kaufman, 2000). This approach assumes that *relative* reaction rates are unaffected at different temperatures, and this is only the case if activation energies for all contributing reactions involved are similar (Miller *et al.*, 2000). Miller *et al.* (2000) tested this assumption for isoleucine (Ile) in *Dromaius novaehollandiae* (Australian emu) eggshell and concluded that the activation energies of hydrolysis and epimerization for Ile were indeed the same, therefore justifying the use of high temperature kinetics to determine rates at low burial temperatures in this case.

Other studies have used a combination of approaches, e.g. independently dated sub-fossil samples are used in order to constrain the observations made from high temperature studies of modern samples (e.g. Kaufman and Miller, 1992; Johnson *et al.*, 1997; Miller *et al.*, 1999; 2000). As temperature records are often not exhaustive, calculation of absolute dates using estimations of palaeo-temperature introduce a large source of error (e.g. Miller *et al.*, 2000; Clarke and Murray-Wallace, 2006). Due to these required assumptions, and difficulties in calculating accurate Arrenhius parameters, AAR geochronology is often limited to relative dating, e.g. aminostratigraphy (e.g. Wehmiller, 1982; Wehmiller, 1993; Ortiz *et al.,* 2006; Penkman *et al.,* 2007; Murray-Wallace *et al.,* 2010). The comparisons of aminostratigraphies are limited to sites from the same geographical regions, or of the same climate histories.

1.2.5. AAR for reconstruction of palaeo-climates

As previously stated, the rate of protein diagenesis is related to temperature. This often limits AAR to relative dating of samples with similar temperature histories (e.g. the same geographic regions). However, the temperature dependence can also be used to aid reconstruction of palaeo-climates, if the samples have been independently dated. For example, AAR on radiocarbon dated land snails from near the Canary Archipelago was used to infer climatic cycles (Ortiz *et al.*, 2006). Similarly, OES samples from Border Cave, South Africa were independently dated using radiocarbon to up to ~38 ka, and the degree of Ile epimerization used to estimate the temperature history at the site, to an accuracy of +/- 1 °C (Miller *et al.*, 1992).

An alternative method for calculating palaeo-climates would involve estimation of both the thermal history and absolute age for a single sample. This could be done by using two different degradation reactions to simultaneously solve the Arrhenius equation. If this could be done it

would prove a very powerful tool, as it would simultaneously link the terrestrial climate to the age of the sample. Indeed, to test this theory, Miller and colleagues (1992) used estimated activation energies for the hydrolysis of Leu and the epimerization of Ile, to analyse independently dated OES samples from Border Cave, South Africa. Unfortunately, the temperature accuracy was poor (+/- 10 °C), and so the method was more applicable for the identification of artificially heated samples.

Johnson *et al.* (1997) have also shown the suitability of the inorganic carbonate fraction of OES for stable isotope analysis. ^{18}O is enriched, in preference to the more abundant ^{16}O when the climate is of relatively low humidity and high temperatures (Johnson, 1997). Indeed, Burk and Stuiver (1981) state that ^{18}O enrichment ($\delta^{18}O$) in the inorganic carbonate is directly related to temperature. Different ratios of the stable carbon isotopes (^{12}C and ^{13}C) result from characteristic photosynthetic pathways of the plants in the ostrich's diet. Trees/shrubs and grasses from a temperate environment photosynthesise via the C3 pathway. Plants photosynthesising via the C4 pathway include mainly grasses from high temperature environments. There is also a third pathway, CAM, which is an intermediate of the 2 other pathways. The amount of ^{13}C enrichment is indicative of the ostrich's diet, and therefore provides information on the environment and the climate at the time of egg mineralization. The analysis of AAR and stable isotopes from the same sample would therefore allow a direct link between the palaeo-environment and age (e.g. Clarke *et al.*, 2006).

1.2.6. Summary of AAR geochronology

AAR geochronology equates the extent of racemization of amino acids within sub-fossil bio-minerals to thermal age (Hare and Mitterer, 1967). AAR is primarily used as a chronological tool, as absolute dating can be complex (Sec. 1.2.4.). Analysis of several amino acids gives a temporal advantage (Sec. 1.2.2.). Many different substrates can be used for AAR, meaning it can be applicable to many sites; e.g. fresh water gastropods from Britain (Penkman *et al.*, 2011), marine molluscs from the Mediterranean (Demarchi, 2005), land snail shells from Israel (Goodfriend, 1987) and ratite eggshells from Madagascar (Clarke *et al.*, 2006) and Africa (Brooks *et al.*, 1990; Miller *et al.*, 1992).

AAR assumes that:

- the initial D/L value is zero
- all racemization is post-mortem
- D/L values increase with a samples thermal age in a reproducible manner

- the amino acids are within a closed system, therefore all variables except temperature, time and species effects can be ignored.

1.3. PROTEIN DEGRADATION

Although the mechanism of racemization of free amino acids in water is fairly simple, in bio-minerals there are many other influencing factors. Some of these can be reduced or removed by limiting analysis to closed system proteins, whilst some, such as the bound state of the amino acids (Sec. 1.3.1.), and the effect of protein structure, cannot. The racemization environment within bio-minerals is therefore more complex than for free amino acids.

1.3.1. The effect of state

The rate of base catalysed racemization is governed primarily by steric effects and the stabilisation of the carbanion intermediate (Matsuo *et al.,* 1967; Smith *et al.,* 1978). Therefore, the state in which the amino acid is bound (i.e. internally bound, terminally bound or free) will have an effect on the rates of racemization. Indeed, a higher rate of racemization has been observed for amino acids in the terminal position. This has been attributed to both the additional electronic stabilisation, and increased flexibility at the end of peptide chains (Kriausakul and Mitterer, 1978; Moir and Crawford, 1988; Smith and De Sol, 1980).

It may be expected that amino acid residues at the N-terminus (with a protonated amino terminus) will racemize faster than those at the C-terminus, due to increased electronic stabilisation; the C-terminus' negatively charged carboxyl group may destabilise the carbanion intermediate (Sec. 1.2.1.1.). Indeed, many studies have shown this to be the case for Ile (Kriausakul and Mitterer, 1978; 1980a; 1980b; Bada, 1985). It has been observed that amino acids in di-peptides racemize significantly faster whilst in the C-terminal position, compared to the N-terminus (Smith and De sol, 1980); however, this was later attributed to diketopiperazine (DKP) formation (Steinberg and Bada, 1981; Sec. 1.3.1.2.). Moir and Crawford (1988) also found that racemization was faster at the terminal positions, that proximity to the N-terminus increased this rate and that the proximity to the C-terminus tend to reduce the rate.

In addition to the bound state of the amino acid, the adjacent residues have an effect on the rate of racemization. For example, Leu in the peptide, Gly-Leu-Gly-Gly racemizes three times faster than when bound in Pro-Leu-Gly-Gly (Moir and Crawford, 1988).

It is clear that there are many factors affecting the rates of racemization within bio-minerals. However, in general, the rates of racemization are: N-terminus > C-terminus >> internally bound ≥

free (Mitterer and Kriausakul, 1984). Notable exceptions to this observation are the formation of diketopiperazines (DKP; Sec. 1.3.1.2.) and the rapid racemization of internally bound Asp and Asn residues (Sec. 1.3.1.1.).

It is often observed that the D/L value of the free fraction of amino acids in sub-fossil samples is higher than for the total hydrolysable fraction (Moir and Crawford, 1988), which may be counter intuitive considering the rates of free amino acid (FAA) racemization are slow. This observation can be explained by the successive hydrolysis of the peptide chains releasing the previously terminally bound, and highly racemized, amino acid residues into the FAA fraction.

1.3.1.1. The special case of Asp and Asn

Rapid racemization of internally bound residues has been observed for Asp and Asn (Lajoie *et al.*, 1980). This rate cannot be explained by the previous base catalysed carbanion mechanism (Fig. 1.7) as the negative inductive effects of the Asp and Asn R groups would destabilise the carbanion intermediate.

Asp and Asn readily undergo nucleophillic attack on the carboxyl of the R group by the nitrogen of one of the amide groups to form a succinimide intermediate (Fig. 1.11; Radkiewicz *et al.*, 1996). This evolves water in the case of Asp, and ammonia for the case of Asn. Nucleophilic addition on the intermediate can then proceed to form either aspartic acid or iso-aspartic acid. The iso-aspartyl product is favoured and accounts for ~75 % at equilibrium (Brennan and Clarke, 1993). Water is generally a more readily available nucleophile than ammonia, so Asn is usually converted to Asp after a succinimide is formed (Vallentyne, 1964; Li *et al.*, 2003).

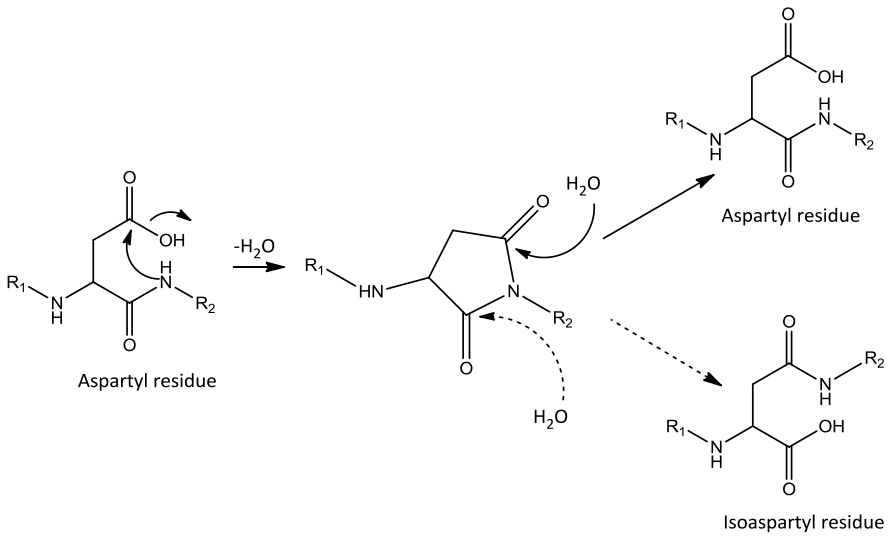

Figure 1.11: Mechanism for succinimide formation with aspartyl residues (R_1 and R_2 symbolise the continuation of the peptide chain)

It was initially thought that the rapid rate of Asp racemization was due to the resonance stabilisation of the succinimide intermediate (Fig. 1.12; Radkiewicz *et al.*, 1996). However, racemization of the Asn residues has also been observed, which therefore may suggest that racemization occurs prior to the formation of the succinimide ring (Li *et al.*, 2003). Li and colleagues (2003) studied the racemization of Asn within the penta-peptide Gly-Gln-Asn-Gln-Gly-Gly. They observed that L-Asn converts to D-Asn, and vice-versa, as well as converting to Asp. Furthermore, they showed that no iso-Asn products were formed, hence providing evidence that the racemization of Asn must occur prior to deamidation. They suggested that racemization may occur via the tetrahedral intermediate (Fig. 1.13). The intermediate may facilitate the base catalysed racemization by forming a more favourable configuration, and/or by the negative inductive effect of nitrogen in the pyrrolidine ring. Although the succinimide intermediate may be resonance stabilised (e.g. Fig. 1.12), this study shows that this does not contribute to the fast rate of Asn racemization, which may also be the case for Asp.

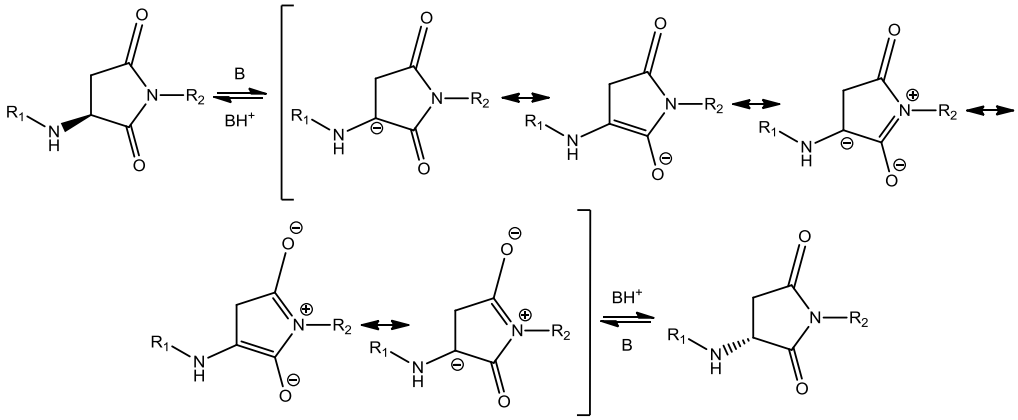

Figure 1.12: From Radkiewicz et al. (1996): the principle resonance structures of the succinimide intermediate which is resposible for the fast rate of racemization of Asp. (R_1 and R_2 symbolise the continuation of the peptide chain; B symbolises a base, e.g. OH^-)

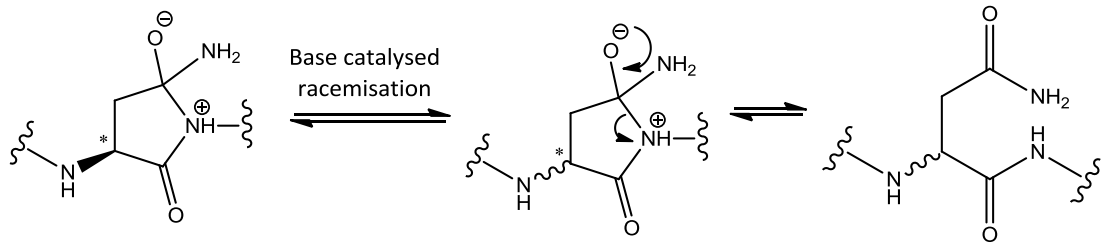

Figure 1.13: Asn tetrahedral intermediate thought to facilitate the racemization of internally bound Asn (Li et al., 2003)

A recent study by Takahashi and colleagues (2010) suggested an alternative mechanism of Asp internal racemization to that suggested by Radkiewicz *et al.,* (1996). Takahashi and colleagues suggest that the rapid racemization of Asp was due to stabilisation of the enolized-succinimide intermediate through the association with two water molecules (Fig. 1.14). They suggested that the succinimide intermediate forms an enolate, facilitated through the concerted bond reorganisation with two water molecules (Fig. 1.14). Reversal of the reaction can result in the reversal of the stereochemistry of the α-carbon (e.g. racemization), in a similar mechanism to that described by Frank *et al.* (1981), for the acidic racemization of free amino acids via an enolized intermediate (Fig. 1.8). Internal racemization is not observed for most other amino acids, including Glu which can also form an analogous cyclic intermediate (see Sec. 1.3.2.1.), thus suggesting that the planar nature of the succinimide ring is necessary for this reaction mechanism.

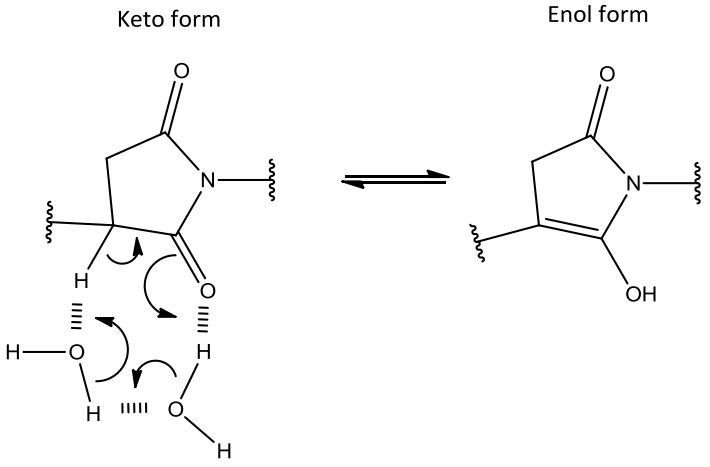

Figure 1.14: Enolisation of Asp succinimide intermediate with mediation by two water molecules (Takahashi et al., 2010).

However, regardless of the mechanism, the irreversible deamination of Asn to form Asp is rapid; for example, at pH7 at 37 °C the half-life is just a few years (Vallentyne, 1964). Therefore, it is unlikely that Asn would persist in the fossil record. Additionally, any Asn preserved in sub-fossil bio-minerals would undergo rapid and irreversible deamination to form aspartic acid under the

acidic conditions used in sample preparation (Hill, 1965; Sec. 2.2.1.). Therefore, when considering the rate of Asp racemization, the rate of Asn racemisation and the rate of Asn to Asp conversion must also be considered, as Asn will contribute towards the overall observed rates of reaction (Brinton and Bada, 1995; Goodfriend and Hare, 1995). As Asp and Asn become analytically indistinguishable, they are referred together as Asx. It has been observed that the initial rate of Asx racemization in corals is faster than at later stages, and it has been proposed that the initial rapid rate of racemization is due to the contribution from Asn to D-Asp (Goodfriend, 1991; Brinton and Bada, 1995).

1.3.1.2. Formation of diketopiperazines

Diketopiperazines (DKPs) are cyclic organic compounds formed from two amino acids joined in a lactam ring; their general structure is given in Fig. 1.15 (Bada, 1991). Formation of DKPs increases the rate of racemization of the residues in the lactam ring (Steinberg and Bada, 1991; Moir and Crawford, 1988), and they may also increase the rate of hydrolysis of the di-peptide from the peptide chain (Kriausakul and Mitterer, 1983; Mitterer and Kriausakul, 1984; Steinberg and Bada, 1991).

DKPs formed from dipeptides have also been shown to invert their sequences, therefore equating rates of amino acid racemization to their original sequence position in short peptide chains should be exercised with some caution (Steinberg and Bada, 1981).

Moir and Crawford (1988) observed that the racemization of Pro in Pro-Leu-Gly-Gly exceeded unity. They showed that the increased extent of Pro racemization was not due to its N-terminal position, and was as a direct result of the DKP formation. Interestingly, Leu racemization was suppressed in this peptide, but was three times faster when in a Gly-Leu-Gly-Gly peptide. This therefore suggests asymmetric induction favours racemization of Pro over Leu. It might be expected that DKPs would preferentially form DL compounds, rather than DD or LL, as the latter would adopt a *cis* conformation resulting in unfavourable steric interactions between the R group). However, it remains unclear why Pro preferentially racemizes over Leu.

These experiments show that DKPs can readily form from peptides, and that as a result the rates of racemization may increase. Furthermore, the rates of racemization, and affinity to form DKPs will be affected by the primary amino acid sequence.

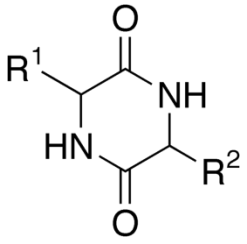

Figure 1.15: General structure of a diketopiperazine

1.3.2. Decomposition

Amino acids may degrade to form other organic compounds and in some cases other amino acids. The pathways can be complex, and may involve decarboxylation, deamination, dehydration or aldol reactions (Bada *et al.*, 1978; Walton 1998).

1.3.2.1. Asp and Glu

Asp decomposes via two main pathways, i) deamidation whilst in the free state to produce fumaric acid and ammonia (Bada and Man, 1980), and ii) decarboxylation to form Ala or β-Ala, depending on whether decarboxylation occurs at the α- or β-carbon (Walton, 1998; Bada 1971; Sohn and Ho, 1995).

Glutamic acid decomposes via two main pathways; decarboxylation, to form aminobutyric acid (Hare and Mitterer, 1967), and dehydration to form pyro-glutamic acid (Wilson and Cannan, 1937). Both free Glu and N-terminal Glu readily form the more stable pyro-glutamic acid (Wilson and Cannan, 1937; Fig. 1.165). Although in theory a similar reaction could occur with Asp, Vallentyne (1964) observed Asp had no affinity to form a lactam ring.

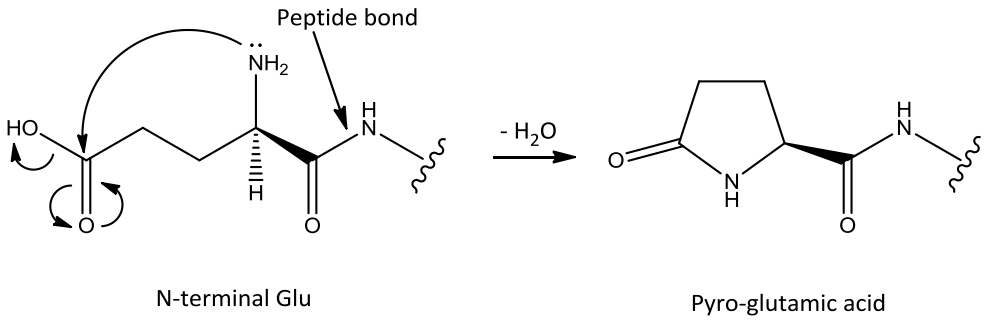

Figure 1.16: Formation of pyro-glutamic acid from N-terminal Glu; this reaction is also applicable for free Glu

Both Asp and Glu form readily from the irreversible deamidation of Asn and Gln, respectively (Brinton and Bada, 1995). Therefore, it is unlikely that Asn or Gln would persist in the fossil record (Walton, 1998).

1.3.2.2. Ser and Thr

Ser is one of the more thermally unstable amino acids and degrades as both a free and bound amino acid, via several pathways; these include decarboxylation to form ethanolamine, deamination to form ammonia, dehydration to form Ala (Bada *et al.*, 1978) and reversible aldol reaction to form Gly (Vallentyne, 1964).

Dehydration has been found to be the dominant degradation pathway of Ser when it is in the free-state, whilst the aldol reaction has been found to dominate whilst Ser is peptide bound (Bada and Mann, 1980).

Similarly to Ser, Thr is also thermally unstable, it can decompose in both the free and peptide bound state, although it is faster whilst bound (Vallentyne, 1964). It degrades via several pathways, including dehydration to form α-aminobutyric acid (α-ABA), aldol cleavage to form Gly, and decarboxylation to form propanolamine (Vallentyne, 1964; Bada *et al.*, 1978; Walton, 1998). It has been found that the aldol reaction can be catalysed by the presence of metal ions (Vallentyne, 1964).

1.3.2.3. Gly and Ala

Gly and Ala are the more thermally stable amino acids (Vallentyne, 1964). Both are formed from the degradation of other amino acids, Gly from Val, Ser, Thr and Tyr (Vallentyne, 1964), and Ala from Ser and Asp (Walton, 1998). Indeed, an increased concentration of Ala is seen in fossil brachiopods dated at > 120 ka (Walton, 1998).

Both Gly and Ala degrade slowly, primarily via decarboxylation to form methylamine and ethylamine, respectively (Vallentyne, 1964).

1.3.2.4. Arg

Arg has been shown to decompose in strong base (pH > 10) to form urea and ornithine (Vallentyne, 1964). However, there is evidence that this route of decomposition also happens at lower pH within the geological record, e.g. ornithine was observed in brachiopods up to 2.2 Ma (Hare and Mitterer, 1967).

1.3.2.5. Val, Leu, Ile and Phe

Leu, Val and Phe are the amino acids which decarboxylate the fastest (Vallentyne, 1964). Phe decarboxylates to form phenethylamine, which later decomposes to form benzylamine (Vallentyne, 1964). The rate of Val degradation was found to be faster whilst in the free-state, opposed to being peptide bound (Walton, 1998). Leu has been found to degrade via deamination and some other unidentified pathways to form ammonia (Walton, 1998).

Walton (1998) found that Ile and Leu decomposition in brachiopods was more rapid than for other amino acids. He also noted that a small amount of Ile and Leu may be temporarily bound by an acid sensitive reaction (see also Sec. 1.3.4.).

1.3.3. Hydrolysis

Peptide bonds are thermodynamically unstable, but the activation energy required to break the bonds prevents spontaneous bond cleavage, therefore giving some kinetic stability. The activation energy varies for the different residues; e.g. serine and aspartic acid are found to break more readily than other amino acids peptide bonds (Walton, 1998).

Hydrolysis of the peptide bonds releases internally bound amino acids to terminal positions, and also creates free amino acids. Hydrolysis therefore has an effect on the rates of both decomposition (Sec. 1.2.2.) and racemization (Sec. 1.3.1.).

The rates of hydrolysis are affected by the primary amino acid sequence (e.g. hydrophobic amino acids will hydrolyse slower than hydrophilic amino acid rich sequences (Bada, 1985)) and by the rate of DKP formation (Sec. 1.3.1.2.). Therefore the rates of hydrolysis are likely to change as protein degradation progresses, as too will the rates of racemization (Liardon and Ledermann, 1986).

The rates of hydrolysis will also be affected by the availability of water, which within a bio-mineral may be limited (Walton, 1998; Sec. 1.3.4.). However, the degradation of some amino acids (e.g. Ser, Thr and Glu) can release water upon degradation, thereby allowing further hydrolysis.

1.3.4. Treating the system as a black box

Most AAR studies use a simplified model of AAR, where only two fractions of amino acids are considered - the total hydrolysable amino acid (THAA) and the free amino acids (FAA) (Fig. 1.17). In reality however, the system is more complex; the primary amino acid sequence, bound state of the amino acid and extent of protein degradation all have contributions to the observed rates of racemization. The rate of racemization is therefore intrinsically linked to the rate of hydrolysis

and other degradation reactions. By treating the system with one rate of racemization per amino acid these underlying parameters are being ignored; the system is effectively treated as a 'black box' (Collins and Riley, 2000).

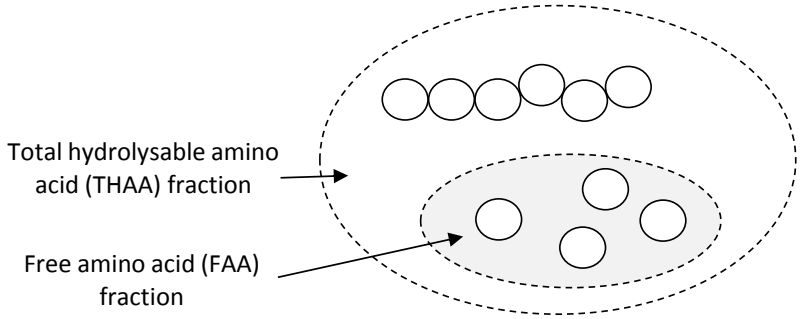

Figure 1.17: THAA and FAA fractions

The generally accepted conceptual model to explain the observed rates of racemization were initially developed by Mitterer and Kriausakul (1984) and Wehmiller (1980). This model is outlined below:

i) Racemization is initially slow due to the majority of amino acids being bound internally in the peptide chains
ii) Progressive hydrolysis produces more terminally bound amino acids, and DKPs which increase the observed rate of racemization
iii) Eventually, the majority of amino acids are free and so the rate of racemization decreases until eventually equilibrium is reached.

However, this model does not fully explain the experimental findings, e.g. in this model the slowest rate of racemization is that of the free amino acids, yet the final rates of racemization in sub-fossil material is often slower than would be predicted (e.g. Kriausakul and Mitterer, 1980b). Collins and Riley (2000) put forward an adapted model (Fig. 1.18) with two explanations as to why this could be the case:

i) Leaching of the highly racemized FAA fraction, resulting in an apparent reduction in the rate of racemization, which should not occur in a truly closed system
ii) Slow hydrolysis of a residual peptide-bound fraction, perhaps due to a lack of water (e.g. Towe, 1980; Miller *et al.*, 2000; Penkman *et al.*, 2008; Demarchi, 2009). Indeed, even for very old samples 100 % hydrolysis is not always reached, e.g. brachiopods from 3.3 Ma were only ~70% hydrolysed (Walton, 1998).

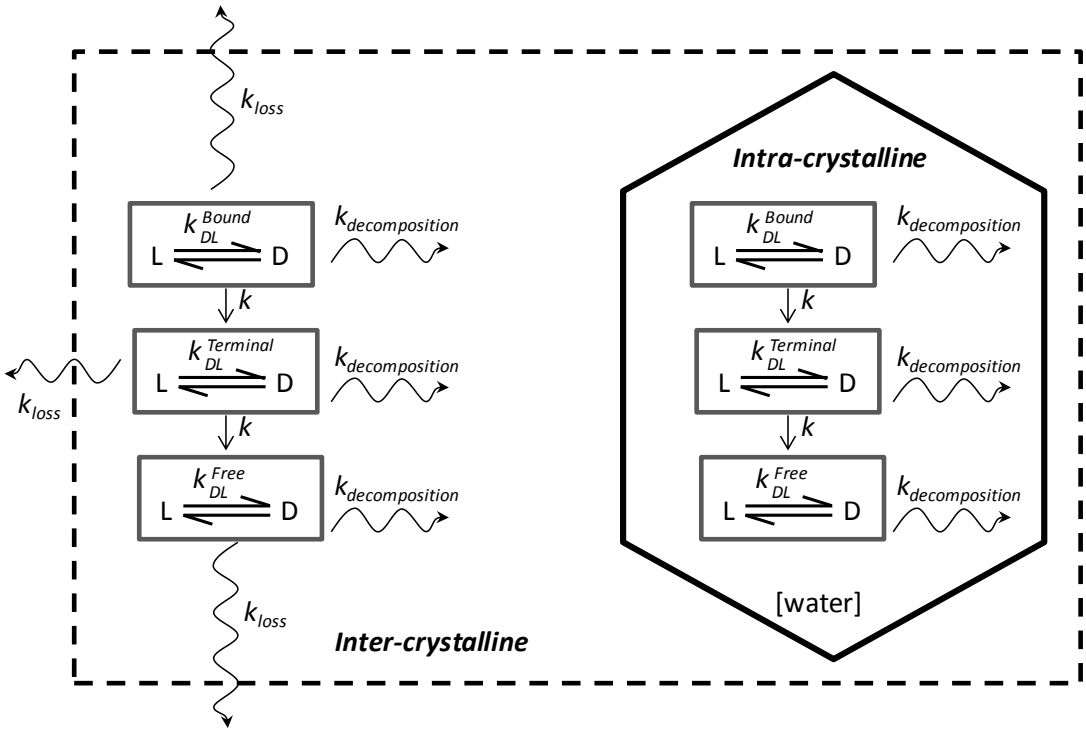

Figure 1.18: Schematic of the different pools of amino acids within a bio-mineral: modified from Collins and Riley, 2000.

Fortunately, treating the system like a 'black-box' gives observed rates of racemization (and hydrolysis) which can sometimes be described mathematically (Chapter 5), even if the underlying chemical rationale is incomplete (Clarke and Murray-Wallace, 2006). However, in order to fully understand the underlying principles more work needs to be done to understand this complex system, and to open the black box. Mass spectrometry (MS) may allow the observation of more than just the FAA and THAA fractions. Indeed, if the starting sequence is known then it may allow direct observation of protein breakdown which can be directly compared to the rates of racemization obtained from chromatographic studies, meaning it would be known which amino acids, and from where, are racemizing at any given moment.

The amount of protein within OES is significantly higher than that found in mollusc shell, the substrate most commonly used in AAR studies. Brooks *et al.* (1990) found OES to have an organic component of 3% w/w, with >99% of this being within the intra-crystalline fraction. This concentration is 50 times more than expected in many mollusc shells (Brooks *et al.*, 1990; Miller *et al.,* 2000). OES has the further advantage that its most abundant proteins (SCA-1 and SCA-2) have been isolated, sequenced and modelled (Mann and Siedler, 2004), which means that there is much more information about the original protein composition than is possible for mollusc shells. SCA-1 is the more abundant of the 2 main proteins in modern OES (Mann and Siedler, 2004). Preliminary MS experiments by Penkman and group (unpublished data) have found that the SCA-1 protein is abundant within the intra-crystalline fraction. The higher concentration of protein

available for analysis, combined with knowledge of the protein's sequence, could enable the characterisation of the key protein degradation mechanisms using mass spectrometry. Studying the degradation of the protein alongside racemization will aid in our understanding of the process of protein diagenesis in sub-fossil bio-minerals, and help develop an improved AAR dating model.

1.4. PROJECT AIMS

It is clear that OES offers an excellent bio-mineral for the preservation of amino acids within the geological record, and is likely to offer the closed system (Brooks *et al.,* 1990; Miller *et al.*, 2000), which is required for accurate AAR dating (Towe and Thompson, 1972; Engel *et al.*, 1994; Sykes *et al.*, 1995; Miller *et al.*, 1999; Collins and Riley, 2000; Penkman *et al.*, 2008).

The application of AAR geochronology to OES from Africa has the potential to provide a time framework for archaeological sites and/or climate histories during the Quaternary (Brooks *et al.*, 1990; Miller *et al.*, 1992; 1999), and could be of particular utility given the widespread use of OES by anatomically modern humans (Ambrose, 1998; Henshilwood *et al.*, 2002; 2004; Texier *et al.*, 2010). This project therefore aimed to develop the method of AAR OES dating, with the ultimate goal of establishing whether this technique may be useful in dating South African Quaternary palaeontological sites, which may aid our understanding of human evolution and climate change over this period. To that end, this project consisted of the following aims:

1. To test for closed system behaviour of proteins in OES (Chapter 3)
    - To develop a robust and defendable method for the isolation of an intra-crystalline fraction of amino acids using modern OES
    - To test the intra-crystalline fraction for closed system behaviour through extensive leaching and heating studies at different pH's
2. To use high temperature studies using modern OES to try and mimic degradation of proteins at lower temperatures over geological time scales (Chapter 4), and to assess the applicability of such high temperature studies to extrapolate to low temperatures (Chapter 4 & 5)
3. To test the utility of using several amino acids in AAR OES studies in giving a temporal advantage, as has been shown for other bio-minerals (Chapters 4 – 6)
4. To assess the applicability of estimating Arrhenius parameters for the degradation of proteins within OES, using both high temperature data and low temperature sub-fossil data (Chapter 5)

5. To analyse a suite of OES sub-fossil samples from independently dated palaeontological sites in South Africa, in order to assess the utility of OES AAR as a dating technique for the Quaternary period in South Africa (Chapter 6)
6. To develop a method for the identification of artificially heated sub-fossil OES samples, such that they could be excluded from AAR age models (Chapter 6)
7. To perform a preliminary study using soft-ionisation protein mass spectrometry, alongside chiral amino acid analysis, in order to better understand the underlying chemical pathways of diagenesis in OES (Chapter 7)
8. To develop a new chromatographic method for the separation of amino acids and their enantiomeric forms, to utilise the developments of ultra-high pressure liquid chromatography (UHPLC; Chapter 8).

CHAPTER 2: ROUTINE EXPERIMENTAL PROCEDURES

2.1. OES SAMPLES

2.1.1. OES Sample details

OES has three structural calcitic layers consisting of a thin outer crystal layer with little organic content (Heredia *et al.*, 2005), a palisade layer, and, on the inside surface of the shell, a mammillary cone layer (Feng *et al.*, 2001; Patnaik *et al.*, 2009) (see Fig. 2.1). The palisade and mammillary layers contain organic components, made of both protein (e.g. Hincke *et al.*, 1995) and polysaccharides (Baker and Balch, 1962). The organic components are speculated to influence nucleation, control crystal growth and have an influence on the mechanical properties of the bio-mineral (Addadi and Weiner, 1992; Arias *et al.*, 1993; Heredia *et al.*, 2005; Lammie *et al.*, 2005). Our analysis did not discriminate between these different layers.

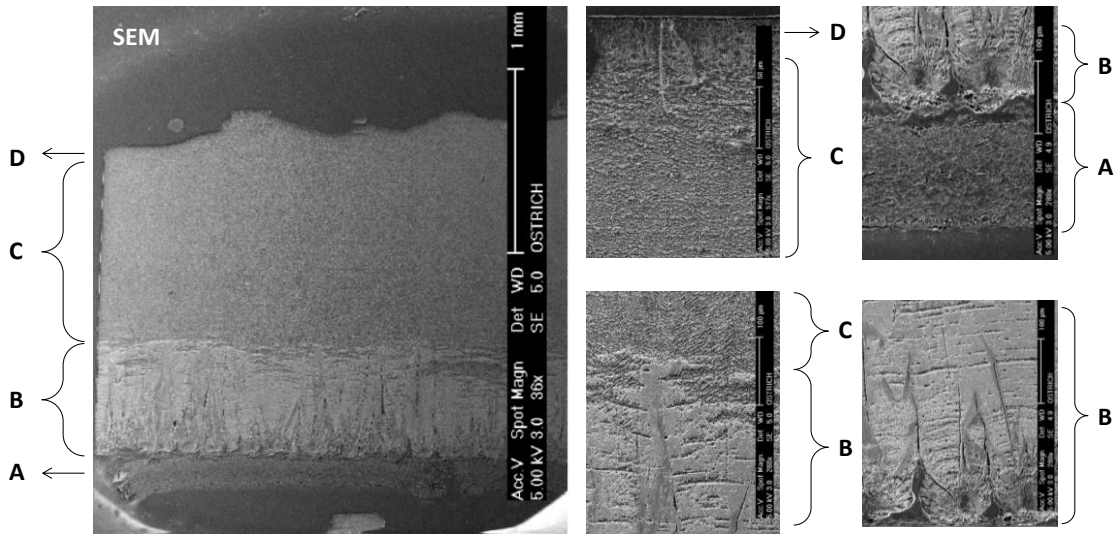

Figure 2.1: Scanning electron microscopy (SEM) images of a cross-sectional plane of OES: A, organic membrane (removed prior to heating and AAR analysis); B, cone layer; C, palisade layer; D, crystal layer (external surface of the OES). The different calcitic layers were not discriminated in this study. Images kindly supplied by Mary Fairweather and Renée van de Locht of the University of York.

The OES samples were cleaned by several rinses and sonication in HPLC-grade water until the water removed was clear. If present, the inner organic membrane was peeled off and excluded

from the analysis. This was done after the first water wash as it was easier to remove once the OES was wet. The OES was then air-dried.

A modern OES was purchased from Oslinc, an ostrich farm based in Boston, Lincolnshire, UK (www.oslinc.co.uk). The shell was less than 1 year old; for the purposes of reproducibility all analyses were done using the same eggshell.

Sub-fossil samples from Pinnacle point were supplied by Curtis Marean, EBC samples were supplied by John Parkington, detailed in Sec. 6.2.1.

2.1.2. Oxidative treatment

The protocol for oxidative treatment was optimised in the process of this thesis (Sec. 3.3.2.); unless otherwise stated, samples were treated as follows. OES samples were powdered using an agate pestle and mortar and sieved to ensure all particles were < 500 μm. Powdered samples were submerged in 50 μL of 12% (w/v) NaOCl per mg of bio- mineral in a sterile plastic universal or eppendorf, depending on the size of the sample. Samples were agitated every 24 h to ensure all powder was exposed to the bleach. After 72 h, the bleach was removed by pipette. The OES was then washed five times in HPLC-grade water, with a sixth wash with HPLC-grade methanol to reduce any leftover bleach. The samples were then air-dried overnight.

2.2. AAR ANALYSIS

2.2.1. Sample treatment

Powder samples were accurately weighed into two fractions for the analysis of the free amino acid fraction (FAA), and the total hydrolysable amino acid fraction (THAA):

- For THAA, samples were hydrolysed by addition of 20 μL of 7 M HCl per mg of OES and subsequent heating at 110 °C for 24 h in N_2 purged vials; this protocol was optimised in the process of this work (Sec. 3.3.1.). The acid was removed using centrifugal evaporation. Unless otherwise stated all samples were prepared using this protocol.
- For FAA, samples were demineralised in a minimal volume of 2 M HCl. The acid was removed by centrifugal evaporation. Approximately 100 μL of 2 M HCl was typically required to demineralise 1 mg of OES.

Samples were solubilised in a rehydration solution comprising 0.01 M HCl, 1.5 mM sodium azide and 0.01 mM L-homo-arginine (L-hArg). This was prepared by dissolution of 8.46 mg of sodium

azide and 1.12 mg of LhArg in 500 mL of 0.01 M HCl. L-hArg is a non-protein amino acid and was used as an internal standard in this study (L-hArg hydrochloride purchased from Sigma-Aldrich; Product code: H1007). THAA samples were rehydrated in 60 µL of rehydration fluid per mg of OES. FAA samples were rehydrated in 20 µL of rehydration fluid per mg of OES.

All glassware used for sample preparation and for the preparation of the rehydration fluid were sterilised by heating at 450 °C for 6 h, or by washing with concentrated nitric acid when this was not possible (as per Penkman, 2005).

2.3.2. High pressure liquid chromatography method

AAR analysis was performed using a high pressure liquid chromatography (HPLC) method based on Kaufman and Manley's 1998 method. The method had been modified with an extended solvent programme such that D-alle and D-Leu could also be separated. The resulting method was 115 min long, inclusive of flush time (Table 2.1; Penkman, 2005). The amino acids within the external standard eluted in the following order: L-Asx, D-Asx, L-Glx, D-Glx, L-Ser, D-Ser, L-Thr, Gly(co-eluting with D-Thr, L-His and D-His), L-Arg, D-Arg, L-Ala, L-hArg, D-Ala, L-Tyr, L-Val, L-Met, D-Met, D-Val, L-Phe, L-Ile, D-Phe, L-Leu, D-alle, D-Leu (e.g. Fig. 1.2). Kaufman and Manley found that this method was capable of quantifying analytes down to 0.1 pmol (Kaufman and Manley, 1998; see also Sec. 8.4.2.1.).

D-Arg and D-Leu are poorly resolved in OES samples, therefore in this thesis they have been excluded from data analysis.

At pH 7 at 37 °C, asparagine (Asn) undergoes rapid irreversible deamination to form aspartic acid and ammonia, with a half-life of just a few years (Vallentyne, 1964). Therefore, it is unlikely that Asn would persist in the fossil record, and any Asn preserved in sub-fossil bio-minerals would undergo rapid and irreversible deamination to form Asp under the acidic conditions used in sample preparation (Hill, 1965). As Asp and Asn become analytically indistinguishable they are referred together as Asx. Similarly glutamine (Gln) undergoes rapid irreversible deamination under acidic conditions to form glutamic acid (Hill, 1965); Glu and Gln are grouped together as Glx.

An Agilent 1100 series HPLC fitted with a quaternary pump, degasser, auto-sampler, heated column compartment and a fluorescence detector was used. Separation was achieved using a HyperSil base deactivated silicon (BDS) column (5 µm, 250 x 4 mm), temperature controlled at 25 °C. The method uses a ternary gradient with sodium acetate buffer (23 mM sodium acetate tri-hydrate, 1.5 mM sodium azide, 1.3 µM EDTA, adjusted to pH 6.00 ±0.01 with 10% acetic acid and sodium hydroxide), methanol (MeOH) and acetonitrile (ACN) (Table 2.1). All solvents used are

HPLC-grade and purchased from Fisher Scientific, UK. HPLC-grade water was prepared using a Millipore Simplicity system. The flow rates and gradient time table are detailed in Table 2.1.

The fluorescence detector uses a Xenon-arc flash lamp at a frequency of 55 Hz, with a 280 nm cut-off filter and an excitation wavelength of 230 nm and emission wavelength of 445 nm.

Run time (min)	%A (sodium acetate buffer)	%C (methanol)	%D (acetonitrile)	Flow (mL / min)
0	95.0	5.0	0.0	0.56
31	76.6	23.0	0.4	0.60
95	46.2	48.8	5.0	0.60
95.9	0.0	95.0	5.0	0.60
99	0.0	95.0	5.0	0.60
100	95.0	5.0	0.0	0.60
115	95.0	5.0	0.0	0.56

Table 2.1: Solvent Gradient programme for RP-HPLC analysis (Penkman, 2005)

Samples were derivatised prior to injection onto the column using an automated injector program: 1.1 µL of a solution of *o*-phthaldialdehyde (OPA) and *N*-iso-butyryl-L-cysteine (IBLC) is drawn into the sample loop followed by 2 µL of sample and then a further 1.1 µL of OPA/IBLC solution. In between each transition the outside of the needle was washed by insertion into a water vial, to reduce cross-contamination of the OPA/IBLC and sample vials. The resulting solution was mixed 13 times within the needle seat (approximately 5 min) prior to injection onto the column. Amino acids with no primary amino acid group, such as Pro, are not derivatised with OPA/IBLC so are not observed using this method. A discussion on why derivatisation is required is included in Section 8.1.2.

The OPA/IBLC derivatising solution consists of 260 mM IBLC and 170 mM OPA in 1 M potassium borate buffer, adjusted to pH 10.4 with potassium hydroxide pellets. OPA/IBLC solution is stable at room temperature for 3 days (Kaufman and Manley, 1998), after which time the sensitivity of the method is reduced (Kaufman and Manley, 1998). Therefore, 100 µL aliquots (enough solution to run a sequence continuously for 3 days), were stored in HPLC auto-sampler vials at – 4 °C and defrosted immediately prior to use. OPA/IBLC solution remaining at room temperature for > 3 days was discarded.

Volumetric flasks and Duran bottles used in the preparation and storage of the OPA/IBLC solutions were sterilized by washing with concentrated nitric acid.

Chromatograms were usually integrated using the automated ChemStation software. However, on occasion peaks were manually integrated when it appeared the software's integration was inappropriate. Analyte concentrations were quantified relative to the area of the internal standard, L-hArg. Areas were also corrected for different fluorescence factors; generally D-amino acids fluoresce ~ 10 % more than the corresponding L-amino acid (Brückner *et al.*, 1991; Kaufman and Manley, 1998; Sec. 8.4.2.3.). Correction factors used in this thesis (except in Chapter 8) were those stated in Penkman, 2005.

Procedural blanks were included at every step of the sample preparation to account for background contamination; amino acid concentrations were low (typically < 50 pmol / mg) and so no corrections were made to account for these.

An external standard solution was run every 10 samples, and was used both as an assessment that the method was working, and to aid in sample peak identification due to slight shifts in retention times. A typical standard solution is presented below (Fig. 2.2).

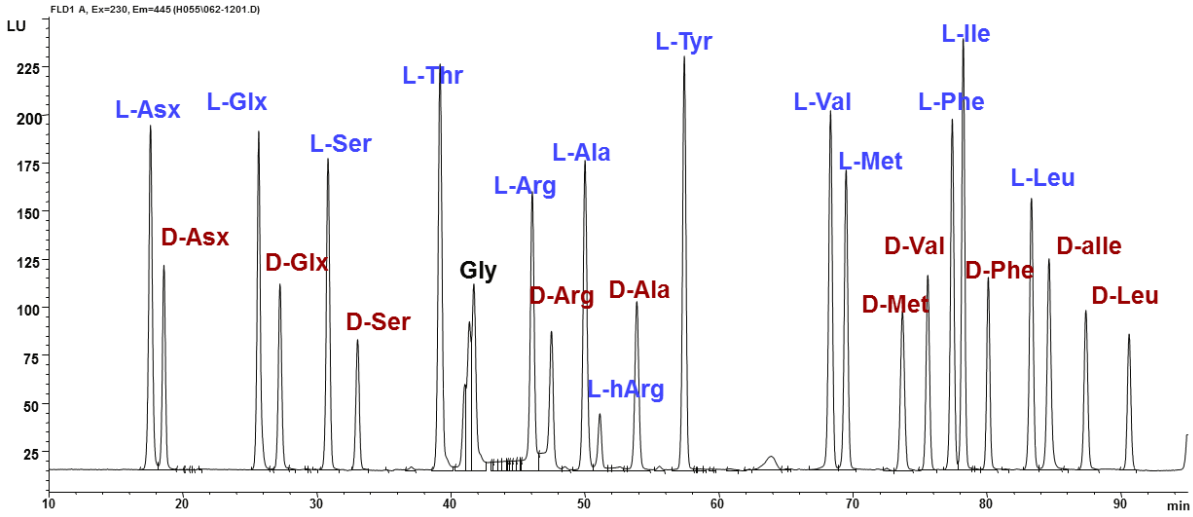

Figure 2.2: Typical HPLC chromatogram of an external standard solution

CHAPTER 3: AMINO ACID PREPARATION DEVELOPMENT AND THE ISOLATION OF THE INTRA-CRYSTALLINE FRACTION

3.1. INTRODUCTION

This study aimed to investigate the presence and closed system behaviour of the intra-crystalline fraction in OES. This was done by first optimising the preparative protocols (Sec .3.1.1.) and then by a series of heating experiments, to test the closed system behaviour of OES (Sec. 3.1.2.).

3.1.1. Optimisation of preparative protocols

3.1.1.1. The hydrolysis protocol

The HPLC method requires amino acids to be in the free form, and not bound (Sec. 2.3.2.). Therefore, the method of hydrolysis of THAA samples was tested to assess whether the maximum concentrations of amino acids were liberated from the OES.

The routine hydrolysis method used in the York AAR laboratories uses 24 h heating at 110 °C (Penkman, 2005). Penkman found that although heating for 24 h does induce some racemization, it is required to liberate the maximum concentration of amino acids, in particular the hydrophobic amino acids (Penkman, 2005).

OES is known to contain higher concentrations of amino acids than molluscan shells (Brooks *et al.*, 1990), for which the routine hydrolysis method was developed (Penkman, 2005). Therefore, shorter hydrolysis times and lower temperatures were not considered. The routine hydrolysis method used in York AAR labs was chosen as a benchmark to compare against longer hydrolysis times, and increased acid volumes (Sec. 3.2.1.).

3.1.1.2. The oxidative treatment protocol

NaOCl (bleach) is expected to oxidise exposed amino acids (i.e. inter-crystalline and exogenous proteins), rendering them unavailable for analysis (e.g. Sykes *et al.*, 1995; Penkman *et al.*, 2008). Previous AAR studies using OES, conducted outside of the York AAR laboratories, have not used an oxidative preparative step (e.g. Brooks *et al.*, 1990; 1991; Miller *et al.*, 1991; 1999). In the light of results from studies using mollusc shells, which showed that oxidative treatment reduces the

variability of AAR data (Sykes *et al.*, 1995; Penkman *et al.*, 2007, 2008), it is important to test whether this observation is also true for OES. A range of oxidative treatments were therefore performed in order to investigate the presence of a stable fraction of intra-crystalline proteins in OES, and optimise this pre-treatment protocol. Powdered OES was exposed to bleach for increasing times and the effect of the oxidative pre-treatment was quantified by monitoring both D/L values and concentrations for several amino acids over time.

3.1.2. Assessment of closed system behaviour

Following optimisation of the oxidative and hydrolytic protocols, the closed system behaviour of the amino acid fraction isolated with oxidative treatment was tested through a series of leaching and heating experiments, summarised in Figure 3.1 and outlined below.

a. Leaching

Many previous AAR studies have performed kinetic experiments in damp sand (e.g. Hare, 1969; Brooks *et al.*, 1990). However, in order to assess the closed system behaviour of a bio-mineral, all of the amino acids within the system need to be accounted for. Therefore, more recent studies designed to assess the closed system behaviour of bio-minerals have used water instead of sand (Brooks *et al.*, 1990; Penkman *et al.*, 2008). By analysing the amino acid concentration in the supernatant water, concentration decreases in the THAA fractions may be accounted for by leaching, if the system is not closed (Penkman *et al.*, 2008). Modern OES samples were therefore heated isothermally in sealed glass vials containing water, in order to simulate diagenesis operating over longer time scales and at lower temperatures.

b. Whole-shell vs. pre-heat vs. post-heat oxidative treatment

The simulated diagenetic trends of both whole-shell and intra-crystalline amino acid fractions of modern OES were compared in order to assess the applicability of using the intra-crystalline fraction or the whole-shell amino acid cohort for further kinetic analysis (see Chapter 4). It was hypothesised that pre-heat and post-heat oxidative treatments would isolate the same fractions of amino acids, therefore this was tested for both 140 °C and 80 °C heated OES (Sec. 3.3.6).

c. The effect of pH

It is expected that open-system proteins undergoing diagenesis in an alkaline burial environment may display a higher rate of racemization (Neuberger, 1948; Hill, 1965; Liardon and Ledermann, 1986). Indeed, elevated pH has been shown to affect the rate of AAR in some bio-minerals (e.g. Bright and Kaufman, 2011b; Orem and Kaufman, 2011). The pH of natural waters are typically in the range of pH 4 – 10 (Eby, 2004), and the environmental pH conditions for geological samples

are very difficult to predict (Davis, 1978; Oviatt, 1989; Dlamini and Hayne, 2004). Differences in pH are likely to increase uncertainties in age estimations when using an open system.

Two recent studies on whole-shell proteins from the lacustrine ostracods *Candona* (*Cypridoidea*) and *Limnocythere* (*Cytheroidea*) (Bright and Kaufman, 2011b) and the bivalve mollusc *Margaritifera falcata* (Orem and Kaufman, 2011), showed that both the rate of amino acid racemization and the extent of amino acid leaching were increased when the samples were heated in conditions of pH > 9. Orem and Kaufman (2011) suggested that this may be due to the physical degradation of the shell structure at higher pH, allowing exposure of a secondary (and possibly more resistant) fraction of amino acids. Interestingly, a sub-study on the intra-crystalline proteins from *M. falcata* showed that the effect of increased pH was magnified when the intra-crystalline amino acids were isolated by oxidative treatment after having been heated (Orem and Kaufman, 2011). This suggests that the intra-crystalline proteins in *M. falcata* are subject to accelerated AAR at high pH, providing evidence that the intra-crystalline proteins in this bio-mineral may not represent a true closed system under the conditions used (Orem and Kaufman, 2011). It is therefore important to test this observation in other bio-minerals, including OES.

The trends in degradation of the intra-crystalline fractions were therefore compared with a pilot study of modern OES heated in mildly basic (pH 9) and mildly acidic (pH 5) conditions, to test whether the degradation of the proteins isolated with oxidative treatment within OES are affected by the external pH conditions.

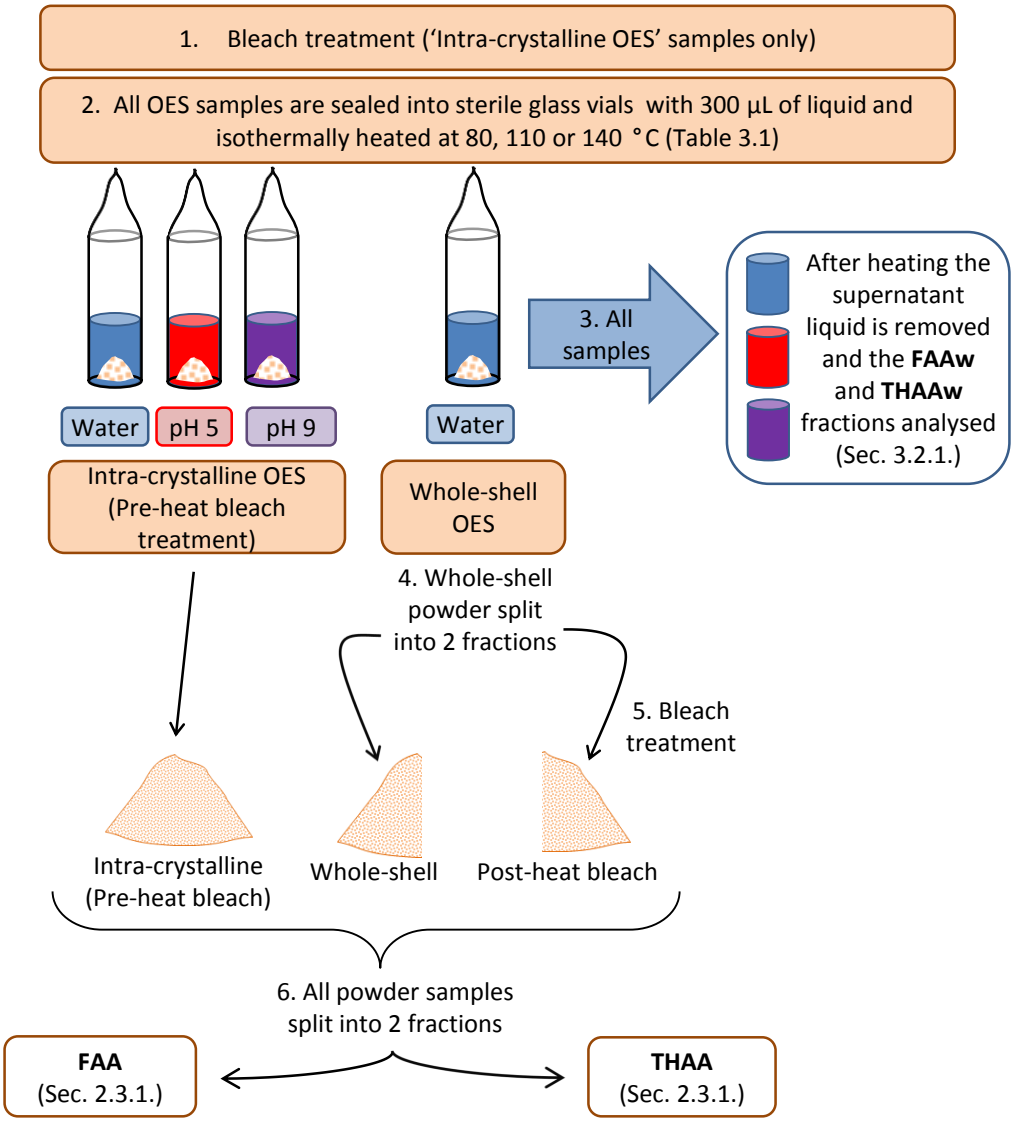

Figure 3.1: Experimental summary for high temperature studies in Chapter 3; FAAw = free amino acid concentration in the supernatant water; THAAw = total hydrolysable amino acid concentration in the supernatant water.

3.2. MATERIALS AND METHODS

3.2.1. Optimisation of hydrolysis method

The routine method of hydrolysis used in the laboratory was compared with four alternative methods which used increased volumes of acid and/or heating times (listed below). The treatment temperature was not increased, so as to keep temperature induced racemization and amino acid degradation at a minimum. Each method was tested in triplicate using modern OES which had been washed with HPLC-grade water and powdered with an agate pestle and mortar, sieved to ensure all particles were < 500 µm and bleach treated for 48 h. This experiment was done prior to the optimisation of the oxidation methodology; therefore samples were treated for

48 h, which is the routine oxidation time for other bio-minerals (e.g. Sykes *et al.*, 1995; Penkman *et al.*, 2007). The hydrolysis methods are outlined below:

"Routine" Method:	20 µL of 7 M HCl per mg of OES, heated at 110 ^{o}C for 24 hours
"30 µL":	30 µL of 7 M HCl per mg of OES, heated at 110 ^{o}C for 24 hours
"40 µL":	40 µL of 7 M HCl per mg of OES, heated at 110 ^{o}C for 24 hours
"48 h":	20 µL of 7 M HCl per mg of OES, heated at 110 ^{o}C for 48 hours
"72 h":	20 µL of 7 M HCl per mg of OES, heated at 110 ^{o}C for 72 hours

3.2.2. Optimisation of oxidation method

The OES was powdered with an agate pestle and mortar and separated by sieving into 4 particle sizes: fine grain (< 100 µm); medium grain (100 µm - 500 µm); coarse grain (500 µm - 1000 µm); and fragments (~1 mm). The different particle sizes were analysed to assess whether surface area affected the effect of the bleach. Samples were submerged in 50 µL of 12% (w/v) NaOCl per mg of OES for 0, 18, 24, 48, 72, 120 and 240 h. Samples were agitated every 24 h to ensure all OES was exposed to the bleach. The bleach was removed by pipette and spotted onto coloured tissue paper to test if the bleach was still active. In all cases the bleach removed was found to still active. The OES was washed five times in HPLC-grade water, with a sixth wash with HPLC-grade methanol to reduce any leftover bleach, before air-drying overnight. The majority of fine and medium size grain samples were prepared in triplicate, the majority of coarse grain and fragment-sized samples were prepared singly.

3.2.3. High temperature studies

Approximately 8 – 10 mg of cleaned, powdered and 72 h bleached OES (as per Sec. 2.1.2.) was weighed and sealed in sterile glass ampoules with 300 µL of HPLC-grade water. Each sample was heated isothermally at 80 °C for up to 6000 h, 110 °C for up to 1200 h or 140 °C for up to 240 h (Table 3.1). The majority of the time points were prepared in triplicate to assess variability during the heating experiment.

After heating, the supernatant water was removed and split into three aliquots (100 µL each). One fraction was analysed for free amino acids in the water (FAAw) and one fraction for the total hydrolysable amino acids in the water (THAAw). The third fraction was stored at -20 °C for future analysis. Both the stored and FAAw samples were placed in eppendorfs, the THAAw samples were stored in sterile 3 mL glass vials.

FAAw samples were dried in a centrifugal evaporator. For HPLC analysis the samples were hydrated in 10 µL of rehydration fluid (Sec. 2.2.1.) per 1/3 of the original mass of OES used.

THAAw samples were hydrolysed by addition of 6 M HCl (20 µL per 1/3 mg of OES) and heated at 100 °C for 24 hours. Prior to heating, the vials were purged for 10 s with N_2, and after 10 min of heating the vial lids were tightened to prevent evaporation of the acid. The acid was removed by centrifugal evaporation. For HPLC analyses, the THAAw samples were rehydrated in 20 µL of rehydration fluid per 1/3 mg of OES. The powder was air-dried overnight, prior to being split into two fractions for FAA and THAA analyses (Sec. 2.3.1.).

The sample preparation and HPLC analyses of the 140 °C heating experiment using bleached OES in water were done by Emily Pilgrim, as part of an undergraduate summer placement.

Several of the 80 °C and 140 °C kinetic experiments were repeated using whole-shell (i.e. unbleached) OES (Table 3.1). Post heating, a sub-set of the whole-shell OES powders were split into two fractions; one fraction was analysed for whole-shell proteins, the second was bleach treated for 72 h (post-heat bleach), prior to amino acid analysis. In addition, the 140 ºC experiment was repeated using 48 h bleached OES. The majority of whole-shell and 48 h bleached samples were run in triplicate, and the post-heat bleached samples were run in duplicate.

A subset of the 80 °C, 110 °C and 140 °C heating experiments were performed as part of an undergraduate project, where sample preparation and HPLC analyses were done by Michael Morgan Williams. The study used washed and powdered OES which had 72 h oxidative pre-treatment (as per Sec. 2.1.2.). OES was submerged in buffered solutions of pH 5 and pH 9 (Table 3. 1). The pH 5 buffer was prepared using sodium acetate trihydrate and acetic acid in HPLC-grade water. The pH 9 buffer was a liquid tetra-borate buffer purchased from Fisher Chemicals (Cat. No. J/2870/15). The pH of the buffer solutions were determined to be 4.96 and 9.20 at room temperature. The majority of the time points were prepared in duplicate. Due to time constraints, the supernatant from all time points of the pH buffered solutions were not analysed.

Temp. (°C)	Samples	Solution	Heating time (h)										
80	Intra-crystalline proteins	Water, pH 5, pH 9	0	24	97	121	480	720	960	1440	2160*	4028 *	5879*
110		Water, pH 5, pH 9	0	24	120	240	384	480	720*	840*	960*	1200 *	
140		Water, pH 5, pH 9	0	1	2	4	6	8*	24	72	96	120	240*
80	Whole shell proteins	Water					480[#]		960[#]		2160[#]		
140		Water	0	1	2[#]	4[#]	6	8	24	72	96	120	240

*Table 3.1: Heating experiments using modern ostrich eggshell; each time point was performed in triplicate (if in water) and duplicate (if pH buffered solutions). * = time point only applicable to eggshell heated in water; [#] = powder samples split into fractions post-heating, and analysed for whole-shell proteins and 'intra-crystalline' proteins*

3.3.1. Optimisation of hydrolysis method

Lower concentrations of some amino acids, most significantly Ser and Gly, were observed for samples hydrolysed for longer than the routine 24 h (Fig 3.2A). The decreased concentration of Ser is presumably due to thermal degradation (Vallentyne, 1964). It is unclear why Gly, a relatively thermally stable amino acid (Abelson, 1954; Vallentyne, 1964), should show a decreased concentration with increased heating time. A possible reason could be the poor resolution of Gly from contaminant peaks in the HPLC method.

Increased heating time also caused a significant increase in the degree of racemization for Asx, Glx, Ala, Val and Phe compared to observed D/L values for samples prepared using the routine method (Fig. 3.2B). This is in broad agreement with Frank *et al.* (1981) who found that the rate of amino acid racemization was accelerated under acidic conditions in the following order: Asp > Glu > Phe > Ala > Val > Ile > Ser; racemization is enhanced where the electronic effects of the side chain stabilise the enolized intermediate (Fig. 1.7; Sec. 1.2.1.1.). These data suggest that an increased hydrolysis time is detrimental.

Increasing the volume of acid did not affect the observed concentrations of amino acids (Fig. 3.2A). However, the increased volume of acid did show a small increase in the observed error of the degree of Ile epimerization (Fig. 3.2B).

The amino acid concentrations and D/L values from the routine method were compared to the alternative methods using a two-tailed student t-test, assuming equal variance in the data sets. The results showed that there was no significant difference between the routine and the 30 µL and 40 µL methods for any of the amino acid concentrations or D/L values, to a 95% confidence level. In contrast, the 48 h and 72 h methods both showed significantly lower Ser and Gly concentrations and higher D/L values for all amino acids, compared to the routine method. However, these statistical tests were performed using small data sets, so should be treated with a degree of caution (routine method had 6 samples; alternative methods had 3 samples each). Nevertheless, it appears that the routine method of hydrolysis, 20 µL of 7 M HCl per mg of OES, heated at 110 ^{o}C for 24 h, appears to show the highest concentrations with the least induced racemization. Therefore, all future samples analysed in this project were prepared using this method.

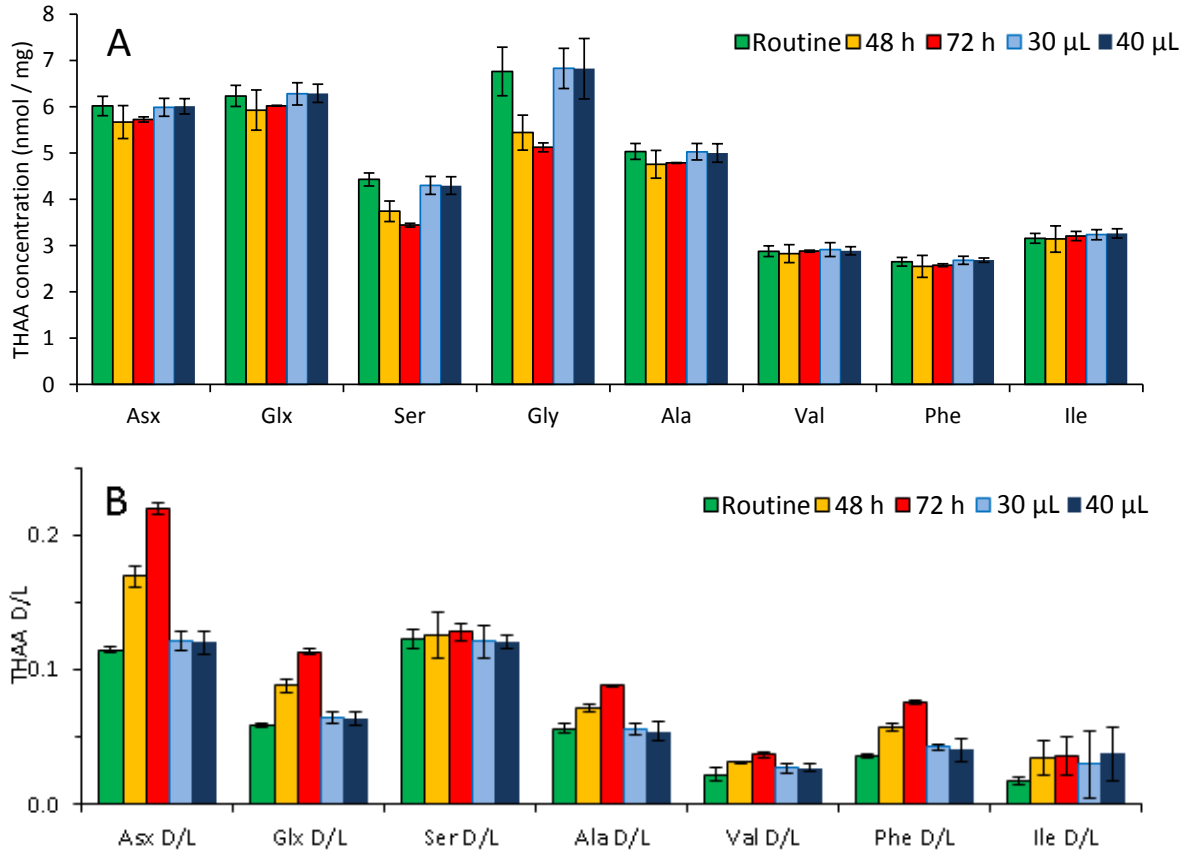

Figure 3.2: THAA concentration (A) and degree of racemization (B) observed for modern OES samples (48 h bleached) prepared using different hydrolysis methods. Error bars indicate 2 x standard deviations based on triplicate samples

3.3.2. Optimisation of oxidative pre-treatment

Bleach (NaOCl) in aqueous solution dissociates to form a weak acid, hypochlorous acid (HOCl), which has the potential to induce racemization in amino acids by aiding proton abstraction (Neuberger, 1948). In a functionally closed system, proteins should be protected from both the hypochlorous acid and NaOCl, so a plateau should be reached for both D/L values and amino acid concentrations following oxidation of the inter-crystalline proteins. Prolonged bleaching of bio-minerals may allow the hypochlorous acid to partially dissolve the calcite, resulting in a further drop in concentration and an increase in the extent of racemization (Penkman *et al.*, 2008).

In the initial stages of oxidative treatment, i.e. between 0 – 72 h, the THAA concentrations of Asx, Glx, Val, Phe, Ile, Ser, Gly and Ala decrease by as much as ~50 % (e.g. Asx in Fig. 3.3A); it is assumed that the amino acids removed represent the inter-crystalline proteins. A stable plateau appears to be reached by 72 h (Fig. 3.3A). Oxidative treatment also reduces THAA concentration variability (Fig. 3.3A).

By 240 h the sum of the THAA concentrations (Asx, Glx, Ser, Ala, Gly, Val, Phe and Ile) reach the same concentration for all of the particle sizes. This suggests that pulverising the OES does not expose additional amino acids to the bleach.

The THAA D/L values of Asx, Glx, Ser, Val, Phe, Ala and Ile (A/I) increase with bleaching time, up to ~72 h (e.g. Asx in Fig. 3.3B). The initial increase of D/L values is probably a consequence of the bleach decomposing the less-racemized inter-crystalline fraction (Sykes *et al.*, 1995; Penkman *et al.*, 2008). The FAA tend to show higher D/L values than the THAA, even though the rate of racemization of free amino acids is slower, presumably because just prior to liberation many residues would have been in terminal positions where racemization is enhanced (see Mitterer and Kriausakul 1984; Liardon and Lederman, 1986; Goodfriend and Meyer, 1991). The inter-crystalline FAA fraction may readily leach from open-system bio-minerals (e.g. Roof *et al.*, 1997; Collins and Riley, 2000), so in general the inter-crystalline fraction has been found to be less racemized than the intra-crystalline fraction (Sykes *et al.*, 1995; Penkman *et al.*, 2008; Demarchi *et al.*, 2013a).

Between 72 h and 480 h the THAA D/L values increase at a far slower rate (Fig. 3.3B; D/L values typically increase by 0.01 – 0.02). The fragment samples take longer than the powder samples to reach the same D/L values and THAA concentrations (Fig. 3.3), presumably due to the reduced surface area to volume ratio restricting the penetration of the bleach.

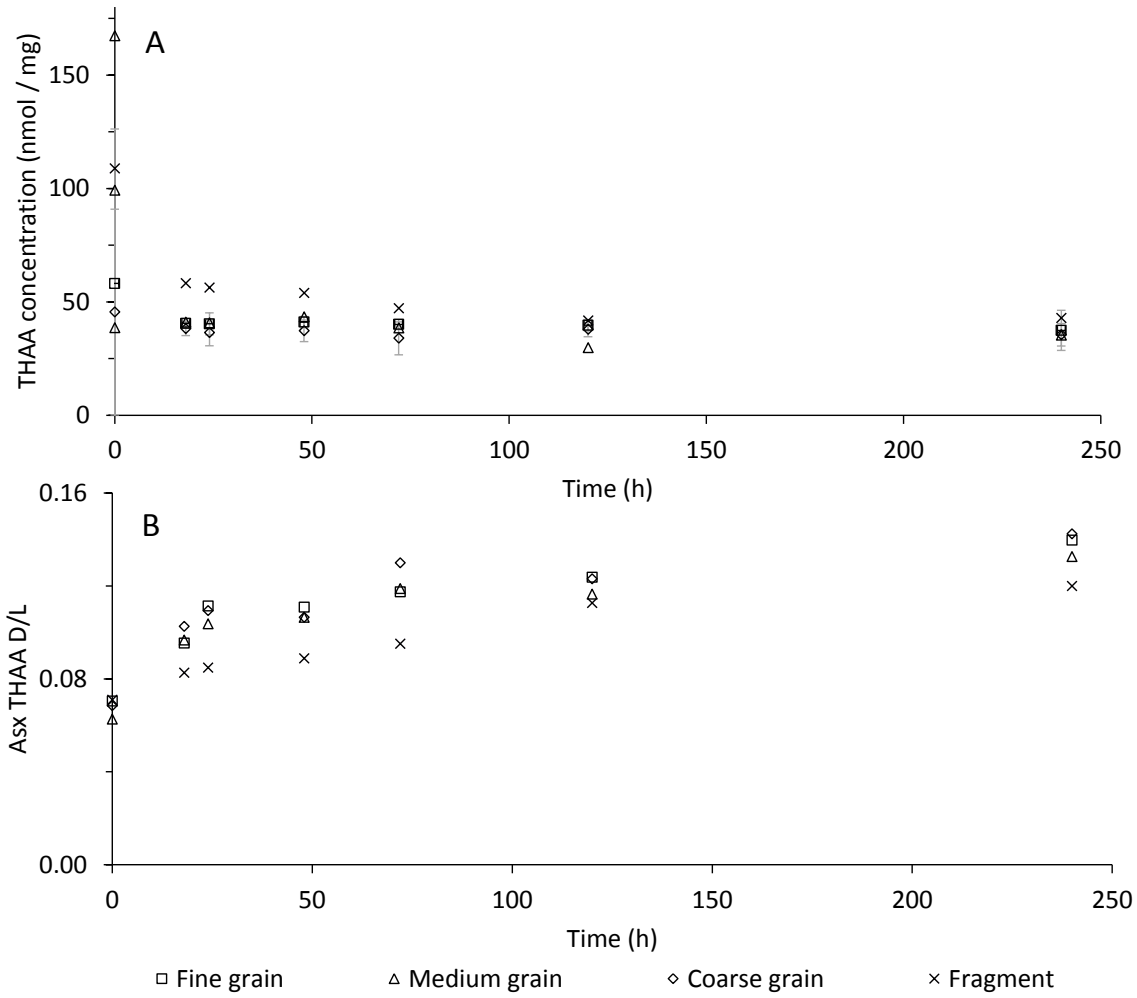

Figure 3.3: Effect of oxidative treatment on the THAA in OES with increased bleach treatment time. A: Sum THAA concentration of Asx, Glx, Ser, Gly, Ala, Val, Phe, Ile; B: Extent of racemization of Asx. (For other amino acids see Appendix A). Error bars for fine and medium sized particles represent 2 x standard deviation based on triplicate samples.

With prolonged bleaching the amino acid concentrations reach a stable plateau. However, whilst the amino acid concentrations remain constant, the THAA D/L values show a small increase (Δ D/L < 0.05 between 72 – 240 h; Fig. 3.3). The same observation was made with some bleach-treated molluscan taxa (Penkman *et al.*, 2008), and could be due to the bleach etching at the carbonate structure, exposing intra-crystalline amino acids to the bleach, and thus inducing racemization, without significantly decreasing the concentrations. An alternative explanation could be the presence of bleach-resistant organic material, which may take longer to oxidise. A slow decrease in concentration with increasing bleaching time observed in ostracods has been attributed to the high concentration of chemically resilient chitin (Bright and Kaufman, 2011a). While eggshell does not contain high concentrations of chitin (Baker and Balch, 1962), other organic matter may provide protection to the amino acids, making it unclear whether the 'intra-crystalline' proteins

are trapped inside crystals or just resistant to oxidative treatment. Although the induced racemization appears to be negligible, it still shows the importance of standardising the oxidative pre-treatment so that the data are comparable.

A stable fraction of amino acids which Is resistant to strong oxidative treatment can be isolated from OES powders of < 1000 µm within 72 h oxidative treatment, but 120 h exposure to bleach is required for OES > 1000 µm (so-called 'fragment' samples). This is demonstrated by the concentration plateau reached with oxidative treatment of 72 h (Fig. 3.3). The 'stable' fraction is operationally defined as the 'intra-crystalline' fraction (Sykes *et al.*, 1995; Sec. 1.2.3.).

The coarse grain (500 – 1000 µm) FAA samples were more time consuming to demineralise, probably due to the reduced surface area to volume ratio, so it was decided not to use powdered particles > 500 µm in size in further experiments.

OES is therefore more resistant to oxidative treatment than certain species of mollusc shells (Penkman *et al.*, 2008; Demarchi *et al.*, 2013a), which require 48 h oxidative treatment to isolate the intra-crystalline proteins.

3.3.3. Comparison of intra-crystalline and whole-shell amino acid compositions

The amino acid composition of the intra-crystalline proteins and the whole-shell proteins in OES are very similar (Fig. 3.4), suggesting that the proteins making up the inter- and intra-crystalline fractions are the same. Mann and Siedler (2004) sequenced the main proteins within OES: struthiocalcin-1 (SCA-1) and struthiocalcin-2 (SCA-2), and found that they are present in OES at a ~ 7:3 molar abundance. The observed composition of amino acids is very similar to the theoretical composition calculated from the sequences of SCA-1 and SCA-2 (Fig. 3.4). The observed concentrations of the more unstable amino acids, e.g. Ser and Arg (Vallentyne, 1964), are slightly lower than the theoretical composition (Fig. 3.4C); it is plausible that the acid hydrolysis procedure causes some degradation (c.f. Hill, 1965; Akiyama, 1980).

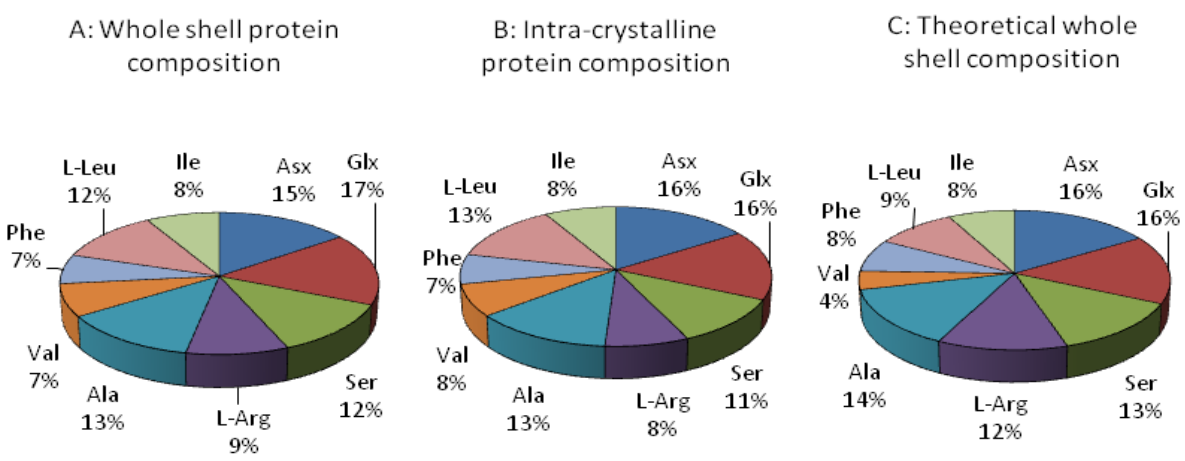

Figure 3.4: THAA composition of OES in: (A) the intra-crystalline proteins, (B) the whole shell proteins and (C) theoretical whole shell composition of OES based on compositions of SCA-1 and SCA-2 at a ratio of 7:3 (Mann and Siedler, 2004). Amino acids not quantified in this study and amino acids < 1% have been omitted. Note that the intra-crystalline and whole shell proteins have very similar compositions and likely the same proteins. The observed amino acid composition of OES is very similar to the theoretical composition of SCA.

The similarities in compositions between whole-shell and intra-crystalline proteins in OES contrast with other bio-minerals used for AAR geochronology. For example, Penkman *et al.* (2008) reported differences in whole-shell and intra-crystalline amino acid compositions for the molluscs *Corbicula fluminalis*, *Margaritifera falcata* and *Bithynia tentaculata.* *Margaritifera* and *Bithynia* displayed increased relative concentrations of Asx in the intra-crystalline fractions and decreases in Ala and Gly. This, they hypothesised, was due to the presence of silk-like proteins (characterised by the high concentration of Ala and Gly) in the inter-crystalline fraction, and acidic proteins (Asx and Glx) in the intra-crystalline fraction (e.g. Falini *et al.*, 2003; Marin and Luquet, 2005). *Corbicula* had similar, but not identical, amino acid composition in the whole-shell and intra-crystalline fractions, with a small decrease in Asx in the bleached shells (Penkman *et al.*, 2008). Demarchi *et al.* (2013a) also reported differences in whole-shell and intra-crystalline composition for the marine gastropod *Patella vulgata.* By contrast with *Margaritifera* and *Bithynia*, *Patella* showed a decrease in relative concentration of acidic amino acids in the intra-crystalline fraction. Significant differences in whole-shell and intra-crystalline protein compositions have also been observed in corals (Ingalls *et al.*, 2003).

It has been suggested that acidic amino acids are involved in the binding of Ca^{2+} ion during bio-mineralisation (Marin *et al.*, 2007), so it might be expected that more acidic proteins are formed in the intra-crystalline fraction, but this is clearly not always the case. Although intra-crystalline

studies are limited, OES is currently unique in having very similar whole-shell and intra-crystalline protein compositions, which may be a consequence of different bio-mineralisation processes to mollusc and corals, e.g. the speed at which OES is formed: 1 egg is laid roughly every 2 days (Jarvis *et al.*, 1985).

Miller *et al.* (2000) reported between species compositional differences between the eggshells of *Genyornis newtoni* (extinct Australian large flightless bird) and *Dromaius novaehollandiae* (extant emu). For the latter they also reported differences in compositions for the outer green layer of the shell and the inner white part. OES has three structural calcitic layers, but as our analysis did not discriminate between the compositions of the different layers, it is unknown whether OES also has different protein compositions within the different calcitic layers.

Comparison of the amino acid compositions of the whole-shell and intra-crystalline proteins from OES (this study) and the published composition of the palisade layer of the *Dromaius* eggshell (Miller *et al.*, 2000) show some small differences. This suggests there may be taxonomic differences between these eggshells, reflected by the protein compositions, as has been observed for other ratite shells (Miller *et al.*, 2000), mollusc shells (Lajoie *et al.*, 1980; Penkman *et al.*, 2008; Demarchi *et al.*, 2013a) and other avian eggshells (e.g. Hincke *et al.*, 1995; Mann and Siedler, 1999; Lakshminarayanan *et al.*, 2002, 2003). However, a more comprehensive data set is required to resolve this fully.

3.3.4. Summary of hydrolysis and oxidative treatment method development

A stable intra-crystalline fraction is isolated from within OES powders of < 1000 µm with 72 h oxidative treatment. However, it was decided to limit future experiments to samples < 500 µm, as particles > 500 µm were difficult to demineralise. OES is more resistant to bleach treatment than certain species of mollusc shells, which require 48 h oxidative treatment to isolate the intra-crystalline proteins (Penkman *et al.*, 2008; Demarchi *et al.*, 2013a). Unlike many other bio-minerals routinely used in AAR studies, the intra-crystalline and whole-shell amino acid compositions appear to be similar in OES.

3.3.5. Testing the closed system behaviour of the intra-crystalline proteins

Oxidative treatment for 72 h isolates an intra-crystalline fraction of proteins; if these proteins are resistant to leaching and immune to changes in environmental conditions (such as pH) then they may represent a closed system with regards to protein degradation. To test this hypothesis, unbleached OES, 48 h bleached OES and 72 h bleached OES were heated isothermally in HPLC-grade water at 140°C in sealed glass ampoules, for various times (Sec. 2.2.; Table 3.1). If the

system were open, the concentrations of amino acids in the water would be expected to increase through leaching. 72 h bleached OES was also heated isothermally at 80 °C, 110 °C and 140 °C in pH 5 and pH 9 buffered solutions to test whether the rates of intra-crystalline amino acid racemization are affected by the pH of the environment.

3.3.5.1. Leaching experiment

After 24 h of heating, the whole-shell OES leached ~ 13 % of the original protein; the 48 h bleached sample leached ~0.7 %; and the intra-crystalline sample ~0.5 % (THAAw concentrations, Table 3.2). These levels are comparable to other bio-minerals, e.g. *Bithynia* which loses ~ 1 % with 24 h heating at 140 °C, which is deemed to approximate a closed system (Penkman *et al.*, 2008).

Sample		Amino acid							
		Asx	Glx	Ser	Ala	Val	Phe	Ile	Total
[THAAw] (pmol / mg)	Whole-shell	943 ± 29	1760 ± 51	420 ± 16	1571 ± 50	729 ± 32	654 ± 38	689 ± 37	7919
	48 h bleached	30 ± 6	46 ± 10	22 ± 16	45 ± 6	20 ± 5	15 ± 7	27 ± 4	251
	72 h bleached	20 ± 4	30 ± 6	16 ± 4	39 ± 7	10 ± 2	11 ± 4	16 ± 3	175
%THAAw	Whole-shell	9.4%	16.2%	5.2%	18.3%	15.1%	14.7%	12.8%	13.1%
	48 h bleached	0.5%	0.7%	0.5%	0.9%	0.7%	0.6%	0.8%	0.7%
	72 h bleached	0.4%	0.5%	0.4%	0.8%	0.4%	0.4%	0.5%	0.5%

Table 3.2: THAAw concentrations of modern OES samples heated isothermally at 140 °C for 24 h in water. The errors represent the standard deviation in the concentrations based on triplicate samples.

It is likely that the amino acids which readily leach would also readily be removed by bleach treatment. It was previously speculated that the increase of THAA D/L values with bleaching time was due to the removal of a highly racemized FAA fraction (Sec. 3.3.2.). This was confirmed by comparing the D/L values of the whole-shell FAAw and THAA fractions (e.g. Fig. 3.5), which showed that the D/L values in the FAAw fraction were slightly higher than the THAA fraction.

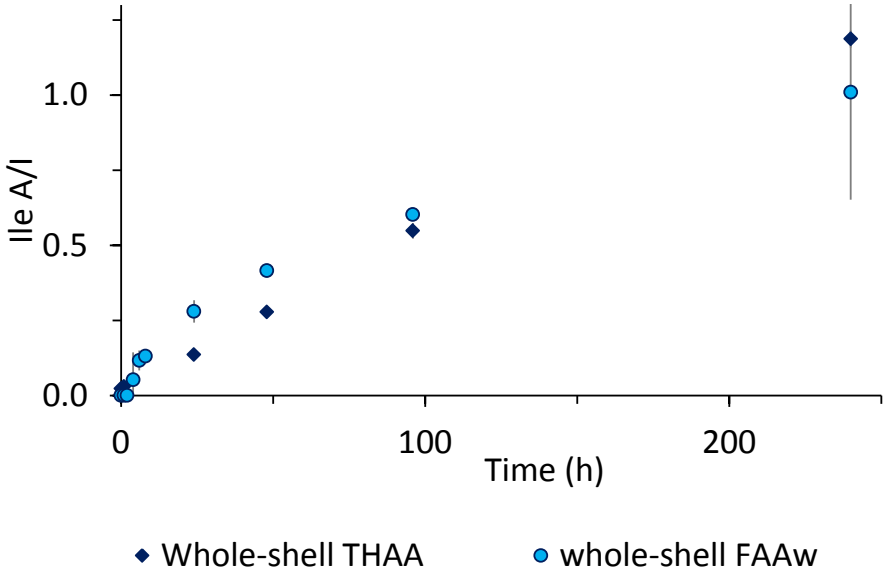

Figure 3.5: A/I values for THAA and FAAw fractions for whole-shell modern OES heated isothermally at 140 °C (for other amino acids, see Appendix A) Error bars indicate 2 x the standard deviation based on triplicate samples.

3.3.5.2. Effect of pH on the degradation of the intra-crystalline amino acids in OES

The extent of racemization and degradation of amino acids in the intra-crystalline fraction of OES was tested at pH 5, 7 and 9 at elevated temperatures, 80 °C, 110 °C and 140 °C. Sample preparation and HPLC analyses of pH 5 and 9 samples were performed by Michael Morgan Williams as part of his undergraduate research project.

There is no discernible change in amino acid concentrations for intra-crystalline samples heated under different pH conditions (e.g. Fig. 3.6 – 3.8). Although the THAA concentrations for samples heated in pH 9 conditions tend to be slightly lower, the difference is not statistically significant.

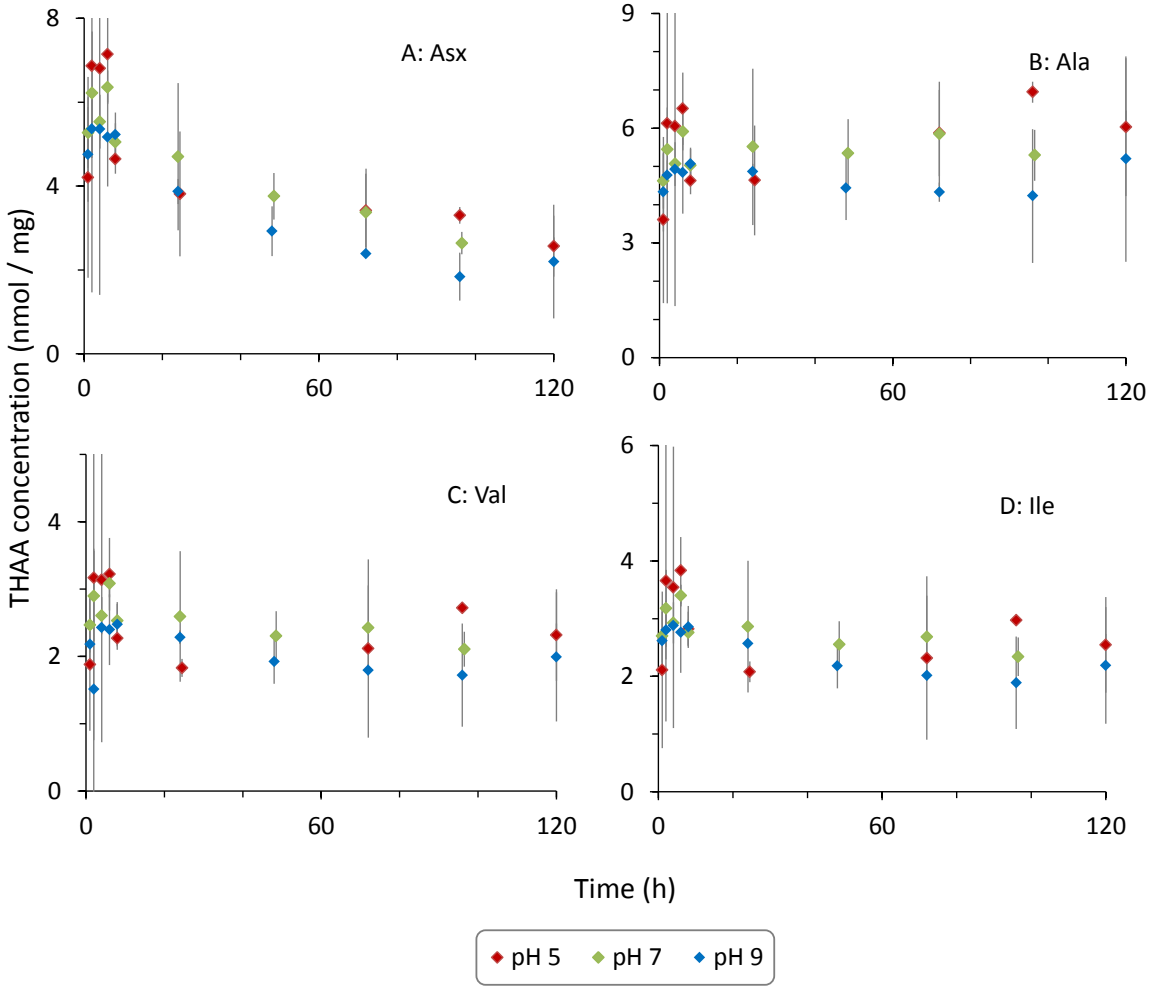

Figure 3.6: Effect on THAA concentrations of intra-crystalline modern OES at pH 5, 7 & 9, heated at 140 °C. A: Asx, B: Ala, C: Val, D: Ile. Error bars represent 2 x the standard deviation about the mean, based on triplicate samples for the majority of samples at pH 7 and duplicate samples at pH 5 & 9.

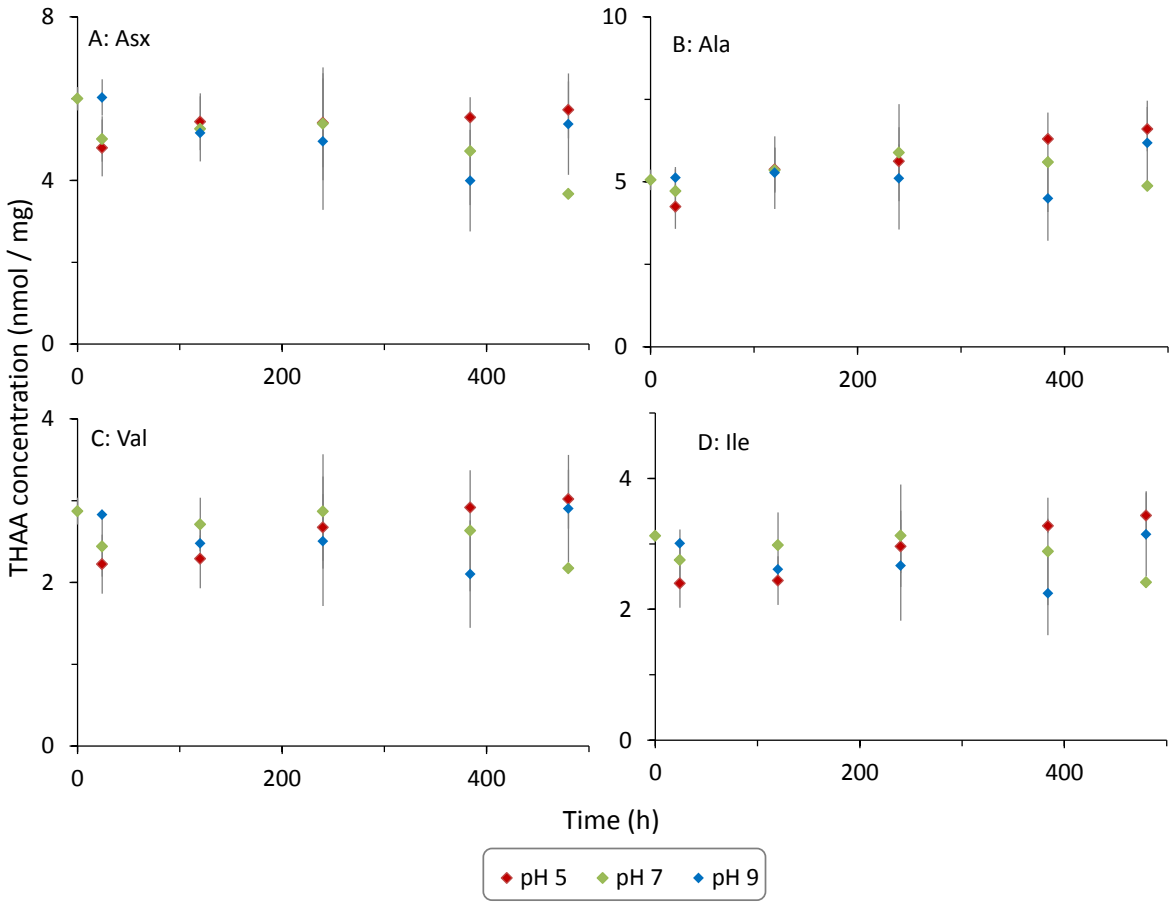

Figure 3.7: Effect on THAA concentrations of intra-crystalline modern OES at pH 5, 7 & 9, heated at 110 °C. A: Asx, B: Ala, C: Val, D: Ile. Error bars represent 2 x the standard deviation about the mean, based on triplicate samples for the majority of samples at pH 7 and duplicate samples at pH 5 & 9.

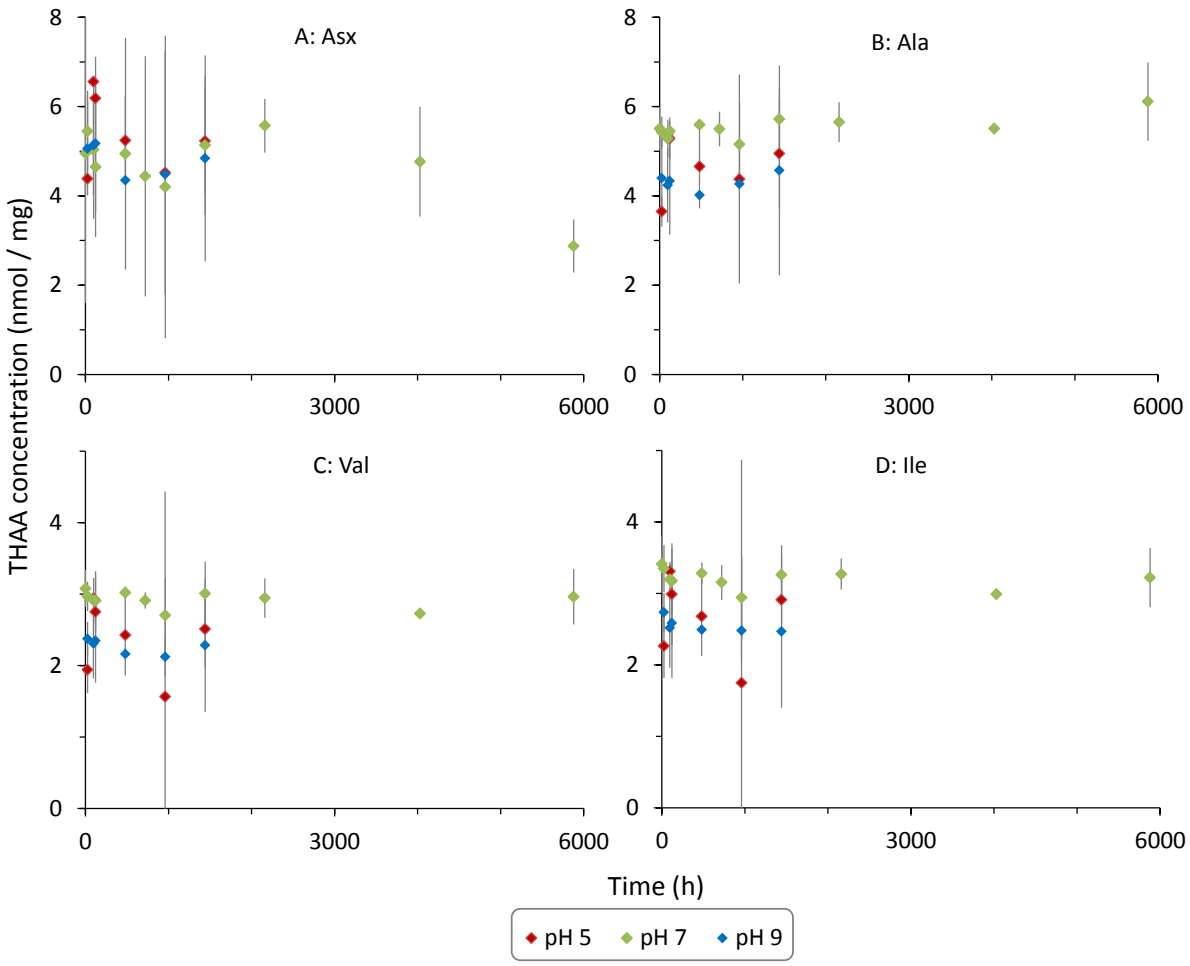

Figure 3.8: Effect on THAA concentrations of intra-crystalline modern OES at pH 5, 7 & 9, heated at 80 °C. A: Asx, B: Ala, C: Val, D: Ile. Error bars represent 2 x the standard deviation about the mean, based on triplicate samples for the majority of samples at pH 7 and duplicate samples at pH 5 & 9.

There was no significant difference in the trends of racemization for intra-crystalline amino acids heated at 140 – 80 °C in solutions of pH 5, 7 or 9 (Fig. 3.9 – 3.11).

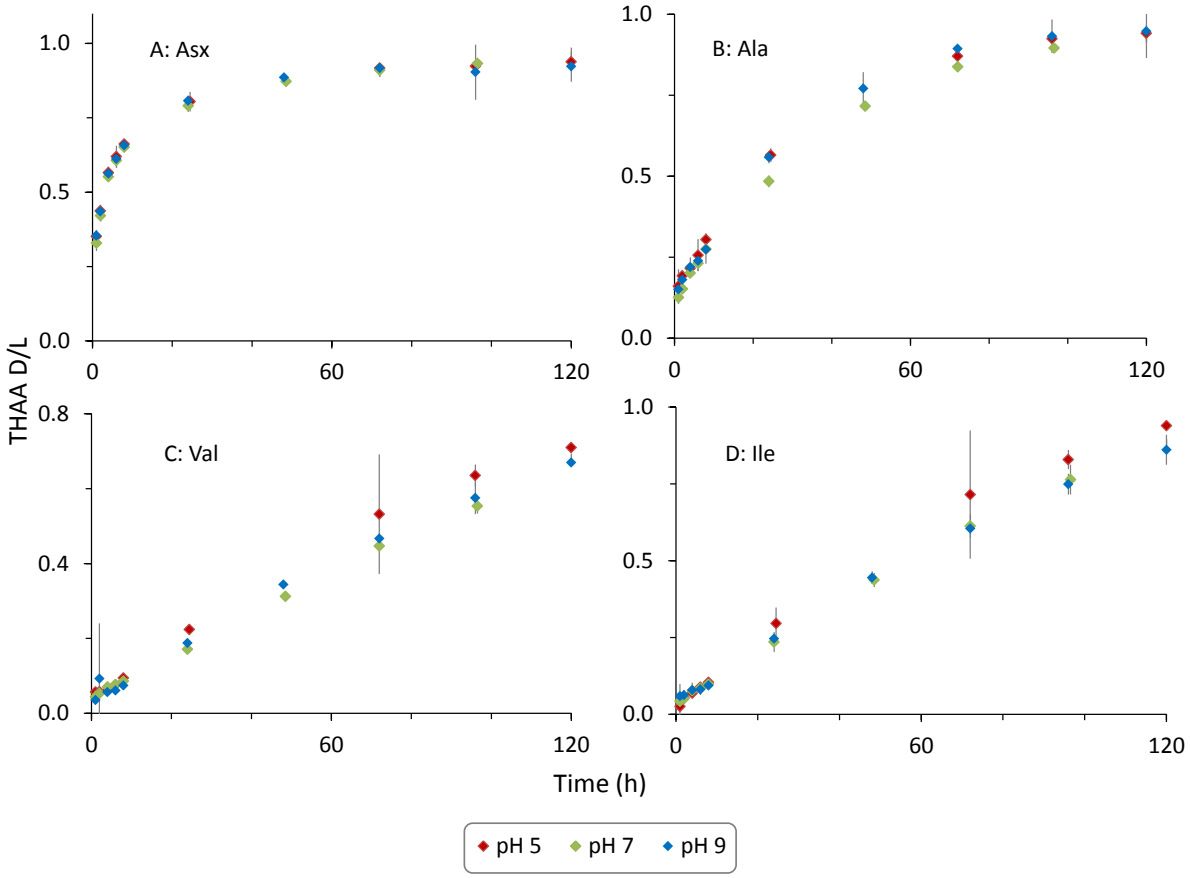

Figure 3.9: Effect on THAA D/L values of intra-crystalline modern OES at pH 5, 7 & 9 heated at 140 °C. A: Asx, B: Ala, C: Val, D: Ile. Error bars represent 2 x the standard deviation about the mean, based on triplicate samples for the majority of samples at pH 7 and duplicate samples at pH 5 & 9.

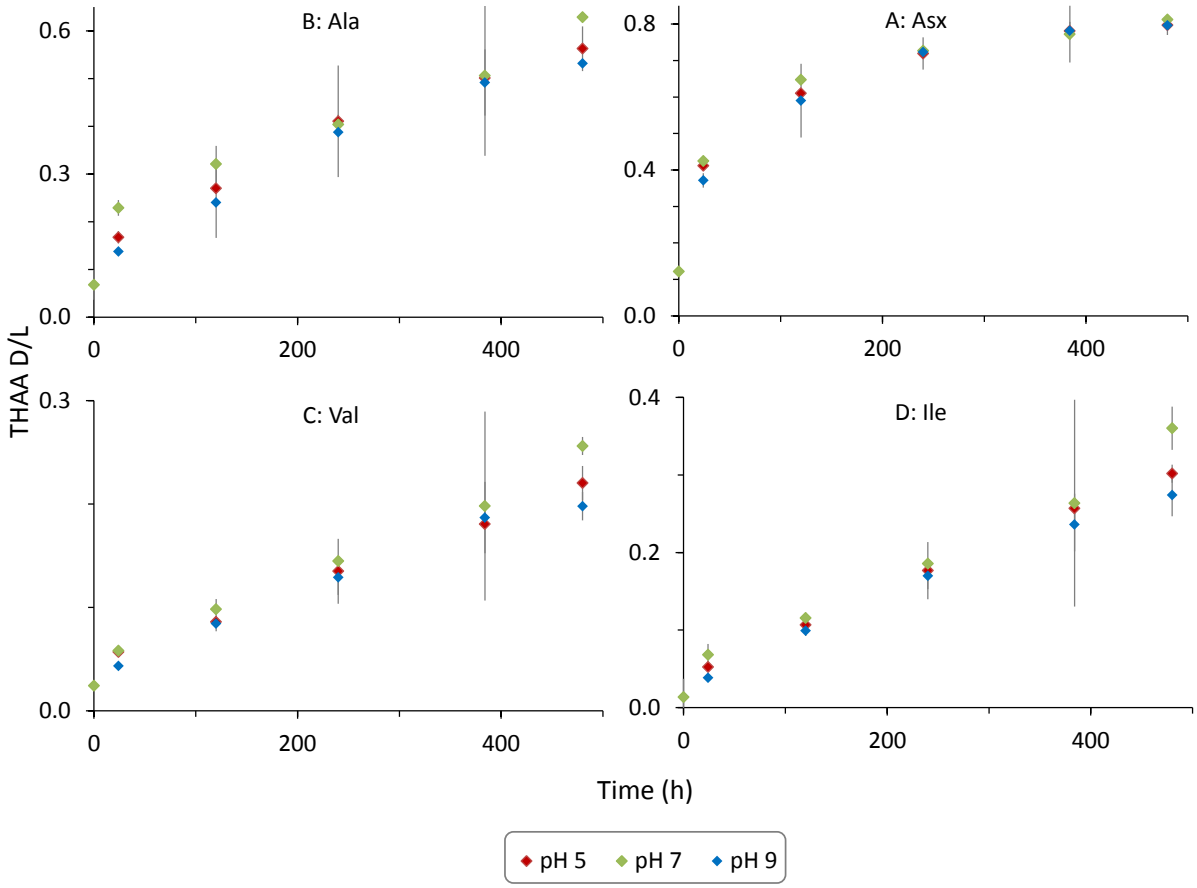

Figure 3.10: Effect on THAA D/L values of intra-crystalline modern OES at pH 5, 7 & 9 heated at 110 °C. A: Asx, B: Ala, C: Val, D: Ile. Error bars represent 2 x the standard deviation about the mean, based on triplicate samples for the majority of samples at pH 7 and duplicate samples at pH 5 & 9.

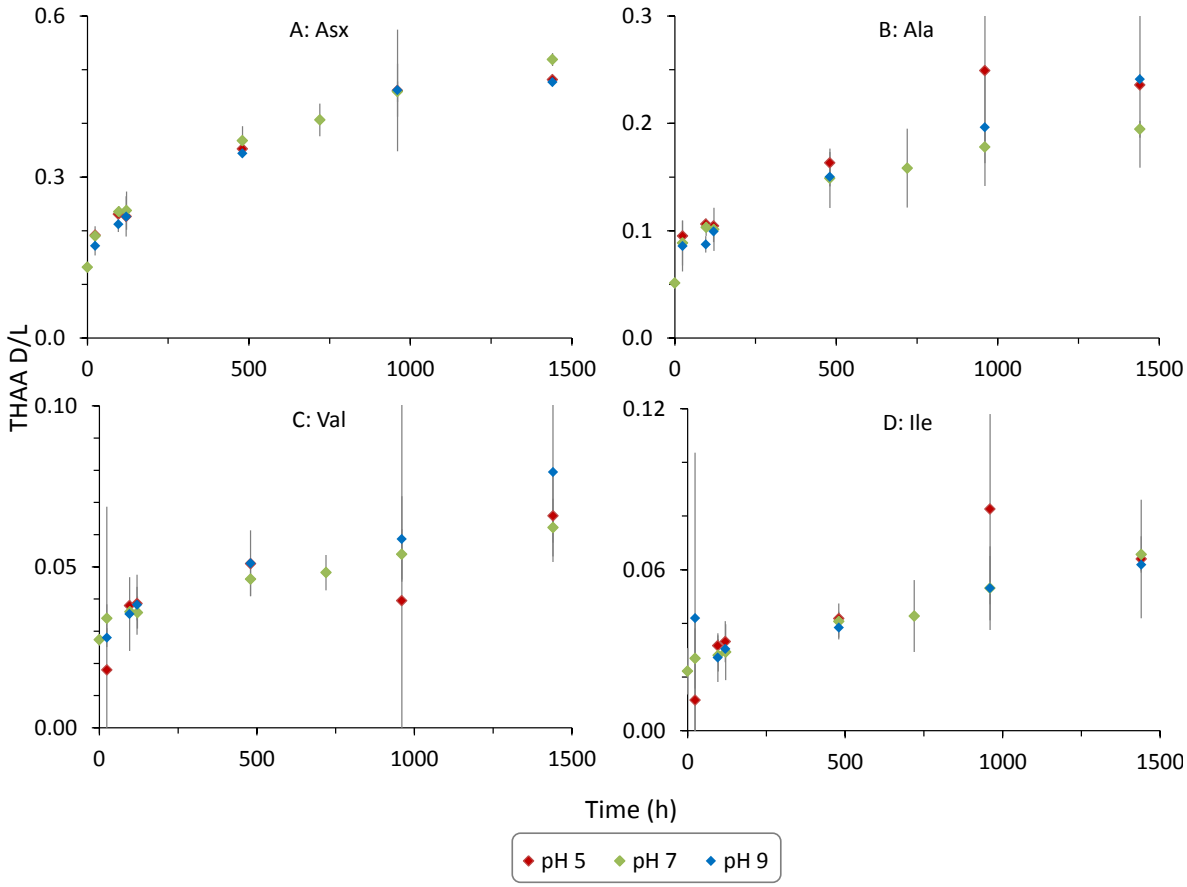

Figure 3.11: Effect on THAA D/L values of intra-crystalline modern OES at pH 5, 7 & 9 heated at 80 °C. A: Asx, B: Ala, C: Val, D: Ile. Error bars represent 2 x the standard deviation about the mean, based on triplicate samples for the majority of samples at pH 7 and duplicate samples at pH 5 & 9.

In a closed system, the FAA D/L and THAA D/L values should be highly correlated; these were therefore compared for samples heated under different pH conditions. The majority of data show no significant difference between FAA and THAA D/L values heated under different pH conditions for all temperatures studied (Fig. 3.12 – 3.14). The 80 °C pH 5 and 9 experiments were not run for very long and so the FAA concentrations remain low and consequently the FAA D/L values show considerable variability. Never-the-less there appears to be no statistical difference in the D/L values for the samples heated at pH 5, 7 or 9.

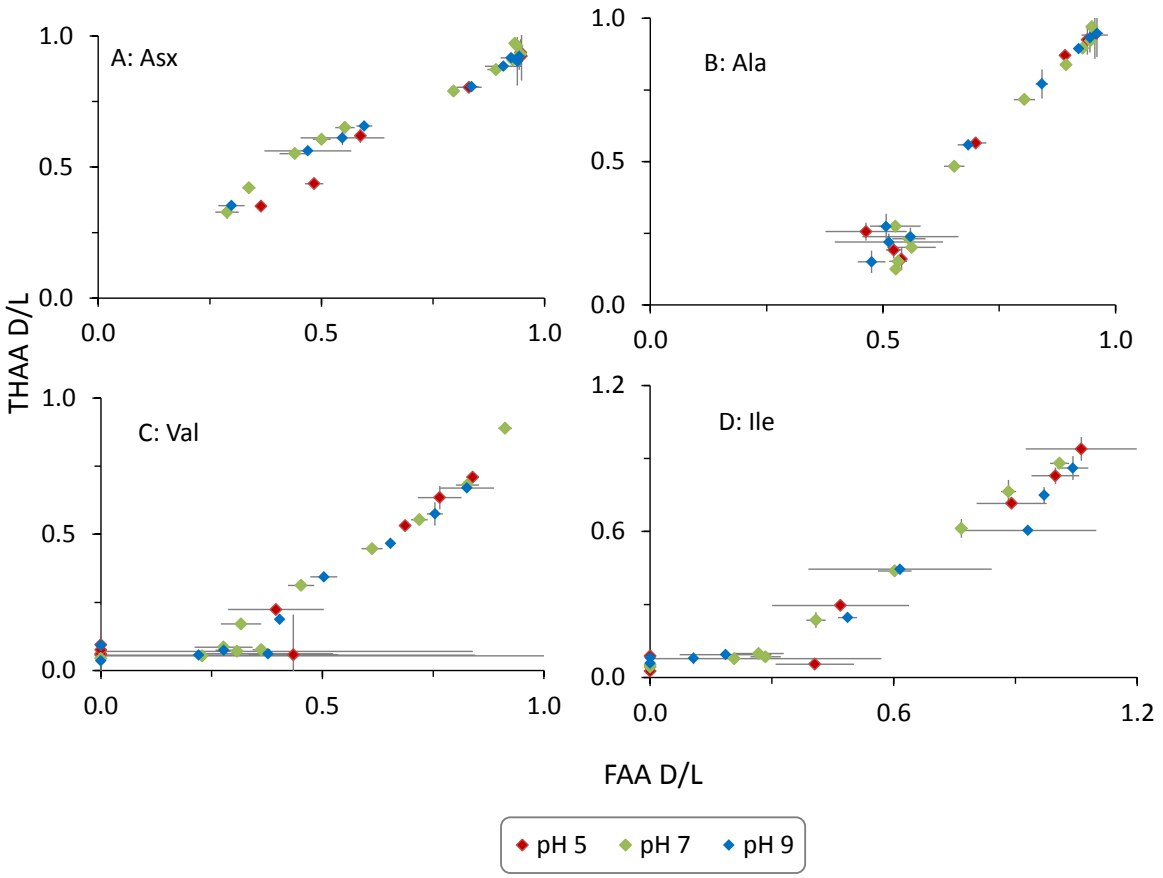

Figure 3.12: FAA D/L vs. THAA D/L values for intra-crystalline modern OES heated at 140 °C, at pH 5, 7 and 9. A: Asx, B: Ala, C: Val, D: Ile. Error bars represent 2 x the standard deviation about the mean, based on triplicate samples for the majority of samples at pH 7 and duplicate samples at pH 5 & 9.

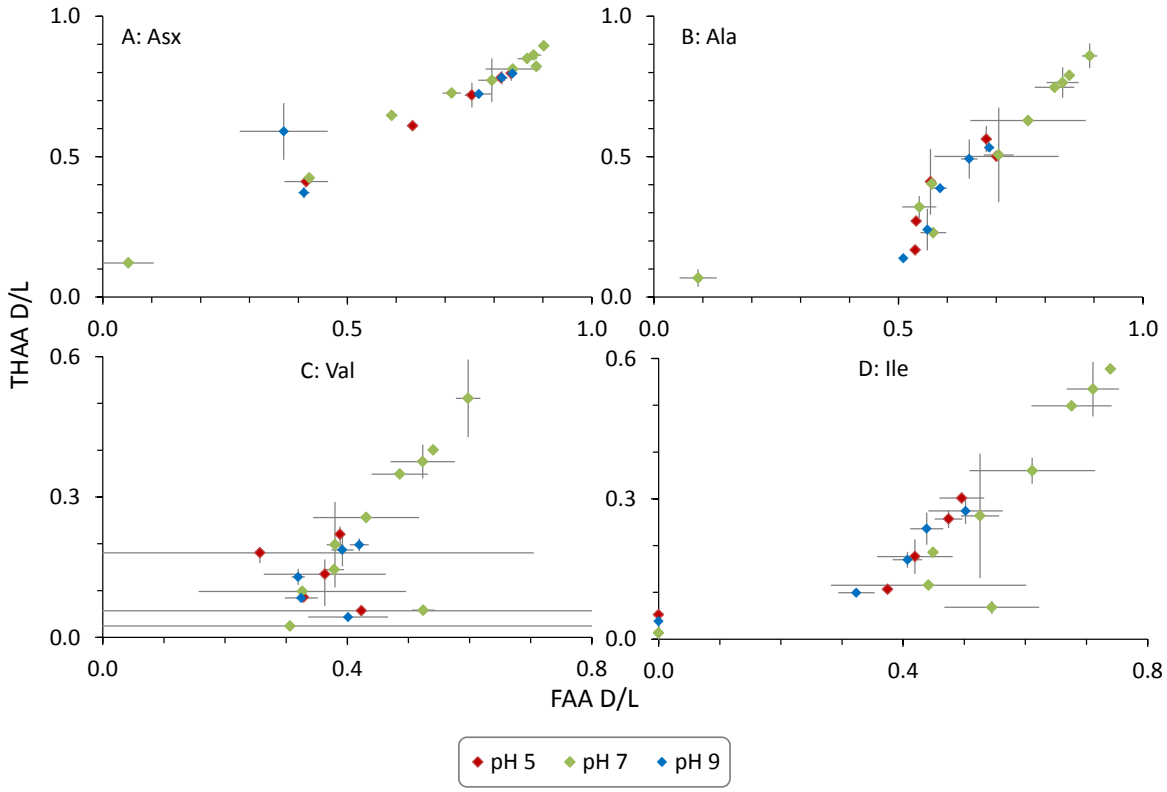

Figure 3.13: FAA D/L vs. THAA D/L values for intra-crystalline modern OES heated at 110 °C, at pH 5, 7 and 9. A: Asx, B: Ala, C: Val, D: Ile. Error bars represent 2 x the standard deviation about the mean, based on triplicate samples for the majority of samples at pH 7 and duplicate samples at pH 5 & 9.

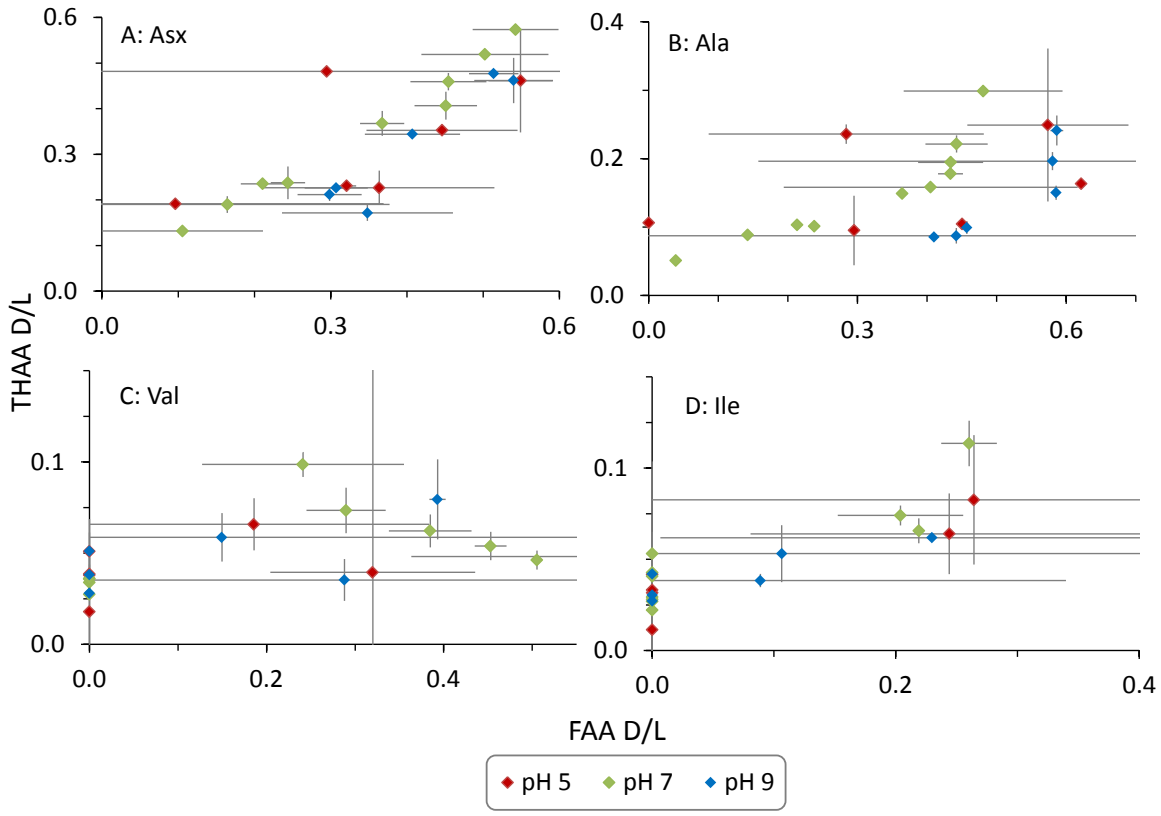

Figure 3.14: FAA D/L vs. THAA D/L values for intra-crystalline modern OES heated at 80 °C, at pH 5, 7 and 9. A: Asx, B: Ala, C: Val, D: Ile. Error bars represent 2 x the standard deviation about the mean, based on triplicate samples for the majority of samples at pH 7 and duplicate samples at pH 5 & 9.

After 6 hours of heating at 140 °C there is no statistical difference between the concentrations of amino acids leached into the supernatant liquid (THAAw) under the different pH conditions (Table 3.3). After 24 h there is an increased concentration in the water for samples heated in pH 5 conditions; however this difference is small and within 2 standard deviations of the pH 7 and 9 data (Table 3.3).

Time (h)	pH	Asx	Glx	Ser	Gly	Ala	Val	Phe	Ile
6	5	27 ± 8	45 ± 5	33 ± 19	104 ± 17	48 ± 4	19 ± 1	19 ± 0	18 ± 1
	7	44 ± 15	48 ± 17	25 ± 10	103 ± 29	53 ± 17	24 ± 6	22 ± 7	23 ± 6
	9	41	44	23	67	39	19	16	17
24	5	173 ± 96	252 ± 132	90 ± 32	427 ± 121	281 ± 119	89 ± 39	99 ± 46	90 ± 40
	7	35 ± 10	54 ± 24	47 ± 54	107 ± 36	57 ± 19	34 ± 19	24 ± 7	28 ± 9
	9	34 ± 12	52 ± 22	32 ± 25	116 ± 17	52 ± 18	26 ± 10	28 ± 10	28 ± 6

Table 3.3: Amino acid concentration in supernatant water (THAAw) of intra-crystalline modern OES samples heated isothermally at 140 °C. Errors shown are standard deviations based on triplicate samples for the majority of pH 7 samples and duplicate for the majority of pH 5 & 9 samples (no error is given for pH 9, 6 h sample as the replicate sample dried out during the hydrolysis preparative step).

3.3.6. The effect of bleaching on OES kinetics

To test whether the method for isolating the intra-crystalline fraction (i.e. bleaching pre-heat) affects the observed trends of protein degradation, a sub-set of 80 °C and 140 °C whole-shell samples were bleached for 72 h (i.e. post-heat bleaching). It was anticipated that bleaching post-heat would isolate the same fraction of intra-crystalline amino acids that are isolated by bleaching pre-heat, as is true for the bivalves *Corbicula* and *Margaritifera* (Penkman, 2005) and for corals (Tomiak *et al.*, 2013).

3.3.6.1. THAA concentration

The THAA concentrations for whole-shell samples heated at both 140 °C up to 96 h and 80 °C up to 2000 h are generally slightly higher than those of the equivalent intra-crystalline samples (Fig. 3.15 & 3.16). By ~ 230 h at 140 °C the concentrations of the whole-shell and intra-crystalline samples approach the same values, presumably because by this point the majority of inter-crystalline proteins from the whole-shell had diffused into the supernatant water. The post-heat bleached samples generally have THAA concentrations which are generally intermediate between

the whole-shell and the intra-crystalline concentrations (Fig. 3.15; 3.16). However, concentration differences are often small and not always statistically significant (Fig. 3.15; 3.16).

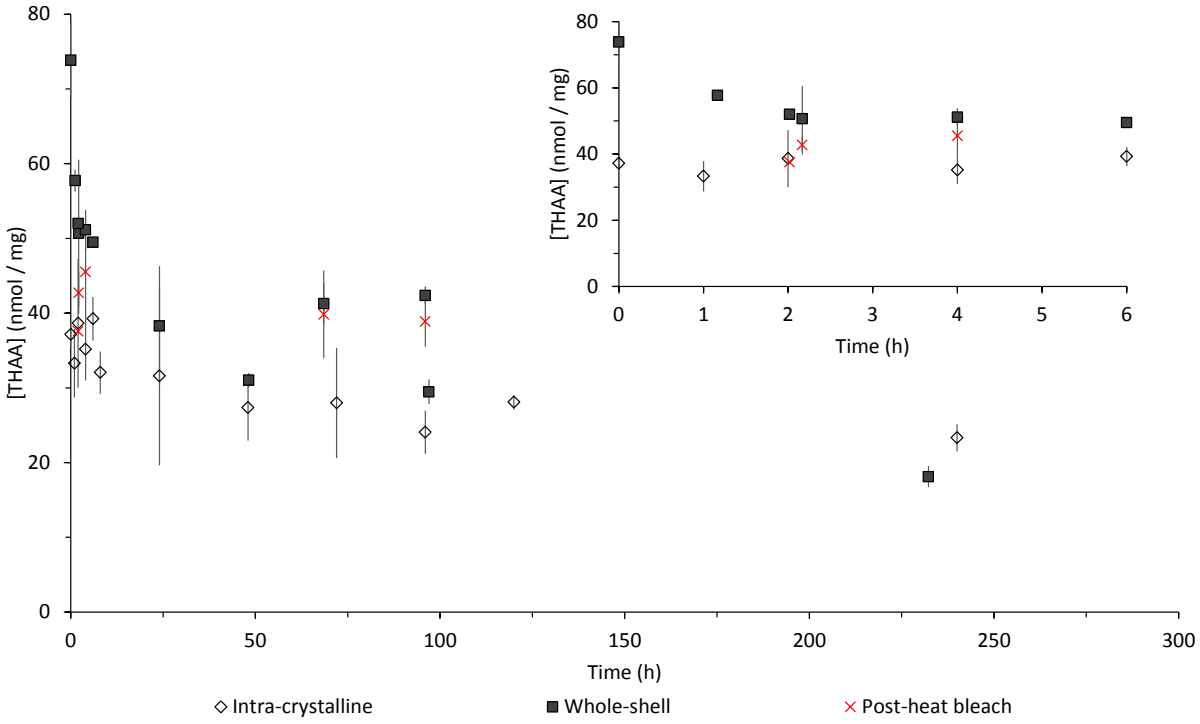

Figure 3.15: Sum of THAA concentrations (Asx, Glx, Ser, Gly, Val, Ala, Phe & Ile) of modern OES samples heated at 140 °C. Error bars represent 2 x the standard deviation, the majority of intra-crystalline and whole-shell samples based on triplicate samples, and post-heated samples using duplicate samples.

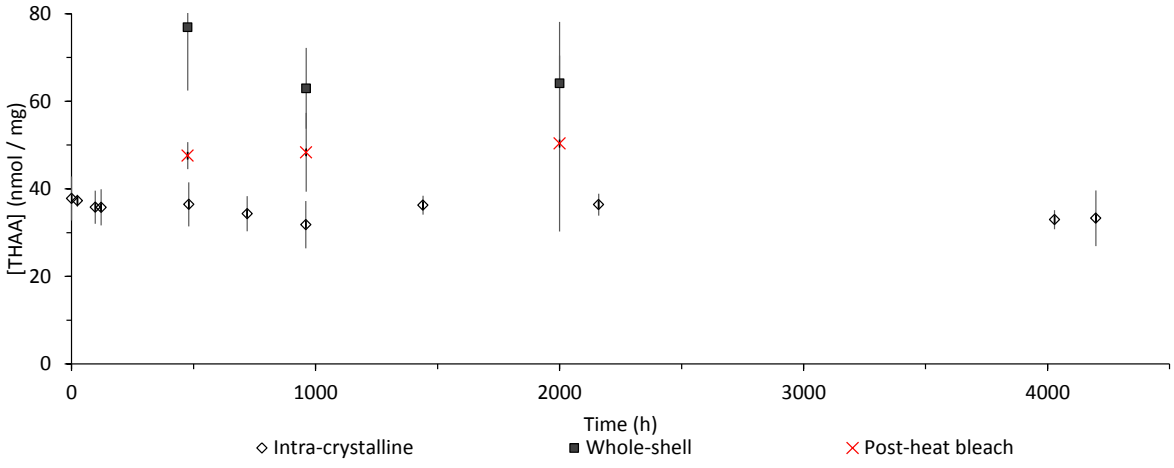

Figure 3.16: Sum of THAA concentrations (Asx, Glx, Ser, Gly, Val, Ala, Phe & Ile) of modern OES samples heated at 80 °C. Error bars represent 2 x the standard deviation based on triplicate samples for intra-crystalline samples, and duplicate samples for post-heat and whole-shell samples.

The THAA compositions of post-heat bleached and whole-shell samples heated at 140 °C and 80 °C appear to be similar (e.g. Fig. 3.17 for samples heated at 140 °C for 96 h, and 80 °C for 960 h). It has already been shown that the amino acid compositions of the intra-crystalline fraction and whole-shells are similar (Fig. 3.4). Here it is shown that the compositions of the post-heat bleached samples and the whole-shell samples also appear to be similar (Fig. 3.17).

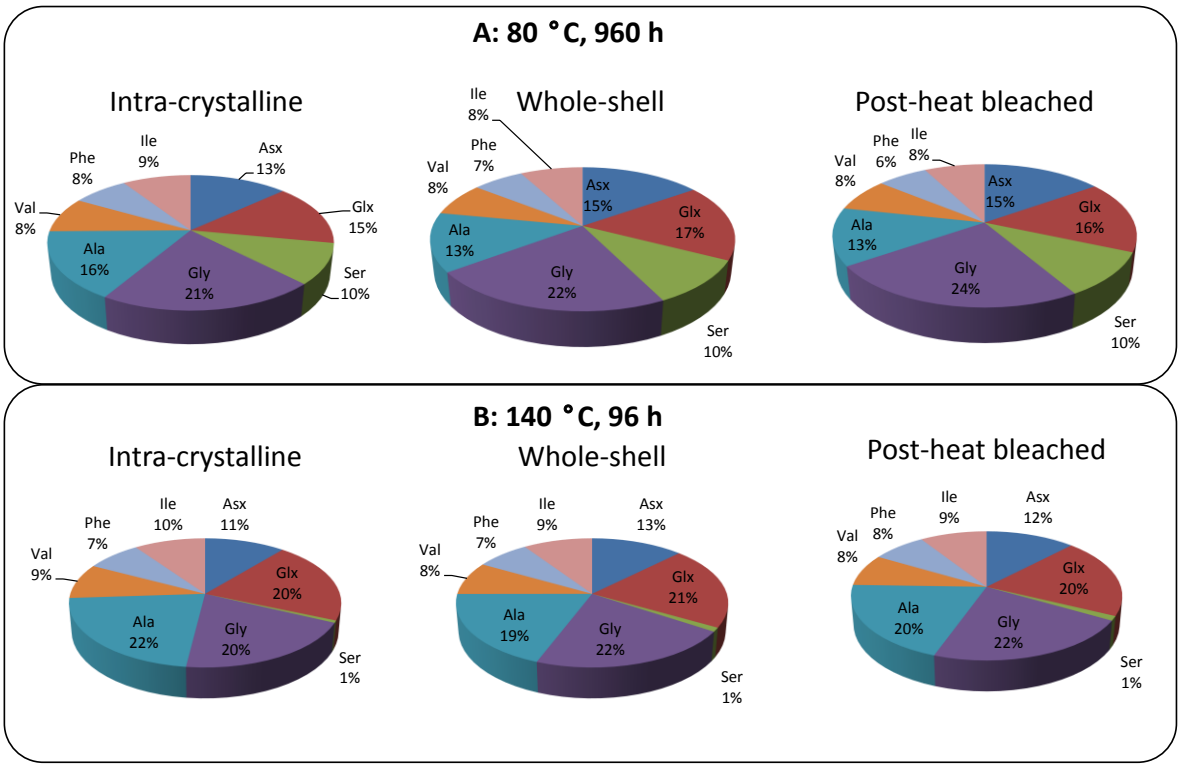

Figure 3.17: THAA compositions for intra-crystalline, whole-shell and post-heat bleached OES samples heated at 80 °C for 960 h (A), and 140 °C for 96 h (B).

3.3.6.2. FAA concentration

The FAA concentrations are presented as percentages relative to the THAA concentrations. Initial results of the 140 °C kinetic experiments using intra-crystalline and whole-shell samples showed there to be slightly higher FAA concentration in whole-shell samples (Crisp *et al.*, 2013). This contrasts with other bio-minerals e.g. mollusc (Penkman *et al.*, 2008), which show similar concentrations of FAA in both the intra-crystalline and whole-shell fractions. A small number of whole-shell time points were repeated, in order that samples could be processed simultaneously using no oxidative and post-heat oxidative treatments. The data showed that differences in concentration were within two standard deviations of the means (Fig. 3.18). However, the samples heated at 80 °C do show a small but statistically significant difference, where the whole-shell FAA concentrations are higher than the FAA concentrations of the intra-crystalline samples, over the limited time points analysed (Fig. 3.19).

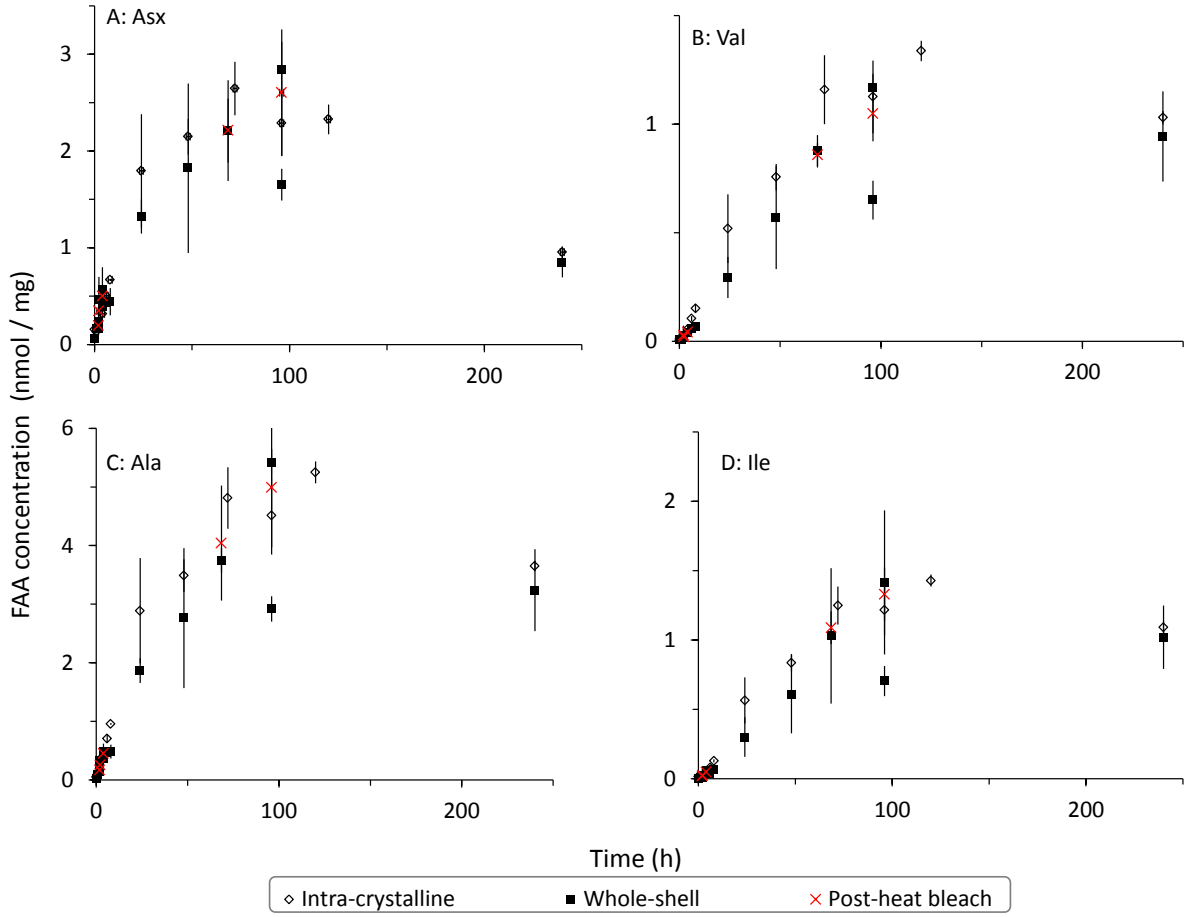

Figure 3.18: FAA concentrations of modern OES samples (whole-shell, intra-crystalline fraction & post-heat bleached samples) heated at 140 °C Error bars represent 2 x the standard deviation about the mean based on triplicate samples for the majority of the intra-crystalline samples and duplicate samples for the majority of post-heat samples and whole-shell samples.

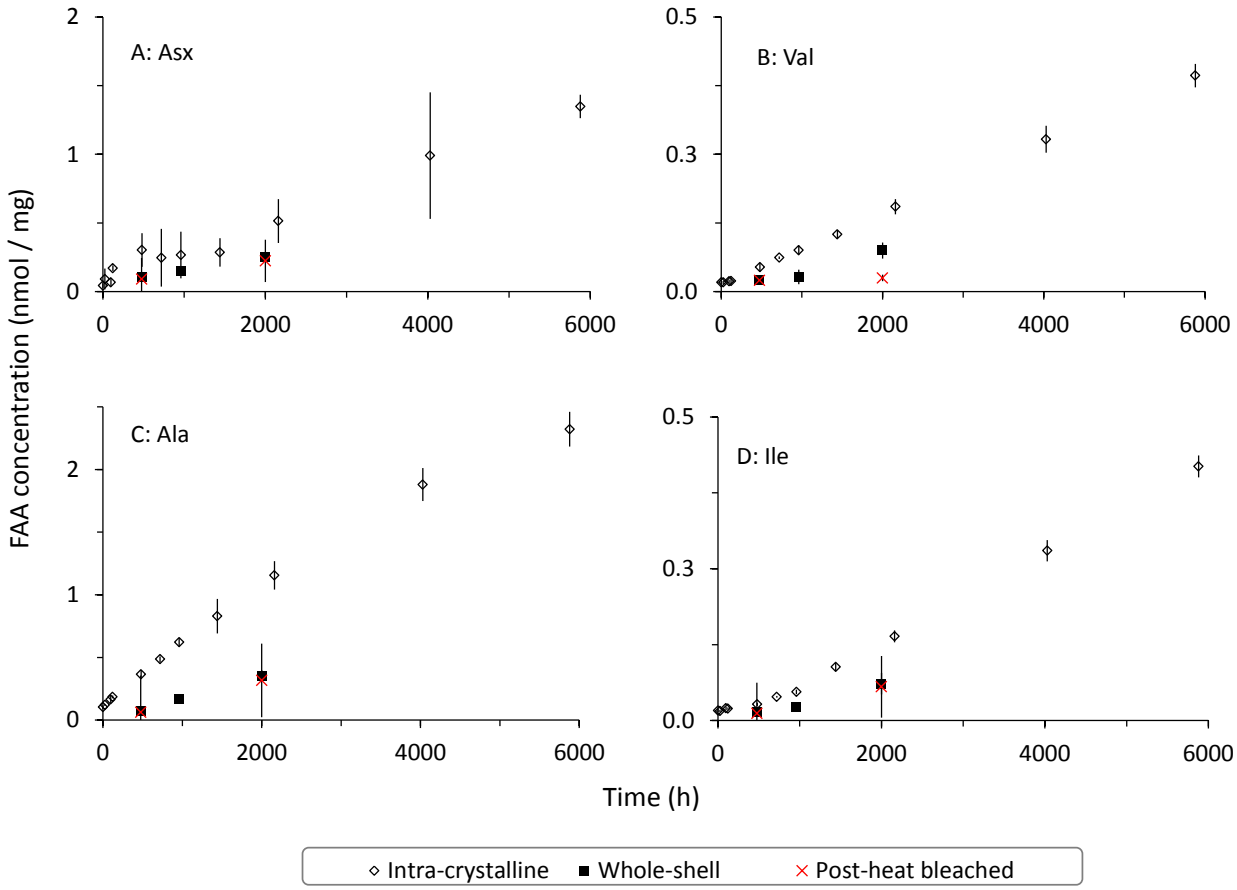

Figure 3.19: FAA concentrations of modern OES samples (whole-shell, intra-crystalline fraction & post-heat bleached samples) heated at 80 °C. Error bars represent 2 x the standard deviation about the mean based on triplicate samples for the majority of the intra-crystalline samples and duplicate samples for the majority of post-heat samples and whole-shell samples.

3.3.6.3. THAA racemization

Whole-shell OES THAA samples show a lower extent of racemization for all amino acids than the intra-crystalline proteins for both 140 °C (Fig. 3.20) and 80 °C (Fig. 3.21) up to 96 h and 2000 h, respectively. At 140 °C the levels of racemization for the whole-shell and intra-crystalline amino acids converge on the same value, at approximately the dynamic equilibrium. Unfortunately, due to time constraints the 80 °C whole-shell experiment was not performed for long enough for racemization to reach a dynamic equilibrium.

The lag in the whole-shell racemization is likely to be a consequence of the highly racemized inter-crystalline FAA fraction leaching from the system, leaving a THAA inter-crystalline fraction with lower D/L values (Sec. 3.3.2.). Indeed, the extent of racemization observed for the amino acids leached into the water is generally higher than that of the THAA fraction (Sec. 3.3.5.1; Fig. 3.5),

and the rate of racemization of FAA in water is too slow to account for this (Wehmiller and Hare, 1971).

It was anticipated that post-heat bleaching would reduce the THAA D/L values from those observed for the whole-shell samples to that observed for the intra-crystalline fraction. However, the post-heat bleached samples retain the THAA D/L values of the whole-shell samples for all amino acids at both 140 °C (Fig. 3.20; Appendix B) and 80 °C (Fig. 3.21; Appendix B).

These data suggest that oxidative treatment of heated whole-shell samples do not remove the fraction of amino acids which are removed by oxidative treatment of samples prior to heating. These data therefore suggest that the whole-shell and post-heat bleach treated samples are equivalent, which is in agreement with the THAA concentration data (Sec. 3.3.6.1.).

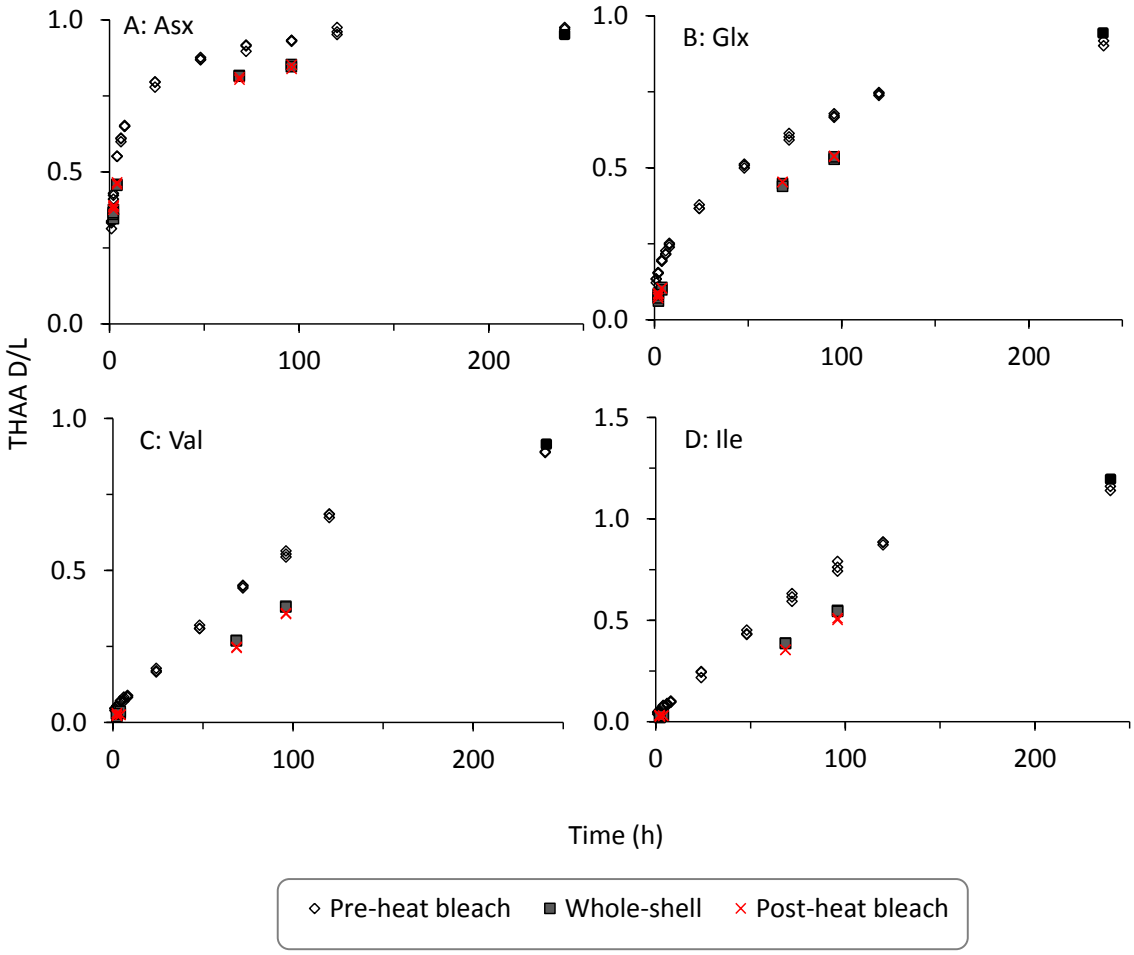

Figure 3.20: Whole-shell modern OES, intra-crystalline modern OES (pre-heat bleach treatment) & post-heat bleach treated modern OES. THAA D/L values of modern OES heated isothermally at 140 °C for (A) Glx, (B) Asx, (C) Val and (D) Ile

.

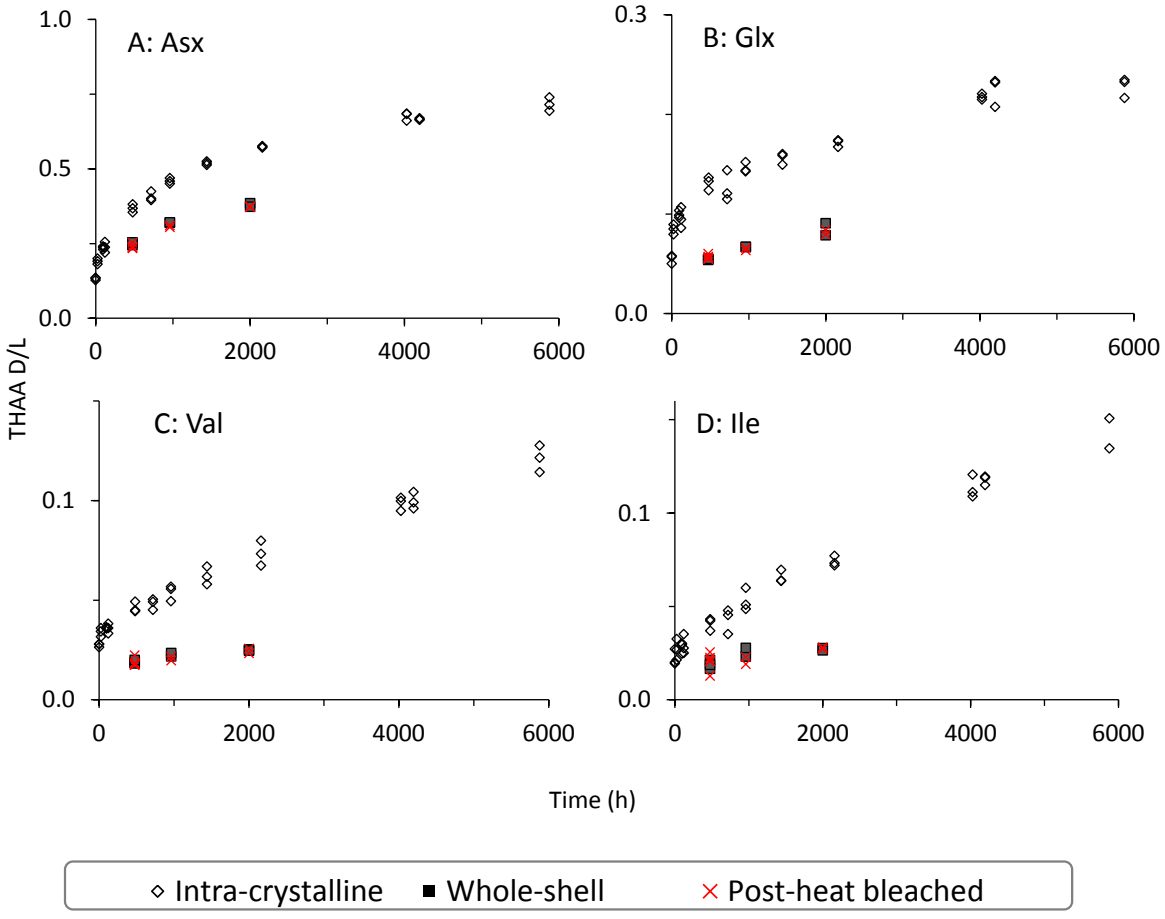

Figure 3.21: Whole-shell modern OES, intra-crystalline modern OES (pre-heat bleach treatment) & post-heat bleach treated modern OES. THAA D/L values of modern OES heated isothermally at 80 °C for (A) Glx, (B) Asx, (C) Val and (D) Ile.

3.3.6.4. FAA racemization

Generally the FAA D/L values for samples heated at 140 °C show similar degrees of racemization, whether they are whole-shell, intra-crystalline or post-heat bleached samples (e.g. Fig. 3.22). The notable exceptions are whole-shell samples (and post-heat bleached samples) heated at 80 °C up to 2000 h, which show lower FAA D/L values for Asx and Ala than the intra-crystalline fraction (Fig. 3.23). This phenomenon is not seen in other bio-minerals, and it is unclear why this is the case for OES.

FAA concentrations are generally more variable than THAA concentrations. This is likely to be due to lower amino acid concentrations and higher relative concentrations of non-amino acid compounds resulting in HPLC chromatograms having increased baseline noise and reduced resolution of some analytes. This is especially true for the earlier time points, where little hydrolysis has occurred.

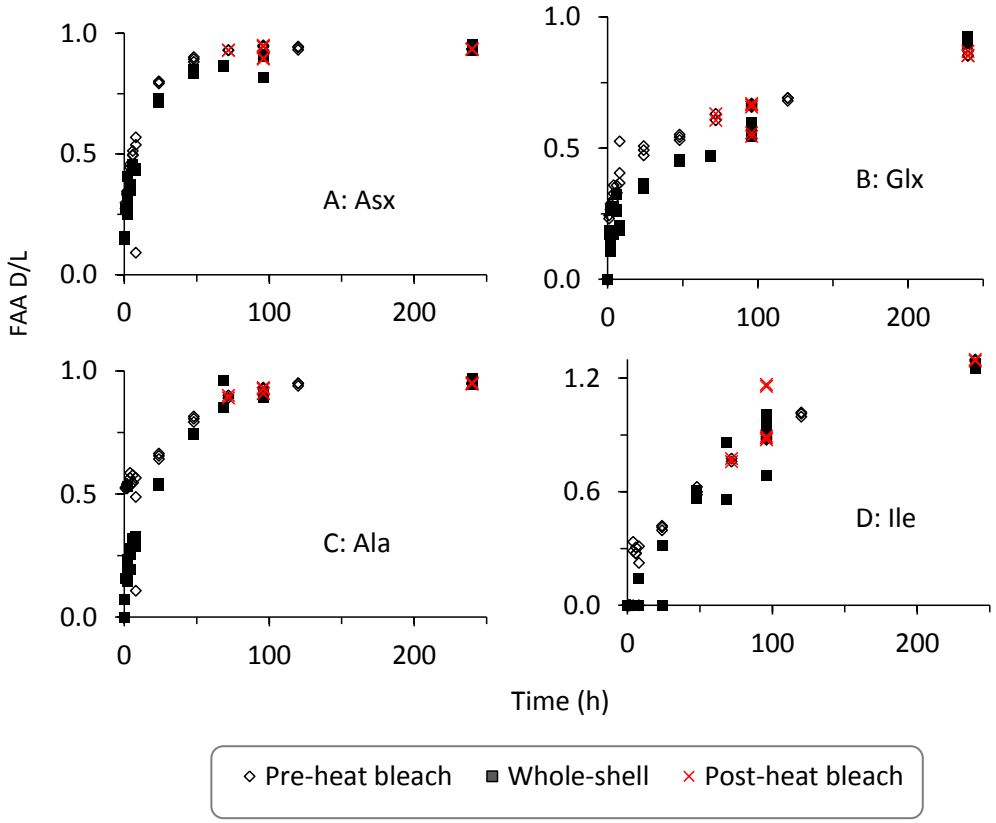

Figure 3.22: FAA D/L values for modern OES samples heated isothermally at 140 °C using whole-shell OES, intra-crystalline fraction only (i.e. pre-heat bleach treated) and post-heat bleach treated OES

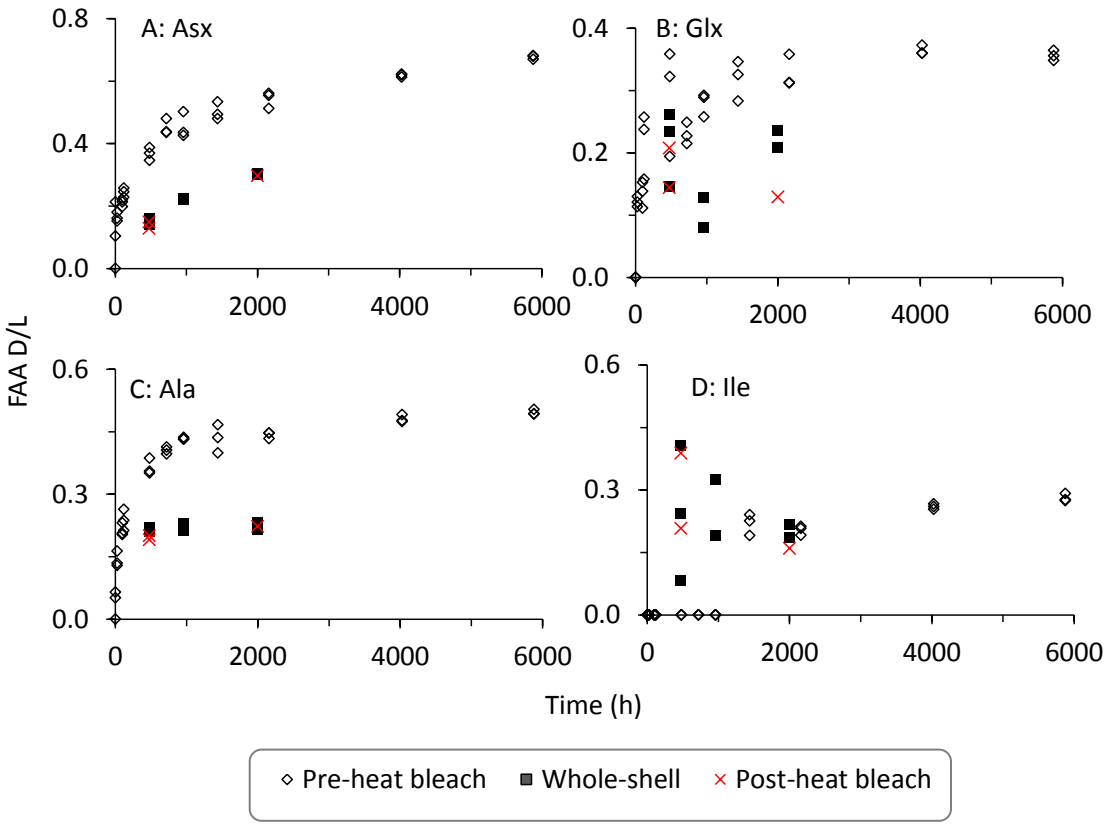

Figure 3.23: FAA D/L values for modern OES samples heated isothermally at 80 °C using whole-shell OES, intra-crystalline fraction only (i.e. pre-heat bleach treated) and post-heat bleach treated OES

3.3.7. Is the intra-crystalline fraction truly closed?

This study demonstrates that oxidative pre-treatment for 72 h with 12 % (w/v) NaOCl isolates a fraction of intra-crystalline proteins in OES. Through leaching studies it has been shown that approximately 99 % of the intra-crystalline THAA concentration is retained after continuous leaching at 140 °C for 24 h (Table 3.2). This has been used in previous studies to prove closed system behaviour of bio-minerals (e.g. Penkman *et al.*, 1998; Tomiak *et al.,* 2013).

Closed system behaviour of the intra-crystalline fraction was confirmed by heating studies at pH 5, 7 and 9. Heating intra-crystalline samples in buffered solutions at both pH 5 and pH 9 did not enhance leaching of the intra-crystalline proteins, nor did either treatment encourage the release of previously inaccessible proteins or enhance racemization in the intra-crystalline fraction, as has been observed for whole-shell ostracods (Bright and Kaufman, 2011b). Therefore, the intra-crystalline proteins of OES appear to maintain closed system behaviour between pH 5 and pH 9.

Contrary to corals (Tomiak *et al.*, 2013) and bivalves (Penkman, 2005), pre-heat and post-heat bleach treatments with OES do not give equivalent AAR results. This raises questions as to the

nature of the intra-crystalline and inter-crystalline fractions of amino acids in OES. This study suggests that heating whole-shell OES samples at 80 – 140 °C prior to removal of the inter-crystalline fractions creates an additional fraction of bleach resistant proteins which would otherwise be removed with 72 h bleach treatment. This additional fraction is likely to comprise inter-crystalline proteins, considering that the whole-shell and post-heat samples appear equivalent (e.g. Figs. 3.6 – 3.8).

The small increase in the FAA concentrations in the intra-crystalline samples may in part be a consequence of sample preparation; bleaching removes organics and perhaps even some carbonate, so the reduction in mass will artificially create a small increase in the apparent FAA concentration. Indeed, SCA 1 & 2 only account for ~20% of the total organic matrix (Nys *et al.*, 1999; Mann and Siedler, 2004; Woodman, 2012). An alternative explanation, that the bleach treatment 'opens' the closed system intra-crystalline amino acids by removing organics from pores, was discounted as if this were the case then it might be expected that: (i) amino acids would leach from the bleached samples, which is not seen (Section 3.3.5.1.); and (ii) there would be differences in the rates of racemization, degradation and hydrolysis for the bleached samples heated at pH 5, 7 and 9, which is also not observed (Section 3.3.5.2.). In the case of the 140 °C experiment the differences in FAA concentration are not significant. The larger difference in concentrations seen for the 80 °C data may be a consequence of the lower temperature being less favourable for the diffusion of inter-crystalline organics (leaching) from the shell structure, thus causing a lesser reduction in mass than at 140 °C; this would result in increased observed amino acid concentrations. It is therefore argued that the observed differences between FAA concentrations in the whole-shell and intra-crystalline fractions are not significant enough to suggest that the intra-crystalline fraction does not approximate a closed system.

The 140 °C whole-shell, post- and pre-heat bleach treated samples do eventually converge onto the same THAA D/L values (Fig. 3.20) and THAA concentrations (Fig. 3.15). This may suggest that the additional bleach resistant fraction is eventually broken down with prolonged heating. Unfortunately, the 80 °C whole-shell/post-heat bleached samples were not heated long enough to see if this is also true at lower temperatures (Fig. 3.16; 3.21).

It is unclear at this point why post-heat bleaching for OES is not equivalent to pre-heat bleaching; whether heating causes subtle changes to the mineral structure, locking in the additional proteins, or perhaps that the water and heat cause chemical reactions, creating the additional bleach resistant fraction. However, no changes in mineral structure can be detected using XRD at temperatures < 500 °C (Heredia *et al.*, 2005; Sec. 6.4.4.). It is possible that during the heating stage the sealed glass ampoules would build up pressure which may facilitate additional reactions. High temperature heating of inter-crystalline amino acids may encourage reactions

with other compounds, organic or inorganic, present in the OES. Reaction pathways could include Maillard reactions, a complex set of reactions involving amino acids and reducing sugars (Maillard, 1912). It is known that chicken eggshells contain polysaccharides (Baker and Balch, 1962), phospholipids (Simkiss, 1958) and protein complexed with acid-mucopolysaccharides (Simkiss and Tyler, 1957), therefore it is likely similar compounds are also present in OES. Maillard reactions can form bleach-resistant melanoidin compounds which may then later be released on acid demineralisation/hydrolysis (e.g. Hoering, 1980; Namiki *et al.*, 1988; Wang *et al.*, 2011).

Additional analysis, perhaps with SEM, would be required to assess whether structural changes result from heating OES at > 80 °C. Perhaps a more aggressive or longer oxidising treatment would be required for samples heated prior to bleach treatment.

Nevertheless, it is clear that oxidative pre-treatment isolates a bleach-resistant fraction of amino acids that is not prone to leaching and is unaffected by changing pH conditions, and thus approximates a closed system.

3.3.8. If, and when to bleach

Kinetic experiments in this study show that whole-shell and intra-crystalline OES amino acids follow different trends of racemization (e.g. Fig. 3.21), and that the inter-crystalline fraction is prone to leaching (e.g. Fig. 3.15). Indeed, the whole-shell OES rapidly leaches amino acids when heated in water, reaching a plateau after 2 h of heating at 140 °C, with a loss of up to 50 % of the original THAA concentration.

It is possible that under geological temperatures, the hypothesised heat-induced bleach resistant fraction observed in the post-heat bleached samples is unlikely to form, and therefore performing kinetic studies using pre-heat bleach treated samples may better mimic the diagenesis of sub-fossil samples.

Under controlled laboratory conditions the extent of leaching between replicates is consistent, but in sub-fossil samples the extent of leaching would be an unpredictable variable, potentially affecting the overall D/L values. It is therefore argued that it is important to remove this source of variability by using an effective oxidative pre-treatment. Subsequent data interpretation of kinetic experiments, in order to estimate Arrhenius parameters, and analysis of sub-fossil samples to build dating models, were therefore limited to pre-heat 72 h bleached samples (i.e. the intra-crystalline fraction).

Previous studies using ratite eggshell have not used an oxidative pre-treatment step, instead cleaning the sample by physically removing the outer layers and then removing one-third of the

sample with acid treatment (Miller *et al.*, 1992). Brooks *et al.* (1990, p. 61) reported that OES retained 99 % of its "stable amino acid content" after 70 h of continuous leaching at 105 °C. Although the purpose of acid cleaning is to remove surface contamination, it may also inadvertently remove some inter-crystalline amino acids, therefore preferentially preserving the intra-crystalline fraction for analysis. The intra-crystalline fraction isolated with oxidative treatment may equate with the previously reported "stable amino acid content" from whole OES of Brooks and colleagues (1990), although it would still be prudent not to directly compare the fractions isolated with bleach and that isolated with acid treatment, as acid treatment would also remove bio-mineral and potentially expose intra-crystalline amino acids.

3.7. CONCLUSIONS

This study suggests that the routine hydrolysis method, using 20 µL of acid per mg of OES and heating at 110 °C for 24 h, was the most appropriate method for hydrolysing the proteins in OES as it induced the least amount of racemization while extracting the highest concentration of amino acids (Sec. 3.3.1.). Even though there is more protein present in OES than in other bio-minerals, and it requires a longer bleach time to remove the inter-crystalline proteins than other bio-minerals, no change in hydrolysis method was required in order to liberate the maximum quantity of amino acids for analysis.

72 h of oxidative treatment isolates a fraction of amino acids which are resistant to chemical oxidation and are therefore defined as the 'intra-crystalline' fraction (Sec. 3.3.2.). This fraction of amino acids are resistant to leaching at increased temperatures (Sec. 3.3.5.1.) and do not show different trends in degradation when heated in solutions of pH 5, 7 or 9 (Sec. 3.3.5.2.). These therefore suggest that the intra-crystalline fraction approximates a closed system.

The whole-shell and intra-crystalline fractions in OES appear to have very similar amino acid compositions, which may suggest similar protein compositions are present (Fig. 3.4). This is unlike other bio-minerals which show different amino acid compositions in the whole-shell and intra-crystalline fractions, e.g. coral (Ingalls *et al.*, 2003) and mollusc (Penkman *et al.*, 2008; Demarchi *et al.*, 2013a). This may be a consequence of the rapid way in which OES is bio-mineralised, as opposed to slow and controlled growths in other bio-minerals used for AAR geochronology e.g. coral and mollusc shells.

Heating whole-shell OES appears to create a fraction of amino acids which are resistant to subsequent oxidative treatment (Sec. 3.3.6.). It seems likely that this fraction is from the inter-crystalline fraction of amino acids, which would otherwise be removed with oxidative pre-treatment (Sec. 3.3.8.). It is likely that sub-fossil samples suitable for dating (i.e. that have not

been exposed to artificial heating, Chapter 6) will not have this additional fraction of amino acids which are resistant to oxidative treatment. Therefore, using pre-heat bleach treatment for heating studies is argued to be a better approach to understanding diagenesis of sub-fossil samples.

In conclusion, the intra-crystalline fraction of proteins within OES approximates a closed system and limiting AAR analysis to these proteins may moderate the variability in sub-fossil data caused by changing environmental conditions such as pH (Sec. 3.3.5.2.), leaching (Walton *et al.*, 1998), and, potentially, microbial action (Child *et al.*, 1993). Furthermore, because the intra-crystalline degradation products are contained within the closed system, potentially other reactions (e.g. hydrolysis, decomposition and racemization of the FAA fraction) may be used for the purpose of amino acid geochronology.

CHAPTER 4: KINETIC STUDIES OF MODERN OES

4.1. INTRODUCTION

It has been established that 72 h oxidative treatment prior to heat treatment of OES isolates a fraction of proteins, operationally defined as 'intra-crystalline', which approximate a closed system (Chapter 3). Therefore, all intra-crystalline amino acids and their degradation products may be accounted for; losses in THAA concentration, for example, may be assumed to be due to degradation, as leaching has been ruled out.

In order to use the protein diagenesis of the intra-crystalline fraction to assign relative ages in sub-fossil samples, specific reactions need to be studied to see how the rates of reaction change with time. Protein diagenesis is too slow at ambient temperatures to be studied in real time, so high-temperature experiments have often been used to simulate reaction kinetics at lower temperatures over lab timescales (e.g. Goodfriend and Meyer, 1991; Brooks *et al.,* 1990; Miller *et al.*, 1991).

There are a number of variables within bio-minerals which may complicate the observed rates of degradation, e.g. primary amino acid sequence and location within the chain (terminally bound/internally bound/free), availability of water and how these conditions change over time (e.g. Sec. 1.3.4.). In addition, the species effect (e.g. Lajoie *et al.*, 1980) means that every bio-mineral intended for the use in AAR studies needs to be studied individually.

If high temperature kinetic experiments are to be used accurately for estimating the rates of diagenesis in sub-fossil OES over geological timespans, it must be shown that all relevant reaction rates are equivalent at high and low temperatures. This is likely to be the case only if all reactions which have influence on one another have similar activation energies (Miller *et al.*, 2000). Although racemization is the reaction of most interest to AAR geochronology, reactions such as hydrolysis and decomposition are also important. Generally speaking, amino acids racemize fastest whilst bound at terminal positions in a peptide chain (Kriausakul and Mitterer, 1978; Moir and Crawford, 1988; Smith and De Sol, 1980; Sec. 1.3.1.). Consequently, the rates of hydrolysis and racemization are intrinsically linked. It is therefore important to show not only that racemization rates are equivalent at increased temperatures, but also that other competing and/or concomitant reactions are too. Miller *et al.* (2000) tested this assumption for isoleucine (Ile) in *Dromaius novaehollandiae* (Australian emu) eggshell, and concluded that the activation

energies of hydrolysis and epimerization for Ile were indeed the same, therefore justifying the use of high temperature kinetics to determine rates at low burial temperatures in this case. In order to assess whether this was also the case for OES, the trends in simulated diagenesis of the intra-crystalline fraction of modern OES at 80 °C, 110 °C and 140 °C were investigated in order to assess whether the protein degradation within the intra-crystalline fraction follow repeatable and predictable rates of reaction. In addition, the trends of protein degradation of the kinetically heated samples and a set of low-temperature sub-fossil samples have been compared to evaluate the applicability of high temperature studies for extrapolation to lower temperatures.

4.2. MATERIALS AND METHODS

4.2.1. Kinetically heated modern OES

Samples were prepared as per Sec. 3.2.3. In this chapter only intra-crystalline samples, heated isothermally at 80, 110 and 140 °C in HPLC-grade water, were considered (Table 4.1).

After heating, the supernatant was removed and the powders air dried. The powders were split into two fractions for FAA and THAA analysis (Sec. 2.3.1.).

Temp. (°C)	Heating time (h)										
80	0	24	97	121	480	720	960	1440	2160	4028	5879
110	0	24	120	240	384	480	720	840	960	1200	
140	0	1	2	4	6	8	24	72	96	120	240

Table 4.1: Kinetic experiment time points using the intra-crystalline fraction of modern OES samples; each time point was performed in triplicate.

4.2.2. Sub-fossil samples

Sub-fossil samples have been included in order to constrain the kinetic experiments with low temperature data. The sub-fossil data are discussed fully in Chapter 6; sample details are given in Section 6.2, and preparation is described in Section 6.3. The sub-fossil data were screened for artificially heated samples and these samples have been excluded for the purposes of this chapter (Sec. 6.6).

4.3.1. Racemization

The racemization of intra-crystalline amino acids follow predictable trends at all temperatures studied, with a general increase in D/L values with heating time (THAA in Fig. 4.1, FAA in Fig. 4.2). Ser is one of the most thermally unstable amino acids (Vallentyne, 1964) and the degradation of the more racemized free Ser molecules results in the apparent reversal of racemization of THAA Ser in the 140 °C experiment (Fig. 4.1, 4.2). Within the THAA fraction, Asx initially displays the fastest rate of racemization (i.e. up to ~0.7 Asx D/L), followed by Ser; the slowest rates were observed for Val and Ile (Fig. 4.1). The observed relative order of racemization rates is in broad agreement with Smith and Evans (1980), who reported the order for the rates of racemization of free amino acids in aqueous solution: Ser > Thr > Asp > Phe > Ala > Glu > Leu > Ile > Val. The main difference in the observed relative order of racemization rate is the rapid initial racemization of Asx, which may be explained by the rapid in-chain racemization via the succinimidyl intermediate (Brennan and Clarke, 1993; Goodfriend and Hare, 1995; Radkiewicz *et al.*, 1996). In addition, the observed rate of Asx racemization will have a small contribution from Asn degrading to form a racemate of Asp (Vallentyne 1964; Hill, 1965; Geiger and Clarke, 1987; Brinton and Bada, 1995). Rapid in-chain racemization of Asp most likely explains the observed fast rate of Asx racemization in OES (Fig.4.1).

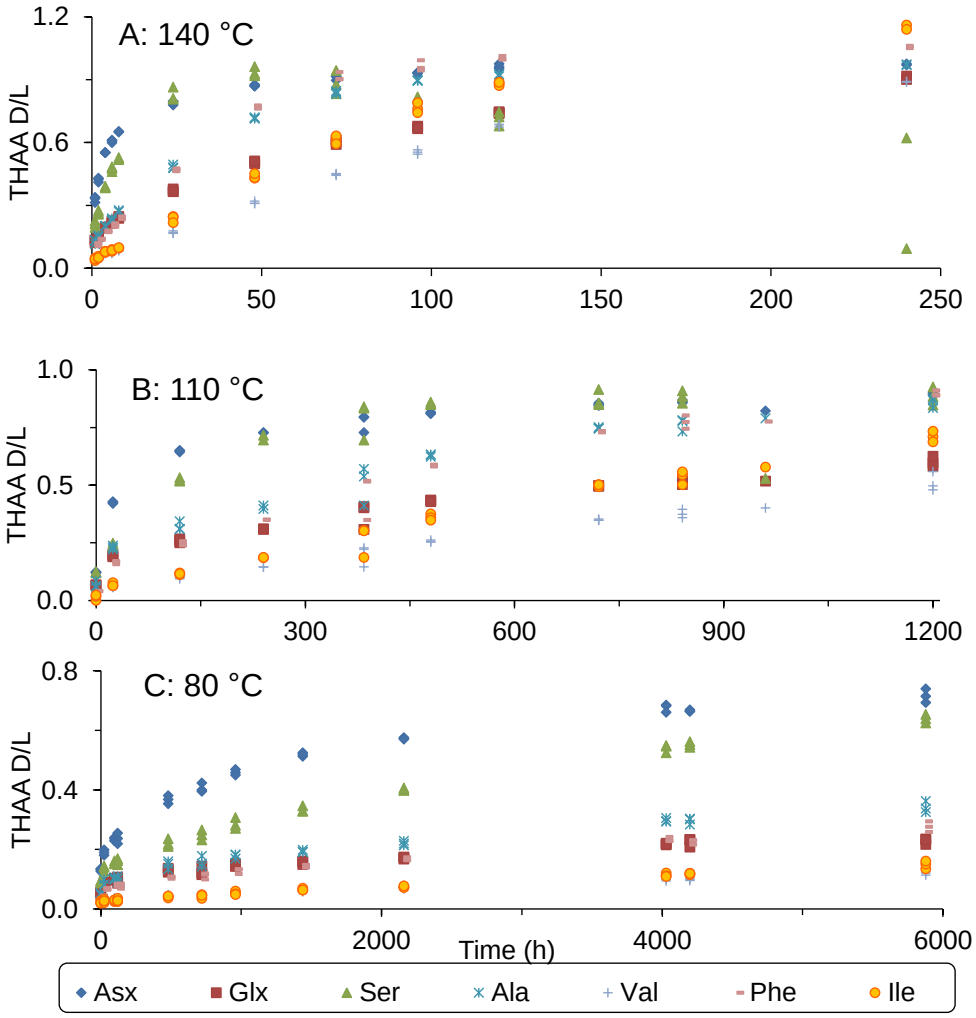

Figure 4.1: Extent of racemization for the THAA in the intra-crystalline protein fraction in modern OES heated isothermally at A: 140 °C, B: 110 °C and C: 80 °C

The FAAs are generally more racemized than those of the THAA fraction (e.g. Fig 4.1, 4.2 and Phe in Fig. 4.3; c.f. Hare, 1971; Smith and Evans, 1980; Liardon and Ledermann, 1986). Unlike all the other amino acids, Asx displays similar rates of racemization in the FAA and THAA fractions (Fig. 4.3); the relationship between racemization and hydrolysis for Asx is therefore fundamentally different from the pathways followed by other amino acids. This is due (at least in part) to the rapid in-chain racemization via the succinimidyl intermediate (Brennan and Clarke, 1993; Goodfriend and Hare, 1995; Radkiewicz *et al.*, 1996) and may therefore not be limited by the rate of hydrolysis to the same extent that other amino acids are.

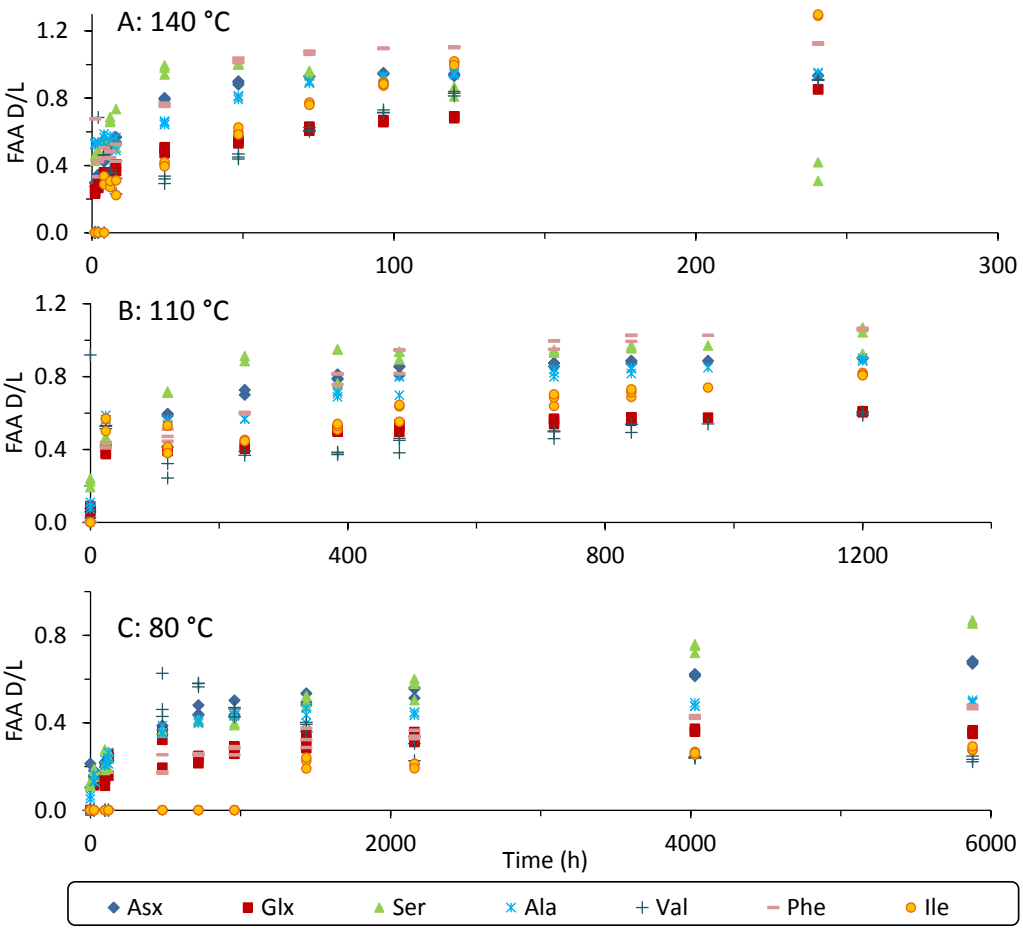

Figure 4.2: Extent of racemization for the FAA in the intra-crystalline protein fraction in modern OES heated isothermally at A: 140 °C, B: 110 °C and C: 80 °C

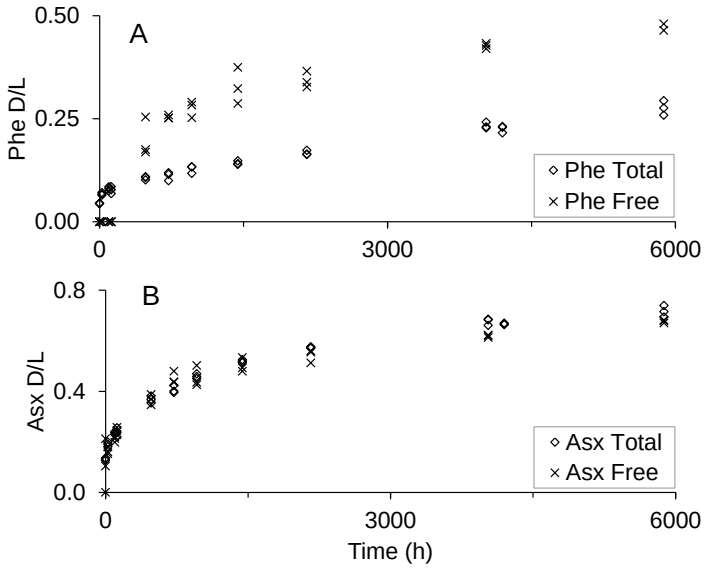

Figure 4.3: Racemization of the FAA and THAA fractions at 80 °C for A: Phe (similar trends are seen for 110 °C and 140 °C and for Ile, Phe and Ala, see Appendix B; B: aspartic acid (Similar trends also seen at 110 °C and 140 °C, see Appendix B).

Val FAA racemization shows a different trend to the other amino acids, with early time points often showing very high D/L values (Fig.4.4). This may be a consequence of a co-eluting peak under D-Val, which impacts on the D/L value with more significance when the FAA concentrations are low. Alternatively, a pocket of highly racemized FAA Val may be present, which eventually degrades and is 'diluted' by newly released Val FAA. Demarchi and colleagues (2013b) observed a similar phenomenon in heating experiments using *Patella* samples; they attributed this observation to low FAA Val concentrations or an initial release of a highly racemized fraction.

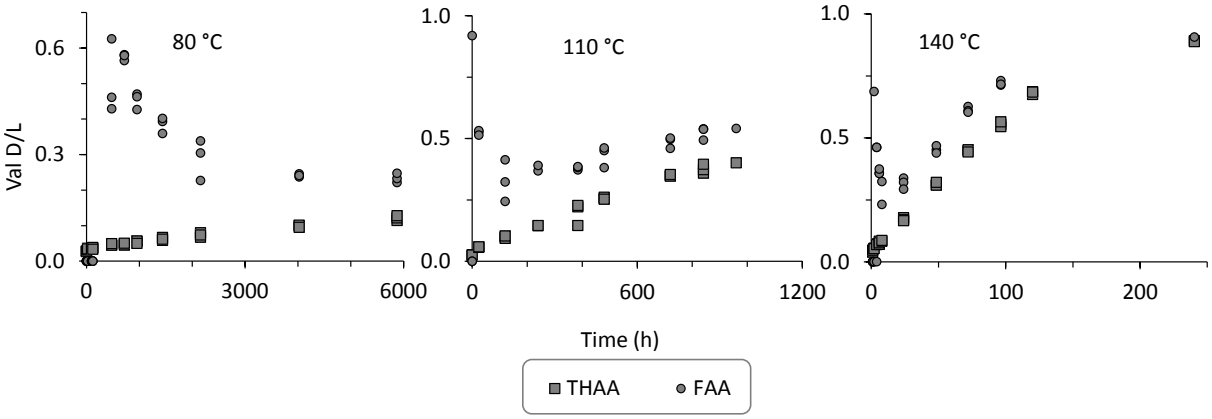

Figure 4.4: Val racemization in the FAA and THAA fractions when heated at 80, 110 and 140 °C

4.3.2. Hydrolysis within the intra-crystalline fraction

As OES is heated, peptide bonds hydrolyse, releasing free amino acids (Hare, 1969). The rate of hydrolysis will depend on the strength of the peptide bond, so it is anticipated that different amino acids will be released at different rates (Walton, 1998).

The observed hydrolysis of Glx appears to be very slow, especially at 110 °C and 140 °C, however, this can be explained by the formation of stable lactams (Vallentyne, 1964). These cannot be derivatised with OPA/IBLC (Kaufman and Manley, 1998), removing their contribution from the observed Glx FAA concentration.

The %FAA values are relative to the THAA concentration of the time point in question, and not the initial THAA concentration at time zero, thereby mitigating against decomposition. Hydrolysis appears to follow predictable trends at all temperatures studied (Fig. 4.5).

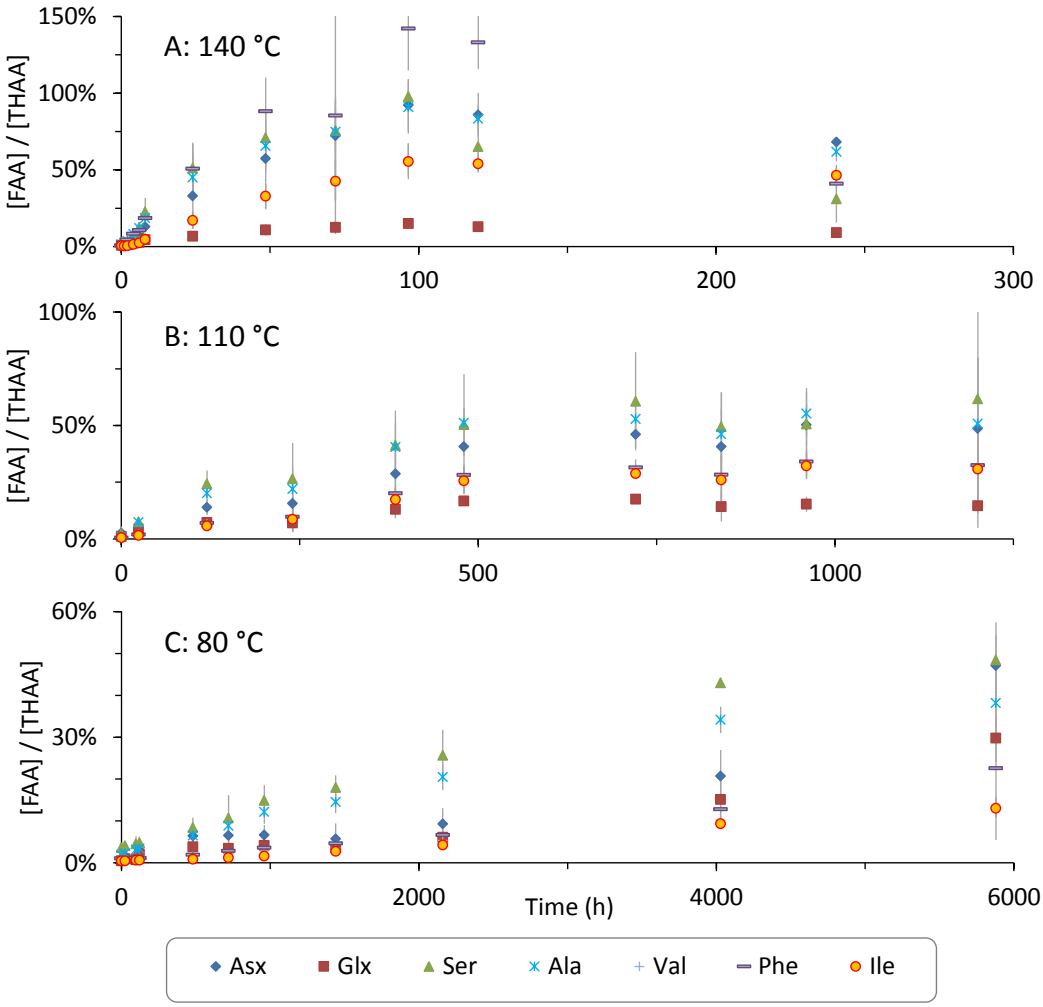

Figure 4.5: % FAA concentration relative to the THAA at time t, for the intra-crystalline proteins of isothermally heated modern OES. A: 140 °C; B: 110 °C; C: 80 °C. Error bars represent the 2 x standard deviation based on triplicate or duplicate samples; where this was not possible due to sample failure (240 h & 960 h at 110 °C), the error represented is the average standard deviation for that amino acid at that temperature

4.3.3. Decomposition

It can be seen that most amino acids slowly degrade with heating, and the rates are greater with increased temperature (Fig. 4.6). Ser, which is known to be a thermally unstable amino acid (Vallentyne, 1964), degrades the fastest. By ~48 h at 140 °C it appears that Asx degrades faster than the other amino acids, with the exception of Ser. Ala consistently shows a high concentration and does not appear to degrade much. This is likely to be a consequence of Ala forming from the degradation of other amino acids such as Ser (Bada *et al.*, 1978) and Asp (Bada *et al.*, 1978; Bada and Man, 1980). All other amino acids at 80, 110 and 140 °C show a slow degradation with heating time, but the rates of degradation are indistinguishable.

The high variability of the amino acid concentrations mean that large changes in concentration are necessary to make the differences statistically significant. The use of amino acid decomposition in respect to giving accurate chronological information from sub-fossil samples may therefore be limited.

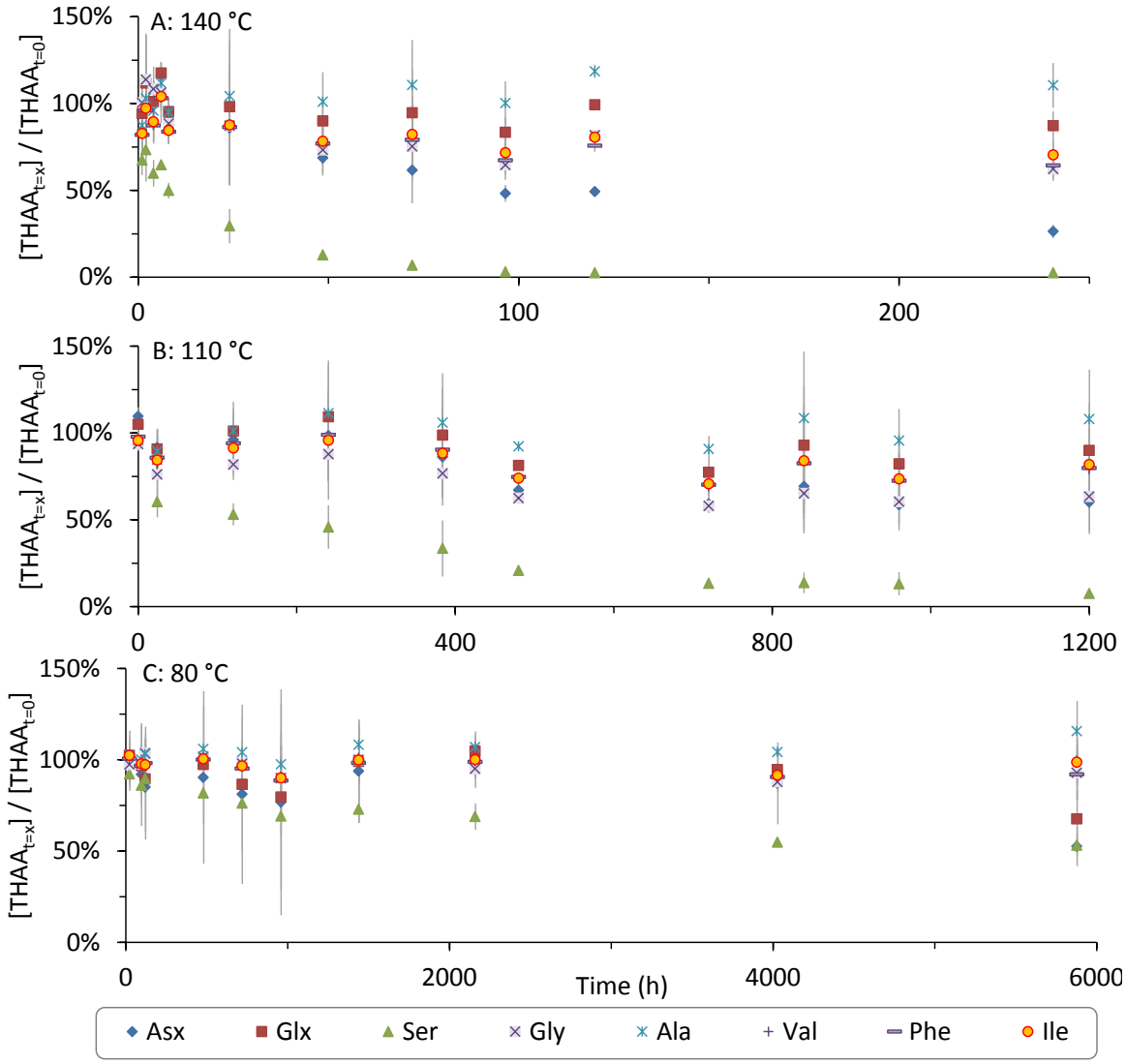

Figure 4.6: THAA concentrations relative to the initial THAA concentration with 0 h heating at A: 140 °C, B: 110 °C, C: 80 °C. Error bars represent 2 x standard deviation, the majority are calculated from triplicate samples, with the exception of 240 h 110 °C and 140 °C which were based on duplicate samples, and, 960 h 110 °C error which is a single sample, so the error represents the average of all samples heated at 110 °C.

4.4.1. Protein degradation of kinetically heated samples compared to low-temperature sub-fossil samples

Using high temperature kinetic data to extrapolate to lower temperatures assumes that all rates of reactions are equivalent at increased temperatures. This assumption was tested by comparing the trends of degradation of the kinetically heated modern samples with a sub-set of unheated sub-fossil samples. Reactions progress faster at higher temperatures; therefore, in order to assess their relative rates at higher temperatures, the trends of hydrolysis, racemization and decomposition of different amino acids were compared.

4.4.1.1. Relative rates of racemization

Miller *et al.* (2000) scrutinised the validity of using high temperature kinetic studies with regards to Ile epimerization in *Dromaius* eggshell. They observed the same trend of epimerization for isothermally heated fossil samples (with different thermal histories and A/I values) as isothermally heated modern eggshell. This they suggest shows that epimerization and all contributing reactions (e.g. hydrolysis) have similar activation energies. The same study also highlighted that the relationship between THAA A/I and FAA A/I was similar for all heated modern and sub-fossil samples. As Ile cannot racemize whilst internally bound (Mitterer and Kriausakul, 1984), they concluded that the activation energies for Ile hydrolysis and epimerization are similar, further confirming the applicability of using high temperature experiments to evaluate Ile epimerization in this case (Miller *et al.*, 2000). Similarly to Ile, the majority of amino acids cannot readily racemize whilst internally bound (Mitterer and Kriausakul, 1984); therefore, THAA D/L and FAA D/L values for several amino acids were compared for OES (Fig. 4.7).

Between 80 and 140 °C the rates of racemization of all amino acids in the FAA and THAA fractions appear to be equivalent (Fig. 4.7). However, when this comparison is extended to include low temperature sub-fossil samples, the relative rates of reaction are not always equivalent:

- Asx appears to show similar trends of FAA and THAA racemization over the temperature range studied (sub-fossil and kinetic samples), within the THAA D/L range of < 0.4 and > 0.8 (Fig. 4.7A). However, there is a small divergence in trends between sub-fossil samples and kinetic samples in the middle THAA range (D/L ~ 0.4 – 0.7), where heated samples show an increased THAA D/L value for a given FAA D/L value.
- Glx shows a fairly good agreement between samples heated at all temperatures, over the D/L range studied (i.e. THAA D/L < ~0.5) (Fig 4.7B).

- Ser initially shows similar extents of FAA and THAA racemization over the full temperature range (THAA D/L < ~ 0.4) (Fig. 4.7C). However, at THAA D/L > 0.5 the low-temperature sub-fossil data generally shows slightly lower THAA D/L values than high temperature data for the same FAA D/L values.
- Ala shows a good agreement between rates, especially at the later time points (THAA D/L > 0.5) (Fig. 4.7D). There is some deviation in the trends at the lower THAA D/L values where the higher temperatures appear to have higher FAA D/L values than samples exposed to lower temperatures.
- The trends of Val's racemization are very similar at all temperatures studied (Fig. 4.7E). The only exceptions are the early time points of the kinetic experiments which show initial high FAA D/L values which rapidly decrease with time (Sec. 4.3.1.; Fig. 4.4). It is speculated that this initial decrease may be from a small pocket of highly racemized free Val which readily degrade, thus reducing the FAA D/L value. Sub-fossil samples do not follow this trend, which suggests that this is a temperature induced effect, although the reason for this remains unclear.
- Phe generally shows a good agreement over the temperature range studied (Fig. 4.7F). However, when the FAA D/L values approach equilibrium, there is a small difference in trends between the sub-fossil samples and kinetically heated samples, where the sub-fossil samples generally show lower THAA D/L values.
- Ile also generally shows a good agreement over the temperature range studied, although it is not possible to extrapolate the sub-fossil data to ascertain whether this is true for THAA D/L > 0.6 (Fig. 4.7G). There are a small number of 110 °C kinetic samples which initially show high FAA D/L values, which then decrease before joining a similar trend to that of the sub-fossil samples. This is a similar, but less extreme phenomenon as seen with Val (Fig. 4.7E).

These comparisons indicate that the relative rates of racemization of amino acids in the intra-crystalline fraction of OES from high temperature studies cannot necessarily be used to extrapolate accurate rates at low temperatures.

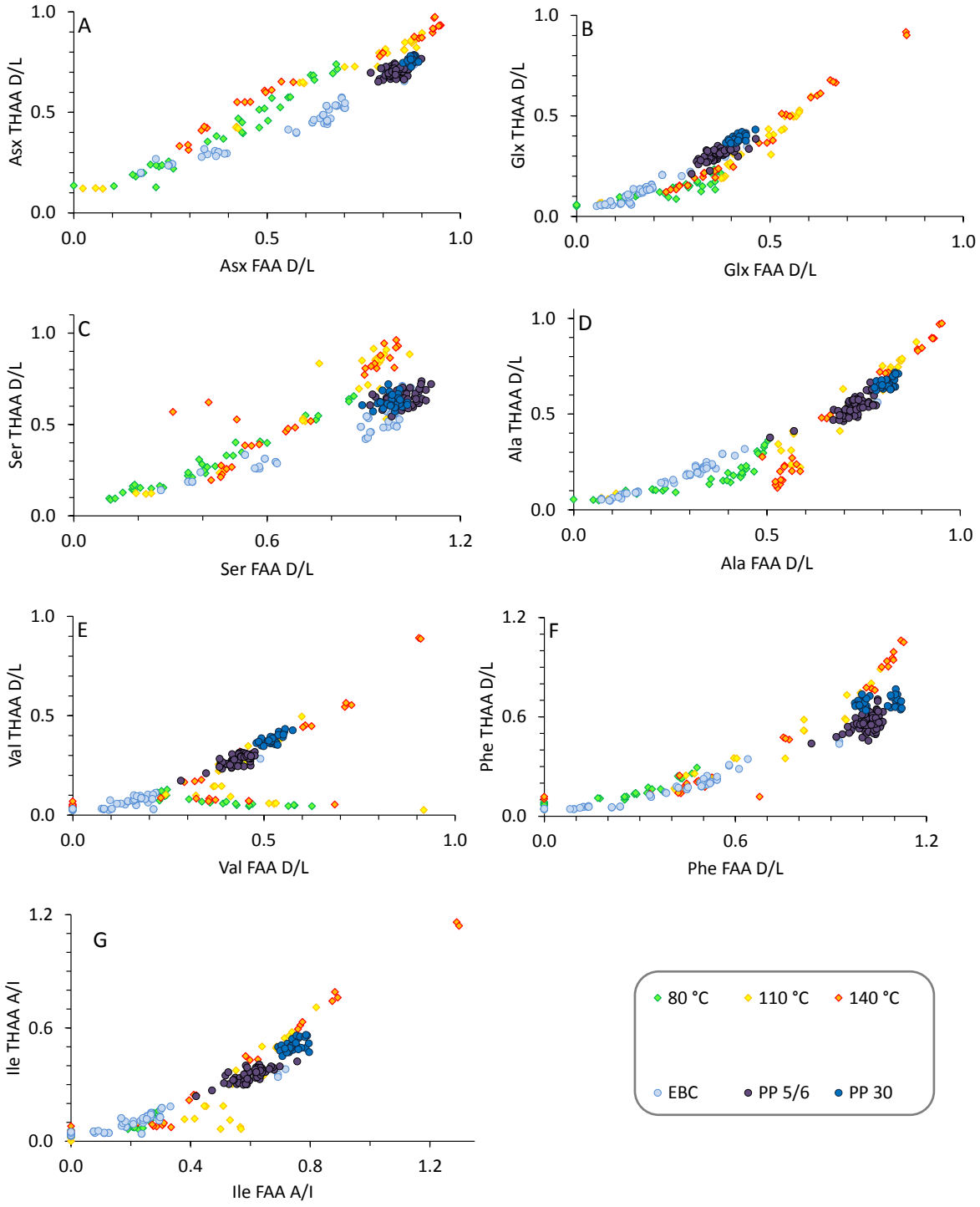

Figure 4.7: Racemization of amino acids within the FAA and THAA fractions for modern samples heated isothermally under kinetic conditions (80 – 140 °C) and unheated sub-fossil samples from Elands Bay Cave (EBC), and Pinnacle point (PP) sites 5/6 & 30. A: Asx, B: Glx, C: Ser, D: Ala, E: Val, F: Phe, G: Ile.

4.4.1.2. Rates of decomposition

Intra-crystalline OES has been shown to act as a closed system; therefore, reductions in THAA compositions are likely to be due to decomposition. The effects of increased temperatures on the THAA concentrations were compared relative to Val THAA D/L (Fig. 4.8). Val was chosen because it generally showed similar trends in FAA and THAA racemization over the temperature range studied, if the initial high FAA D/L values are ignored. Therefore, by comparing decomposition to Val D/L, it is hoped that the variables are limited primarily to Val racemization and the decomposition of the amino acid in question (Fig. 4.8).

Ser, the most thermally unstable amino acid (Vallentyne, 1964), is the only amino acid which displays a rapid decrease in concentration with time (Fig. 4.8C). With the exception of Asx, it appears that the concentrations of all amino acids relative to the extent of Val THAA racemization are similar regardless of the sample's thermal history (Fig. 4.8). This may suggest that for most amino acids decomposition and all directly connected reactions have similar activation energies. Asx is the notable exception as it appears in higher concentrations in sub-fossil samples than heated modern samples for Val THAA D/L values of > 0.2 (Fig. 4.8A). It is therefore unclear whether the concentration differences between the series are significant, or if the pathways of Asx degradation are affected by changing temperatures.

4.4.1.3. Rates of hydrolysis

The rates of racemization and hydrolysis for each amino acid are intrinsically linked (Sec. 1.3.1.). In order to assess whether the temperature dependencies for hydrolysis and racemization were similar for each amino acid the extents of hydrolysis, represented by the absolute FAA concentrations, were compared to the THAA D/L values (Fig. 4.9).

The data indicate that the relative rates of hydrolysis to racemization are higher for sub-fossil samples than samples heated under kinetic conditions (Fig 4.9). Indeed, for some amino acids this difference can even be seen between the 80 °C and 110 °C data sets, most significantly for Glx (Fig. 4.9B), Ser (Fig. 4.9C) and Ala (Fig. 4.9D).

Equating FAA concentration to hydrolysis assumes that the FAAs are only formed through hydrolysis and that decomposition of the FAA fraction is not significant. Although this may be true for most amino acids, notable exceptions are Ala, Glu and Ser:

- Ser is the most thermally unstable amino acid and is seen to readily degrade even at low temperatures in the geological record (e.g. Fig. 4.8C). Therefore, free Ser concentration is

unlikely to give a good representation of the rates of Ser hydrolysis at increased temperatures (Fig. 4.9C).

- Ala is formed from the degradation of Ser (Bada *et al.*, 1978) and Asp (Bada *et al.*, 1978; Bada and Man, 1980). Therefore, it might be expected that the FAA concentration will overestimate the extent of hydrolysis (Fig. 4.9D).
- Free Glu readily form lactams, which depletes the signature in the FAA pool (Wilson and Cannan, 1937), therefore the apparent rates of Glx hydrolysis will be underestimated (Fig. 4.9B).

To assess whether the differences in FAA concentration at increased temperature were due to decomposition, the relative concentrations (e.g. [FAA]/[THAA]) were compared (Fig. 4.10). Assuming that the rates of decomposition are similar for free and bound amino acids, using relative concentrations helps to mitigate against decomposition.

Asx, Glx, Ala, Val and Ile all showed similar trends for the relative FAA concentration (Figs. 4.10A, B, D, E & G) as was observed for the absolute concentrations (Figs. 4.9A, B, D, E & G), albeit to a lesser extent. This indicates that the differences in FAA concentrations may be due to the temperature dependencies of hydrolysis and racemization in these cases. The rates of hydrolysis and racemization at increased temperatures might be expected to be the same if the activation energies were similar. These data suggest that the activation energies for hydrolysis for most amino acids are lower than for racemization, resulting in hydrolysis progressing faster relative to racemization, at lower temperatures.

The differences in absolute free Phe concentration for kinetically heated and sub-fossil samples are suppressed when relative free concentrations are considered (Fig. 4.9F vs. Fig. 4.10F). This may suggest that the differences between hydrolysis and racemization activation energies for Phe are smaller than for other amino acids.

When the relative concentrations of free Ser are considered (Fig. 4.10C) there is a small difference in trends between samples of different temperatures during early degradation (e.g. Ser THAA D/L < 0.3), where the FAA concentrations for sub-fossil samples are higher than that observed for kinetically heated samples. However, when Ser THAA D/L > 0.5 there is no significant difference in FAA concentrations with increased temperatures, this may be because decomposition dominates observed trends of Ser degradation.

As a general rule, racemization progresses at a faster rate when the amino acids are terminally bound. An increase in the rate of hydrolysis, exposing an increased number of terminally bound amino acids, may therefore also increase the rate of racemization. However, if the temperature is low enough (e.g. < 80 °C), then racemization, which requires more energy, may not be able to

'keep up' with the hydrolysis, resulting in a lower extent of racemization in the FAA fraction than if the sample were exposed to temperatures > 110 °C. To test this, the FAA D/L values were compared to the FAA concentrations (Fig. 4.11). For a given FAA concentration the FAA D/L values of heated samples were indeed lower than for unheated samples; this was most clear for Asx (Fig. 4.11A), Ala (Fig. 4.11D), Val (Fig. 4.11E), Phe (Fig. 4.11F) and Ile (Fig. 4.11G). This supports the interpretation that the activation energies for hydrolysis are less than the activation energies for racemization in the intra-crystalline fraction of OES.

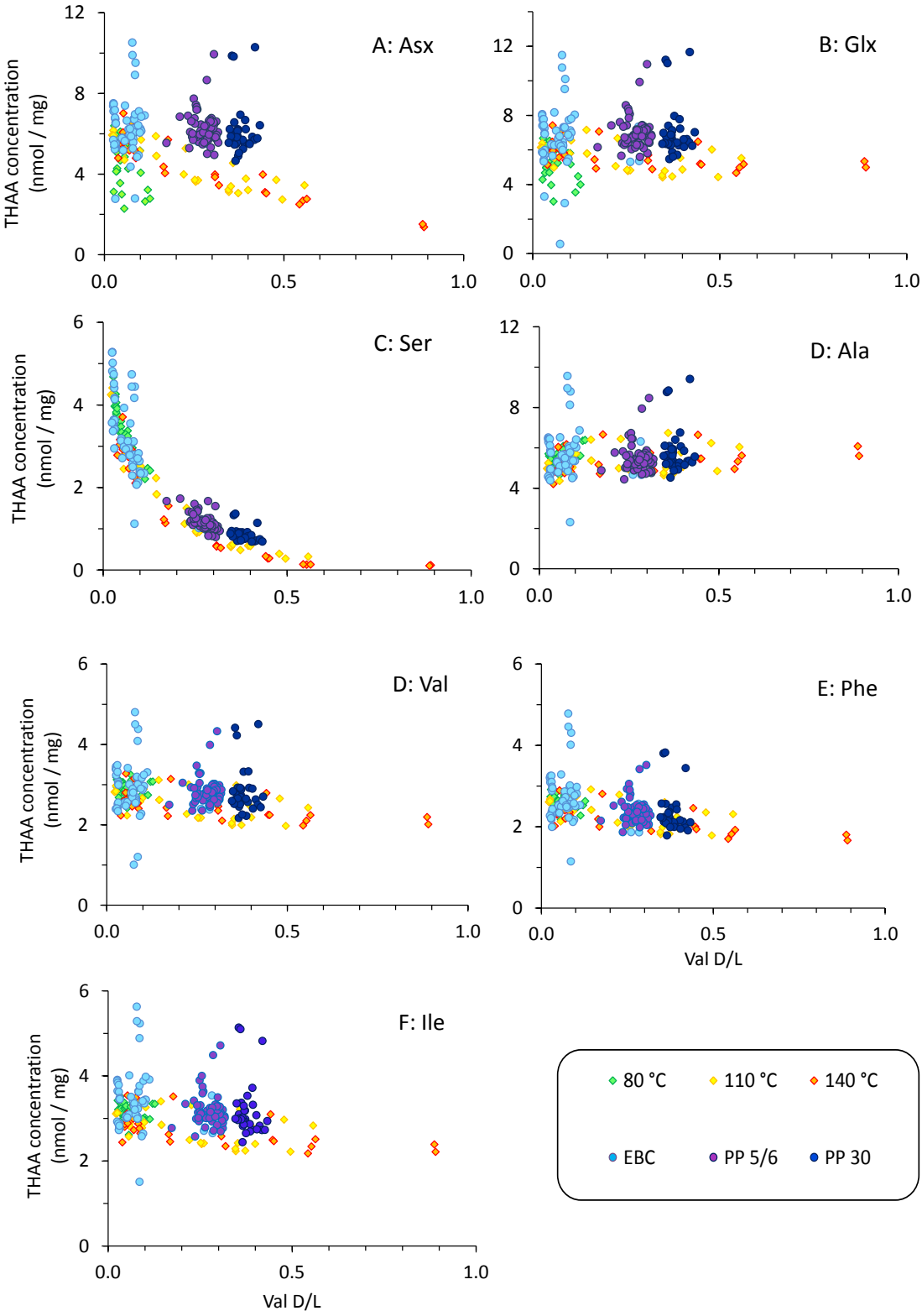

Figure 4.8: THAA concentration of amino acids for modern samples heated isothermally under kinetic conditions (80 – 140 °C) and unheated sub-fossil samples from Elands Bay Cave (EBC), and Pinnacle point (PP) sites 5/6 & 30. Concentrations are plotted against Val THAA D/L values. A: Asx, B: Glx, C: Ser, D: Ala, E: Val, F: Phe, G: Ile.

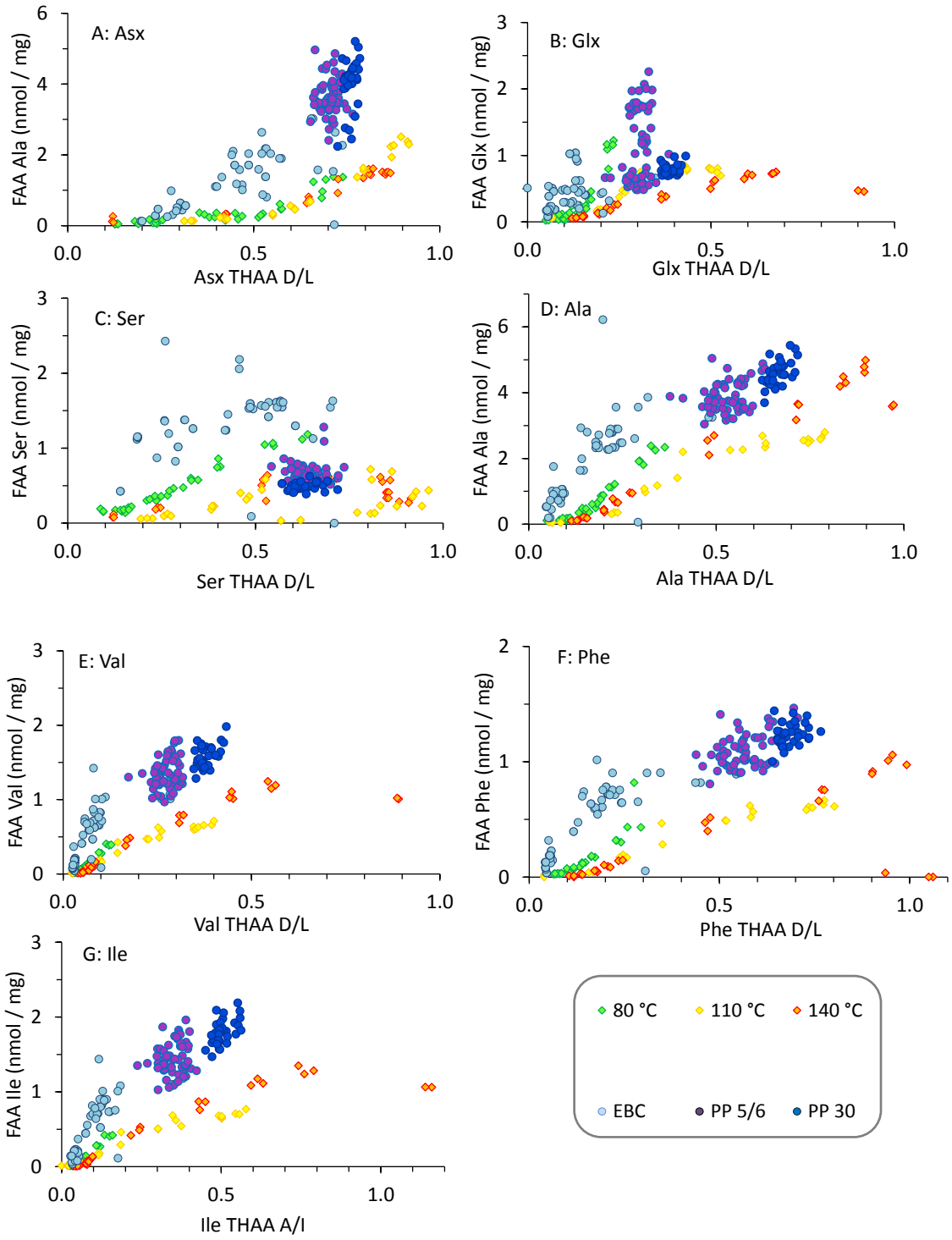

Figure 4.9: Absolute FAA concentrations of amino acids for modern samples heated isothermally under kinetic conditions (80 – 140 °C; diamonds) and unheated sub-fossil samples from Elands Bay Cave (EBC), and Pinnacle point (PP) sites 5/6 & 30 (circles). Concentrations are plotted against THAA D/L values. A: Asx, B: Glx, C: Ser, D: Ala, E: Val, F: Phe, G: Ile.

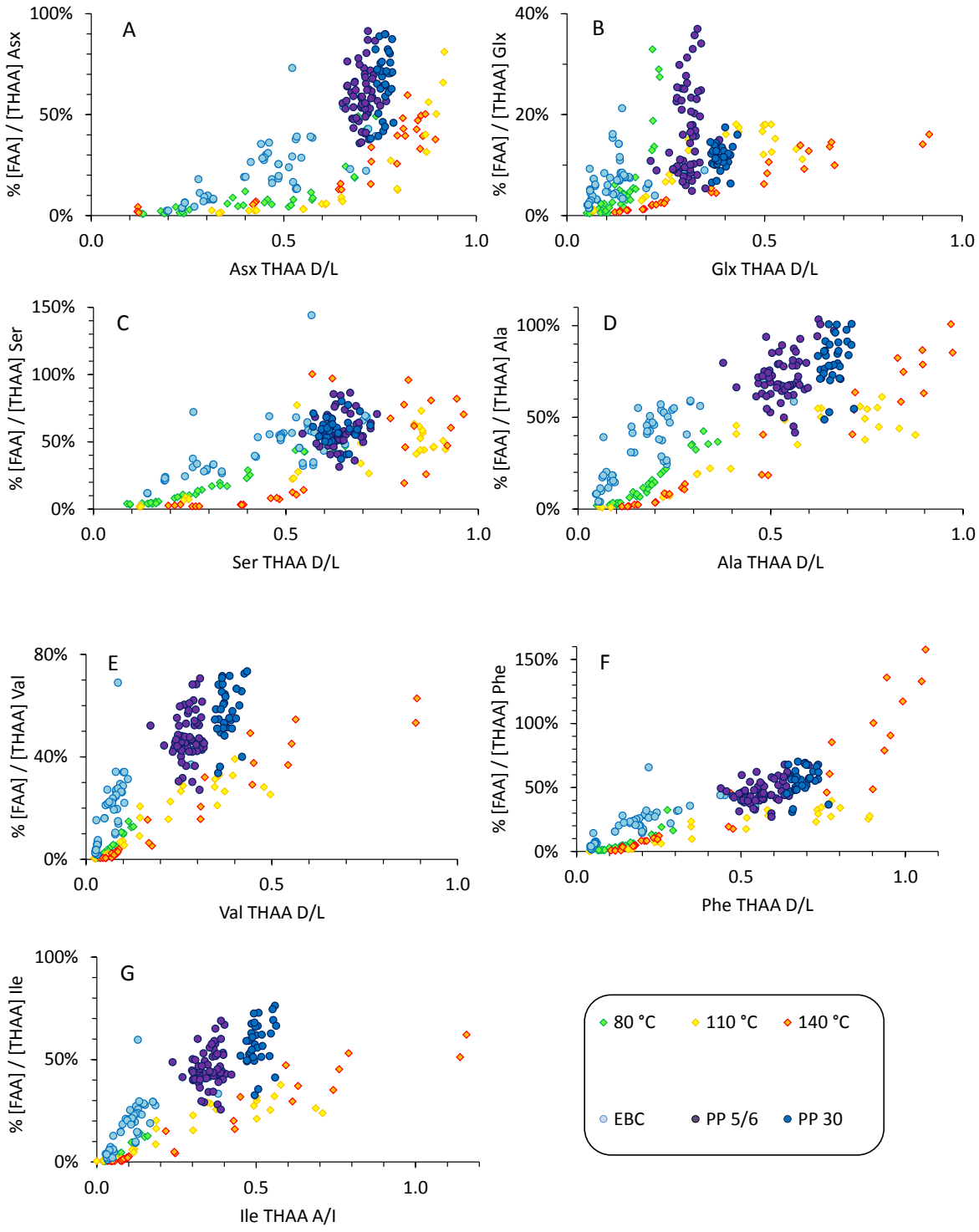

Figure 4.10: Relative FAA concentrations of amino acids for modern samples heated isothermally under kinetic conditions (80 – 140 °C; diamonds) and unheated sub-fossil samples from Elands Bay Cave (EBC), and Pinnacle point (PP) sites 5/6 & 30 (circles). Concentrations are plotted against THAA D/L values. A: Asx, B: Glx, C: Ser, D: Ala, E: Val, F: Phe, G: Ile.

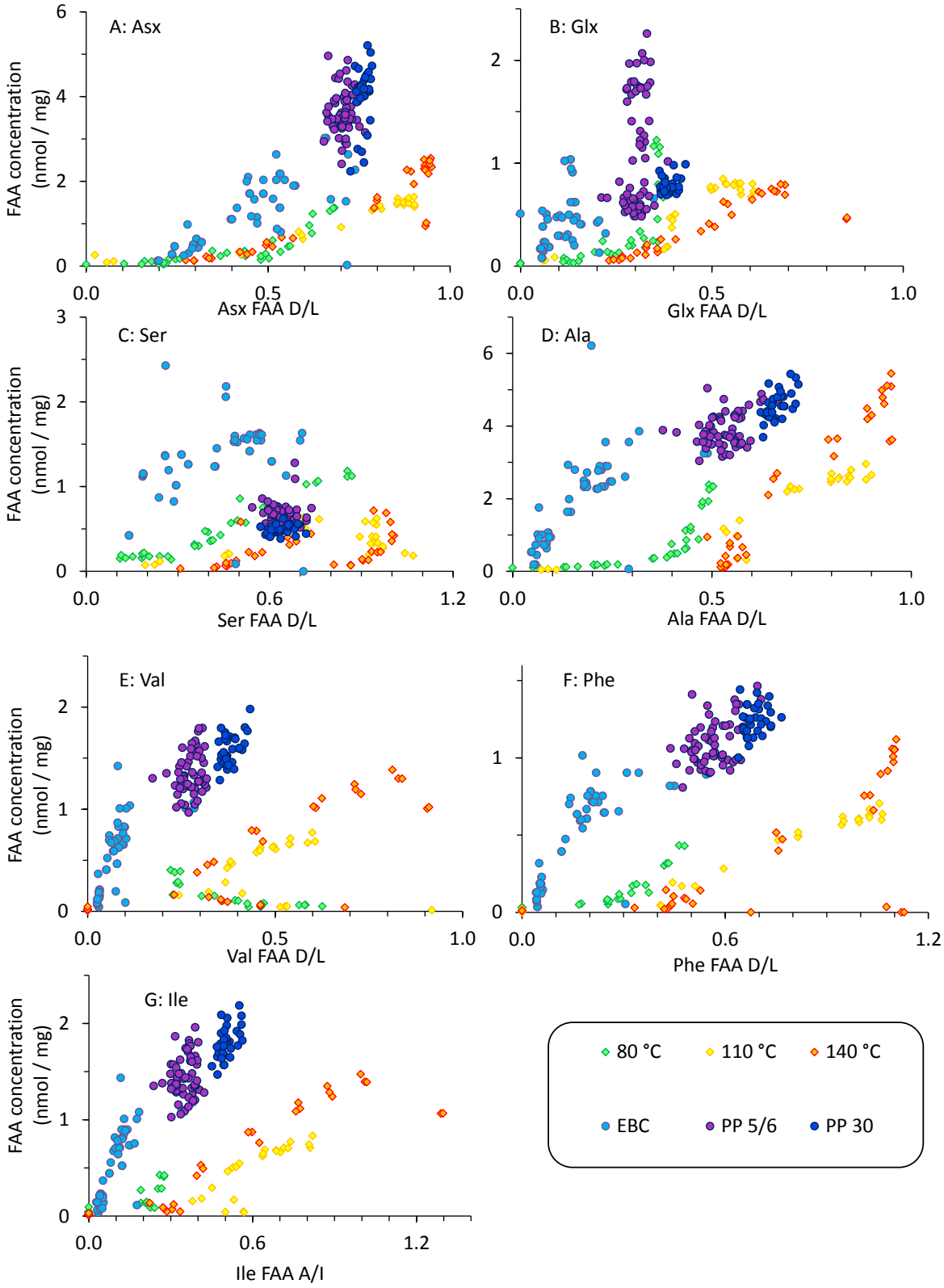

Figure 4.11: Absolute FAA concentrations of amino acids for modern samples heated isothermally under kinetic conditions (80 – 140 °C; diamonds) and unheated sub-fossil samples from Elands Bay Cave (EBC), and Pinnacle point (PP) sites 5/6 & 30 (circles). Concentrations are plotted against FAA D/L values. A: Asx, B: Glx, C: Ser, D: Ala, E: Val, F: Phe, G: Ile.

4.4.1.4. Residual bound fraction

In theory, the FAA concentrations should increase from 0 % to 100 % of the THAA concentration as more amino acids are hydrolysed; the THAA concentrations should slowly decrease due to decomposition. Eventually, it is expected that the FAA and THAA fractions should converge to the same concentration (i.e. when % FAA = 100 %). To that end, the FAA and THAA concentrations for each amino acid were plotted against Val THAA D/L for both kinetically heated modern samples and sub-fossil samples (Fig. 4.12).

The FAA and THAA concentrations do not reach a convergence for samples heated at 80 °C within the time constraints of this study (Fig. 4.12). This is also the case for samples heated at 110 °C, with the exception of Ser (Fig. 4.12B).

The FAA and THAA concentrations of Asx, Ser, Ala and Gly from sub-fossil samples and modern samples heated at 140 °C all converge at the same concentrations. It should be reiterated at this point that the free concentrations of both Gly and Ala have contributions not only from hydrolysis, but also from the degradation of other amino acids (Vallentyne, 1964; Walton, 1998). The FAA concentrations of Glx, Ile, Val and Phe from sub-fossil samples and modern samples heated at 140 °C do not reach 100 % FAA within the time limits of our experiments; for Glx this is likely to be a consequence of the effective removal of free Glx by lactam formation (Wilson and Cannan, 1937). These data imply that there is a fraction of Ile, Val and Phe which does not readily hydrolyse, which may be a consequence of the hydrophobic nature of these amino acids. A fraction of peptides which are resistant to hydrolysis may have implications on the rate of racemization of amino acids which cannot racemize whilst internally bound. A similar phenomenon was observed for Ile, Glx, Phe and Leu in modern heated *Patella* shells (Demarchi, 2009). It has been postulated that this 'residual fraction' may be a consequence of a limited supply of water within the intra-crystalline sites, or perhaps the formation of a hydrolysis resistant fraction of amino acids (Collins and Riley, 2000; Miller *et al.,* 2000).

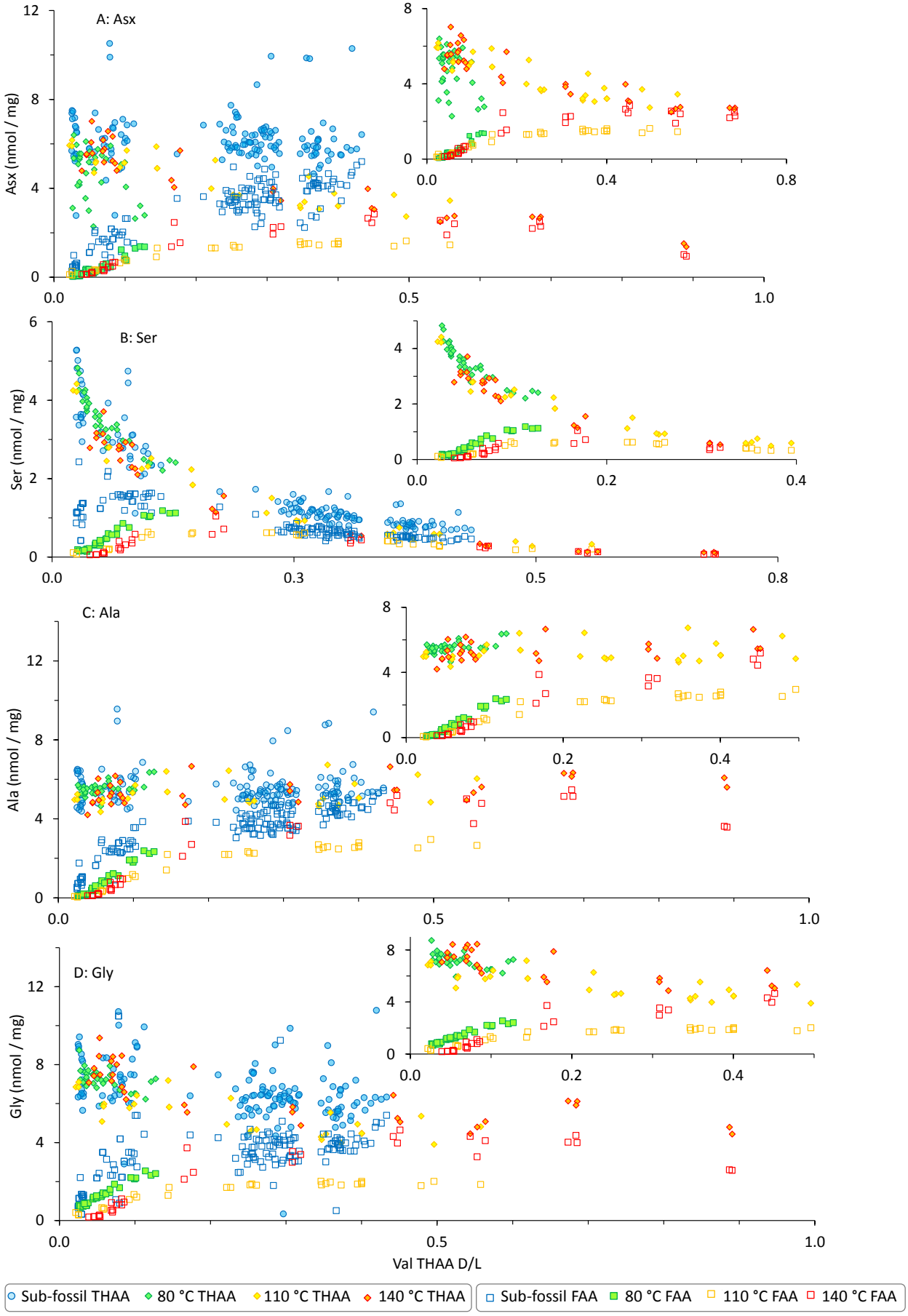

Figure 4.12A-D: FAA and THAA concentrations plotted against Val THAA D/L for modern kinetic samples and sub-fossil samples (inset = kinetic samples only)

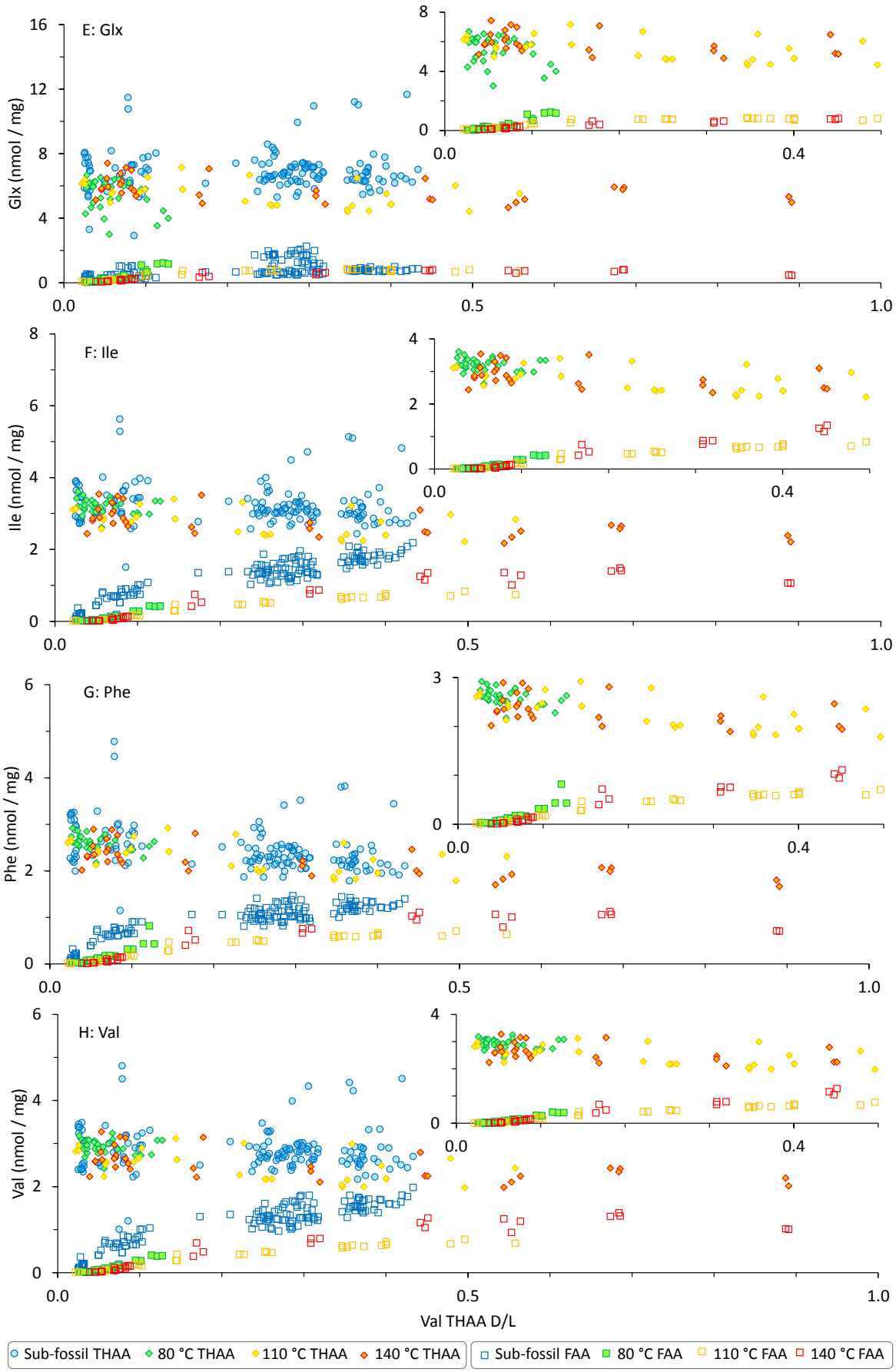

Figure 4.12E-H: FAA and THAA concentrations plotted against Val THAA D/L for modern kinetic samples and sub-fossil samples (inset = kinetic samples only)

4.4.2. Why are plots of FAA D/L vs. THAA D/L insufficient in assessing the relative activation energies of hydrolysis and racemization?

Miller *et al.* (2000) scrutinised the validity of using high temperature kinetic studies with regards to Ile epimerization in *Dromaius* eggshell. They observed the same trends for epimerization of isothermally heated fossil samples (with different thermal histories and A/I values) as isothermally heated modern eggshell. This suggested that the rates of epimerization are independent of a sample's thermal history; they concluded this could only be true if epimerization and all contributing reactions (e.g. hydrolysis) have similar activation energies. The same study also observed that the relationship between THAA A/I and FAA A/I was similar for all heated modern and unheated sub-fossil samples. As Ile cannot racemize when internally bound in a peptide chain, its epimerization is related to its hydrolysis (Mitterer and Kriausakul, 1984). They therefore concluded that the activation energies for Ile hydrolysis and epimerization are similar, further confirming the applicability of using high temperature experiments in regards to Ile epimerization (Miller *et al.*, 2000).

Similarly to Ile in whole-shell *Dromaius* (Miller *et al.,* 2000), the intra-crystalline Ile in OES also shows similar trends of FAA A/I vs. THAA A/I for modern samples heated at 80 -140 °C and sub-fossil samples (Fig. 4.7G). Glx, Phe, Val and Ala also show similar trends of FAA vs. THAA racemization for kinetically heated and sub-fossil samples (Fig. 4.7). As Ile, Glx, Val and Ala cannot racemize whilst internally bound, this may suggest the activation energies for their hydrolysis and racemization reactions are similar (Miller *et al.*, 2000). However, plots of FAA concentrations vs. racemization suggest that hydrolysis may have lower activation energies for Asx, Ala, Val, Phe and Ile (Fig. 4.11).

If the activation energy of Ile hydrolysis is indeed less than the activation energy for Ile epimerization then two hypothetical scenarios may be considered:

1. At high temperatures:
    a. Hydrolysis creates terminally bound Ile
    b. The high temperatures supply sufficient energy to allow the rapid epimerization of the terminal Ile, increasing the Ile THAA A/I value
    c. Hydrolysis releases the highly racemized terminal Ile into the FAA fraction
2. At low temperatures:
    a. Hydrolysis creates terminally bound Ile
    b. The low temperatures impede the rates of epimerization of the terminal Ile, therefore hydrolysis proceeds releasing a fraction of Ile with a lower A/I value than at high temperatures

c. The result of this hypothetical situation is that the A/I values in both the FAA and THAA fractions are lower than for samples of the same extent of hydrolysis but where heated at higher temperatures

This situation, where the lower activation energy of hydrolysis impacts on both the extent of THAA and FAA epimerization, could explain the observation that plots of FAA A/I vs. THAA A/I show the same trends in racemization at different temperatures, whereas plots of FAA concentration vs. THAA A/I do not. This study indicates that similar trends of FAA D/L vs. THAA D/L at increased temperatures may not be sufficient evidence alone to prove that the temperature dependencies of hydrolysis and racemization are similar.

4.4.3. Can high temperature kinetic experiments be used to understand diagenesis at lower temperatures?

The data presented in Sec. 4.3.1. demonstrate that the relationships between competing and/or related degradation reactions are often complex, and the relative rates of these reactions are dependent on the temperatures a sample is exposed to. This study may have important implications for using high temperature kinetic studies to extrapolate rates to lower temperatures, as it suggests that the underlying pathways of degradation are different at higher temperatures. However, without well stratified and well dated deposits of OES and old samples showing the advanced stages of diagenesis, there is little alternative but to use high temperature experiments. Therefore, high temperature studies still have an important part in understanding the diagenetic routes of amino acids within sub-fossil bio-minerals, but caution should be taken as the relative rates of reaction may not be the same at all temperatures. The use of low-temperature data to constrain the observed rates is therefore necessary.

4.5. CONCLUSIONS

Kinetic studies of the intra-crystalline fraction in OES show that Ile, Phe, Val, Ala, Asx, Glx and Ser give predictable trends of hydrolysis and racemization in both the FAA and THAA fractions, and therefore show potential for estimating relative ages of OES samples from archaeological and geological contexts. Previous studies have focused on the use of Ile epimerization, whilst this study shows that other amino acids may also be useful and that studying amino acids with different rates of racemization may have a temporal advantage. Furthermore, studying several rates may act as an internal check for compromised samples as all AAR values should converge at the same ‘age’ (see also Chapter 6).

In order to use these reactions for absolute dating, the Arrhenius parameters need to be calculated accurately, or the rate of racemization needs to be calibrated for a given region and species. The trends of racemization for all amino acids studied over the sub-fossil – 140 °C temperature range are similar, but plots of hydrolysis vs. racemization indicate that hydrolysis reactions are generally more favoured than racemization at lower temperatures. This has also been seen for other bio-minerals, e.g. *Porites* coral (Tomiak *et al.*, 2013) and *Patella* shell (Demarchi *et al.*, 2013b).

Although there are differences between the relative rates of racemization and hydrolysis for amino acids in sub-fossil OES and those heated at 80 – 140 °C, it should be noted that the difference is often small, and that the differences are not uniform for all amino acids. High temperature experiments for some amino acids may therefore be more applicable than for others. It is clear that high temperature kinetic experiments help us to gain an insight into how proteins degrade within OES over geological time. However, caution needs to be taken if these are used solely to extrapolate rates to lower temperatures, as rates are not always equivalent at low and high temperatures, especially in regards to hydrolysis. This argument will be developed in the next chapter by application of mathematical transformations to derive Arrhenius parameters using kinetic data, and kinetic data constrained with low temperature data.

CHAPTER 5: KINETIC MODELLING: CALCULATION OF ARRHENIUS PARAMETERS

5.1. Introduction

In order to utilize AAR as an absolute (rather than a relative) dating method, protein diagenesis needs to be accurately described and calibrated for a given geographic region (see Chapter 6), and ideally, accurate kinetic parameters derived. Arrhenius parameters (e.g. activation energies and frequency factors) may then be used to extrapolate ages over geological time spans (e.g. Bada and Schroeder, 1972; Brooks *et al.,* 1990; Miller *et al.*, 1999; Kaufman, 2000). Indeed, if the activation energies of several reactions with different energies can be calculated accurately, this may negate the need to know the thermal history of the sample, as the Arrhenius equation may be solved simultaneously (e.g. Miller *et al.,* 1999).

Racemization of free amino acids in aqueous solution has been shown to follow reversible first order reaction kinetics (RFOK) (cf. Bada and Schroeder, 1972, 1975; Smith *et al.*, 1978; Smith and Reddy, 1989); where the forward rate constant (k_1) and reverse rate constants (k_2) are the same. Therefore the rate equation can be expressed as:

$$-d[L] / dt = k_1 [L] - k_2 [D] \qquad \textit{(Equation 5.1)}$$

where [L] and [D] are the concentrations of the L and D amino acids. The integrated rate for this reaction can be expressed as (Bada and Schroeder, 1972, 1975):

$$ln \{ (1 + D/L) / (1 - K' (D/L)) \} - constant = (1 + K') k_1 t \qquad \textit{(Equation 5.2)}$$

where $K' = 1 / K = k_2/k_1$, t = time (s) and the *constant* accounts for racemization induced by sample preparation. For most amino acids $k_1 = k_2$, therefore Eq. 5.2 can be simplified to:

$$ln \{ (1 + D/L) / (1 - (D/L)) \} - constant = 2kt \qquad \textit{(Equation 5.3)}$$

If $ln\{(1+D/L)/(1-D/L)\}$ yields a straight line when plotted against time (Eq. 5.3), then it suggests that the mechanism may follow first order reversible kinetics where the gradient = $2k$.

Amino acids with two chiral centres (such as Ile), may exhibit forward and reverse rates of racemization that are not equal. The favoured racemization reaction for L-Ile (I) is the epimerization to D-alle (A), where k_1 is the rate constant for L-Ile → D-alle and k_2 for D-alle → L-Ile

and $k_1 > k_2$ (Bada and Schroeder, 1975). The epimerisation of Ile has been found to equilibrate at A/I of 1.3, and thus the integrated rate law becomes (Wehmiller and Hare, 1971; Bada and Schroeder, 1975):

$$ln \{(1 + A/I) / (1 – 0.77 \times A/I)\} – constant = 1.77\ kt \qquad \textit{(Equation 5.4)}$$

Assuming conformity to the Arrhenius equation (Eq. 5.5), the calculated rate constants (k) from different temperatures can be used to calculate the kinetic parameters (E_A and A) by way of a plot of the integrated form of the Arrhenius equation (Eq. 5.6), i.e. a plot of $ln\ (k)$ vs. $1 / T$ should give a straight line with a gradient equal to $– E_A / R$ and y-axis intercept of $ln\ A$.

$$k = A\ exp(-E_A / RT) \qquad \textit{(Equation 5.5)}$$

$$ln(k) = (-E_A / RT) + ln\ A \qquad \textit{(Equation 5.6)}$$

where k = rate constant (s^{-1}), A = frequency factor (s^{-1}), E_A = activation energy (kJ mol^{-1}), R = molar gas coefficient (kJ mol^{-1} K^{-1}), T = temperature (K).

Many kinetic AAR studies have focused on whether the racemization of amino acids in bio-minerals show conformity to RFOK; indeed, many studies have shown that this is the case for some bio-minerals within certain D/L ranges (Brooks *et al.*, 1990; Miller *et al.*, 1991, 1992, 1997, 2000; Clarke, 2005). Studies using ratite eggshells have mainly focussed on Ile epimerization, with some evidence that this reaction obeys RFOK. However, due to the inherent complexity of the system within bio-minerals (e.g. degradation of the protein, decomposition and condensation reactions, different and changing environments of the amino acids), it is unlikely that racemization within bio-minerals truly conforms to RFOK (e.g. Wehmiller and Hare, 1971; Wehmiller, 1980; Mitterer and Kriausakul, 1989; Stephenson and Clarke, 1989; Collins and Riley, 2000; Clarke and Murray-Wallace, 2006; Crisp *et al.,* 2013; Demarchi *et al.,* 2013b; Tomiak *et al.,* 2013). Therefore, in this chapter 'RFOK' is suffixed with 'a' to denote the 'apparent' conformity to RFOK (RFOKa, notation as used by Clarke and Murray-Wallace, 2006).

Due to the well-documented non-conformity of many amino acids to RFOK, there has been a shift towards using empirical mathematical transformations to linearize the extent of racemization with time, for example power transformations (e.g. Manley *et al.,* 2000; Sec 5.2.1.2.) and parabolic curves (Mitterer and Kriausakul, 1989) (see review by Clarke and Murray-Wallace, 2006). It is recognised that these transformations are not ideal as they lack a full underlying chemical rationale, aiming instead to calculate a single apparent activation energy from observed racemization, which is itself the result of several different rates. However, the complexity of the underlying mechanisms and non-conformity to RFOK leaves little alternative.

In this chapter a number of approaches have been used in an effort to estimate the Arrhenius parameters for amino acid racemization and hydrolysis. No attempt was made to derive kinetic parameters for the degradation reactions, as within the timescales of the kinetic experiments degradation had not progressed far enough. The rate of amino acid degradation is slower than racemization and hydrolysis; by 241 h of heating at 140 °C the majority of amino acids still persist at > 60 % of their initial concentrations, the only exceptions being Asx and Ser (Sec. 4.3.3.; Fig. 4.5).

The approaches used to describe the rates of racemization are:

- Reversible first order kinetics (RFOK; Sec. 5.2.1.1.),
- Constrained power kinetics (CPK; Sec. 5.2.1.2.), and
- Scaling method (Sec. 5.2.1.3.).

The approaches used to describe the rates of hydrolysis are:

- Irreversible first order kinetics (IFOK; Sec. 5.2.1.4.), and
- Scaling method (Sec. 5.2.1.5.).

This chapter is divided into two main sections; the first considers the high temperature kinetic data only, the second part considers the impact of the inclusion of low temperature sub-fossil data on the estimated Arrhenius parameters.

5.2. DESCRIBING THE RATES OF REACTION FOR HIGH TEMPERATURE KINETIC DATA

5.2.1. Apparent reversible first order kinetics (RFOKa) of racemization

Plots of *ln{(1+D/L)/(1-D/L)}* vs. *t* (Eq. 5.2; 5.3) for the intra-crystalline proteins in OES show linearity for most amino acids over limited ranges of D/L values (Fig. 5.1, Table 5.1; Appendix B). A cut-off value was chosen to exclude data with an R^2 value < 0.97 (where R^2 refers to the coefficient of determination); these data are not presented, as it is not possible to linearize them using this transformation. The kinetic parameters (E_A and A) were then calculated using a plot of the integrated form of the Arrhenius equation (Eq. 5.6), e.g. a plot of *ln (k)* vs. *1 / T* giving a straight line with the gradient = - E_A / R (Fig. 5.2; Table 5.1; Appendix B).

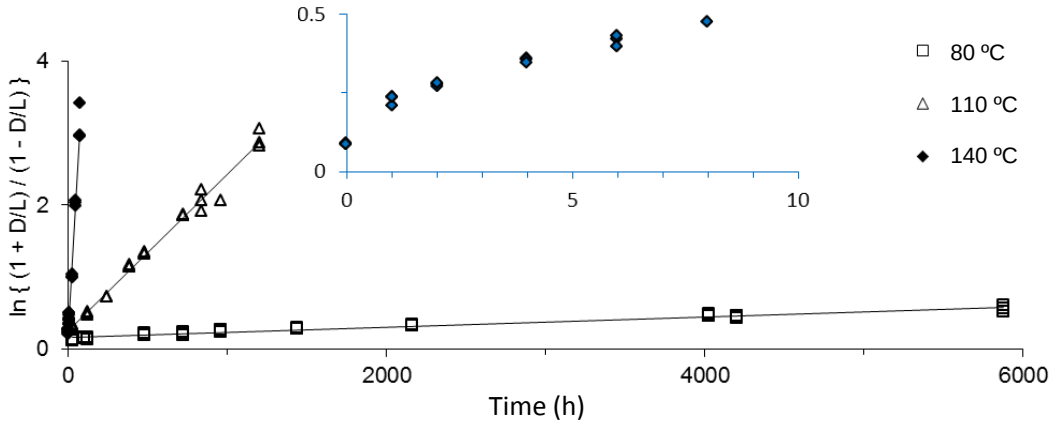

Figure 5.1: D/L data transformed assuming apparent reversible first order kinetics (Eq. 5.2) for the total hydrolysable fraction of Phe in OES isothermally heated at 80 °C, 110 °C and 140 °C. The inset shows the 140 °C data zoomed in to show the non-conformity to the expected linear relationship during the early stages of racemization. A linear relationship suggests reversible first order kinetics are obeyed, with the gradient proportional to the rate constant for that temperature.

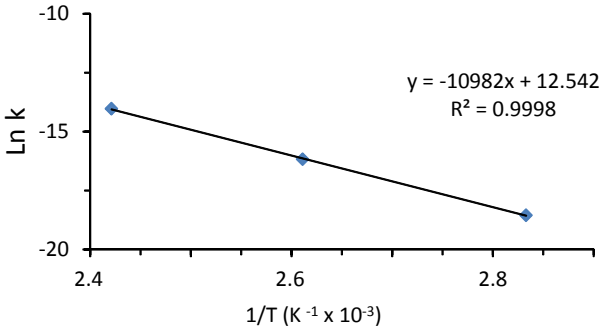

Figure 5.2: Arrhenius plot for Phe racemization with rates estimated using RFOKa

Amino acid	Plot of ln{(1+D/L)/(1-D/L)} vs. time						Arrhenius Plot		
	80 °C		110 °C		140 °C		R^2	E_A (kJ mol^{-1})	lnA
	D/L range	R^2	D/L range	R^2	D/L range	R^2			
Ala	0.1 – 0.3*	0.9699	0.20 – 0.75	0.9934	0.1 – 0.83*	0.9916	1.0000	117	22
Val	0 – 0.15*	0.9729	0.00 – 0.60	0.9850	0.0 – 0.89*	0.9944	0.9989	120	22
Phe	0.1 – 0.3*	0.9713	0.15 – 0.90	0.9885	0.1 – 0.90*	0.9912	1.0000	127	25
Ile	0 – 0.16*	0.9749	0.00 – 0.73	0.9884	0.0 – 0.88*	0.9880	0.9992	121	22
Ser	0.1 – 0.6*	0.9821	0.10 – 0.85	0.9839	0.1 – 0.85	0.9686	0.9999	121	24

*Table 5.1: R^2 values from plots of ln{(1+D/L)/(1-D/L)} vs. time over given linear ranges (as Fig. 5.1) and the activation energies, frequency factors (A) and R^2 values calculated from Arrhenius plots as in Fig. 5.1 inset; full data are available in Appendix B. * indicates that the upper limit is due to the time limit of the experiment and therefore it is unknown whether the data deviates from linearity beyond this point.*

The racemization of several amino acids (e.g. Ile, Phe, Val and Ala) shows some conformity to RFOKa in OES for a limited range of D/L values. However, early stages of racemization often deviate from linearity (Fig. 5.1, inset) and the correlation between *ln(1+D/L)/(1-D/L)* and time are in all cases better described by a non-linear correlation, rather than linear trend-lines dictated by RFOK (i.e. R^2 values for second order polynomials in all cases were higher than for linear regression lines). Furthermore, the calculated rate constants vary depending on the range of D/L values included, which should not be the case in true RFOK, i.e. for free amino acids in water (Bada, 1985). The observed kinetics of amino acids in the intra-crystalline fraction of OES are not fully described by a linear relationship. This indicates that the assumption that racemization proceeds via RFOK is unlikely to be valid for intra-crystalline amino acids in OES.

5.2.2. Constrained power-law kinetics (CPK) applied to Asx and Glx racemization

Asx and Glx, unlike other amino acids, show very little conformity to RFOKa (Fig. 5.3), and so alternative transformations were used to linearize the observed racemization with respect to time. Asx racemization reaction kinetics are more complex than many other amino acids, due in part to the contribution of Asn (Hill, 1965; Geiger and Clarke, 1987; Brinton and Bada, 1995) and the succinimidyl-mediated racemization of both Asn and Asp (Goodfriend and Hare, 1995).

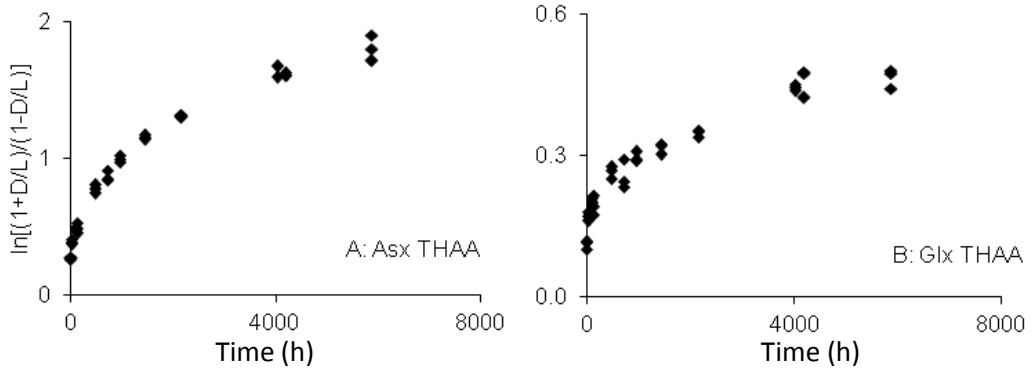

Figure 5.3: D/L data transformed assuming apparent reversible first order kinetics (Eq. 5.3) for the intra-crystalline total hydrolysable fraction (THAA) in OES isothermally heated at 80 °C (same trend observed at 110 °C and 140 °C). The deviation from a linear relationship suggests reversible first order kinetics are not obeyed for A: Asx and B: Glx.

A number of commonly-used mathematical transformations were tested to linearize the observed Asx racemization, including parabolic curves (Mitterer and Kriausakul, 1989), RFOK (e.g. Sec. 5.2.1.) and simple power transformations (e.g. Manley *et al.,* 2000) (see Appendix B). The strongest correlation between transformed D/L values and time was achieved using the constrained power–law kinetic (CPK) transformations (e.g. Kaufman, 2000; Manley *et al.,* 2000; Kaufman, 2006):

$$ln[(1 + D/L) / (1 - D/L)]^n = kt + constant \qquad \textit{(Equation 5.7)}$$

CPK was developed to describe the racemization of Asx and Glx within the whole shell protein of molluscs (Manley *et al.,* 2000), ostracods (Kaufman, 2000) and foraminifera (Kaufman, 2006). CPK has an advantage over alternative transformations in that it has an asymptote converging on one, mimicking the D/L equilibrium, therefore better describing the observed racemization.

A heuristic approach was taken to find the power (n) which gave the highest R^2 value for all of the temperatures, which was found to be 2.3 for Asx (D/L range used: 0 – 0.7 for 80 °C and 140 °C; 0 – 0.73 for 110 °C). A plot of $ln[(1 + D/L) / (1 - D/L)]^n$ vs. time gives a gradient equal to k (Fig. 5.4). Using the Arrhenius equation, a plot of *ln (k)* vs. *1 / T* gives a straight line with gradient = $- E_A / R$; E_A was calculated as 131 kJ mol^{-1} for Asx using CPK (Table 5.2). CPK was also used to linearize the racemization observed for Glx, which showed poor conformation to RFOKa and parabolic curve fitting (Appendix B.). The power (n) which gave the highest R^2 value for all of the temperatures was found to be 2.2. Using this model, the E_A for Glx racemization was calculated to be 147 kJ mol^{-1}, when D/L < 0.6 (Table 5.2).

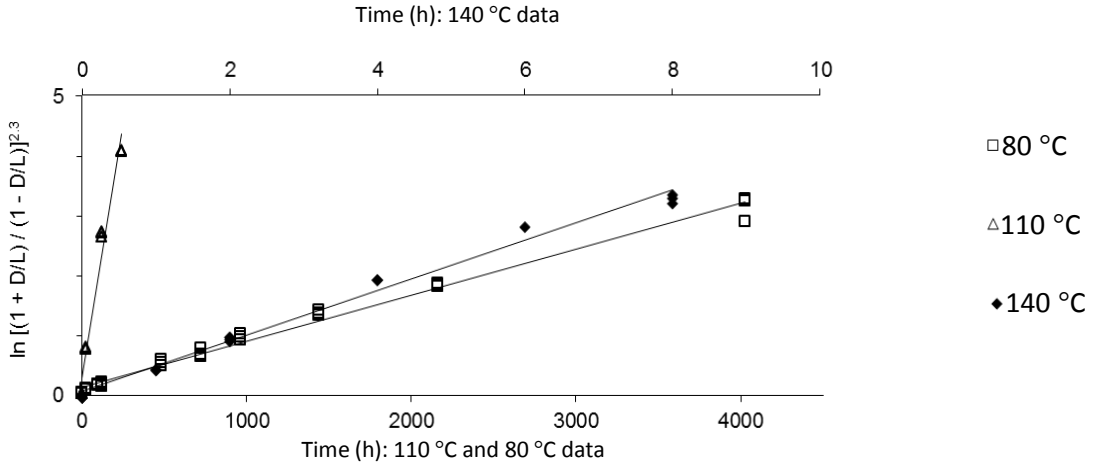

Figure 5.4: D/L values transformed using constrained power-law kinetics (Eq. 5.7) for the total hydrolysable fraction of Asx amino acids in the intra-crystalline fraction of OES heated isothermally at 80 °C, 110 °C and 140 °C. This transformation describes a linear relationship with the gradient proportional to the rate constant at each of the temperatures. Note: the 140 °C data are scaled differently (upper x-axis) to the 110 °C and 80 °C data sets (lower x-axis).

Amino acid	Integrated rate plot summary (Fig. 5.3; Appendix B)						Arrhenius Plot		
	140 °C		110 °C		80 °C		R^2	E_A (kJ mol^{-1})	Ln A
	D/L range	R^2	D/L range	R^2	D/L range	R^2			
Asx	< 0.65	0.9959	< 0.65	0.9957	< 0.68	0.9945	1.0000	123	26
Glx	< 0.61	0.9729	< 0.62	0.9714	< 0.23*	0.9706	0.9973	138	28

*Table 5.2: Summary of Arrhenius parameters estimated for Asx and Glx racemization using rates estimated using the constrained power-law kinetics. * = highest D/L value dictated by final time point in the experiment.*

5.2.3. Scaling method applied to rates of racemization

A new 'scaling method' was also attempted, with the aim of estimating the kinetic parameters of racemization using relative rate constants (Demarchi *et al.*, 2013b; Tomiak *et al.*, 2013), as opposed to absolute rate constants. The rationale behind this method is based on the observation that the curve describing racemization (and hydrolysis), for the three different temperatures studied may be characterised by the same shape.

Plotting against time (e.g. in minutes) biases towards later time points, e.g. a reasonably high R^2 value can be achieved even when there is an initial non-conformity to RFOK. Therefore, time is

plotted as a log value- reducing this bias. Third order polynomial expressions were found to best describe the shape of the log time vs. racemization (or hydrolysis) trend (Demarchi *et al.*, 2013b; Tomiak *et al.*, 2013).

The observed trends of racemization (or hydrolysis) for each temperature are then overlapped, by scaling of the log-scaled time axis. To ensure the best fit, third order polynomial functions are used to describe the observed racemization (or hydrolysis) (Fig. 5.5). An advantage of this approach is that the data are not forced to conform to a straight line, which can result in later time points prejudicing against earlier ones (an issue for RFOKa). Using a Generalized Reduced Gradient Algorithm (Microsoft Solver), the scaling factors for the 80 °C and 140 °C data were optimised to minimise the least squares difference between the fitted curves (sum of squares; Table 5.2).

An arbitrary relative apparent rate constant for racemization of '1' is assumed for the 110 °C data; the relative rates for 80 °C and 140 °C are calculated by multiplying the assumed 110 °C rate by the scaling factors. Due to the nature of the experiment itself, the 140 °C data are mainly fitted over the later stages of reaction and the 80 °C over the earlier stages. The 'scaling factors' are therefore synonymous with the relative reaction rates calculated using other techniques, such as RFOK. The apparent relative rates can then be applied to the Arrhenius equation (e.g. Eq. 5.6) to estimate the effective activation energies, although the use of relative rates prohibits the calculation of the frequency factors. Using this method, activation energies for all seven well-resolved amino acids can be estimated (Table 5.3).

It is important to note that this new approach has no underlying chemical rationale, analogous to some of the alternative mathematical transformations (e.g. Sec. 5.2.2.). A single apparent activation energy is still estimated from observed racemization, which is itself not a single rate, as the observed racemization has contributions from a number of rates (for example, differently bound amino acids: free, internally bound, terminally bound, etc.).

The activation energies reported are the average energies calculated from the 80 – 110 °C range and the 110 – 140 °C range; therefore representing the estimated activation energies over the 80 – 140 °C temperature range. These should be equivalent to the energies calculated using alternative techniques over similar ranges. Reporting an average value assumes that the activation energies for the two temperature ranges are similar, which is not always the case (e.g. Glx, Ala and Phe, Table 5.3; Appendix B) and may represent the changing simulated diagenetic environment at different temperatures.

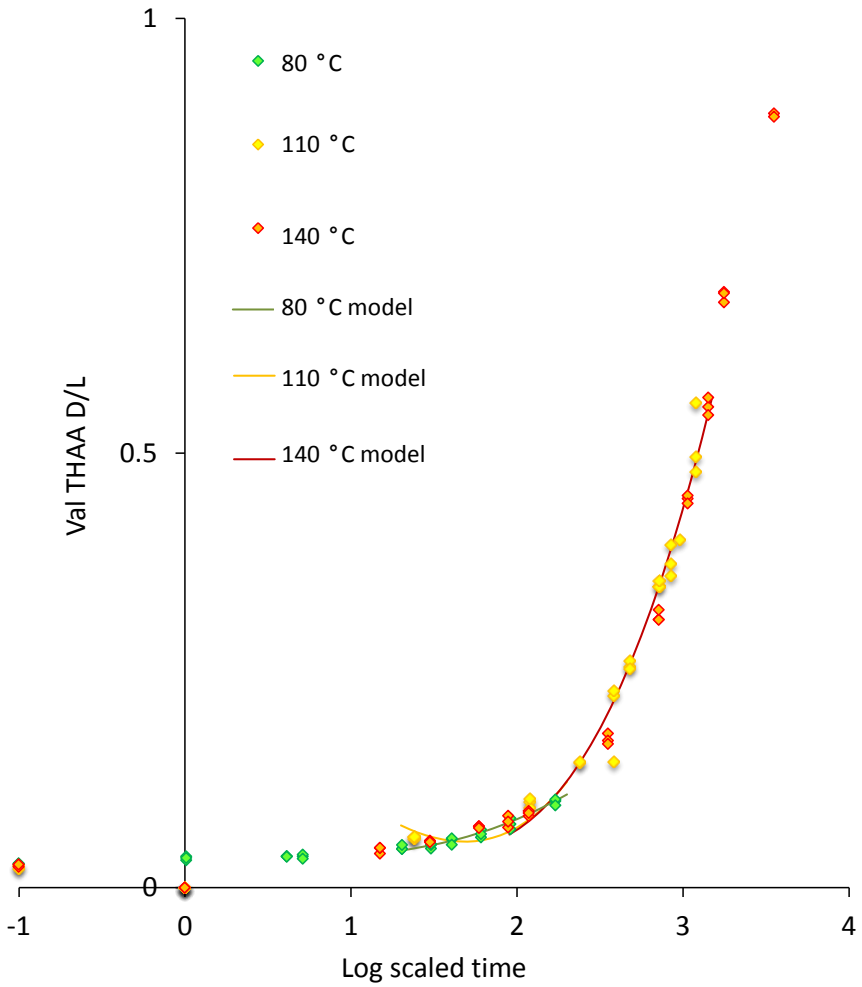

Figure 5.5: D/L values of the total hydrolysable amino acid (THAA) fraction of intra-crystalline proteins within OES. The data are transformed using the scaling method, where the log time x-axes of 80 °C and 140 °C are scaled relative to 110 °C data series to get the maximum overlap of D/L values between the temperatures. Models are second order polynomials of the data within limited D/L ranges (Table 5.2). Val THAA D/L is shown, for Asx, Glx, Ser, Ala, Phe and Ile see Appendix B.

Amino acid	80 °C relative to 110 °C				140 °C relative to 110 °C				Summary data from Arrhenius plot (80 – 140 °C)	
	Relative rate	Range (D/L values)	Sum of squares	E_A (kJ mol^{-1})	Relative rate	Range (D/L values)	Sum of squares	E_A (kJ mol^{-1})	E_A (kJ mol^{-1})	R^2
Asx	0.03	0.37 ↓ 0.72	0.003	122	16.0	0.44 ↓ 0.93	0.010	128	125	0.9998
Glx	0.01	0.19 ↓ 0.26	0.002	122	16.2	0.25 ↓ 0.69	0.001	162	144	0.9937
Ser	0.03	0.22 ↓ 0.69	0.008	120	15.2	0.20 ↓ 0.86	0.001	131	126	0.9992
Ala	0.02	0.21 ↓ 0.36	0.004	112	12.7	0.19 ↓ 0.94	0.036	143	129	0.9952
Val	0.04	0.06 ↓ 0.11	0.003	118	14.8	0.06 ↓ 0.57	0.000	118	118	1.0000
Phe	0.02	0.14 ↓ 0.29	0.006	125	17.3	0.17 ↓ 0.95	0.067	142	134	0.9987
Ile	0.04	0.06 ↓ 0.15	0.004	116	14.1	0.08 ↓ 0.79	0.006	123	120	0.9997

Table 5.3: Summary of racemization kinetic parameters calculated using the scaling method with kinetic OES samples. Rates are expressed relative to a 110 °C rate of '1'. Cells highlighted in grey indicate a poor correlation between the calculated activation energies (E_A) for the different temperature ranges (> 15 kJ mol^{-1} difference).

5.2.4. Irreversible first order reaction kinetics for hydrolysis

The rates of hydrolysis were estimated by application of irreversible first order reaction kinetics (IFOK), as Miller *et al.* (1992) applied to Leu hydrolysis, where:

$$Rate\ of\ hydrolysis = -d\,[Bound] / dt = [Bound]\,k \qquad (Equation\ 5.8)$$

Where *[Bound]* is the concentration of amino acids within peptides, *k* = rate constant for hydrolysis, *t* = time

The integrated rate law is given as:

$$Ln\,([Bound] / [Total]) = -kt \qquad (Equation\ 5.9)$$

To help account for decomposition reactions, the total concentration is calculated individually for each time point. This method is also beneficial when analysing archaeological samples, as an initial THAA concentration need not be assumed.

As with RFOKa, the 'a' denotation is employed to show that even if IFOK can describe the observed kinetics, it is very unlikely the reactions are true first order reactions, due to the complexity of the system and different amino acid environments.

Plots of the integrated rate law (Eq. 5.9) for each temperature (e.g. Fig. 5.6; Appendix B) allow the observed rate constants to be calculated from the gradient (gradient = $-k_{obs}$), which should yield a straight line if the reaction mechanism conforms to IFOKa. The observed rates of hydrolysis for most of the amino acids showed poor conformity to linearity (Fig. 5.6; Table 5.4; Appendix B). This suggests that the mechanism of hydrolysis is not a true first order reaction mechanism, although it may be used to describe the hydrolysis over limited %FAA ranges. An Arrhenius plot (e.g. Eq. 5.6) allows calculation of the activation energy and frequency factors from the observed rate laws (Table 5.4).

Miller *et al.* (2000) found that the initial stages of Leu hydrolysis followed IFOK, while at later stages of degradation (A/I > 1) it was hypothesized that decomposition and other competing reactions cause deviation from IFOK. Unfortunately, using our RP-HPLC method, D-Leu has a co-eluting peak, compromising the accuracy of the estimates of Leu hydrolysis, and so it was not possible to make a direct comparison with the reported results for *Dromaius* (Miller *et al.,* 2000).

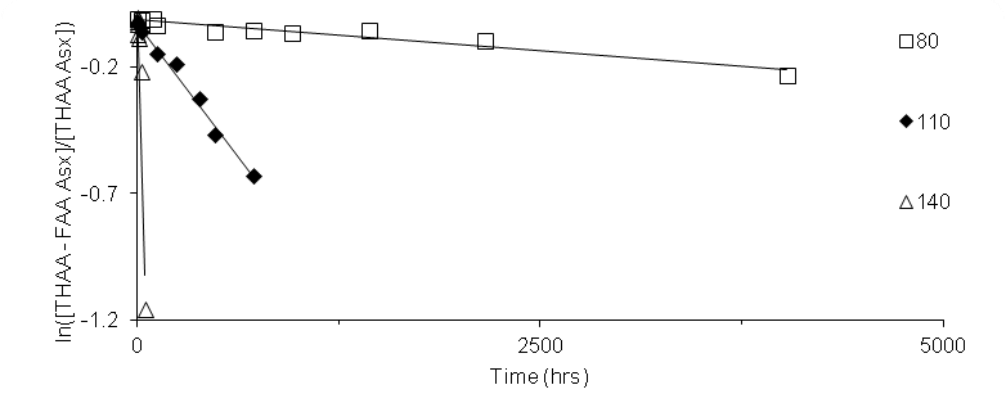

Figure 5.6: Natural log of the relative concentration of free amino acid (FAA) to total hydrolysable amino acids (THAA) in the intra-crystalline fraction of OES when heated isothermally at 80 °C, 110 °C and 140 °C. This transformation, assuming irreversible first order kinetics (Eq. 5.8 & 5.9) should yield a linear correlation where the gradient is proportional to the rate constant for hydrolysis at each temperature. Asx is shown above; for Glx, Ser, Ala, Phe, Ile and Val see Appendix B.

Amino acid	IFOKa: $[Bound]_t = [THAA]_t - [FAA]_t$								
	Calculation of rate constants						Arrhenius Plot		
	80 °C		110 °C		140 °C				
	%FAA Range	R^2	%FAA Range	R^2	%FAA Range	R^2	E_A (kJ mol^{-1})	ln A	R^2
Asx	< 21	0.8308	< 47	0.9771	< 46	0.9582	99	24	0.9973
Glx	< 15	0.8511	< 18	0.9454	< 9	0.9245	83	18	0.9951
Ser	< 48*	0.9799	< 69	0.9531	3 – 12	0.9280	107	27	0.9977
Ala	< 38*	0.9764	< 53	0.9642	< 78	0.9076	119	31	0.9776
Val	< 13*	0.9898	< 38	0.9250	< 42	0.9085	114	31	0.9810
Phe	< 18*	0.9891	< 26	0.9108	< 44	0.9673	91	28	0.9962
Ile	< 13*	0.9794	< 34	0.9254	< 73	0.9082	114	21	0.9998

*Table 5.4: Hydrolysis kinetic parameters calculated using IFOKa; E_A is the activation energy, A is the frequency factor; cells highlighted in grey indicate a poor correlation to first order kinetics ($R^2 < 0.90$). * indicates that the upper limit is due to the time limit of the experiment and not that the data deviates from linearity.*

The observed rates of hydrolysis for most amino acids were poorly described using IFOKa (Table 5.4). Therefore an alternative scaling method was also used, similar to that described in Section 5.2.3., using time log plots vs. %FAA (Table 5.5). The activation energies are calculated using relative rates of hydrolysis, so it is not appropriate to report frequency factors.

Amino acid	80 ℃ relative to 110 ℃			140 ℃ relative to 110 ℃			Arrhenius Plot	
	Relative rate	%FAA Range	Sum of squares	Relative rate	%FAA Range	Sum of squares	E_A (kJ mol^{-1})	R^2
Asx	0.03	5 – 10	0.001	17.8	10 – 42	0.030	132	0.9995
Glx	0.04	3 – 6	0.000	5.0	4 – 17	0.000	100	0.9772
Ser	0.08	5 – 45	0.007	15.0	6 – 43	0.020	106	0.9963
Ala	0.06	5 – 23	0.005	14.4	6 – 33	0.009	110	0.9990
Val	0.05	1 – 3	0.000	15.8	5 – 27	0.014	118	0.9998
Phe	0.05	0 – 7	0.000	42.6	8 – 22	0.006	136	0.9878
Ile	0.04	0 – 10	0.000	14.4	3.1 – 23	0.008	118	1.0000

Table 5.5: Hydrolysis kinetic parameters calculated using the scaling method. %Free amino acid (FAA) calculated relative to the total hydrolysable amino acid (THAA) concentration from the respective time point: $\%FAA_t = [FAA]_t / [THAA]_t$. Cells highlighted in grey indicate a poor correlation between the calculated activation energies (E_A) for the different temperature ranges (> 20 kJ mol^{-1} difference).

5.3. HIGH TEMPERATURE KINETIC DATA CONSTRAINED WITH LOW TEMPERATURE SUB-FOSSIL DATA

The effect of inclusion of low temperature data in to the Arrhenius calculations was assessed. Sub-fossil OES samples were used as the low temperature data. These data were screened for artificially heated samples (see Chapter 6), and these have been excluded for the purposes of this chapter. Independent ages of sub-fossils were assumed from the age of the horizons from which they were recovered (Sec. 6.2.). It is expected that this will introduce some error as these are only average ages for each horizon, and inevitably the OES samples will be dispersed throughout the layer.

The average temperature of the sub-fossil samples was estimated using a free on-line software programme which takes into account the location, age and burial depth (thermal-age.eu). These temperatures are calculated using non-peer reviewed models. However, this study was not performed in order to calculate absolute activation energies, and these temperature estimates are therefore appropriate in this case. The average temperatures were calculated to ~ 14 °C for PP, and slightly higher at ~ 19 °C for EBC (Appendix B). As the temperatures between the two sites varied, each data set was considered separately in the following kinetic calculations.

5.3.1. RFOKa for racemization of low temperature constrained data

The R^2 values for the sub-fossil data linearized using RFOKa are lower than those observed for kinetic samples (Table 5.6), the principal cause of this is most likely that the age of each sub-fossil sample is an average age from its horizon; inevitably, there will be a mix of sample ages throughout each stratigraphic layer (Table 5.6). The initial non-linearity observed for the kinetic samples (e.g. Fig. 5.1) is also seen for the sub-fossil samples (Fig. 5.7).

			Ser	Ala	Val	Phe	Ile
Integrated rate law plot	14 °C (PP)	D/L range	0.14 - 0.61	0.05 - 0.56	0.02 - 0.28	0.04 - 0.54	0.03 - 0.38
		R^2	0.7931	0.8270	0.8061	0.7759	0.8008
	19 °C (EBC)	D/L range	NA	0.38 - 0.71	0.17 - 0.39	0.44 - 0.72	0.24 - 0.52
		R^2		0.7820	0.8564	0.6922	0.8832
	80 °C	D/L range	0.1 – 0.6	0.1 – 0.3	0 – 0.15	0.1 – 0.3	0 – 0.16
		R^2	0.9723	0.9125	0.9693	0.9506	0.9749
	110 °C	D/L range	0.1 - 0.85	0.1 - 0.75	0 – 0.6	0.15 – 0.9	0 – 0.73
		R^2	0.9839	0.9664	0.9850	0.9345	0.9884
	140 °C	D/L range	0.1 - 0.85	0.1 - 0.83	0 – 0.9	0.1 – 0.9	0 – 0.88
		R^2	0.9629	0.9916	0.9717	0.9913	0.9982
Arrhenius plot	14 – 140 °C	E_A (kJ mol^{-1})	137	139	138	140	137
		lnA	29	28	27	29	27
		R^2	0.9978	0.9970	0.9983	0.9985	0.9932
	80 – 140 °C	E_A (kJ mol^{-1})	121	117	120	127	121
		lnA	24	22	22	25	22
		R^2	1.000	0.9996	0.9993	1.0000	0.9972

*Table 5.6: RFOKa constrained with low temperature data compared with unconstrained data. * The rapid degradation of Ser meant that the data was limited to EBC samples.*

In all cases, inclusion of the sub-fossil data resulted in an increase in the estimate for the activation energies for racemization (Table 5.6; Fig. 5.8). There was generally a poor agreement for the activation energies estimated using high temperature only data, and low temperature constrained data (Table 5.6). If activation energies were to be used to calculate the age of a sub-fossil sample, an underestimation of the energy would result in the calculated age being younger than its real age (Fig. 5.8). For example, if a 151 ka sample from PP 30 is considered with a Val THAA D/L value of 0.38, the calculated age using rate constants calculated using the low temperature constrained kinetic data is ~240 ka, compared to only 30 ka if the rate constant is estimated from extrapolated from high temperature data only. Likewise, if a modern sample heated at 80 °C for ~ 6000 h is considered, the calculated age using low temperature constrained data is 9859 h, compared with 6131 h when only high temperature data is considered. These calculations highlight the errors introduced to calculated absolute ages when rates of racemization from high temperature data are used to extrapolate rates at low temperatures. In

addition, they show that using low temperature data to constrain Arrhenius plots of high temperature data may not be sufficient to calculate accurate activation energies, as the rate constants for high and low temperatures are not described fully by a linear trend-line (Fig. 5.8).

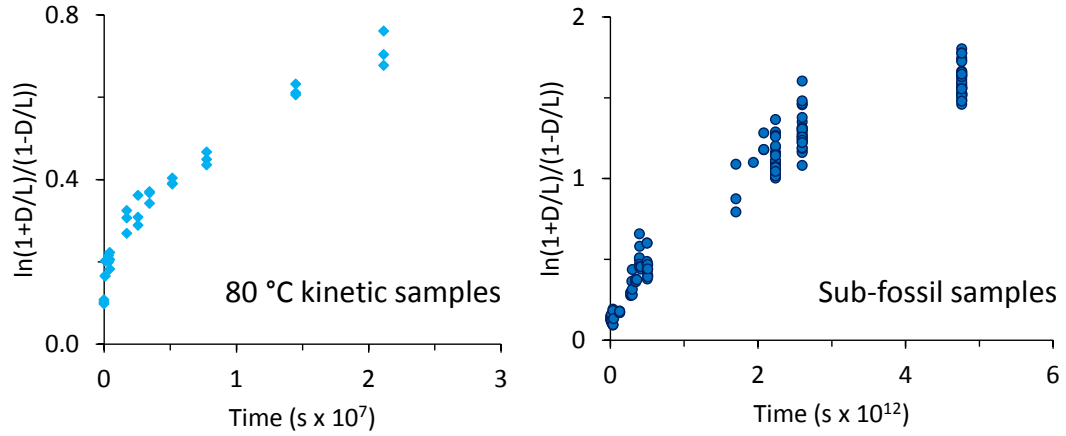

Figure 5.7: RFOK applied to modern OES samples heated under kinetic conditions at 80 °C (left), and unheated sub-fossil samples (right); Ile is shown, but other amino acids show a similar trend

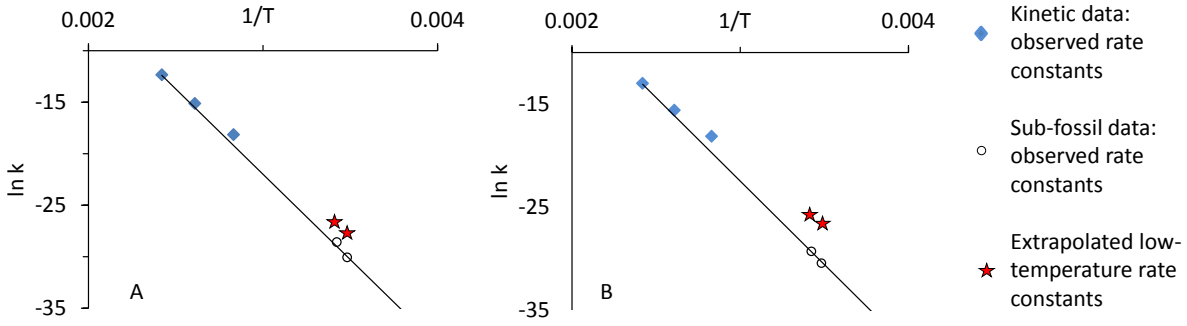

Figure 5.8: Arrhenius plots showing the observed ln k for racemization within sub-fossil samples, and the predicted ln k of sub-fossil samples based on extrapolation from kinetic data. A: Ala, B: Ile, for other amino acids see Appendix B.

5.3.2. Power transformation of racemization of Glx and Asx for low temperature constrained data

The same sub-fossil temperature assumptions were made for the CPK calculations as were made for the RFOKa calculations (Sec. 5.3.1.). The sub-fossil data was poorly described by CPK. Never-the-less the low temperature constrained activation energies were estimated. Inclusion of the

sub-fossil data to the kinetic data resulted in a small increase in the estimated E_A for Asx racemization and a decrease in Glx racemization (Table 5.7).

Analyte	Data included	D/L range	Temp (°C)	R^2	lnA	E_A (kJ mol^{-1})	R^2
Asx	Kinetic data only (n = 2.20)	< 0.7	80	0.9945	26	123	1.0000
			110	0.9957			
			140	0.9959			
	Kinetic and sub-fossil samples (n = 2.70)	< 0.7	80	0.9969	28	129	0.9942
			110	0.9991			
			140	0.9976			
			19	0.8704			
			14	0.5041			
Glx	Kinetic data only (n = 2.30)	< 0.6	80	0.9706	28	138	0.9973
			110	0.9714			
			140	0.9729			
	Kinetic and sub-fossil samples (n = 2.26)	< 0.6	80	0.9721	20	114	0.9920
			110	0.9882			
			140	0.9957			
			19	0.7290			
			14	0.9008			

Table 5.7: Arrhenius parameters calculated for Asx and Glx using the CPK transformation and both kinetic data and the kinetic data with the sub-fossil data

5.3.3. Scaling method applied to racemization of low temperature constrained data

Generally speaking, sub-fossil racemization follows a similar trend to that of the kinetic samples, therefore allowing the application of the scaling method (Sec. 5.2.3.; Fig. 5.9). The same D/L ranges were used for the kinetic samples as those used earlier to estimate activation energies without low-temperature data (Sec. 5.2.3.; Table 5.8). The sum of least squares for sub-fossil and 110 °C heated samples were generally of similar magnitude to that of the 140 °C and 80 °C data. Inclusion of sub-fossil data generally causes an increase in the estimated activation energies (Table 5.9), as was true for energies calculated assuming RFOK (Sec. 5.3.1.).

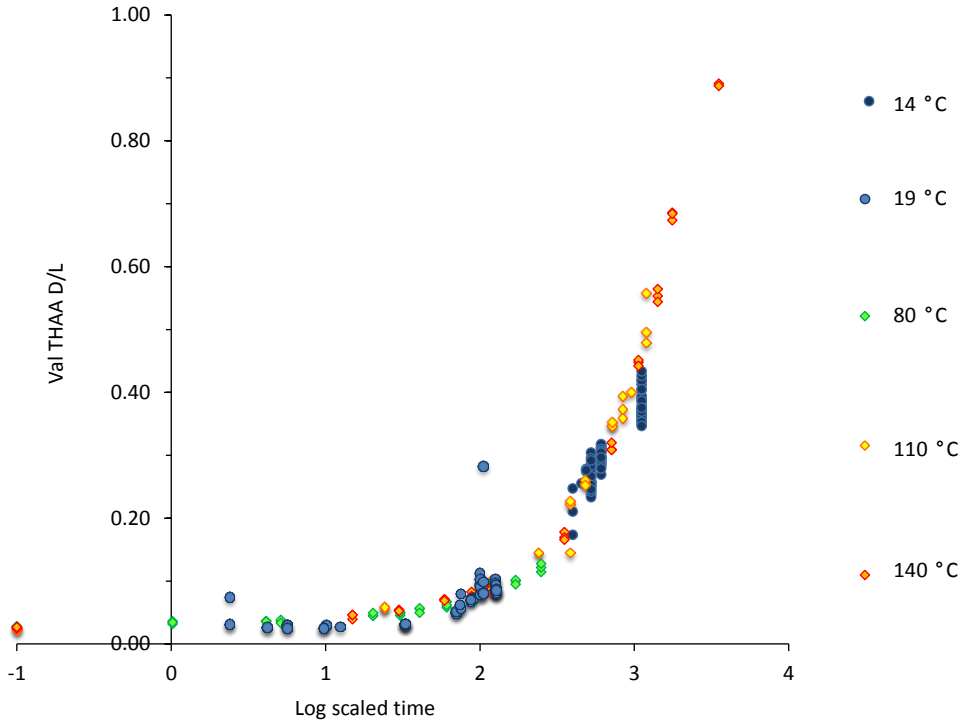

Figure 5.9: Scaling method applied to Val racemization including kinetic data and sub-fossil samples

	Rate of racemization relative to the 110 °C kinetic data (x 10^{-7})		Sum least squares (14 – 140 °C)
	14 °C (PP)	19 °C (EBC)	
Asx	3.2	3.8	0.000
Glx	2.6	0.8	0.011
Ser	2.6	11.5	0.043
Ala	5.2	3.0	0.002
Val	8.5	9.0	0.001
Phe	6.2	5.5	0.139
Ile	14.8	7.2	0.035

Table 5.8: Relative rates of reaction and sum of least squares for racemization sub-fossil samples used to constrain high temperature kinetic data transformed using the scaling method

	Arrhenius outputs constrained with low temperature data (140 – 14 °C)		Arrhenius outputs unconstrained (140 – 80 °C) (for full data set see Table 5.2)	
	E_A (kJ mol^{-1})	R^2	E_A (kJ mol^{-1})	R^2
Asx	144	0.9963	125	0.9998
Glx	151	0.9913	144	0.9937
Ser	144	0.9994	126	0.9993
Ala	141	0.9939	129	0.9952
Val	136	0.9966	118	1.0000
Phe	139	0.9970	134	0.9987
Ile	134	0.9988	120	0.9997

Table 5.9: Comparison of racemization activation energies calculated using the scaling method with and without inclusion of low-temperature data

The low temperature FAA concentrations were poorly linearized using IFOKa (e.g. Fig. 5.10), probably due to the variability of the FAA concentrations. This was true even when limiting the range to the initial stages of hydrolysis (E.g. Fig. 5.10C & D; Table 5.10). The hydrolysis activation energies using the low-temperature constrained data set were therefore not calculated.

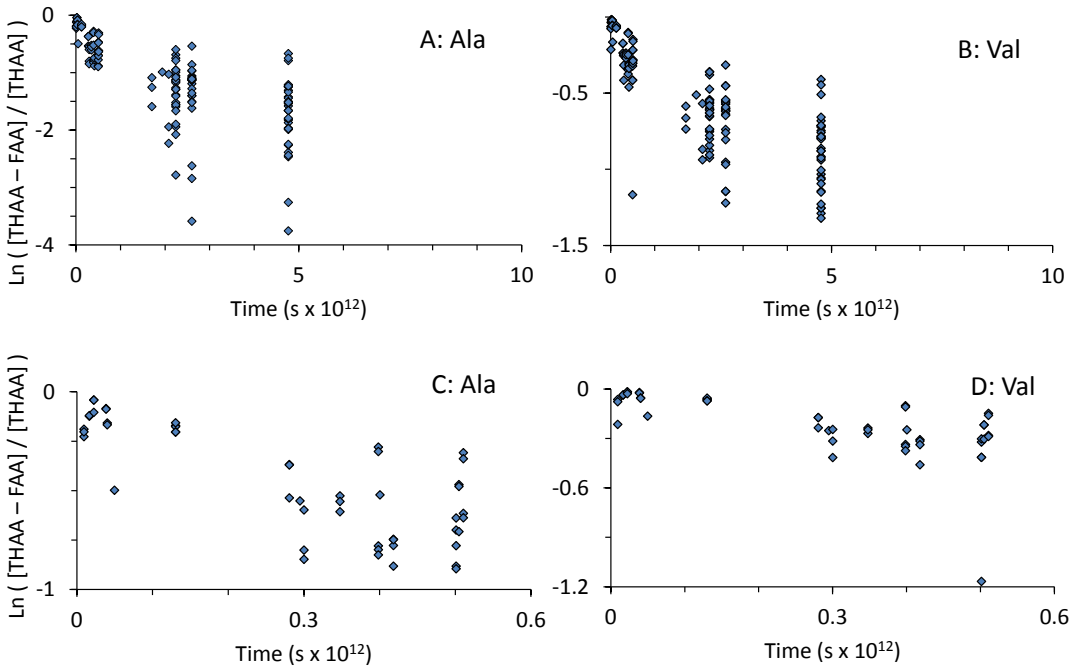

Figure 5.10: Sub-fossil hydrolysis reaction transformed assuming IFOK for Ala (A: all data, C: early hydrolysis only), and for Val (B: all data, D; early hydrolysis only).

	R^2
Asx	0.6834
Glx	0.3122
Ser	0.4809
Ala	0.6436
Val	0.6576
Phe	0.7324
Ile	0.6972

Table 5.10: Coefficients of determination values for hydrolysis data from EBC sub-fossil samples transformed assuming IFOKa

The low temperature hydrolysis data was better described using the scaling method than using IFOKa (Table 5.11; Fig. 5.10 & 5.11; Appendix B), but it could not describe all of the sub-fossil data, in particular Glx and Ser. Inclusion of low temperature data generally caused an increase in estimated activation energies, the only exception being Asx, which remained the same (Table 5.11). For example, Glx, Ser, Ala and Ile all increase by > 8 kJ /mol whereas Asx and Phe decrease by > 6 kJ / mol (Table 5.11).

		Asx	Ala	Val	Phe	Ile
14 °C relative to 110 °C ($x 10^{-6}$)		2.3	3.4	3.8	3.7	3.2
19 °C relative to 110 °C ($x 10^{-6}$)		1.4	0.9	1.0	1.0	0.8
14 - 140 °C	Range (%)	0 - 27%	0 - 64%	1 - 56%	0 - 36%	4 - 40%
	Sum least squares	0.1835	0.1832	0.0420	0.5797	0.0179
E_A (kJ mol^{-1})	Low-temperature constrained (140 - 14 °C)	132	132	131	139	129
	Non constrained (140 - 80 °C; Sec. 5.2.5.)	132	110	118	136	118

Table 5.11: Summary of hydrolysis data from kinetics and low temperature samples transformed using the scaling method

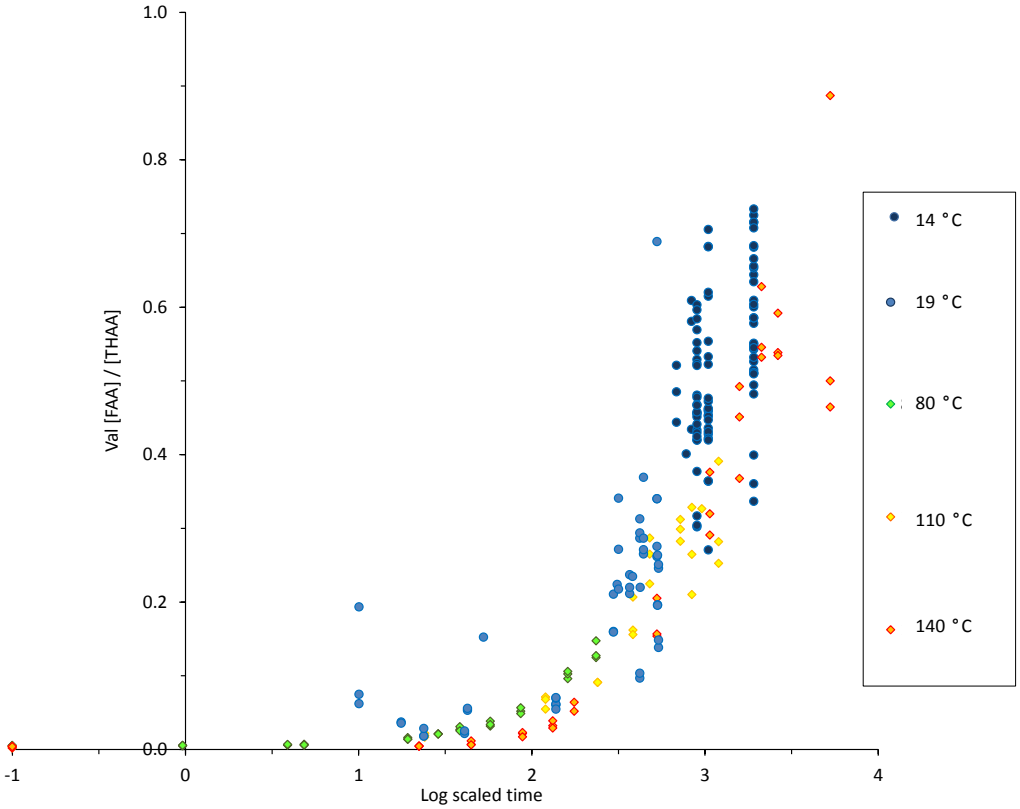

Figure 5.11: Val hydrolysis for kinetic samples and low-temperature samples, transformed using the scaling method

5.4. CONCLUSIONS

The epimerization of Ile in ratite eggshells has previously been shown to approximate RFOK (Brooks *et al.*, 1990; Johnson *et al.*, 1997; Miller *et al.*, 1999, 2000). This can now be extended to include Phe, Val and Ala (and epimerization of Ile), all of which have regions where they appear to follow RFOKa within limited D/L ranges (e.g. Table 5.7). However, it is very unlikely that the amino acids within a bio-mineral truly follow RFOK (e.g. Wehmiller and Hare, 1971; Wehmiller, 1980; Mitterer and Kriausakul, 1989; Collins and Riley, 2000; Clarke and Murray-Wallace, 2006). Therefore, RFOK loses its chemical rationale, and is instead a mathematical transformation used to linearize the data, in the same way as does CPK.

The scaling method has the benefit of not forcing the data to form a straight line, which in many cases was difficult to achieve over large D/L and %[FAA] ranges. However, this method also has no underlying chemical rationale. Considering the lack of understanding of the complete system operating within OES there is little alternative but to use mathematical transformations.

Addition of low-temperature data to kinetic models changed the estimated activation energies for both hydrolysis and racemization for the majority of cases (Table 5.12). Any agreement between

the different models for the estimated activation energies does not necessarily suggest that these are accurate results. The differences in estimated activation energies, calculated using the different mathematical models and different data, highlight the problems of assigning activation energies from a single overall rate constant without considering the underlying mechanisms and contributing rate constants. This phenomenon is also seen for the intra-crystalline amino acids in *Patella* shell (Demarchi *et al.*, 2013b) and in *Porites* coral (Tomiak *et al.*, 2013).

If the activation energies of several reactions with different energies can be calculated accurately, this may negate the need to know the thermal history of the sample, as the Arrhenius equation may be solved simultaneously (e.g. Miller *et al.*, 1999). In order to do this there is a need to better understand the underlying mechanisms controlling the reaction rates to give chemical rationale to the rate laws. As has been shown in this study, using different models can result in different, and equally plausible, activation energies.

Amino acid	Racemization						Hydrolysis		
	RFOKa		CPK		Scaling method		IFOKa	Scaling method	
	140 – 80 °C	14 – 140 °C	140 – 80 °C	140 – 14 °C	140 – 80 °C	140 – 14 °C	140 – 80 °C	140 – 80 °C	140 – 14 °C
Asx	ND	ND	123	129	125	144	99	132	132
Glx	ND	ND	138	114	144	151	83	100	ND
Ser	121	137	ND	ND	126	144	107	106	ND
Ala	117	139	ND	ND	129	141	119	110	132
Val	120	138	ND	ND	118	136	114	118	131
Phe	127	140	ND	ND	134	139	91	136	139
Ile	121	137	ND	ND	120	134	114	118	129

Table 5.12: Summary of activation energies calculated using various models and using both kinetic only data and low temperature constrained data (ND = not determined)

CHAPTER 6: ANALYSIS OF SUB-FOSSIL OSTRICH EGGSHELL SAMPLES FROM SOUTH AFRICA

6.1. INTRODUCTION

Previous studies have used the degree of Ile epimerization of whole shell proteins of OES as a proxy for thermal age (Brooks *et al.*, 1990; Miller *et al.,* 1992; 1999). Through kinetic studies of modern OES samples, both intra-crystalline and whole-shell, it has been shown that the rates of protein degradation are predictable for several amino acids, including Ile (Chapter 4). It is therefore important to test whether this also holds with sub-fossil samples. To that end, a series of samples from archaeologically and palaeontologically important sites in South Africa have been analysed; two sites from Pinnacle Point (~151 – 48 ka; Location: 34.21S: 22.09E, PP 5/6 and PP 30), and one from Elands Bay Cave (~16 – 0.3 ka; Location: 32.18S 18.19E) (Section. 6.2.).

Pinnacle Point (PP) contains 28 known archaeological sites, 21 of which are from the Middle Stone Age (MSA) and 15 of which are caves or rock shelters (Marean *et al.*, 2004). There is evidence at Pinnacle Point for early modern humans using pigments and producing bladelets (Marean *et al.,* 2007; Brown *et al.*, 2012). In addition, the earliest evidence to date for the use of pyro-technology in stone tool manufacture has been recognised at site PP 5/6 at ~164 ka (Brown *et al.* 2009), and for the systematic human exploitation of marine resources at site PP 13B at ~164 ka (+/- 12 ka) (Marean *et al.,* 2007). This is therefore an important series of sites in regards to the development of 'modernity' in early humans (McBrearty and Brooks, 2000; Henshilwood and Marean, 2003). The PP sites were occupied by *Homo sapiens* between approximately 164 – 40 ka (Marean *et al.*, 2007), the coastal site offering a favourable location with plentiful marine resources, compared to harsh and arid conditions across much of Africa during this time (Marean *et al.*, 2007; Compton, 2011).

In addition to the archaeological sites at PP, site PP 30 is a palaeontological site thought to have had a short occupation by hyenas at ~ 151 ka (Rector and Reed, 2010), a species which also utilized ostrich eggs as a food source (e.g. Kandel, 2004). This site was targeted specifically for its older age, and because it was hypothesised that none of the OES samples would have been affected by human occupation, e.g. anthropogenic fire (pers. comm. Curtis Marean).

Elands Bay Cave (EBC) is a well stratified post-glacial cave site, also on the south coast of South Africa. It was targeted because it is younger than the PP sites (occupation between ~16 – 0.3 ka; Parkington, pers. comm. unpublished data), but is likely to have a similar climate and is therefore comparable to PP.

There are a number of potential sources of variability that have been identified which may affect the AAR results for sub-fossils, that are not a problem for modern samples heated in a controlled lab environment:

(i) Sample re-working/intrusion

Cave sites (such as EBC, PP 5/6 and PP 30) often have complex sample deposition, due in part to cave collapses, foraging animals and erosion (Karkanas *et al.*, 2000; Marean *et al.*, 2010). Consequently, a sample may be associated with non-contemporaneous strata. A sample showing a greater D/L value than expected could be a genuinely older sample which has been re-worked into a younger horizon; likewise a young sample may be intruded within an older horizon. Sample re-working would be difficult to identify, and would have to be assigned on a sample by sample basis, based on the specific sample, site history and the D/L values of a suite of samples from the site.

(ii) Natural variability

Different ostriches, diets and environmental stresses may potentially affect protein composition in OES resulting in natural variability between samples (Sec. 6.5.2.).

(iii) Artificial heating

Evidence of anthropogenic fire as early as ~164 ka has been found at Pinnacle Point (Brown *et al.*, 2009) and there are numerous hearth deposits throughout the PP 5/6 and EBC sequences (Marean *et al.*, 2007; Brown *et al.*, 2009; Marean *et al.*, 2010; Parkington, pers. comm.). In addition to anthropogenic fire, veld fires may provide another source of artificial heating, which may affect both archaeological (EBC and PP 5/6) and palaeontological (PP 30) sites (pers comm. Curtis Marean). Proximity of OES to fire, either pre- or post-deposition, would result in some eggshells from these cave deposits having been heated, artificially increasing the extent of protein degradation, and therefore the apparent AAR age. Indeed, Brooks *et al.* (1991) attributed much of the variability they observed in Ile epimerization in OES from a series of sites in Africa to anthropogenic fire (including Boomplaas, Mumba Shelter, Qafzeh and Apollo 11).

Based on the site details (e.g. human activity and veld fires), and the previous work by Brooks and colleagues (1990; 1991), it was anticipated that many OES samples from archaeological sites (e.g. PP 5/6 and EBC) and potentially some from palaeontological sites (e.g. PP 30) may have been exposed to increased temperatures. It is imperative that these samples can be identified and excluded from age models so that only samples with similar thermal histories are compared. Therefore the identification of artificially heated sub-fossil samples is an integral part of this study. A high-temperature heating study on modern OES was performed between 110 – 500 °C, in order to assess the effect of artificial ageing of OES samples through exposure to high temperatures. Furthermore, a suite of samples from the palaeontological site (PP 30) were analysed as they were expected to have less variability introduced from artificial heating than archaeological sites.

A previous heating study by Brooks *et al.* (1991) using untreated modern OES fragments dry heated at temperatures between 160 – 360 °C reported that the amino acid composition of 'moderately heated' samples was often dominated by Glu ('moderate heating' = 1 hr at 200 – 230 °C). Furthermore, they noted that the concentration of ammonia and an unknown analyte (speculated to be γ-aminobutyric acid, known to form from the decarboxylation of Glu; Hare and Mitterer, 1967) increased with heating. An alternative approach for identifying artificially heated OES samples was adopted by Miller *et al.* (1992). They used two degradation reactions with different activation energies to simultaneously solve the Arrhenius equation to calculate the average environmental temperature of that sample. The reactions utilised were the hydrolysis of Leu and the epimerization of Ile, assuming irreversible and reversible first order kinetics respectively, in order to calculate their activation energies. Using this technique they were able to identify and exclude a small number of early late stone age OES samples from Heuningsneskrans, South Africa which showed no visual indication of heating. Both Brooks *et al.* (1991) and Miller *et al.* (1992) use ion-exchange chromatography for their AAR analysis, but unfortunately as D-Leu in the RP-HPLC method used in this study often co-elutes with other compounds in OES samples, this method for identifying heated samples is not possible. However, the RP-HPLC method is able to quantify other degradation reactions (e.g. racemization as well as epimerization) so it may be possible to find additional ways for identifying heated OES samples. In addition to these chromatographic methods, it has been noted by Professor Julia Lee-Thorp, (pers. comm.) that often OES samples which have been visually identified as having been heated release a powerful smell when the sample is broken; the smell is often quite potent, with a slight sulfurous odour. The problem of heated samples in AAR studies is not exclusive to OES samples; indeed Demarchi (2009; Demarchi *et al.*, 2011) found that heating in the mollusc shell *Patella* may be identified by the relative rates of Glx and Asx racemization.

A thorough artificial heating study was carried out using modern OES samples and analysis with HPLC, gas chromatography (GC) and X-ray diffraction (XRD) (Sec. 6.3.1.). The data from this study was compared with data from sub-fossil samples in order to develop a robust method capable of identifying heated sub-fossil samples and exclude them from AAR age models. Once heated samples can be excluded, the applicability of AAR using sub-fossil OES samples can be assessed, using several amino acids from samples up to 151 ka.

6.2. SAMPLE DETAILS

6.2.1. Elands Bay Cave, South Africa

Approximately 40 OES samples have been analysed from the archaeological site, Elands Bay Cave (EBC; Fig. 6.1), ranging in age from ~0.3 – 16 ka; the strata have been independently dated using radiocarbon analysis (Parkington, pers. comm. unpublished data), with calibration using CalPal_2007_HULU.

Strata name	No. of samples
Kaunda	2
Mrs Balls	1
George Best	2
Jesus Christ	2
D. Lamour	1
Soynika	3
Maroon Robson	2
Bero	1
Nero	2
PW Botha	1
Neptune	2
Crayfish	1
Brian Statham	1
Foam	2
Smoke	3
Dust	1
Ashes	2
GBS 1	3
GBS 2	2
OBS 1	2
OBS 2	3
SS 1	3

Table 6.1: Summary of samples from Elands Bay Cave

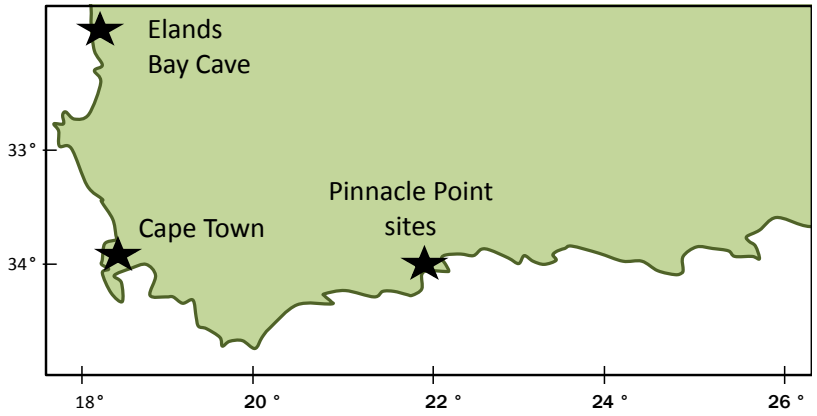

Figure 6.1: Map of South Africa showing locations of sample sites, Elands Bay Cave and Pinnacle Point site

6.2.2. Pinnacle Point, South Africa

Site PP 5/6 is an archaeological MSA cave shelter from which approximately 120 OES samples have been analysed from 6 horizons dated between 54 – 86 ka (Table 6.1). These horizons have been independently dated using optically stimulated luminescence (OSL) dating (Brown *et al.*, 2009; Brown *et al.*, 2012; Table 6.2).

37 OES samples were analysed from the palaeontological site "PP 30". PP 30 is thought to have been occupied by hyenas for a short period of time at ~151 ka, dated using OSL (Rector and Reed, 2010).

Site	Horizon	Independent age	MIS stage	No. of samples
PP 5/6	Orange Brown Sand (OBS)	66 ka ± 3	4	8
PP 5/6	Shelly Ashy Dark Brown Sand (SADBS)	71 ka ± 2	4	36
PP 5/6	Ashy Light Brown Sand (ALBS)	71 ka ± 2	4	22
PP 5/6	Medium Brown Sand and Roof-spall (MBSR)	54 ka ± 2	3	4
PP 5/6	Shelly Grey Sand (SGS)	58 - 65 ka ± 4	3	7
PP 5/6	Light Brown Sand and Roof-spall	~ 86-79 ka	5	38
PP 30	Single horizon	~ 151 ka	6	37

Table 6.2: Sample details for sub-fossil OES samples from Pinnacle Point

6.3. EXPERIMENTAL

6.3.1. Artificial heating samples

Fragments of OES were dry heated isothermally between 110 °C and 500 °C on pre-heated watch-glasses in a furnace (Table 6.3). Post-heating, the samples were treated as per sub-fossil samples (Section 6.3.1.); a small fragment was removed, washed, powdered and bleach treated for 72 h prior to FAA and THAA analysis (Chapter 2).

Temperature (°C)	Time points (min)
110	0, 60, 138, 207, 1440, 28945, 59335, 113760
200	2, 5, 10, 15, 40, 60, 150, 240, 480
300	5, 10, 15, 20, 45, 80, 120
400	1, 2, 3, 5, 10, 20
500	1, 2, 3, 5, 10

Table 6.3: Temperatures and time points for modern OES fragments used in artificial heat experiment

Heating large OES fragment samples could cause localised hot spots, where, for example the sample was in contact with the watch-glass. This may be exacerbated at shorter time points where the whole fragment may not have time to reach the desired temperature. In contrast, the kinetic experiments were carried out using powdered samples and heated in water, which would act to diffuse the heat more equally through the whole OES sample (see Sec. 3.2.3.; 4.2.1.). In order to assess the variability introduced by heating fragment samples in a watch-glass (as opposed to homogenised powder in water), the artificial heating study was also carried out at 110 °C, so that they could be compared to the 110 °C kinetic experiment data (i.e. intra-crystalline OES samples isothermally heated in water; Sec. 4.2.1.). In addition, by including the kinetic data, a greater temperature range could be studied, i.e. from 80 °C – 500 °C.

Low temperature sub-fossil OES data was used to constrain the observations from the heating studies. Samples were chosen from each age bracket at PP 5/6 and PP 30 based on which samples showed the lowest AAR values for their age group. In this way it can be assumed that these samples have been exposed to minimal heating. 5 samples from PP 30 and 5 samples from each of the horizons at PP 5/6 were used, with the exception of the 48 ka horizon, where only 4

samples were available in total and so only one sample was used. The average data from each age group was used.

6.3.2. Archaeological Samples

Surface dirt was removed from the archaeological OES samples with physical abrasion using a Dremel drill with silicon polishing head. Samples were washed in ultrapure water with 2 min sonication, until the water removed was clear; 3 rinses were usually sufficient.

Samples were dried and powdered with an agate pestle and mortar to < 200 µm particle size. The powder was bleached for 72 h and agitated every 24 h. Bleach was removed by pipette and tested on coloured tissue to ensure the bleach was still active; for all samples the bleach was found to be still active. To ensure all the bleach was removed the sample was then washed 5 times with HPLC-grade water followed by a final wash with HPLC-grade methanol, which was left for a number of minutes prior to removal, in order that the methanol is oxidized by any remaining bleach. The sample was air dried overnight.

The powder was split into two fractions for analysis for the FAA and THAA fractions (Chapter 2).

6.3.3. Gas chromatography

When heavily burnt samples are broken or ground up they emit a strong 'burnt' odour. It was therefore suspected that volatiles were being created in the heating process which could act as a marker for the identification of heated samples. Gas chromatography (GC) seemed a natural choice of technique, given its utility for analysing vapour phase analytes. Headspace-GC is often used in the flavour and fragrance analysis industries (e.g. Snow and Slack, 2002), therefore a static headspace experiment was used in an attempt to isolate these volatiles to see whether they could be used as a marker for heat exposure. Static headspace analysis is not the most sensitive of techniques, therefore a large (~ 2 by 2 cm square fragment) modern OES fragment was heated at 400 °C for 5 min, such that the odour it released was very powerful. Although this size of sample is very unlikely to be available for sub-fossil samples, this experiment was designed as a proof of concept. After heating, the OES sample was broken into pieces and quickly sealed in a GC vial.

Two types of detection methods were used, flame ionised detection (FID) and flame photometric detection (FPD); the former is used to analyse compounds containing carbon to hydrogen bonds, the latter is used for the detection of sulfur containing compounds.

A Thermo Trace GC Ultra fitted with a Triplus Headspace autosampler, splitless injection port, flame ionisation detector (FID) and flame photometric detector (FPD) was used. The syringe for sample injection was maintained at 40 °C. Sample vials were incubated (80°C, 10 min) prior to injection in order to increase the concentration of volatile components in the headspace of the vial and an aliquot of the headspace (1 mL) was injected via a splitless inlet (230°C, splitless time 1 min) onto the gas chromatograph. Separation was achieved using a DB-wax capillary column (J&W Scientific, 60 m in length, 0.25 mm internal diameter and 0.25 µm film thickness) and the following oven programme; initial temperature 30°C (hold time 10 min) to 230°C at a rate of 6°C min^{-1} (hold time 3 min). Helium was used as the carrier gas at a flow rate of 2 mL / min. The FID detector was maintained at 230°C. The FPD detector was fitted with a 394 nm narrow band optical filter for sulfur and the detector and detector base were held at 150°C and 230°C, respectively.

6.3.4. X-ray diffraction

X-ray diffraction was used to look for changes in crystal structure that may be linked to the physical changes occurring in OES at increased temperatures. Indeed, Heredia *et al.* (2005) noted a change in crystallinity for OES samples heated at > 550 °C.

XRD was attempted on samples heated at < 500 °C focussing on the regions noted by Heredia *et al.* (2005), namely 2 ϑ = 30 – 60°. Modern unheated whole-shell OES were compared with samples heated at 200 °C for 15 min, 280 °C for 15 min and 280 °C for 30 min. In addition, two whole-shell sub-fossil samples from PP 5/6 were analysed, both of which were not identified as having been heated (Sec. 6.5.3.) and were independently dated to 71 ka +/- 2.

Powdered samples were packed into an aluminium plate with a circular well. Analysis was carried out using a Bruker-AXS D8 diffractometer with a copper anode (1.54 λ). Each sample was scanned between 30 – 60 ° 2 θ using a 0.025 degree increment with a measurement time of 0.5 seconds per step.

6.4. RESULTS: ARTIFICIAL HEATING STUDY

6.4.1. Appearance and olfactory analysis

Heating at 110 °C – 200 °C, for up to 79 days and 8 hours, respectively, caused subtle changes in colour, notably a slight darkening on the outer crystal layer (Fig. 6.2).

Heating OES at 300 °C almost instantly caused a darkening of the outer crystal layer, with an orange colour observed at 5 min and a black/brown colour from 10 min (Fig. 6.2). From the earliest time points for samples heated at > 400 °C, the outer crystal layer and the inner surface of the OES turn a dark brown/black (Fig. 6.1).

Heating at 300 °C for more than 10 min, or at > 400 °C, caused different colour changes in the palisade layer (Fig. 2.1, layer 'C') and the adjacent cone layer (Fig. 2.1, layer 'B'); the former darkens and the latter whitens, creating a defined line between the layers (Fig. 6.2 D & E). The dark colour on the outer crystal surface and the palisade layer appeared to propagate from the pores (e.g. Fig. 6.2 E). After 3 min of heating at 500 °C the cone layer spalled from the palisade and crystal layers (Fig. 6.2 G). After 10 min of heating at 500 °C the outer crystal layer developed a subtle iridescent green colour.

No discernible smell was released when powdering 110 °C heated samples, and only a slight smell was released from samples heated at 200 °C for more than 480 h. A strong odour was released when powdering any sample heated at > 300°C, similar to the smell released from archaeological samples suspected of having been exposed to high temperatures which had been identified through visual inspection. This smell, especially from samples heated at > 400 °C, was very intense.

Figure 6.2: Modern OES fragments from artificial heating study. Side profile shots show the outer side on the top. Where only one side profile is shown, fractured and exposed sides looked the same.

When heavily burnt samples are broken or ground up they emit a strong 'burnt' odour. It was therefore suspected that volatiles were being created in the heating process which could act as a marker for heated samples. A modern sample was therefore heavily heated and analysed using static gas head space GC. Unfortunately, there were no discernible peaks in any of the analyses. It is likely that this technique was not sensitive enough for our analyses, especially considering the large sample that was used for the test runs, approximately 100 % larger than a typical sized OES archaeological sample required for AAR analysis. It is therefore unlikely that this method, as it stands, will prove to be an appropriate technique for the identification of artificially heated OES samples.

6.4.2. AAR analysis

The extents of protein degradation reactions were compared at different temperatures in an attempt to differentiate samples by their temperature exposure. In order to help constrain the lower temperatures the kinetic data sets from Chapter 4 were also included in the following comparisons. It should be noted, however, that the experimental set up was different for the artificial heating and the kinetic experiments, e.g. the kinetic samples were powdered and bleach treated prior to heating in water; the artificial heating samples were unbleached fragment samples which were heated and then a sample of this fragment was powdered and bleached prior to AAR analysis. As discussed earlier (Chapter 3), pre- and post- heat bleaching are not equivalent. However, for the purposes of this study it is useful to include data from the kinetic studies, which were performed at lower temperatures.

6.4.2.1. Decomposition

The amino acids in modern OES samples rapidly degrade when heated at the high temperatures used in the artificial heating experiments, e.g. the sum of THAA concentrations (Asx, Glx, Ser, Gly, Ala, Val, Phe, Ile & Tyr) reduce by ~70 % with 10 min heating at 300 °C, ~70 % with 2 min heating at 400 °C and > 99 % with 1 min of heating at 500 °C. Indeed, the decrease in concentration was so rapid at 500 °C that Gly was the only amino acid persisting at > 1 % of its initial concentration after 1 min of heating. Therefore, AAR analyses on samples heated over 500 °C are not useful in studying the comparative rates of protein degradation.

It was noted that the composition of the THAA fraction changes with heating (Fig. 6.3). The more thermally unstable amino acids, e.g. Ser (Vallentyne, 1964), readily degrade with heating. The Asx concentration also reduces considerably with heating. The relative concentration of Glx increases

with heating, as was observed by Brooks and colleagues (1991), for all samples heated at < 400 °C. Indeed, an increase from ~ 16 % for an unheated sample to > 50 % Glx was seen in samples heated at > 300 °C for 45 min, and Glx appears to be the only amino acid which persists when samples are heated at 500 °C.

Interestingly the relative concentration of Ala decreases when heated at 300 °C but increases for samples heated at > 400 °C. In order to assess whether the changes in composition were different at different temperatures, they were normalised by plotting against D/L values. The profiles of Asx, Glx, Ser and Ala are focused on as these amino acids appeared to show the most significant changes with heating (Fig. 6.3).

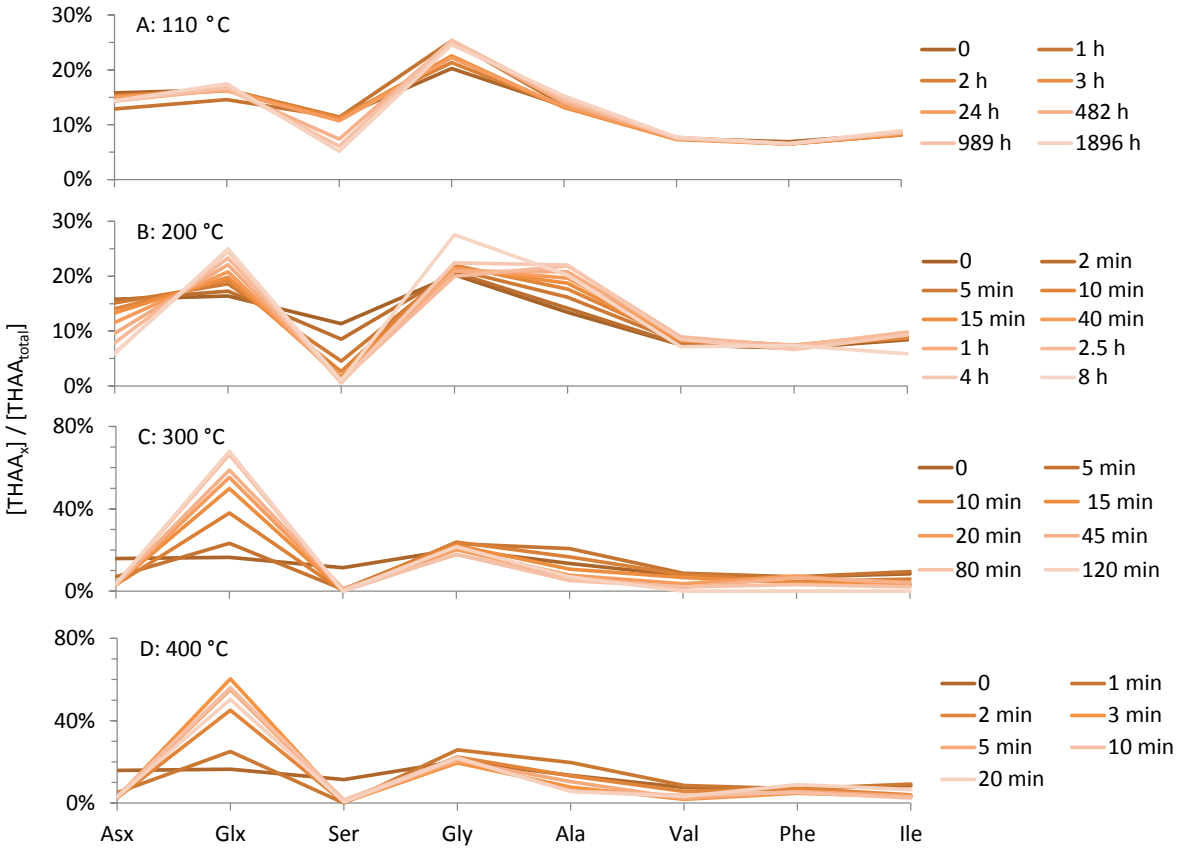

Figure 6.3: Amino acid concentrations ($THAA_x$) relative to the total of all THAA concentrations ($THAA_{total}$) of modern OES samples heated isothermally at, A: 110 °C, B: 200 °C, C: 300 °C and D: 400 °C. Concentrations represent the average of duplicate samples (See Appendix C for standard deviations).

The %Glx composition for heated samples was plotted against the Asx THAA D/L values (Fig. 6.4), Asx was chosen because it showed the best differentiation between the different temperatures and the strongest trends. This comparison suggests that all samples follow a similar trend upon heating at ≤ 200 °C, with a small increase in %Glx with increasing Asx D/L values (Fig. 6.4). In

contrast, samples heated at ≥ 300 °C show a rapid increase in % Glx which deviates from the trend followed by samples heated at lower temperatures.

Similarly, the % Ala composition was plotted against the Ala THAA D/L (Fig. 6.5). Samples heated at ≤ 200 °C show a strong correlation, with a small increase in % Ala with increasing Ala D/L values. Samples heated at ≥ 300 °C show far more variable results than those heated at lower temperatures, and show a decreased % Ala for samples of the same Ala D/L values.

Both the % Asx and % Ser concentrations appear to be reduced for samples heated at > 300 °C (Fig. 6.6 & 6.7), although the 80°C data show considerably more variability for % Asx than for % Glx (Fig. 6.4).

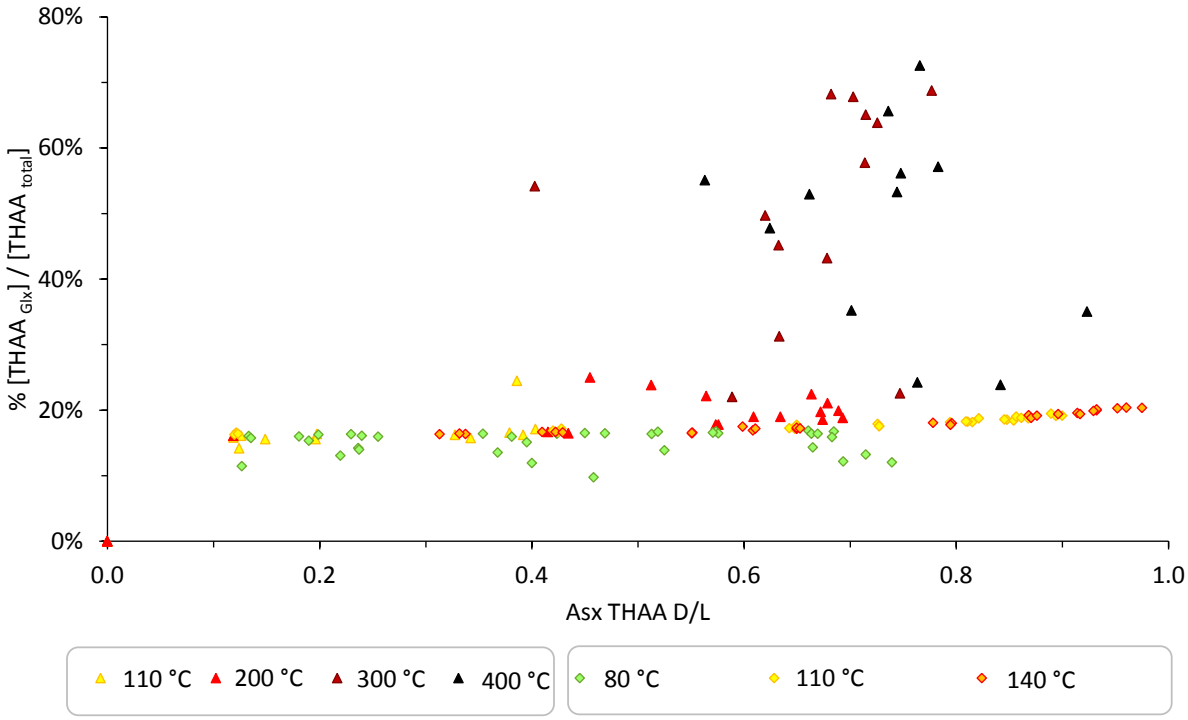

Figure 6.4: % Glx concentration of the total amino acid concentrations (Asx, Glx, Ser, Gly, Ala, Val, Ile & Phe) of modern OES samples heated at 80 – 140 °C under kinetic conditions (diamonds) and 110 – 500 °C under artificial heating conditions (triangles); concentrations are plotted against the Asx THAA D/L values.

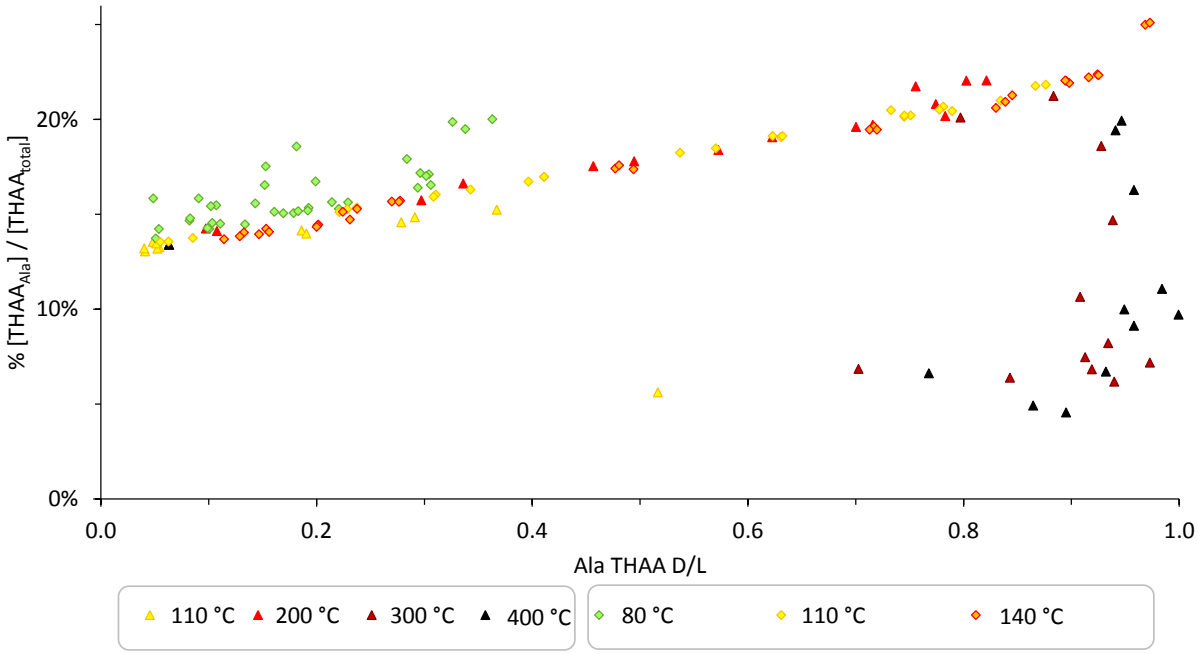

Figure 6.5: % Ala concentration of the total amino acid concentrations (Asx, Glx, Ser, Gly, Ala, Val, Ile & Phe) of modern OES samples heated at 80 – 140 °C under kinetic conditions (diamonds) and 110 – 500 °C under artificial heating conditions (triangles); concentrations are plotted against the Ala THAA D/L values.

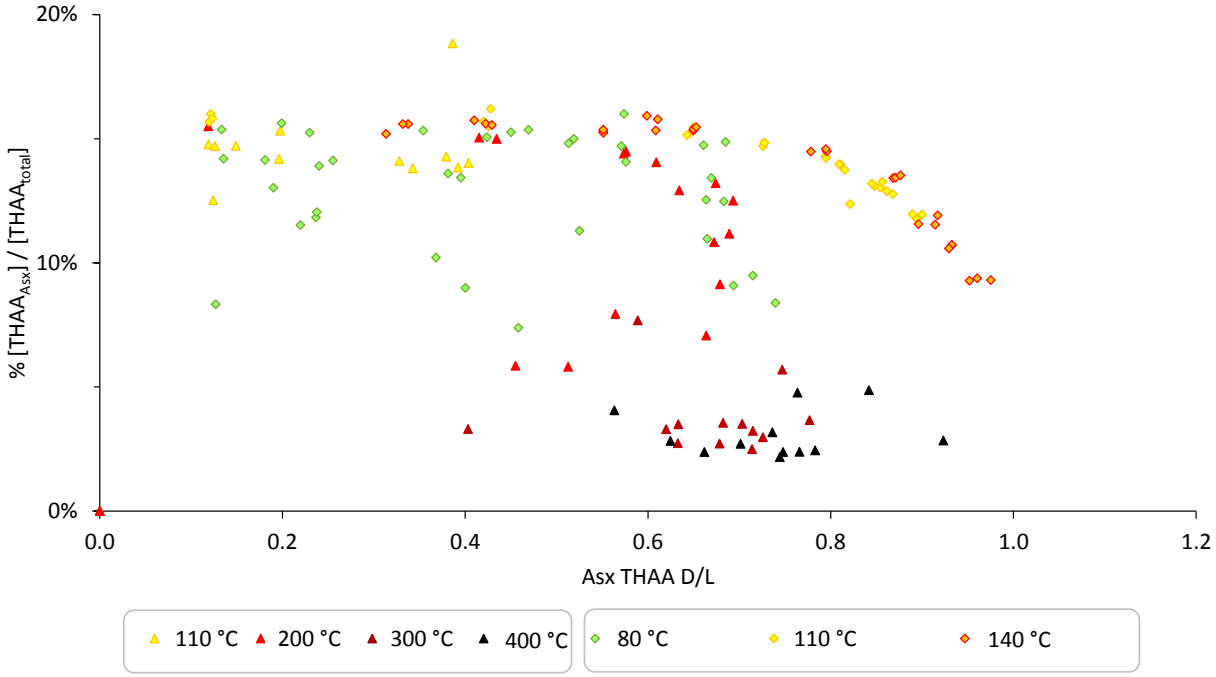

Figure 6.6: % Asx concentration of the total amino acid concentrations (Asx, Glx, Ser, Gly, Ala, Val, Ile & Phe) of modern OES samples heated at 80 – 140 °C under kinetic conditions (diamonds) and 110 – 500 °C under artificial heating conditions (triangles); concentrations are plotted against the Asx THAA D/L values.

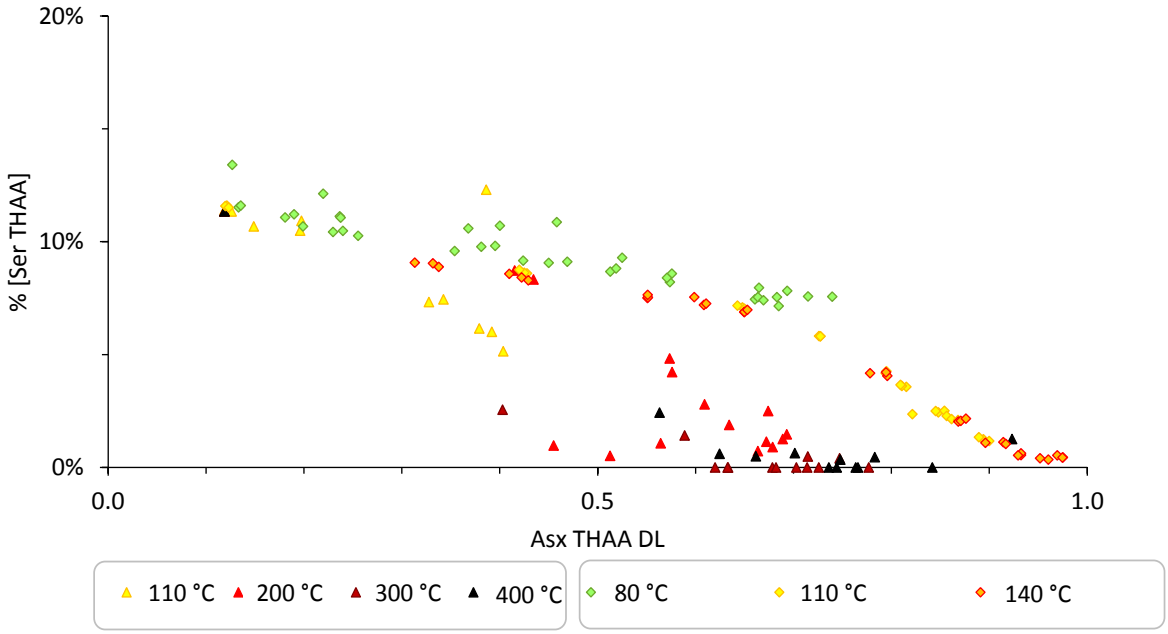

Figure 6.7: % Ser concentration of the total amino acid concentrations (Asx, Glx, Ser, Gly, Ala, Val, Ile & Phe) of modern OES samples heated at 80 – 140 °C under kinetic conditions (diamonds) and 110 – 500 °C under artificial heating conditions (triangles); concentrations are plotted against the Ala THAA D/L values.

In addition, the % Glx, % Ala, % Ser and % Asx compositions were compared relative to each other at different temperatures (e.g. Figs. 6.8 – 6.11). Comparing the % Glx and % Asx, a different trend is observed for the 80 °C kinetic data and that of samples heated at ≥ 110 °C (Fig. 6.8). Comparing % Glx and % Ala, different trends are observed for samples heated at ≥ 300 °C, those heated at 80 – 200 °C and those heated at 80 °C (Fig. 6.9). Comparing the % Glx and % Ser (Fig. 6.10), it can be seen that Ser rapidly degrades with heating and that a similar trend is followed by all samples heated at < 300 °C.

The comparisons in this section suggest that a sample showing a high % Glx (Fig. 6.4) and a low % Asx (Fig. 6.6; 6.8), % Ala (Fig. 6.5; 6.9) and % Ser (Fig. 6.7; 6.10) for a given D/L value, may indicate that a sample has been heated at ≥ 300 °C. The amino acid composition of OES samples may therefore be used to identify artificially heated samples. The relative compositions of amino acids in kinetic and sub-fossil samples were not previously considered in Chapter 4 (Sec. 4.3.4.), only the THAA concentrations relative to Val THAA D/L. These graphs only showed a difference when considering Asx concentrations (Fig. 4.8).

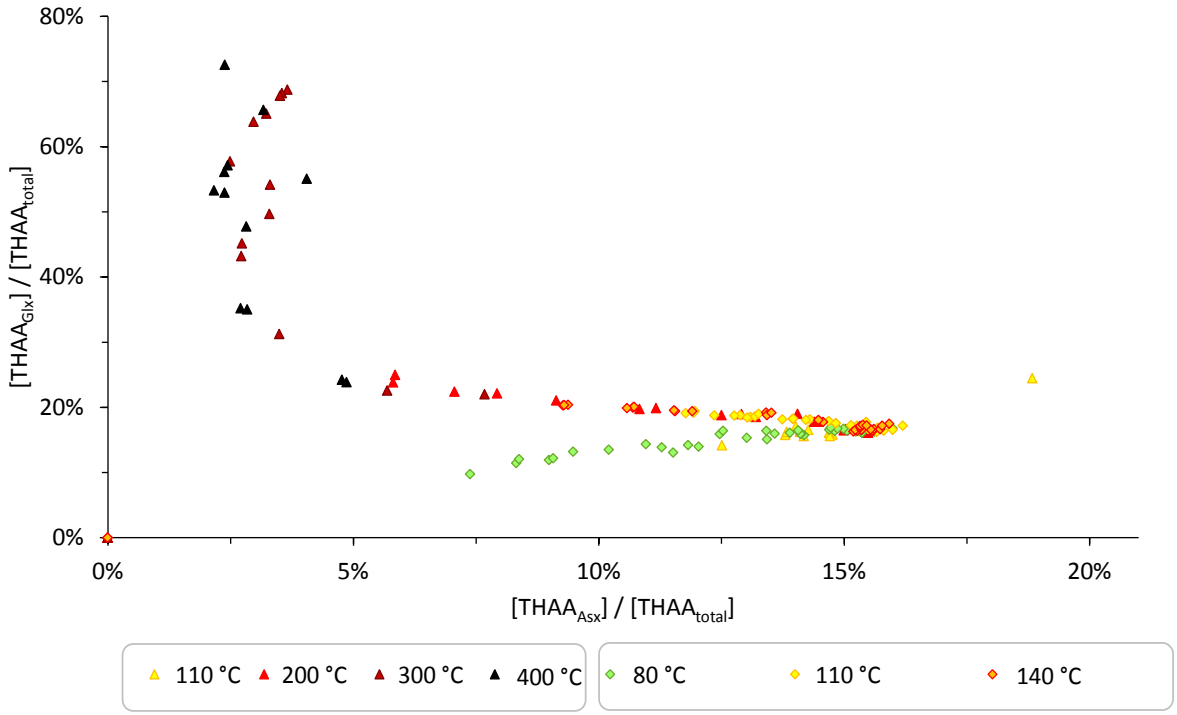

Figure 6.8: % Glx concentration compared to the % Asx concentration, both relative to the total amino acid concentrations (Asx, Glx, Ser, Gly, Ala, Val, Phe & Ile) of modern OES samples heated at 80 – 140 °C under kinetic conditions (diamonds) and 110 – 500 °C under artificial heating conditions (triangles).

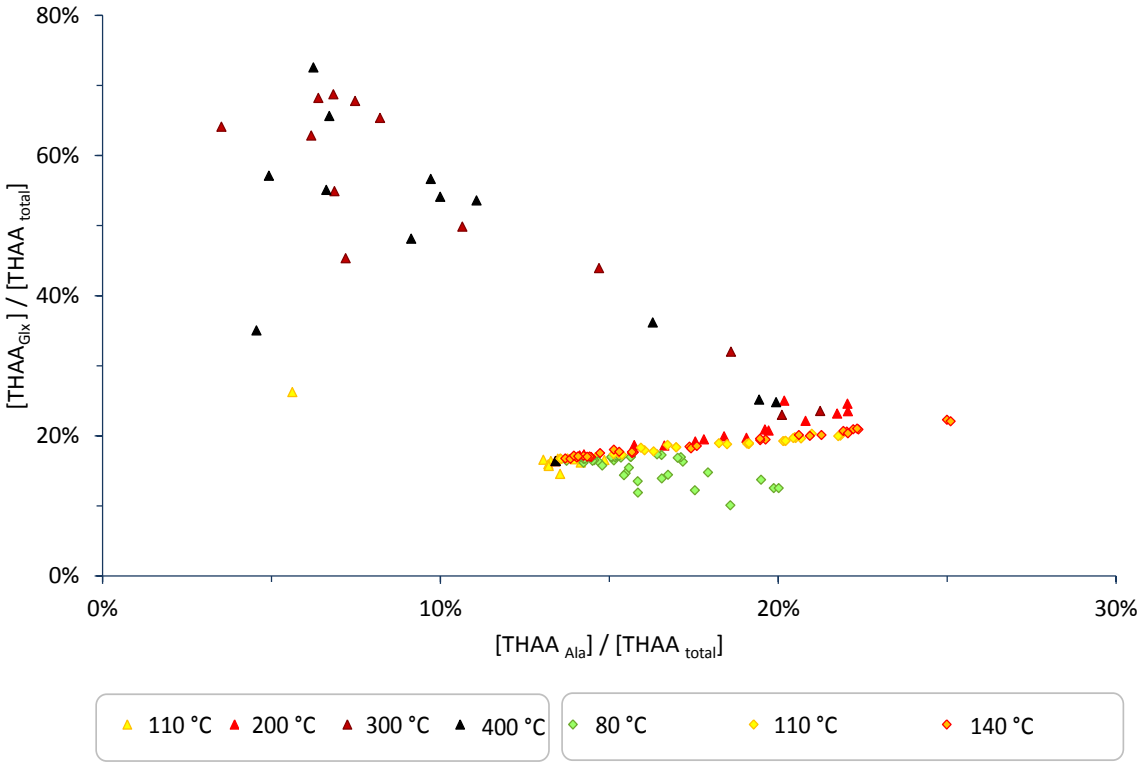

Figure 6.9: % Glx concentration of the total amino acid concentrations (Asx, Glx, Ser, Gly, Ala, Val, Phe & Ile) compared to % Ala concentration of modern OES samples heated at 80 – 140 °C under kinetic conditions (diamonds) and 110 – 500 °C under artificial heating conditions (triangles).

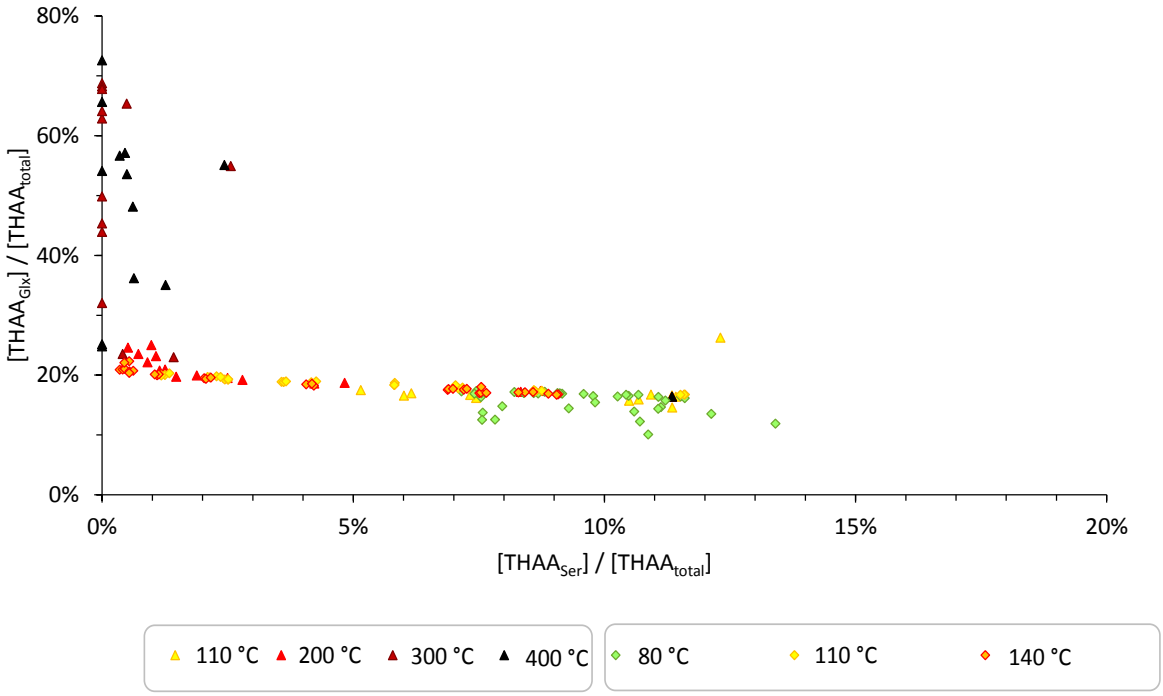

Figure 6.10: % Glx concentration of the total amino acid concentrations (Asx, Glx, Ser, Gly, Ala, Val, Phe & Ile) compared to % Ser concentration of modern OES samples heated at 80 – 140 °C under kinetic conditions (diamonds) and 110 – 500 °C under artificial heating conditions (triangles).

6.4.2.2. THAA racemization

The relative extents of Asx and Glx racemization for all the kinetic samples (i.e. 80 °C, 110 °C and 140 °C) appear to follow similar trends irrespective of the different temperatures (Fig. 6.11). However, samples heated at >200 °C for > 10 min deviate from this trend, showing a higher Glx D/L value for a given Asx D/L value (Fig. 6.11).

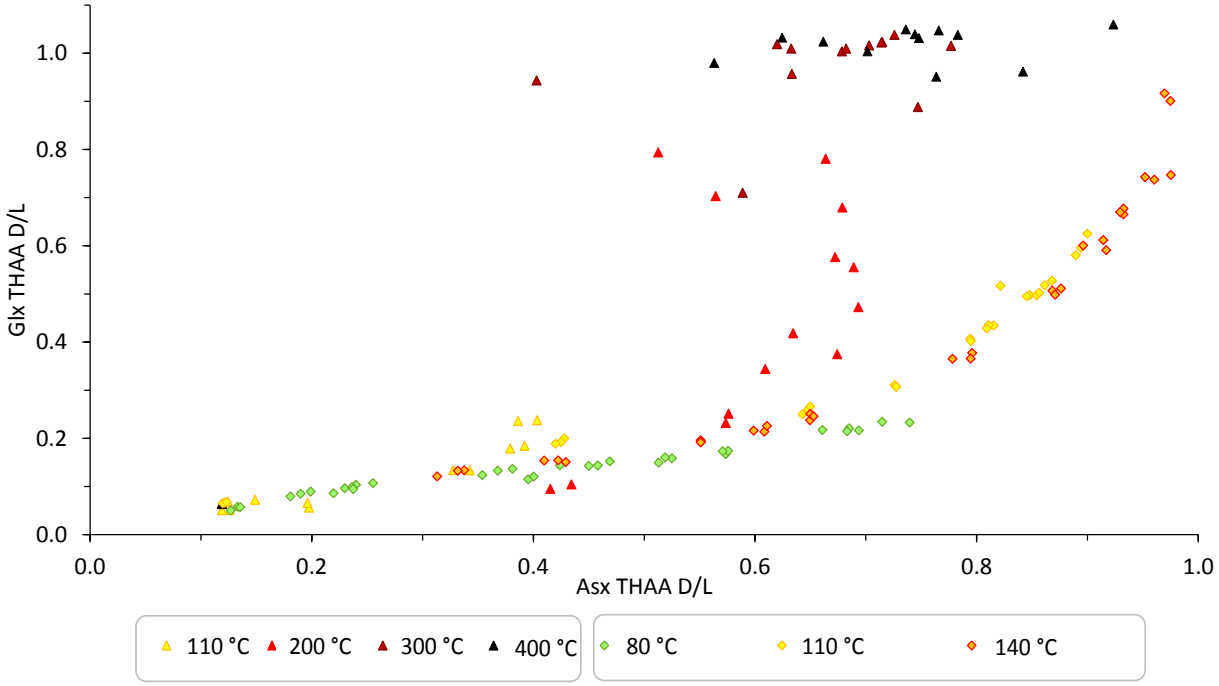

Figure 6.11: Asx THAA D/L vs. Glx THAA D/L of artificially heated modern OES samples (triangles) and kinetically heated modern OES samples (diamonds)

When the extents of Ile epimerisation and Glx racemization are considered, samples heated at 110, 140 and 200 °C appear to follow slightly different trends (Fig. 6.12); at lower temperatures, Ile epimerization appears to be favoured over Glx racemization. Indeed, comparing Ile and Glx appears to show some deviation in trends between samples artificially heated at 200 °C and the kinetic samples heated at 140 °C, there is also a small difference between the 110 °C and 140 °C kinetic trends over a limited Glx D/L range (approx. 0.5 – 0.7) (see also Chapter 4). The relative extents of Ile epimerization and Glx racemization may therefore be useful in identifying artificially heated sub-fossil OES samples.

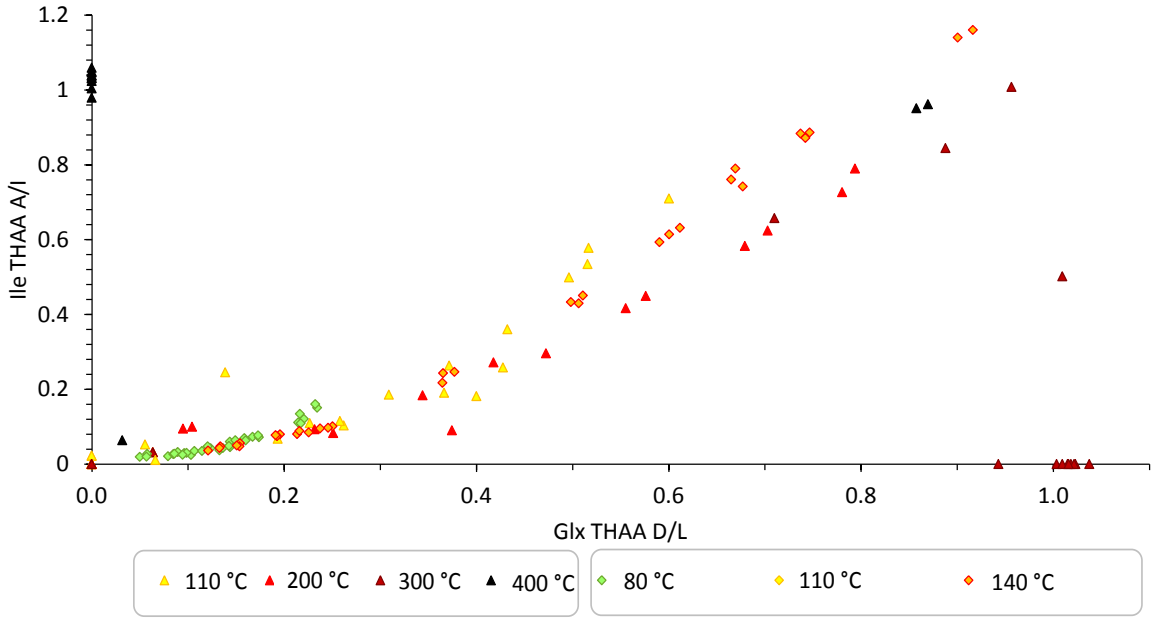

Figure 6.12: Glx THAA D/L vs. Ile THAA A/I of artificially heated modern samples (triangles) and kinetically heated modern samples (diamonds)

6.4.2.3. Hydrolysis

It has previously been shown that the trends in hydrolysis of kinetically heated samples and sub-fossil samples are not always equivalent at increased temperatures (Sec. 4.4.1.3.). Indeed, Ala hydrolysis follows a different trend for kinetically heated samples heated at 80 °C to those of ≥ 110 °C during the early stages of degradation (e.g. D/L < 0.4; Fig. 6.14). When artificially heated samples are included in these comparisons, e.g. for Ala (Fig. 6.13), there is not a clear differentiation between the trends of samples heated at different temperatures, as the 110 °C artificially heated samples do not follow the same trend as the 110 °C kinetically heated samples. It is unclear if this is a consequence of the different preparative methods.

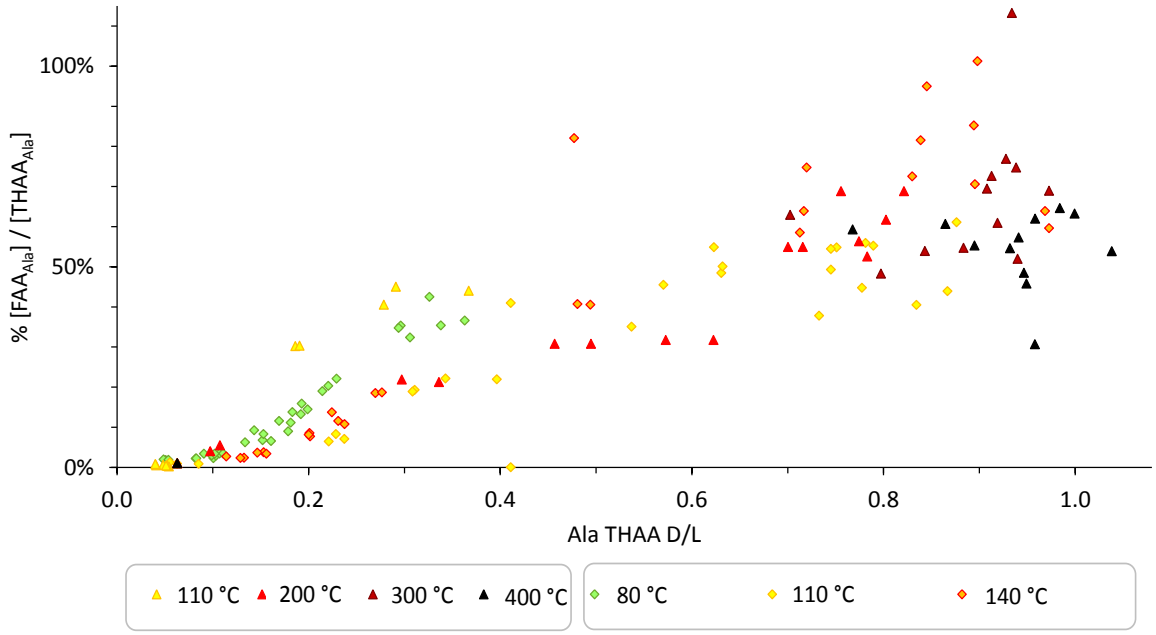

Figure 6.13: Extent of Ala hydrolysis under kinetic conditions between 80 – 140 °C (diamonds) and artificially heating conditions (triangles) between 110 – 400 °C, concentrations are normalised against the Ala THAA D/L values

6.4.3. Unidentified products of heating

It might be anticipated that heating OES at high temperatures not only increases the rate of protein degradation, but also enables reactions with higher activation energies to occur. Identification of the hypothetical degradation products may act as an additional indicator of whether a sample has been artificially heated. Indeed, heated samples consistently showed a small number of unidentified compounds which are not normally observed in the HPLC analysis, e.g. peaks at ~ 50 min and a collection of peaks from ~70-75 min (Fig. 6.14). Often these peaks were present even when the sum of THAA's concentrations had decreased to < 1 % of their initial concentrations (e.g. Fig. 6.14F). Heated samples also tended to show a lot of late-eluting compounds, e.g. the raised baseline from 60 min. These have also been reported from heated *Patella* samples (Demarchi, 2009), and so may be a common marker for heating in bio-minerals.

Areas of the resolved unidentified peaks were plotted against the degree of Asx racemization, as this was often the only amino acid showing well-resolved L and D peaks at temperatures > 400 °C. Unfortunately, no correlation between these peaks and increased temperature was found. However, it shows the potential that some compounds are very resistant to heating, but further identification of these analytes is needed, for example using LC-MS.

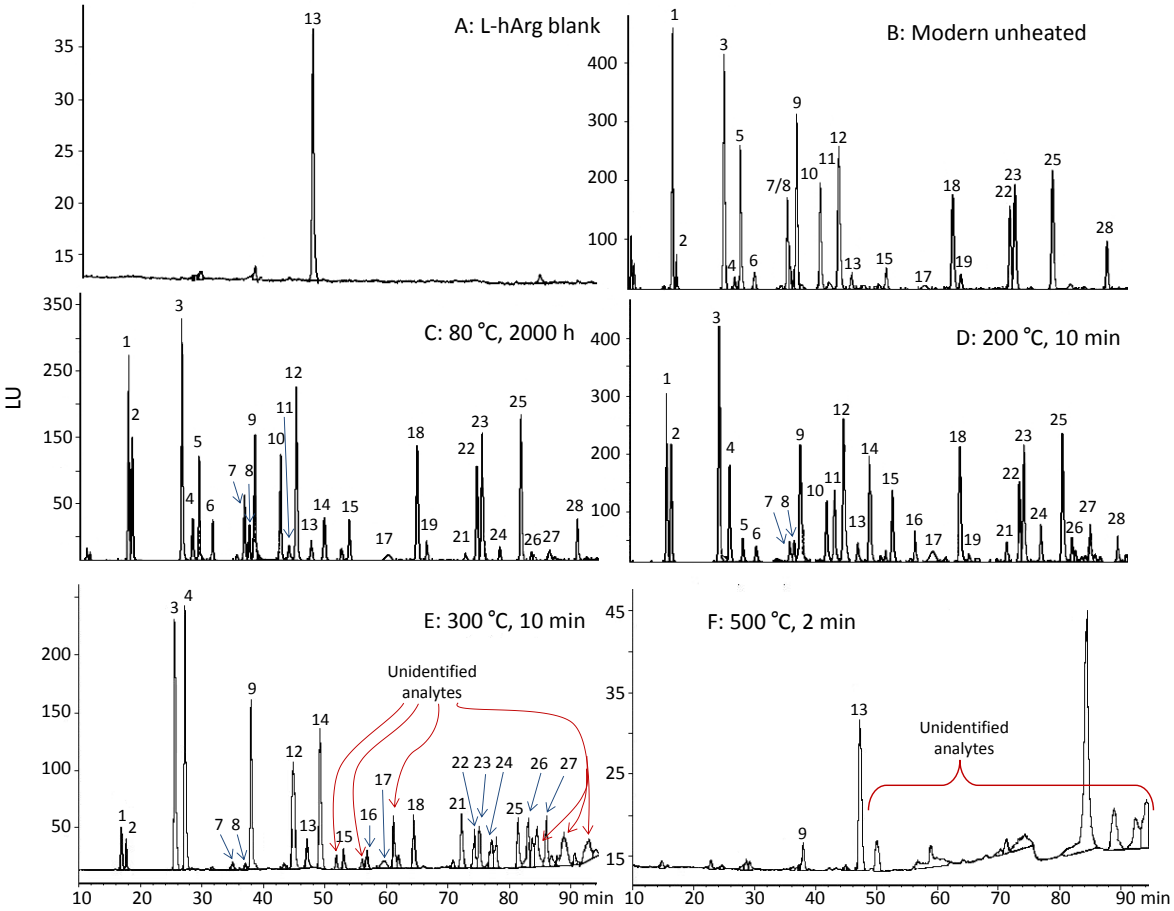

Figure 6.14: HPLC chromatograms: A: L-hArg blank; B: Modern unheated, bleached OES; C: Modern OES, intra-crystalline fraction, heated at 80 °C for 2000 h heated under kinetic conditions; D: Modern OES heated at 200 °C for 10 min using artificial heating method; E: Modern OES heated at 300 °C for 10 min using artificial heating method; D: Modern OES heated at 500 °C for 2 min using artificial heating method. (1. L-Asx, 2. D-Asx, 3. L-Glx, 4. D-Glx, 5. L-Ser, 6. D-Ser, 7. L-Thr, 8. L-His. 9. Gly (& D-Thr & D-His), 10. L-Arg, 11. D-Arg, 12. L-Ala, 13. L-hArg, 14. D-Ala, 15. L-Tyr, 16. D-Tyr, 17. Gly (secondary), 18. L-Val, 19. L-Met, 20. D-Met, 21. D-Val, 22. L-Phe, 23. L-Ile, 24. D-Phe, 25. L-Leu, 26. D-alle, 27. D-Leu, 28. L-Lys)

6.4.4. Structural changes

It has been observed by Heredia and colleagues (2005) that structural changes to the mineral in the cone and palisade layers of OES samples heated at > 500 °C can be observed by powder X-ray diffraction. They noted that the cone and palisade layers showed different thermal behaviour to the palisade layer, which showed no change in the mineral structure even when heated at 550 °C for 30 min. This work agrees with the visual analysis from this study (Sec. 6.4.1.), which showed a difference in thermal behaviour at temperatures as low as 200 °C.

Samples heated at > 500 °C are unlikely to have amino acids remaining (Sec. 6.4.2.1.), therefore cannot be identified as having been heated through comparative rates of protein degradation. However, it is likely that these samples will be easy to identify visually (Sec. 6.4.1.) and hence unlikely that these samples would be mistaken as genuinely old.

Powder XRD analysis was carried out on modern OES, modern OES heated at 200 °C for 15 min, modern OES heated at 280 °C for up to 30 min and two 71 ka unheated sub-fossil OES samples. The diffraction peak heights, widths and shifts were compared for all samples. However, no correlation could be found between changes in these parameters and thermal treatment. Therefore, it is assumed that the differences in peak shape and intensities in Fig. 6.14 are due to the natural variability.

XRD may have some use in identifying samples heated to very high temperatures (e.g. > 500 °C), but not at lower temperatures. The changes in mineral structure are likely to occur in the palisade and cone layers, which were observed to spall off when the OES fragments were heated at 500 °C for more than 2 min, therefore it is unlikely that these layers would persist in the fossil record.

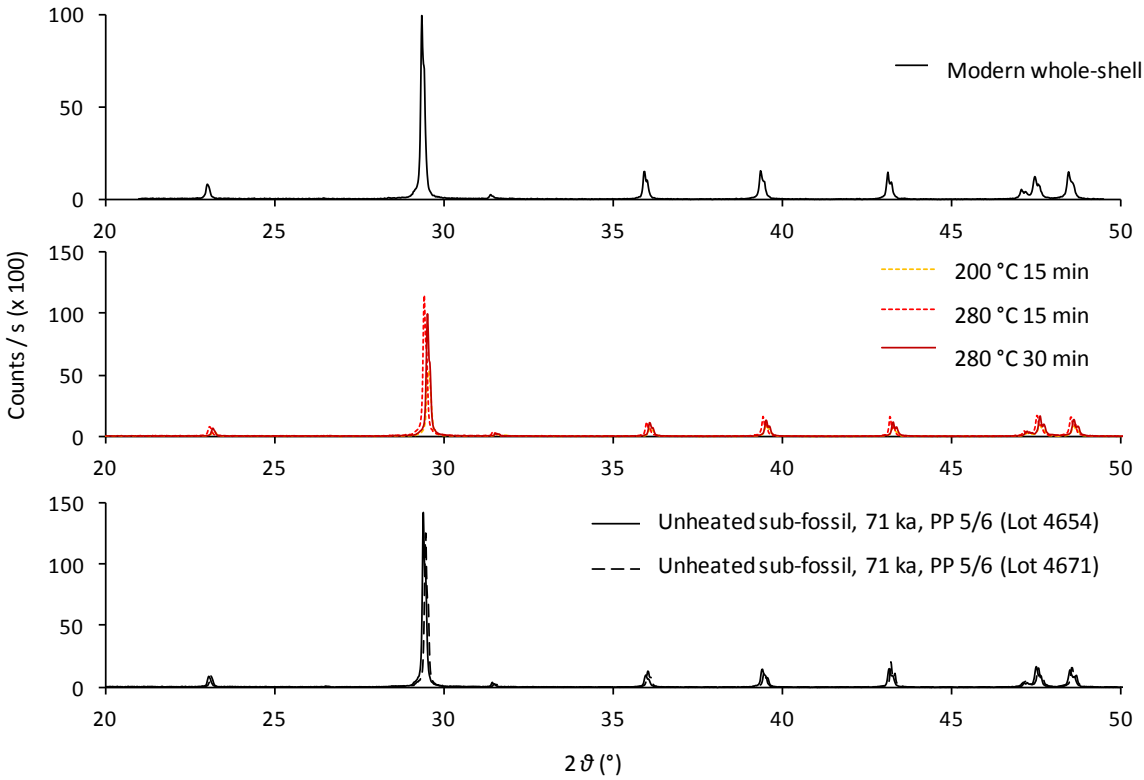

Figure 6.15: X-ray diffraction of modern (top), modern heated (middle) and unheated sub-fossil (bottom) OES samples: modern heated samples heated at: 200 °C for 15 m, 280 ° for 15 min and 280 °C for 30 min.

6.4.5. Summary of Artificial heating study

It has been shown that several protein degradation reactions in modern OES samples have different temperature dependencies, and therefore may be used to identify sub-fossil samples which have been exposed to high temperatures. It was found that the following show a potential use as indicators for exposure to increased temperatures:

- Physical appearance and olfactory analysis
- High % Glx, low % Ala, low % Ser and low % Asx composition for a given D/L value (Figs. 6.4 – 6.10)
- Different trends in relative rates of racemization: Glx vs. Asx (Fig 6.11) & Glx vs. Ile (Fig. 6.12), samples heated at high temperatures have higher Glx D/L values for given Asx D/L and Ile A/I values than samples heated at lower temperatures
- Relative rates of Ala hydrolysis and Ala racemization (Fig. 6.13); hydrolysis appears to be favoured at lower temperatures
- Additional analytes observed in HPLC-chromatograms for samples heated at high temperatures, e.g. ≥ 300 °C (Fig. 6.14)

- Samples heated at > 500 °C preserved little, if any, amino acids; therefore comparative rates of protein degradation could not be used to identify these heated samples. Instead visual, olfactory, or perhaps changes in mineral structure must be used as indicators (Sec. 6.4.4.).

This study suggests that it is unlikely that there will be one single 'marker' for a sample having been heated, especially for sub-fossil samples where their history is likely to be more complex than the isothermal experiments performed for this study. It is possible that sub-fossil samples are not exposed to only one heating episode; there may be many, of different intensities over many years, or indeed no heating episodes at all. Ideally at sites where there is a lot of evidence for the use of fire, many samples would be obtained for AAR analysis as the chances of samples having been heated are high. It would be expected that some large fragment OES samples may have local areas which have been heated to a greater extent than the rest of the fragment. Therefore, several analyses of the same sample may be required especially for those samples which have a questionable thermal history. However, the identification of potential markers of high temperature exposure could be very useful; therefore these potential markers are explored in the next section by comparison with the archaeological data set.

6.5.1. All data

Analysis of the entire suite of sub-fossil samples showed considerable variability of D/L values compared with the independent ages provided by radiocarbon or OSL (Fig 6.16; Ile shown, other amino acids show a similar spread of D/L values, see Appendix C).

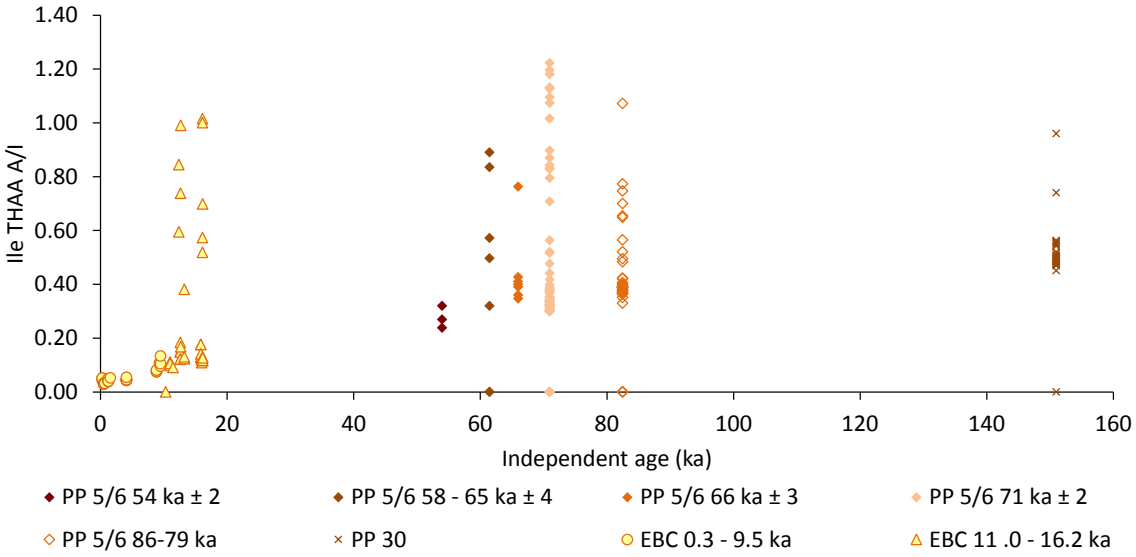

Figure 6.17: Degree of epimerization for Ile in the THAA fraction, colour coded by independent ages determined using radiocarbon dating for EBC and OSL for PP (Section 6.1.)

6.5.2. Variability

The likely causes of the variability of D/L values for samples of the same independent age have already been discussed (Sec. 6.1.). In order to assess the variability induced by the preparation method, three samples covering the age range represented by PP 5/6 were prepared in triplicate. The variability observed is not enough to account for the variability seen in Fig. 6.16 (e.g. Table 6.4 & 6.5). The relative standard deviations (RSD) of the THAA concentrations were generally < 5 % (except Gly from sample '4689' which was higher at 6.6 % RSD; Table 6.4). The error associated with the FAA concentrations was higher, with RSD values as high as 31.6 % (Table 6.4). The RSD values of the D/L values, for THAA were < 6.4 % and for FAA were < 7.6 % (Table 6.5).

These errors are generally lower than the errors reported in a recent proficiency testing study for 10 modern 48 h bleached OES samples analysed in the AAR labs at York, the % RSDs were

generally < 8 % for THAA concentrations and < 10 % for D/L values (Powell *et al*., 2012). These errors were calculated on samples prepared by different analysts at different times and using two different HPLC machines. This may explain the higher error than reported in this study, where samples were prepared at the same time, by the same analyst and all samples were analysed using the same HPLC machine.

			Concentration (pmol / mg)								
			Asx	Glx	Ser	Gly	Ala	Val	Phe	Ile	Total
4689 (~151 ka)	THAA	Average	6687	7841	873	7284	6647	3010	2871	3603	38815
		%RSD	3.2	4.0	1.5	6.6	1.6	3.0	3.3	3.4	2.6
	FAA	Average	3624	1199	411	5028	4269	1460	1191	1761	18943
		%RSD	9.0	8.3	10.9	7.8	8.7	6.4	8.0	6.4	8.0
4668 (~66 ka)	THAA	Average	8023	9253	1485	8887	7325	3611	3263	4197	46044
		%RSD	3.4	3.8	4.8	4.0	3.9	3.4	3.7	3.4	3.5
	FAA	Average	2714	991	654	254	3972	1397	1133	1610	12726
		%RSD	23.7	31.6	17.8	6.2	21.3	23.1	18.9	21.8	11.1
4613 (~54 ka)	THAA	Average	8760	9748	2105	10015	7392	3945	3324	4362	49650
		%RSD	2.1	3.5	2.6	4.5	2.3	3.0	4.0	3.2	3.1
	FAA	Average	2675	965	861	208	3198	1139	863	1271	11180
		%RSD	16.3	13.2	18.7	14.0	19.7	20.0	19.2	19.0	18.0

Table 6.4: Three sub-fossil OES samples from PP 5/6 were prepared in triplicate. %RSD = standard deviation relative to the mean average concentration.

			D/L values						
			Asx	Glx	Ser	Ala	Val	Phe	Ile
4689 (~151 ka)	THAA	Average	0.77	0.39	0.68	0.61	0.33	0.67	0.49
		%RSD	0.4	0.7	1.6	3.2	2.3	1.4	1.1
	FAA	Average	0.85	0.43	1.05	0.80	0.54	1.22	0.69
		%RSD	0.8	2.6	2.8	2.0	2.6	2.3	1.4
4668 (~66 ka)	THAA	Average	0.69	0.29	0.68	0.48	0.23	0.53	0.34
		%RSD	0.9	1.0	0.7	1.8	1.3	1.3	1.5
	FAA	Average	0.82	0.33	1.05	0.72	0.46	1.19	0.59
		%RSD	0.9	2.7	1.1	0.7	4.9	4.7	2.1
4613 (~54 ka)	THAA	Average	0.66	0.23	0.70	0.40	0.18	0.46	0.26
		%RSD	1.7	1.8	2.4	2.6	6.4	2.9	3.1
	FAA	Average	0.78	0.28	1.04	0.58	0.36	1.09	0.45
		%RSD	1.6	4.5	0.7	1.6	7.6	3.1	2.7

Table 6.5: Three sub-fossil OES samples from PP 5/6 were prepared in triplicate. %RSD = standard deviation relative to the mean average concentration.

The inter-shell variability within a horizon was measured by consideration of all samples from PP 30 (excluding the 3 samples which have been identified as having been artificially heated, presumably through veld fires, see Sec. 6.5.3.). This showed that the RSDs in THAA D/L values are generally < 6 % and < 5 % for FAA D/L values (Table 6.6). The THAA concentrations showed higher variability of ~ 20 %. The variability in THAA compositions were lower than that of the absolute concentrations, generally < 4 %, except Ser and Gly which showed slightly higher RSDs at 7 % and 6 %, respectively. Considering concentrations relative to each other compensates for some of the analytical error introduced by, for example, inaccurate dilutions. Therefore, the amino acid compositions and D/L value errors give a better indication of the between sample reproducibility.

These inter-shell errors are in line with previous studies, e.g. Miller and colleagues (1992) who quoted 3 – 5 % for the THAA D/L values of 5 sub-fossil OES samples, and for that quoted by Penkman *et al.* (2011) for 13 sub-fossil opercula samples at < 4 % for the THAA D/L values. A higher variability has been observed for mollusc samples; 6 – 8 % for THAA D/L values for 5 samples (Miller and Brigham-Grette, 1989) and as high as 10 % for some THAA D/L values for *Patella* samples (Demarchi, 2009). Demarchi speculated this higher variability was due to low D/L values and mixed-age populations.

		Asx	Glx	Ser	Gly	Ala	Val	Phe	Ile
FAA D/L	Average	0.87	0.42	0.99	NA	0.81	0.52	1.04	0.74
	% RSD	0.9	3.6	2.9		2.0	4.2	5.2	3.8
THAA D/L	Average	0.76	0.39	0.63		0.66	0.38	0.69	0.50
	% RSD	1.9	4.4	5.6		3.9	6.1	4.6	5.8
[THAA] (nmol / mg)	Average	6.2	7.0	0.9	6.3	5.8	2.8	2.3	3.2
	% RSD	21.1	20.9	18.3	19.0	19.1	19.7	20.4	20.1
THAA composition	Average	18%	20%	2%	18%	17%	8%	7%	9%
	% RSD	3.3	2.2	7.2	5.8	2.3	3.5	4.5	3.5

Table 6.6: Average values and relative standard deviations (RSD) for all unheated sub-fossil samples from PP 30

Errors associated with analytical reproducibility (Table 6.4; 6.5) and inter-shell variability (Table 6.6) are therefore not significant enough to explain the variability observed in the complete sub-fossil data set (e.g. Fig. 6.16). The visual appearance of some samples (areas of charring and discolouration) and a characteristic 'burnt' odour emitted from some of these samples on grinding leads to the suspicion that artificial heating is responsible for the majority of the variability between degree of racemization and horizon age in PP 5/6 and EBC (Fig. 6.16). In contrast, OES from PP 30 show less variability, presumably because of the lack of human activity (Fig. 6.16). The main source of variability in the PP 30 samples may be because the samples are not all of the same age.

6.5.3. Application of heating markers to sub-fossil data

The sub-fossil data was further assessed using the heating criteria described in Section 6.4.5.

6.5.3.1. Appearance and olfactory analysis

Many OES samples from PP 5/6 and EBC show visual characteristics of having been heated (areas of charring and discolouration, Fig. 6.17) and a characteristic 'burnt' odour was emitted from some of these samples on grinding. In contrast, OES from PP 30 showed less variability, presumably because of the lack of human activity, with only one sample emitting a smell when broken up.

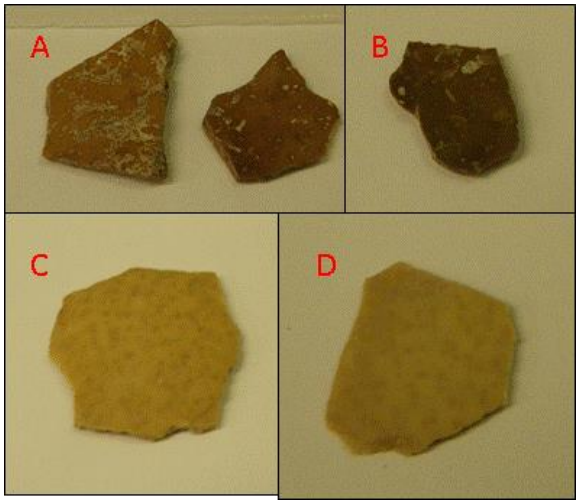

Figure 6.17: Examples of archaeological OES samples from PP 5/6. A: 86 – 79 ka, visual presence of charring; B: 72 – 70 ka, visible presence of charring; C: 72 – 70 ka, no visible signs of heating; D: 48 ka, no visible signs of heating.

6.5.3.2. Amino acid decomposition

The sub-fossil sample data was added to each of the comparisons of THAA compositions of artificially heated OES (Figs. 6.7 – 6.9 & Fig. 6.20). It was found that the majority of sub-fossil samples fell onto the trend-lines set by the modern samples artificially heated at < 200 °C (Figs. 6.18), with a smaller number of samples falling into the regions occupied by the modern samples artificially heated at temperatures ≥ 300 °C.

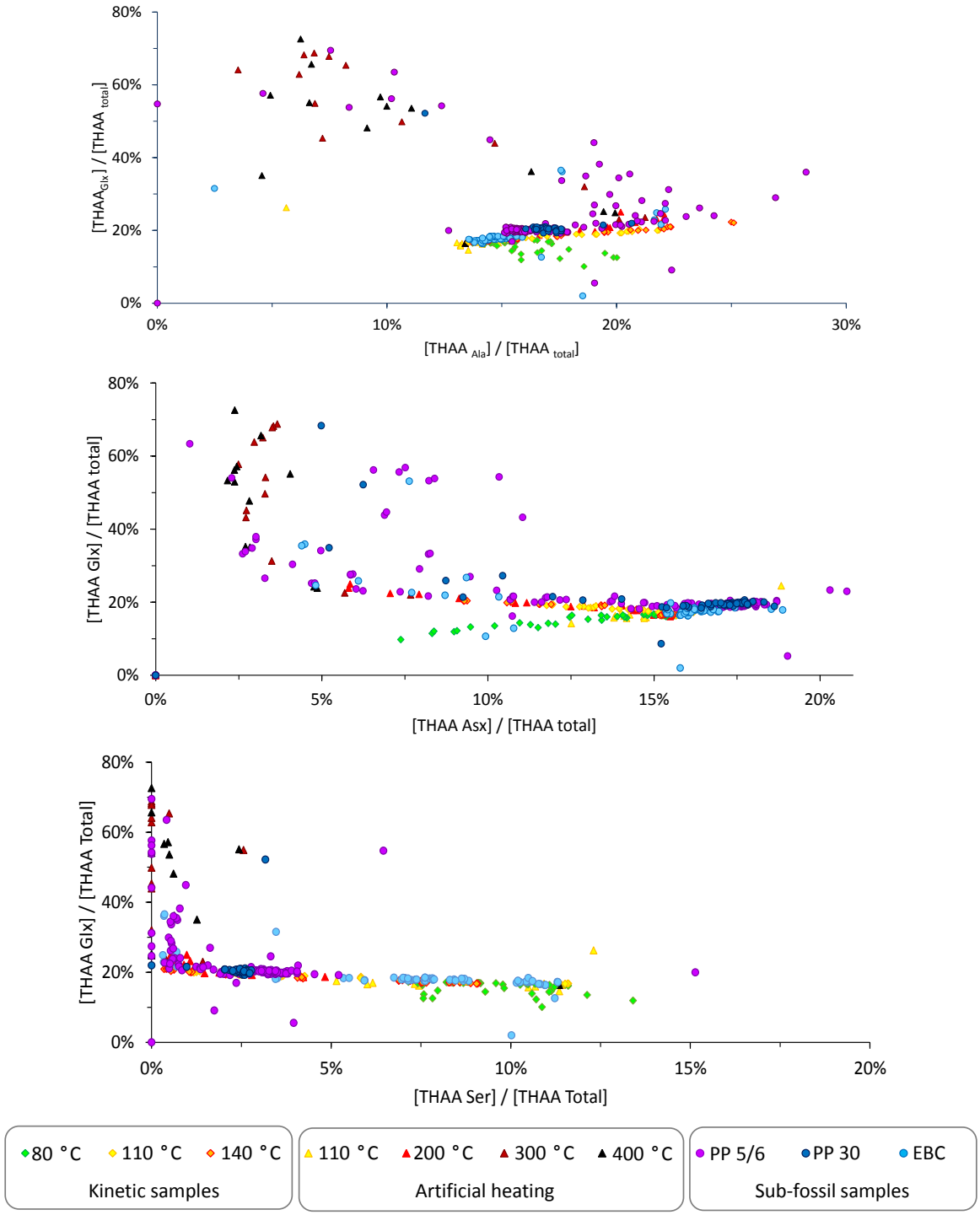

Figure 6.18: Comparison of THAA compositions for kinetic samples (diamonds), artificially heated samples (diamonds) and sub-fossil samples (circles) for, top: Ala composition vs. Glx composition; middle: Asx composition vs. Glx composition; bottom: Ser composition vs. Glx composition.

It was observed that the composition of amino acids in sub-fossil samples varied considerably, even from samples from within the same horizon. The majority of sub-fossil samples showed a similar composition to that of modern unheated OES samples. However, many showed

compositions dominated by Glx (Fig. 6.19), as was observed for modern heated samples in this study (Sec. 6.4.2.1., Fig. 6.2) and by Brooks *et al.* (1991). Indeed, sub-fossil samples identified as having been heated through olfactory and visual analysis (e.g. Sec. 6.5.3.1.), all showed a composition higher in Glx and lower in Asx than samples of similar age that did not display a burnt appearance or emit a smell. Within the time limits of our artificial heating experiments, compositions containing > 50 % Glx were only observed for modern OES samples when heated at > 300 °C (e.g. Fig. 6.2).

A small number of samples from each horizon at PP 5/6/30 were selected which didn't show visual signs of heating, did not smell upon grinding and that showed the lowest degrees of racemization for their horizon. As such, these samples were assumed not to have been exposed to high temperatures. 5 samples were selected from every horizon, except the 48 ka horizon from PP 5/6 where only 2 samples were available. All of these samples selected displayed compositions very similar to those seen in modern samples (Fig. 6.19).

It was noted that the % Ala concentrations in some heated samples showed higher and some showed lower concentrations than unheated samples (Fig. 6.19). Therefore, the use of THAA composition for identifying heated sub-fossil samples was limited to Glx and Asx, which showed the largest increase and decrease, respectively, with artificial heating (Fig. 6.18 top; 6.19).

The compositions of all the 'unheated' sub-fossil samples were used to calculate a single standard deviation for each amino acid. Sub-fossil samples were tentatively assigned as heated if they had both a % Glx concentration that was greater than the average of the unheated sub-fossil samples plus 3 standard deviations, and, a % Asx concentration lower than the unheated average plus 3 standard deviations (e.g. % Glx > 21.1 % and % Asx < 14.9 %). Using this method, 3 samples from PP 30, 37 samples from PP 5/6 and 8 samples from EBC were identified as possibly having been heated. This included all of the samples which were identified visually and/or by olfactory analysis.

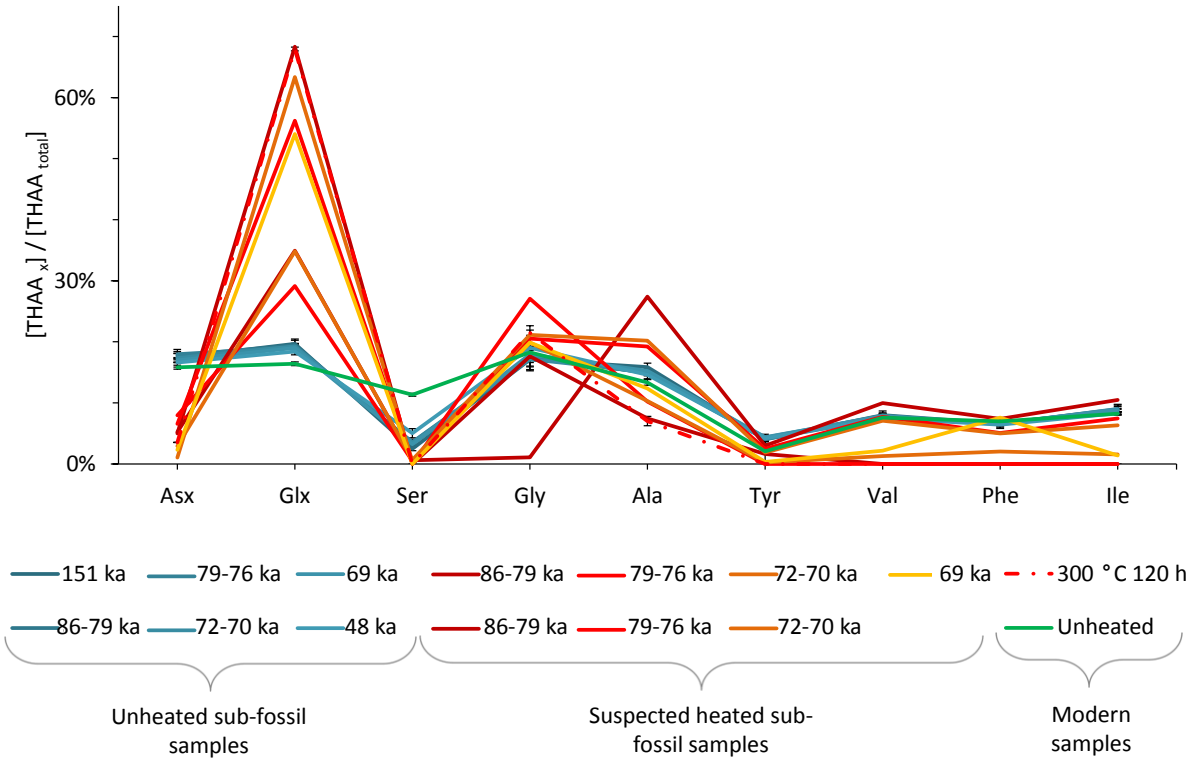

Figure 6.19: THAA composition of selected sub-fossil and modern OES samples. Five samples from each horizon showing the lowest degrees of racemization and no visual or olfactory signs of heating were selected as 'unheated sub-fossils'; error bars represent 2 x standard deviation of these 5 samples. Error bars for modern samples represent 2 x standard deviation based on triplicate samples.

6.5.3.3. Comparison of Asx and Glx racemization

The artificial heating study showed that a comparison of the relative extents of Asx and Glx racemization may serve as a useful marker for identifying heated samples, as there was a deviation in trends between samples heated at ≥ 200 °C and ≤ 140 °C (Sec. 6.4.2.2.). When the sub-fossil data is added to the artificial heating data, it shows that the majority of sub-fossil samples appear to follow the trend set by the kinetic samples (≤ 140 °C), however a number also fall above this trend, showing similar D/L values to modern samples heated at ≥ 200 °C (Fig. 6.20). The vast majority of PP 30 samples, which are less likely to have been exposed to artificial heating, plot onto the trend set by the kinetically heated modern samples. This suggests that the kinetic data (80 – 140 °C) sufficiently describes the trends of Asx/Glx racemization at lower temperatures. Therefore, sub-fossil samples falling off this trend line are suspected as having been heated.

In order to mathematically differentiate between 'heated' and 'unheated' samples, a third order polynomial was calculated using all of the 80 °C and 110 °C data and all but the last time point

(240 h) of the 140 °C (as this would require extrapolating beyond the range of the sub-fossil samples). A third order polynomial was chosen purely because it best described the data set. Using the observed Asx D/L values theoretical Glx D/L values were calculated using the third order polynomial expression (Fig. 6.20) and compared to the observed Glx D/L values; the standard deviation of the differences were then calculated. Artificially heated modern samples which showed a difference between their calculated and observed Glx D/L values of more than 4 times the standard deviation calculated from the kinetic samples were marked as having been heated. By employing this method all modern samples heated at > 300 °C and at > 200°C for > 10 min were marked. This method therefore allowed differentiation between samples heated at 200 °C > 10 min and those heated at < 140 °C, and was therefore applied to the sub-fossil samples as well. Using this method 3 samples from PP 30, 8 samples from EBC and 42 samples from PP 5/6 were marked as potentially having been exposed to high temperatures e.g. ≥ 200 °C for ≥ 10 min (samples highlighted with squares in Fig. 6.20); this included all of those samples having been identified as possibly having been heated through the amino acid composition (Sec. 6.5.3.2., Fig. 6.19).

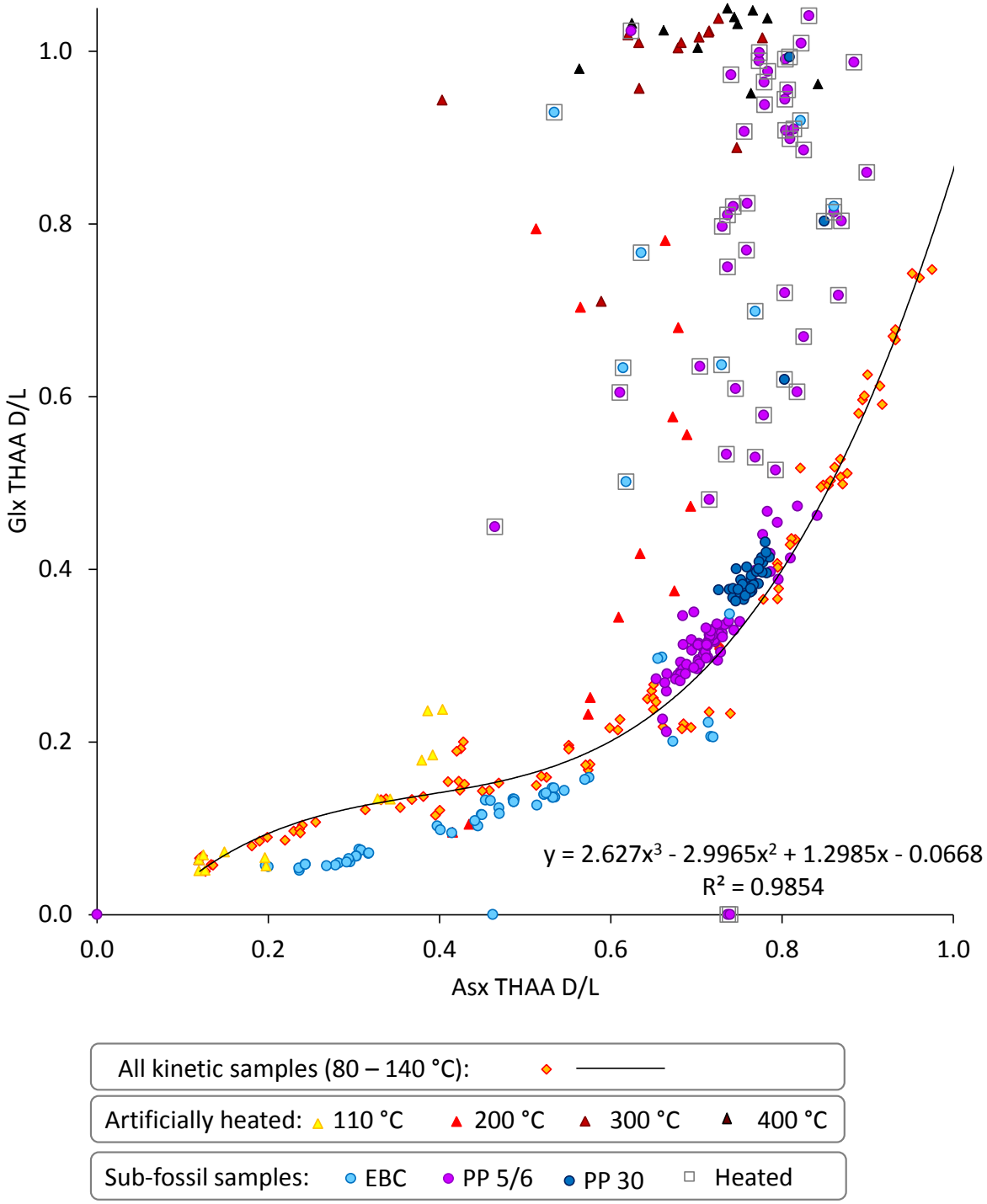

Figure 6.20: Asx THAA D/L vs. Glx THAA D/L of sub-fossil samples and artificially heated modern samples; samples marked with a grey square are suspected to be heated samples, as they fall away from the trend line of the kinetic samples

6.5.3.4. Comparison of Ile and Glx racemization

Similarly to the comparison of Asx/Glx racemization (Sec. 6.5.3.3.), the relative rates of Ile and Glx racemization in modern heated samples (Fig. 6.11) indicated that Ile epimerization may be

favoured over Glx racemization at lower temperatures, and therefore may be used to identify heated sub-fossil samples.

The majority of sub-fossil samples form a trend line above that of the kinetic and artificially heated modern samples, where Ile epimerization is even more favoured than Glx at lower temperatures (Fig. 6.21). This observation was confirmed on three fronts:

1. The vast majority of PP 30 samples, which are unlikely to have been exposed to anthropogenic fire, form a tight group on the 'unheated' trend (Fig. 6.21A)
2. A sub-set of 'unheated' sub-fossil samples (see Sec. 6.5.3.1.), shown as green square symbols in Fig. 6.21, also plot onto the 'unheated' trend (Fig. 6.21A)
3. Sub-fossil samples all previously identified as having been heated (through composition, olfactory or visual analysis) all fall onto the trends set by the kinetically and artificially heated modern samples (Fig. 6.21A)

In order to systematically identify heated samples, a trend-line was fitted to the assumed unheated sub-fossil samples; a second order polynomial was used as this best described the trend (Fig. 6.21). Theoretical Ile A/I values were calculated for all sub-fossil samples based on their observed Glx D/L value and the second order polynomial based on the trend of the unheated sub-fossil samples. The standard deviation of the differences between the observed and calculated Ile A/I values of the unheated sub-fossil samples was calculated. Samples have been identified as heated where the calculated and observed Ile A/I values deviate by more than 5 times the standard deviation calculated from the unheated samples (Fig. 6.21B).

This method of identifying heated samples is better suited in identifying the more subtly heated samples with Glx D/L values of approximately < 0.4, values higher than this require extrapolation beyond the known trend of the unheated sub-fossil samples. Using this method in conjunction with the previously described visual analysis (Fig. 6.212A; Sec. 6.5.3.1.), composition (Fig. 6.21A; Sec. 6.5.3.2.) and racemization of Glx/Asx (Fig. 6.21A; Sec. 6.5.3.3.) methods, an additional 15 samples from PP 5/6 and one from EBC were identified as having been heated (Fig. 6.21B). There were however a small number of border-line sub-fossil samples which were not identified as having been heated; these borderline samples have not been excluded in this study. The cut-off value of 5 times the standard deviation erred on the side of caution so as to not identify samples as heated which could not be justifiably removed. However, with further analysis of more sub-fossil samples and perhaps independent methods of identifying heated samples, these border-line samples may also be justifiably removed.

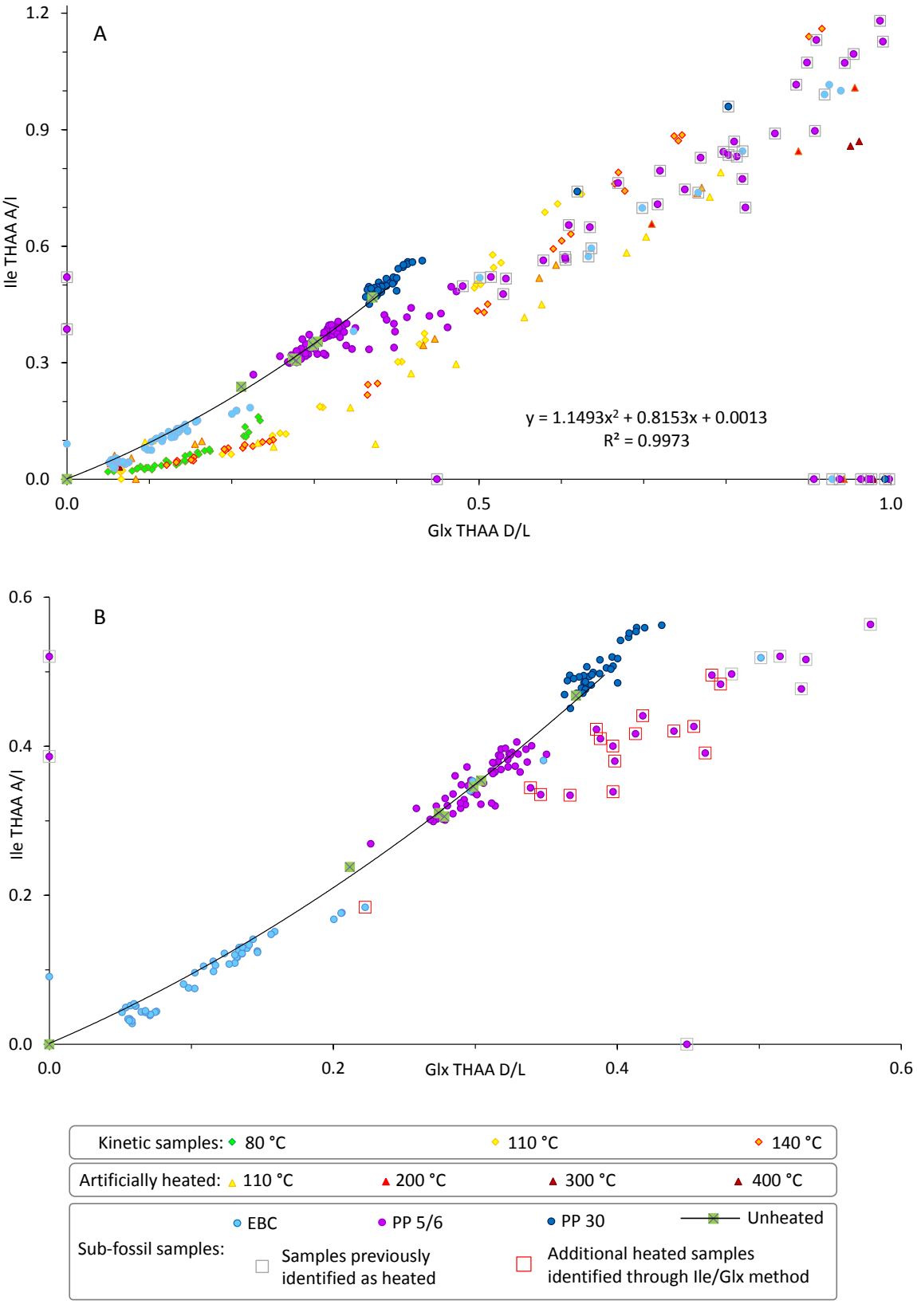

Figure 6.21: A: Ile THAA A/I vs. Glx THAA D/L of sub-fossil samples and artificiality heated modern samples showing heated samples identified through previous methods (Sec. 6.5.3.1.; 6.5.3.2.; 6.5.3.3.); B: Sub-fossil samples only, indicating additional samples identified as heated through Ile/Glx D/L method

6.5.3.5. Rates of Ala hydrolysis and racemization

Previously it has been shown that the temperature dependencies of the hydrolysis and racemization of Ala may also be used to identify samples exposed to high temperatures (Fig. 6.12). However, when the sub-fossil data is added into the comparison, the temperature dependence is unclear, largely due to the large range of Ala concentrations of the sub-fossil samples (Fig. 6.22). The younger samples from EBC plot to the left of the 80 °C data, which suggests that hydrolysis is indeed favoured at lower temperatures, as has been seen previously (Chapter 4 & 5). However, a small number of 110 °C artificially heated samples also plot to this side of the 80 °C trend. As the resolution is not as clear as previous methods (e.g. Sec. 6.5.3.2. - 6.5.3.4) this method was not pursued for the identification of heated sub-fossils.

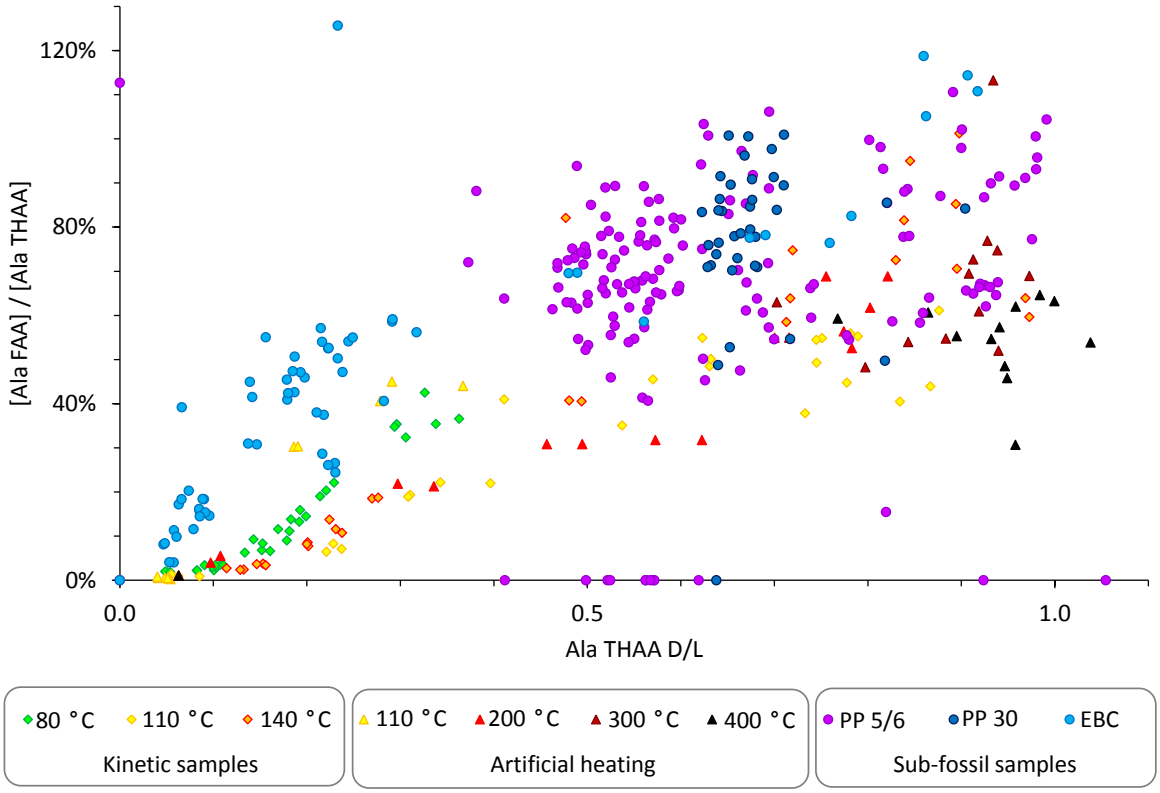

Figure 6.22: Hydrolysis of Ala of modern OES samples heated under kinetic conditions and artificial heating conditions and sub-fossil samples from EBC, PP 5/6 and PP 30 normalised against Ala THAA D/L

6.5.3.6. Additional analytes

Sub-fossil samples which were identified as having been heated (Sec. 6.5.2 – 6.5.3) show the same characteristic HPLC chromatograms as artificially heated modern samples (Fig. 6.13), e.g. a sharp unidentified peak at approximately 59 min and many additional hydrophobic analytes eluting

from approximately 65 min onwards (Fig. 6.23), which sub-fossil samples of similar age which have not been identified as heated do not show (Fig. 6.23). No correlation could be found between the area of the peak at 59.7 min and the degree of heating or the sample's independent age, therefore this is not useful as a quantitative measure of artificial heating. However, the presence of this peak and additional hydrophobic analytes can still be used to identify artificial heating in many sub-fossil samples.

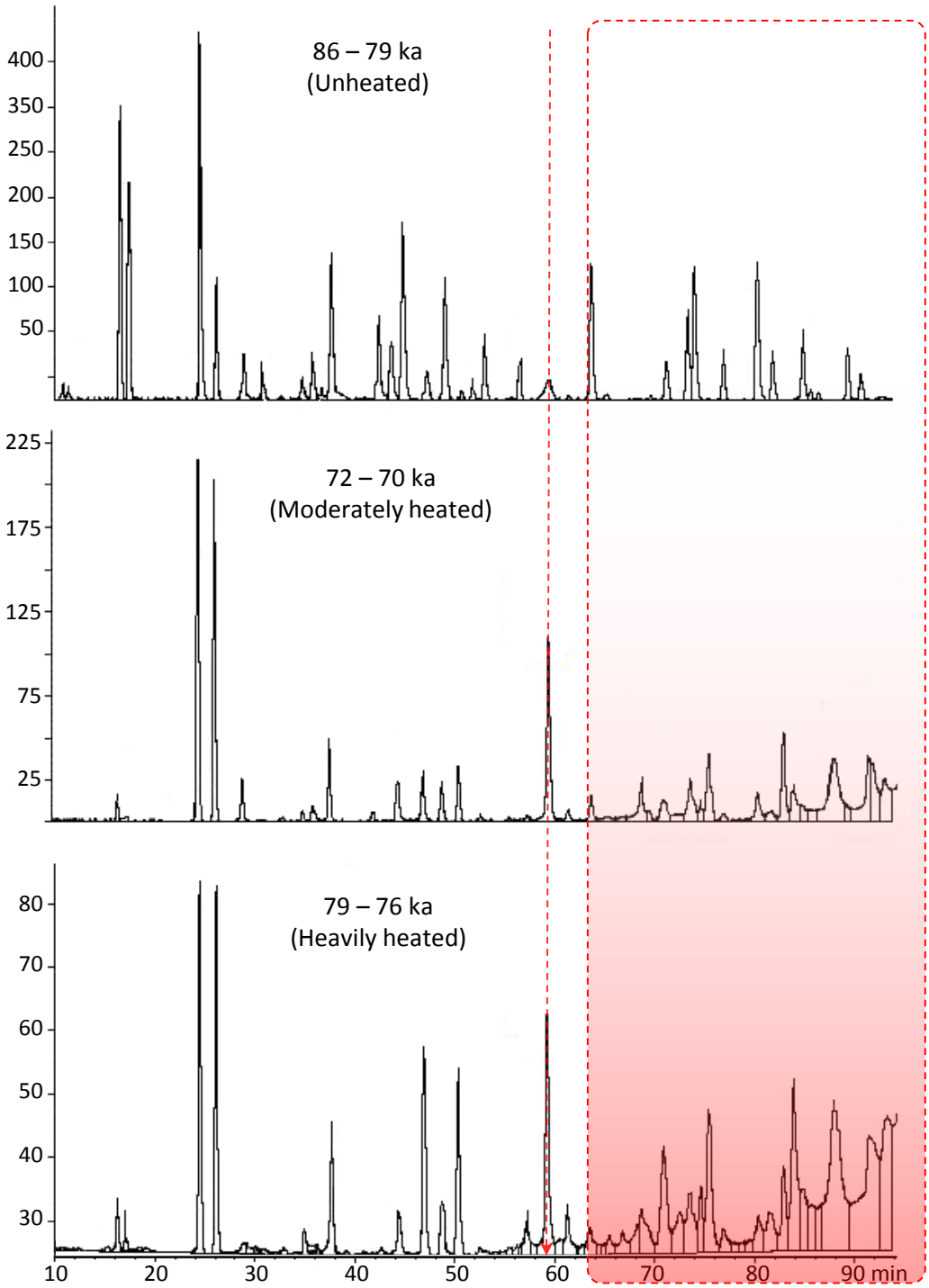

Figure 6.23: HPLC chromatograms from Pinnacle Point OES sub-fossil samples: TOP: un-heated; MIDDLE: suspected slightly heated; BOTTOM: suspected heavily heated. Heated samples are characterised by a sharp peak at ~ 59 min (highlighted by red dotted line) and multiple unresolved peaks eluting from ~ 65 min (highlighted by red box)

6.5.4. Summary of identification of artificially heated samples

It is very important for the application of AAR to OES (and indeed other bio-minerals used for AAR) to be able to distinguish between genuinely old samples and those which have been artificially 'aged' by increased temperatures (Brooks *et al.*, 1991). To that end, the amino acid compositions and rates of racemization and hydrolysis have been compared at different temperatures, normalised against the D/L values. The temperature dependencies for many of these reactions are sufficiently different to be able to differentiate between samples heated at different temperatures, as previously noted for Leu hydrolysis and Ile epimerization in OES (Miller *et al.*, 1992).

It seems there may not be one key indicator for identifying heated samples, as these markers will vary depending on the degree of heating and the age of the sample. Compositional changes (Figs. 6.3 – 6.6), for example, can differentiate between most samples heated < 200 °C and those at > 300 °C with the same Asx D/L values, but it cannot differentiate between samples heated between 80 – 200 °C. Heating a sample at 200 °C for only 2 min increases Ile A/I from ~ 0.03 to ~ 0.10, and Asx D/L from ~ 0.12 to ~ 0.42, which are similar to the levels of racemization observed for samples aged ~ 9 ka. Therefore, using composition alone to identify heated samples may leave a significant number of artificially heated samples unidentified which would increase the error associated with OES AAR age estimates.

The relative extents of Glx and Asx racemization were able to differentiate between samples heated at ≤ 140 °C and those heated at ≥ 200 °C for > 10 min. These measures have previously been suggested to be useful in identifying heated samples in the mollusc shell *Patella* (Demarchi, 2009; Demarchi *et al.*, 2011).

The most sensitive technique for identifying samples at intermediate temperatures was comparison of the relative extents of Ile and Glx racemization (Fig. 6.21). Applying this comparison, samples heated at > 80 °C and those unheated in geological conditions can be distinguished. All samples previously identified as having been heated fall onto the trend lines set by the high temperature experiments, but in addition a further 18 samples from PP 5/6 can be identified as probably having been heated. This method is limited at present to samples with Ile A/I approximately < 0.6 and Glx D/L approximately < 0.45, as samples showing higher D/L values than this would require extrapolation beyond the extents of low temperature sub-fossil data. This study would therefore benefit from the analysis of older, unheated, sub-fossil samples. Although this method appears to be the most sensitive, it would be prudent to use all the

comparisons (smell, appearance, composition and Asx D/L : Glx D/L) to screen the more heavily heated samples first to give greater confidence in the identification of heated samples.

Interestingly, 3 samples from PP 30 were consistently identified as having been artificially heated. Although PP 30 has not been identified as having had human activity, the heated OES samples may be a consequence of veld fires (pers. comm. Curtis Marean).

6.5.4.1. Criteria for identification of artificially heated sub-fossil samples

The criteria to identify artificially heated sub-fossil samples are listed below; the list begins with the more crude methods and end with the most sensitive methods. Therefore, it is very unlikely that a heated sample would only show the first markers without the other markers proceeding it, e.g. an OES sample > 151 ka may show a composition of high % Glx and low % Asx, but if it doesn't fulfil the proceeding conditions (e.g. Asx/Glx and Ile/Glx racemization), it would not be identified as having been heated. However, a lightly heated sample may be identified using chemical markers (e.g. Asx/Glx and Ile/Glx racemization) but would otherwise not be identified by using visual analysis alone.

1. Visual analysis: a darker colour was indicative of heating in modern samples, but care needs to be taken here as geological processes and the burial environment may have an effect on the sample's appearance. Therefore, these are not strong enough indicators by themselves.

2. Olfactory analysis: Samples identified as having been heated often emit a strong smell when the sample is broken or ground up. The smell can be fairly potent and it has a burnt, oily and sometimes sulfurous odour. Artificially heated modern OES samples emitted a strong smell for samples heated at > 300 °C or 200 °C for > 480 h.

3. Visual analysis of the HPLC chromatogram: Modern OES samples artificially heated at > 300 °C had a sharp peak at ~ 60 min and following this the chromatogram may be dominated by a series of late-eluting hydrophobic analytes and a poor baseline causing a loss of resolution of the late eluting amino acids (Fig. 6.14). This observation was also made with heated sub-fossil samples.

4. Composition: A higher % Glx and a lower % Asx are indicative of heating. It was calculated that samples showing % Glx > 21.1 % and % Asx < 14.9 % are likely to have been heated. This was based on the averaged compositions of 'unheated' sub-fossil data.

5. Relative extents of Asx and Glx racemization (Sec. 6.5.3.3.): Heated samples show a higher than expected Glx D/L value for a given Asx D/L value. The third order polynomial was

calculated using the 80 °C, 110 °C and 140 °C kinetic data. Glx D/L values for the kinetic data were calculated based on their Asx D/L values, and compared to the observed Glx D/L values. Similarly, sub-fossil samples that showed a difference between the calculated and observed Glx D/L value of more than 4 times the standard deviation (calculated from the kinetic samples), are marked as having been heated.

6. Relative extents of Ile and Glx racemization (Sec. 6.5.3.4.): Heated samples show a higher than expected Glx D/L value for a given Ile A/I value. A second order polynomial was fitted to the suspected unheated sub-fossil samples. Ile A/I values were calculated for each sub-fossil sample based on this trend-line and the observed Glx D/L values. Sub-fossil samples where the calculated and observed Ile A/I values deviated by more than 5 times the standard deviation calculated from a set of unheated sub-fossil samples were assigned as having been heated. The cut-off limit of 5 times the standard deviation may be refined when more low-temperature and older sub-fossil data becomes available.

6.5.5. Corroded samples from PP 30

Two samples from PP 30 had an altered appearance to other samples from this site (Fig. 6.24), with the appearance of corrosion, possibly either through physical abrasion with liquid or sand, or ingestion by the hyenas who occupied the cave.

These samples were not identified in any of the relative rate comparisons as potentially having been heated. They showed 'normal' compositions and degrees of racemization compared to other samples from the same site. It is therefore suggested that however this 'corrosion' may have occurred, it does not seem to have had an effect on the AAR composition and the samples appear to have remained 'closed system'.

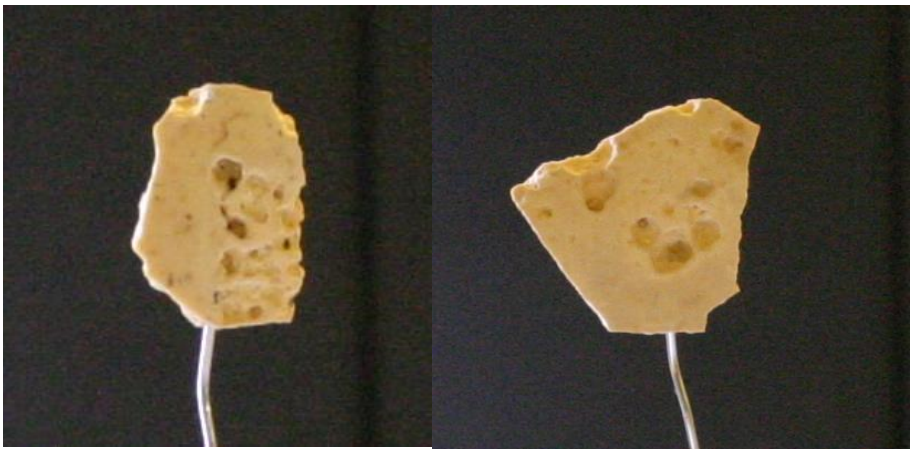

Figure 6.24: OES samples from PP 30 which appear to have been corroded; AAR lot numbers: Left: 4713, Right: 4708

6.5.6. Intra-crystalline vs. whole-shell samples

A small number (~18) of sub-fossil samples from all 3 sites were analysed for their whole-shell proteins as well as their intra-crystalline fraction. It was found that for the vast majority of samples, oxidative treatment had little effect on the amino acid concentrations (Fig. 6.25). For example, for Glx concentration plotted against the independent sample ages, only 2 samples showed a large decrease in concentration with oxidative treatment. These were samples from EBC dated to < 4 ka. It may be possible that leaching of the inter-crystalline fraction in older samples meant only small concentration changes are observed with oxidative treatment, due to the natural isolation of the intra-crystalline fraction.

Two of the samples selected for analysis were visually identified by archaeologists as having been heated, this means unbleached and post-heat bleached samples are effectively compared. As with the modern heated samples, there is no significant difference in concentration for whole-shell and post-heat bleached samples (Sec. 3.3.6.).

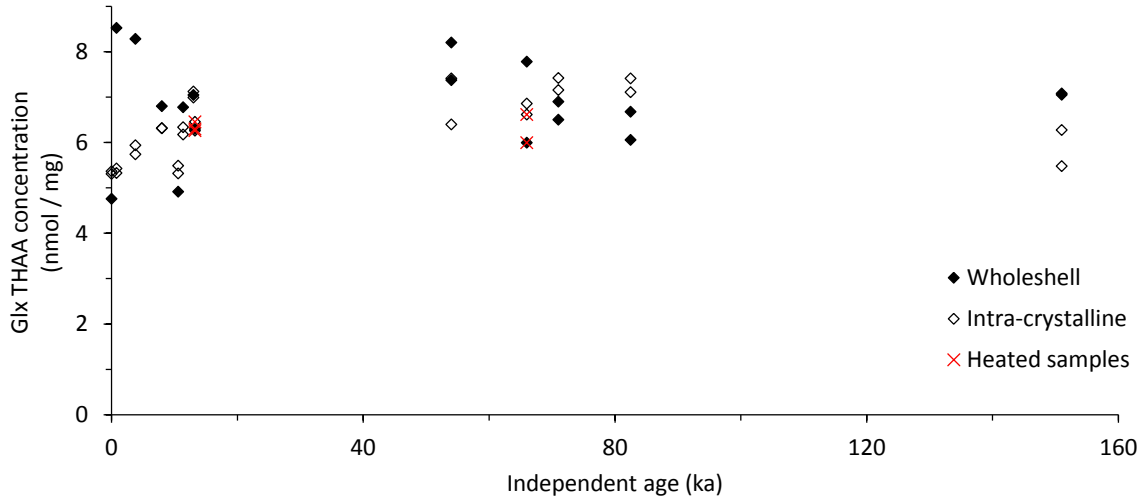

Figure 6.25: Glx concentration compared to the average independent age from each sample's horizon; samples were analysed twice, once with bleach pre-treatment and once with no bleach treatment.

The whole-shell fractions in sub-fossil samples generally show similar D/L values to the intra-crystalline samples for all amino acids (e.g. Fig. 6.26). This differs to the lab heated whole-shell and intra-crystalline samples which showed increased D/L values in the intra-crystalline fractions. This may be a consequence of leaching of the inter-crystalline fraction amino acids in sub-fossil samples into the surrounding ground, which might not be possible at the faster time scales involved in kinetic experiments, despite the increased temperatures. This is in agreement with the majority of sub-fossil concentration data, which generally showed little difference between whole-shell and intra-crystalline samples (Fig. 6.25). This is in line with observations made when comparing bleached and un-bleached sub-fossil gastropods and bivalve shells (Penkman *et al.*, 2008).

However, one sample in particular shows a large difference in D/L values in the whole-shell and intra-crystalline fraction (Fig. 6.26), although the same sample shows little difference in concentration. This sample was identified as likely to have been heated (Section 6.5.3.). It may be possible that in-situ heating caused a localised hot spot, such that the whole-shell and intra-crystalline sub-samples were exposed to different temperatures, or that the sample had been

contaminated *in-situ* with a more highly racemized substance, which was removed in the intra-crystalline sample.

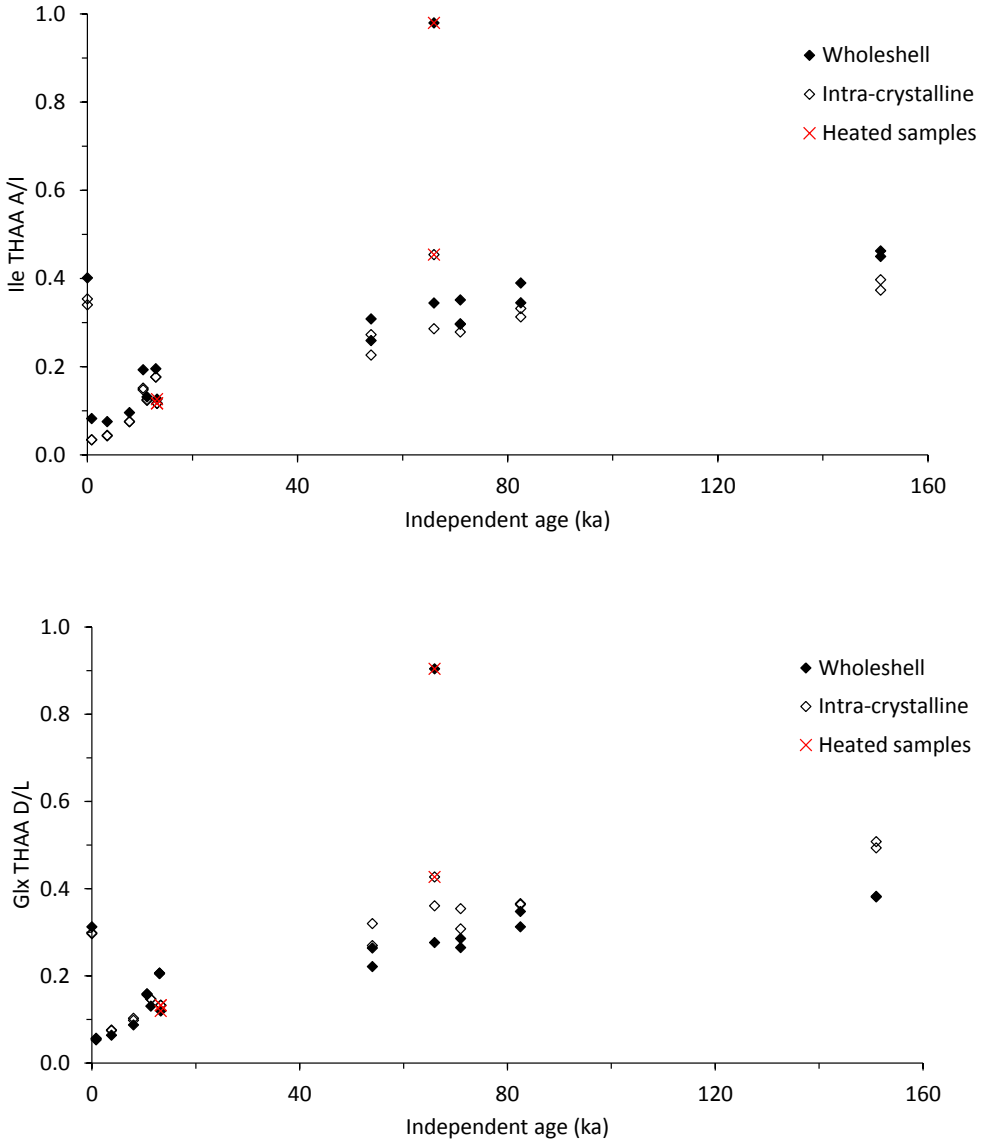

Figure 6.26: Ile THAA A/I (top) and Glx THAA D/L (bottom) for the same sub-fossil samples with and without bleach treatment (i.e. whole-shell and intra-crystalline fractions). Samples with a cross have been exposed to high temperatures (Sec. 6.5.3.)

In Chapter 3 it was argued that bleaching was required to isolate a fraction of closed system intra-crystalline amino acids. However, here it has been shown that for the majority of sub-fossil samples bleaching makes little difference, as the majority of inter-crystalline amino acids have probably leached from the system by the time of sampling. However, a small number of sub-fossil samples showed significantly higher concentrations of amino acids in the whole-shell samples

than the intra-crystalline fractions. It is therefore argued that oxidative treatment removes the uncertainties associated with different rates of leaching of the inter-crystalline fraction and indeed contamination from external sources.

6.5.7. Sub-fossil data excluding artificially heated samples

Archaeological samples were all screened using the key indicators for heating (Section 6.5.4.1.) prior to AAR data interpretation. Removing the samples which are suspected of having been heated gives a stronger correlation between D/L values and independent age for all amino acids studied (e.g. Ile in Fig. 6.27). In addition to removal of samples with anomalously high A/I values, a number of samples with A/I values of zero were also removed. These samples were often heavily heated samples, such that the Ile peaks were unresolved in the HPLC chromatograms resulting in A/I values of 0. These samples were therefore identified as heated through amino acid composition (Sec. 6.5.3.2.), appearance (Sec. 6.5.3.1.) and/or Asx/Glx racemization (Sec. 6.5.3.3.), and did not use the Ile/Glx racemization method (Sec. 6.5.3.4.).

One sample from EBC which came from a horizon independently dated at ~ 13 ka using radiocarbon (Parkington, pers. comm. unpublished data), which shows an Ile A/I value indicative of a far older sample yet does not display any of the markers that have been identified which may imply a sample has been heated. It is therefore suggested that this sample may have been reworked from an older horizon, possibly through the action of animal burrowing (Julia Lee-Thorp, pers. comm.).

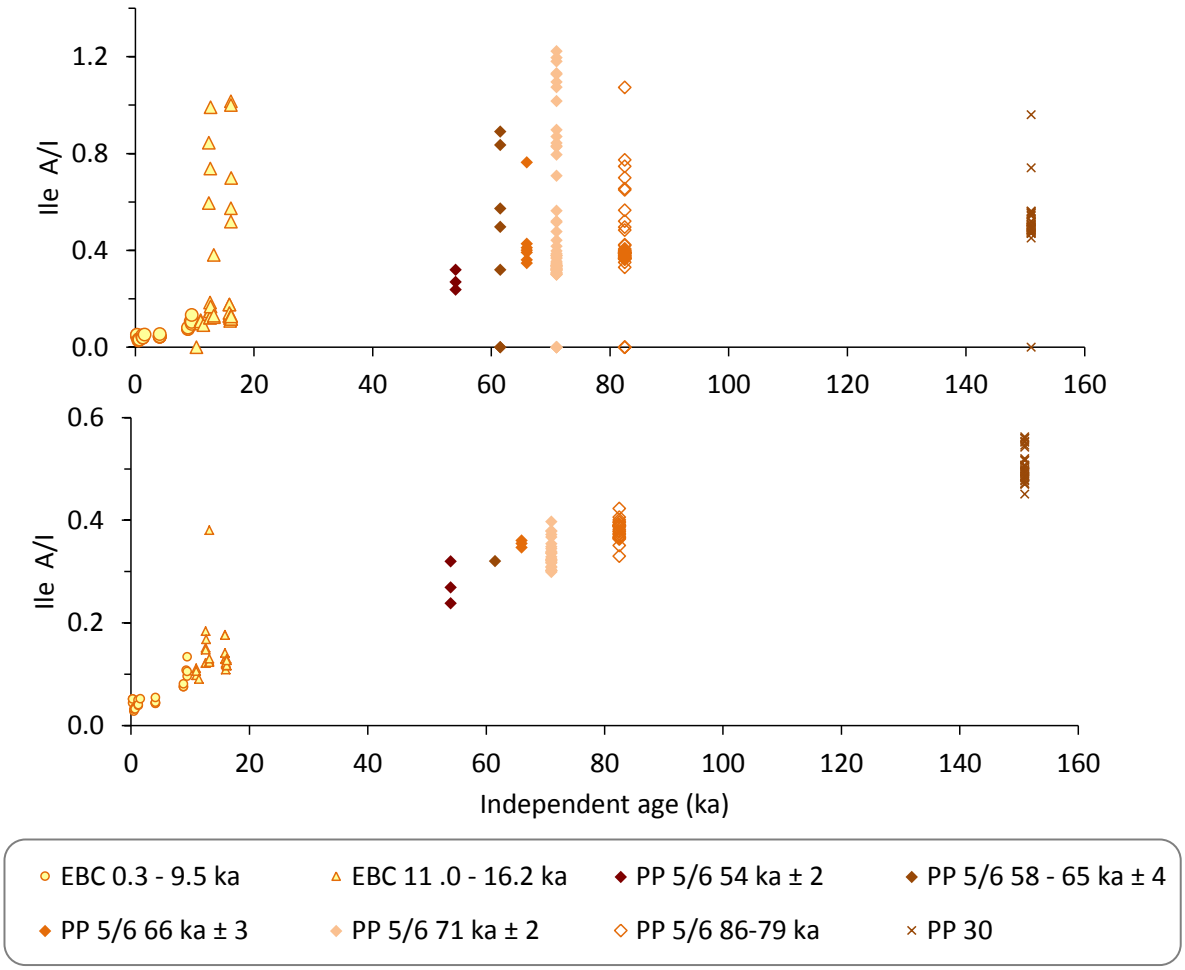

Figure 6.27: Ile THAA A/I values plotted against the average independent ages of the sample's horizon (see Section 6.2). Top: all data. Bottom: data screened for heated samples.

The degree of racemization in the FAA and THAA fractions should be highly correlated in a closed system (e.g. Preece and Penkman, 2005), which is shown to be the case for the screened sub-fossil OES samples (Fig. 6.28). This suggests that a closed system is maintained under geological conditions up to at least ~151 ka (Fig. 6.28) in OES, and that it is possible to relate the degree of racemization to thermal age (Towe and Thompson, 1972; Engel *et al.*, 1994; Sykes *et al.*, 1995; Miller *et al.*, 1999; Collins and Riley, 2000; Penkman *et al.*, 2008). Furthermore, at ~151 ka the Ile THAA A/I is far from equilibrium at ~ 0.6, therefore showing AAR's utility for OES samples far older than 151 ka.

In addition to providing evidence for closed system behaviour, FAA D/L vs. THAA D/L plots of samples with similar temperature histories are able to separate samples based on their relative AAR ages; young samples will have both low FAA and THAA D/L values, older samples will have

higher D/L values. Calibrating these plots with a number of independently dated samples creates a chronological framework for a given geographic region which then may be used to assign ages to samples of unknown age (e.g. Penkman *et al.*, 2007; Miller *et al.*, 2000; Demarchi, 2009; Penkman *et al.*, 2011).

By comparing the degree of epimerization in the free and total fractions (Fig. 6.28), there is a separation between samples from PP 30 (151 ka) and those from the later stage of occupation at PP 5/6 (~ 86 ka). However, using Ile A/I values there is poor resolution between the younger samples from EBC (< 16 ka). Using a faster racemizing amino acid, such as Asx (Fig. 6.28), resolution between samples from EBC of < 5 ka and those of > 9 ka can be achieved. However, Asx reaches equilibrium far faster than Ile, so it cannot distinguish between any samples older than approximately 50 ka. There is therefore a clear temporal advantage to studying several amino acids.

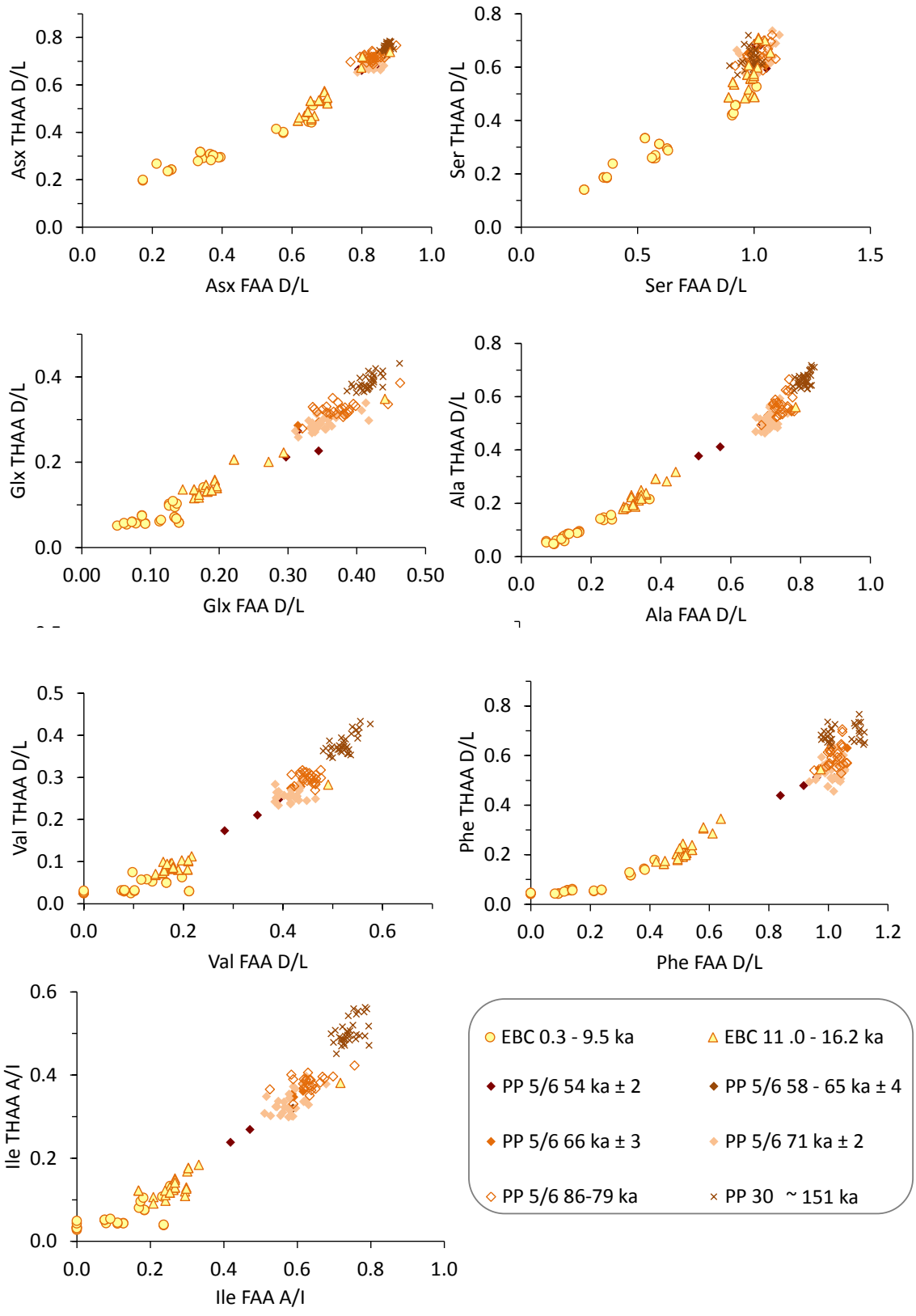

Figure 6.28: FAA D/L vs THAA D/L values for screened sub-fossil samples from EBC and PP; samples are colour coded with their horizon's independently determined ages.

In order to assess statistically whether AAR could be used to distinguish between samples from different MIS stages, a student t-test was performed for each amino acid for both FAA and THAA

fractions. A two tailed test was used, as this assumes no prior knowledge in regards to the relative ages of the two data sets, and is therefore a more rigorous test. The data from MIS 3 and 4 were grouped because of the small number of samples in MIS 4. For the majority of amino acids a significant difference was seen for all MIS group comparisons (assuming a 95% confidence level). The exceptions were Ser and Asx, which showed poor separation for MIS 3/4 vs. MIS 5; and Ser and Phe which showed poor separation for MIS 5 vs. MIS 6.

The student t-test assumes that the data is normally distributed; therefore the skew and kurtosis for the FAA and THAA D/L values from PP 30 were tested to give an indication of the normality of the distribution for all OES samples. PP 30 was chosen because it has the largest number of samples, all from within a small time window. It is assumed that if these data are normally distributed then the student t-test is valid in this instance. A skew and kurtosis value of zero signifies a normal distribution. A negative skew signifies a left hand tail; a positive value shows a right hand tail. The kurtosis value indicates the relative flatness compared to a normal distribution; a positive value indicates a sharp peak, a negative value indicates a flattened peak. The results indicate that the data does not form a perfect normal distribution. Therefore, for completeness the THAA and FAA D/L values were also analysed using a Mann-Whitney u-test. This test is similar to the student t-test but does not assume a normal distribution. A two-tailed Mann-Whitney u test was performed assuming 95% confidence level, for the different MIS stages and for the THAA and FAA D/L values (Table 6.9). The results from the student t-test (Table 6.6) and the Mann-Whitney u-test (Table 6.10) are in broad agreement, with the exceptions that when a normal distribution is not assumed there are fewer statistically significant differences between the D/L values of Asx at the MIS 5/6 boundary, and the D/L values of Phe at the MIS 3/4 boundary.

	No. of observations with $p < 0.05$						
	Asx	Glx	Ser	Ala	Val	Phe	Ile
MIS 1 vs. MIS 2	2	2	2	2	2	2	2
MIS 2 vs. MIS 3/4	2	2	2	2	2	2	2
MIS 3/4 vs. MIS 5	1	2	0	2	2	2	2
MIS 5 vs. MIS 6	2	2	1	2	2	1	2

Table 6.7: Two-tailed student t-test of FAA and THAA D/L values of sub-fossil OES samples

		Asx	Glx	Ser	Ala	Val	Phe	Ile
MIS 6 (n = 34)	Average	0.87	0.42	0.99	0.81	0.52	1.04	0.74
	st dev	0.01	0.01	0.03	0.02	0.02	0.05	0.03
	Skew	**-0.38**	**0.49**	**-1.16**	**-0.36**	**0.22**	**0.22**	**0.28**
	kurtosis	**0.94**	**1.61**	**2.22**	**-0.74**	**-0.19**	**-1.83**	**-0.71**

Table 6.8: Assessment of normal distribution of FAA D/L values from PP 30

		Asx	Glx	Ser	Ala	Val	Phe	Ile
MIS 6 (n = 34)	Average	0.76	0.39	0.63	0.66	0.38	0.69	0.50
	St. Dev	0.01	0.02	0.03	0.03	0.02	0.03	0.03
	Skew	**-0.28**	**0.72**	**0.73**	**0.46**	**0.86**	**0.64**	**0.70**
	Kurtosis	**-0.39**	**-0.17**	**0.16**	**-0.69**	**-0.16**	**-0.32**	**-0.36**

Table 6.9: Assessment of normal distribution of THAA D/L values from PP 30

	No of observations with $p < 0.05$						
	Asx	Glx	Ser	Ala	Val	Phe	Ile
MIS 1 vs. MIS 2	2	2	2	2	2	2	2
MIS 2 vs. MIS 3/4	2	2	2	2	2	2	2
MIS 3/4 vs. MIS 5	1	2	0	2	2	1	2
MIS 5 vs. MIS 6	1	2	1	2	2	1	2

Table 6.10: Mann-Whitney test applied to THAA D/L values of sub-fossil OES

6.6. CONCLUSIONS

Human activity at archaeological sites results in many OES samples being exposed to anthropogenic fire, artificially increasing the apparent AAR age. The exclusion of these artificially aged samples from AAR age models will decrease the uncertainty associated with dating OES by AAR. Through extensive artificial heating studies on modern OES samples a checklist has been developed to identify samples exposed to high temperatures (Sec. 6.5.4.1.). It seems there is not a single key indicator for identifying heated samples, as these markers will vary depending on the degree of heating and the age of the sample. However, a series of 6 markers have been identified (Sec. 6.5.4.1.), some indicators are more sensitive than others, e.g. Ile THAA A/I vs. Glx THAA D/L (Fig. 6.22). It is prudent to use several markers so as to not remove samples of 'genuine' AAR age without just cause. Using these criteria, 8 samples from EBC (18.6 % of all EBC samples analysed), 56 samples from PP 5/6 (48.7 %) and 3 samples from PP 30 (7.0 %) were identified and excluded from age models. The unheated sub-fossil OES data appear to suggest that a closed system is maintained to at least 151 ka (Fig. 6.27).

Oxidative treatment of sub-fossil samples does not affect the AAR results for the majority of samples, where this was tested. This is presumably because sufficient time has passed allowing the vast majority of the inter-crystalline fraction to leach from the bio-mineral, leaving only the intra-crystalline fraction. However, ~1 % of unbleached samples showed a significant change in the degree of racemization with oxidative treatment, i.e. a decrease in both amino acid concentration and THAA D/L values with treatment. This agrees with previous AAR studies using other bio-minerals, which show that oxidative pre-treatment reduces the variability in D/L values and amino acid concentrations (Sykes *et al.*, 1995; Penkman *et al.*, 2007; 2008), and is therefore a necessary pre-treatment procedure for AAR analysis.

Plots of FAA D/L vs. THAA D/L (e.g. Fig. 6.27) have been used to build a chronological framework for South Africa using OES samples from independently dated layers. Using plots such as these, samples from similar geographic localities, of unknown age, could be dated. Faster racemizing amino acids, such as Asx, give better age resolution for younger samples (i.e. MIS 2 – 3). Slower racemizing amino acids, such as Ile, give better resolution for the older samples, e.g. between samples from MIS 5 and 6. Indeed, Ile THAA A/I at 151 ka is approx. 0.6, therefore showing the utility of OES AAR for samples far older than 151 ka in South Africa, or places with similar or colder climates. The temporal advantage of using several amino acids is clear in these examples (Sec. 6.6.2.).

Over the time range studied, OES AAR probably cannot compete with the resolution offered by alternative dating techniques, e.g. OSL. However, OES AAR has been shown to have the potential to date samples far older than 151 ka, and so has the potential to date sites older than the present typical upper age limit for OSL, of ~ 200 ka (Walker, 2005; but see also Wang *et al.*, 2006).

In addition to dating there is the potential for the analysis of OES to be used to gain further insights into the terrestrial climate record through stable isotope analysis of the dated OES (Johnson *et al.* 1997), or through AAR analysis of independently dated OES samples.

OES is ubiquitous to archaeological sites in Africa and therefore may be useful to date many diverse archaeological and geological contexts. Unfortunately, at sites where fire is readily utilized, it is likely that a large number of OES samples would need to be excluded from age interpretations. In these cases, it is likely a large number of OES samples would need to be available for analysis. However, OES AAR analysis is both cheap and rapid, therefore this does not pose a major problem. Using OES AAR, samples from MIS 1, 2, 3/4, 5 and 6 could be successfully differentiated. It has been shown that OES AAR offers a useful additional dating technique for palaeontological sites in Africa up to at least 151 ka.

CHAPTER 7: MASS SPECTROMETRY ANALYSIS OF KINETIC AND SUB-FOSSIL OES SAMPLES

7.1. INTRODUCTION

High temperature studies and analysis of a suite of independently dated sub-fossil samples have been used to observe the trends in protein degradation within bio-minerals (Chapters 4 and 6, respectively). However, these studies (using chromatographic separation methods) are limited to the study of only two fractions of amino acids, the THAA and FAA fractions. The racemization in the FAA and THAA fractions, and hydrolysis in the THAA fraction, can be observed and often mathematically described (Chapters 4 & 5). Activation energies calculated using these methods are describing a single observed rate of racemisation (or hydrolysis), which is in reality a composite of many different rates of reaction (e.g. Chapter 5). The underlying chemical rationale for the observed rates is so far unexplained, due in part to the complex nature of the system.

Attempts have been made to describe the system, e.g. the 3 box model (Fig. 1.8). In a closed system, this model considers the rates of racemization of the terminally bound, internally bound and free amino acids (and in a slightly more complex version, the contribution from DKPs is also considered; see Sec. 1.3.4.). However, this is insufficient to describe the observed rates of racemization, e.g. the model predicts that the slowest rate of racemization is achieved when the amino acids are fully hydrolysed, therefore racemizing at the rate of FAA. However, the observed rates of racemization in the later stages of degradation are slower than this (Kriausakul and Mitterer, 1980b); it is speculated that a lack of water or a hydrolysis resistant fraction may be responsible (Collins and Riley, 2000). Nevertheless, it would be difficult to differentiate between these protein pools using chromatography alone.

Mass spectrometry (MS) may offer the chance to observe more fractions than just the FAA and THAA fractions. Indeed, if the starting sequence is known, then it could allow direct observation of protein breakdown, which can be directly compared to the rates of racemization obtained from HPLC studies. In theory, at any given moment, the locations of racemizing amino acid could be known.

A recent study by Demarchi and colleagues (in press) analysed the degradation of a model hepta-peptide using a combination of RP-HPLC, matrix assisted laser desorption-MS (MALDI-MS) and MS/MS to give further evidence that Asn racemizes in-chain, and revealed the first direct

evidence that Ser is capable of racemizing whilst internally bound. Their work benefitted from using a single hepta-peptide, of known sequence, where each of the residues of interest (Ser and Asn) occurred only once in the sequence. Although it is clear that the application of this kind of study may be useful in unravelling the diagenetic reaction kinetics within sub-fossil bio-minerals, the system within bio-minerals is far more complex than model peptides in solution. For example, it is highly likely that there will be more than one peptide present, and that these peptides will be significantly longer than 7 residues in length, and that the majority of amino acids will have more than one position in the protein sequence. Furthermore, the protein structure may play a role in the rates of degradation; for example the restrictive nature of collagen is hypothesised to limit the racemization of internally bound Asn (Collins *et al.*, 1999). Application of HPLC, MS and MS/MS to directly link racemization to residue position within a bio-mineral system would require the sequences of the intact proteins to be known, and an assessment of which parts of the protein remain intact at any given time.

OES has already been shown to be an excellent substrate for AAR (Chapters 3 – 6) and also has the potential to be an excellent substrate for investigating direct protein breakdown for two main reasons:

1. The protein concentration in OES is far higher than for other bio-minerals used for AAR, therefore the chances of observing the relevant peptides is higher;
2. The two main proteins in OES have been identified and sequenced (Mann and Seidler, 2004), this is not the case for other bio-minerals so far used in AAR geochronology. These two proteins are struthiocalcin-1 (SCA-1) and struthiocalcin-2 (SCA-2), both lectin like proteins, of roughly 7:3 molar abundance (SCA-1 : SCA-2). SCA-1 is analogous to the goose eggshell protein, ansocalcin, showing 65 % shared sequence identity (Fig. 7.1). SCA-2 is similar to both ansocalcin and the chicken eggshell protein, ovocleidin-17 (OC-17), showing 47 % and 36 % sequence identity, respectively (Fig. 7.1). Unfortunately, the crystal structures of SCA-1 and SCA-2 are not yet known.

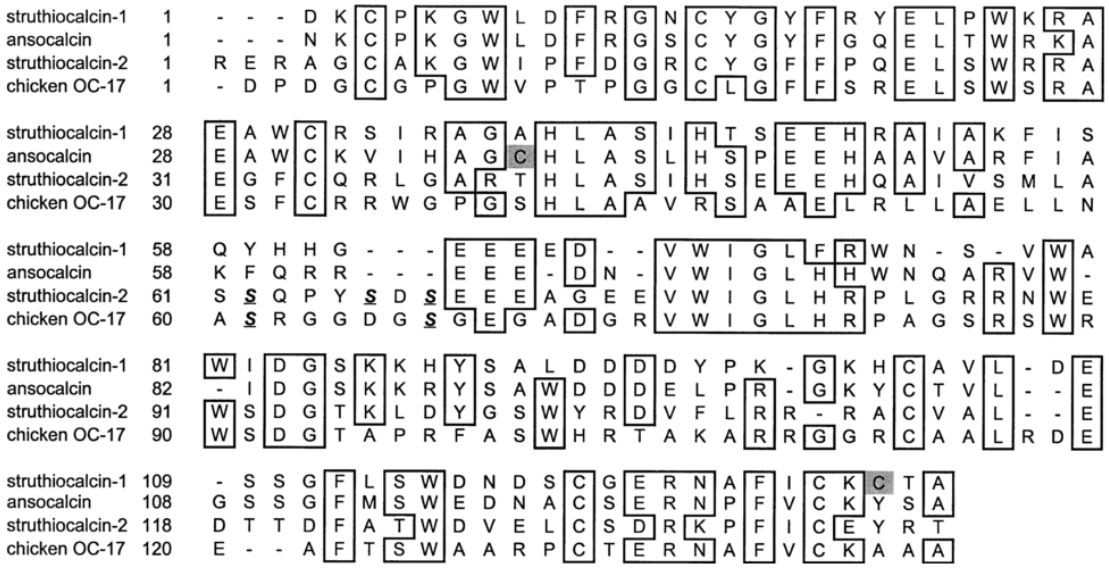

Figure 7.1: The peptide sequences of SCA-1 and SCA-2 with their analogous proteins, ansocalcin (goose) and ovocleidin (chicken, OC-17) Reproduced from Mann and Seidler, 2004.

A preliminary study done by the Penkman group at York (Cappellini *et al.*, unpublished data) has already shown the potential for using MS to understand the diagenetic pathways in sub-fossil OES. A 48 h bleached sub-fossil OES sample was analysed using nano-LC electronspray ionisation (ESI) MS/MS. An SCA-1 sequence coverage of 82 % was attained (Fig. 7.2), along with a small number of SCA-2 peptides and peptides from an ovotransferrin-like protein.

D K C P K G W L D F R **G N C Y G Y F R Y E L P W K R A E A W**
C R S I R **A G A H L A S I H T S E E H R** A I A K **F I S Q Y H**
H G E E E E D V W I G L F R W N S V W A W I D G S K K H Y S
A L D D D D Y P K G K **H C A V L D E S S G F L S W D N D S C**
G E R N A F I C K C T A

Figure 7.2: Sequence coverage of SCA-1 in a bleached sub-fossil OES sample, highlighted in bold. Single underline indicates positions of sequential hydrolysis; double underline indicates a site of deamidation/succinimidyl formation.

A series of sequential points of hydrolysis were also observed. Unfortunately, at this time the crystal structure of SCA-1 or its closest analogue, ansocalcin, have not been published, therefore SCA-1 was superimposed onto the structure of OC-17 (Reyes-Grajeda *et al.*, 2007). This showed that the positions of hydrolysis were on the exterior of the protein, where they may be more susceptible to hydrolytic damage (Cappellini *et al.*, unpublished data). This may be the first example of the observation of the direct hydrolysis of peptides within a fossil protein, although it may be possible that the hydrolysis was induced by the preparative acid demineralisation.

Nevertheless this study clearly shows the utility of using MS to link the degradation of the protein to the processes of racemization in OES.

7.1.1. Protein Mass Spectrometry

Mass spectrometers use the differences in mass to charge ratios (*m/z*) to separate charged gaseous molecules or atoms (e.g. de Hoffmann and Stroobant, 2007). The mass and fragmentation of these molecules can be used to elucidate structural properties of the analyte. In general, an MS consists of three components: i) an ion source, ii) a mass analyser (a method of separating the different *m/z* ions), and iii) a detection method. Although generally MS is run in the positive mode (where only positive molecular ions are analysed), it is also possible to run in a negative mode (where only negatively charged ions are analysed). In tandem MS (MS/MS) a specific ion is isolated and fragmented into product ions, so that more detailed structural information about the precursor ion can be deduced.

The aims of most protein MS studies are to, i) identify the proteins present in a sample, and/or, ii) to ascertain the amino acid sequence of a protein or peptide, and/or, iii) identify the presence and positions of any post-translational modifications.

The first step in protein identification, prior to MS analysis, is usually an enzyme digestion, which cuts the amino acid chain at predictable sites into smaller, more manageable sized peptides. The most widely used digestive enzyme is trypsin, which cuts the peptide chains at the C-terminal side of Lys and Arg, except where the subsequent residue in the peptide chain is Pro. Therefore, a protein of known sequence digested with trypsin will have a predictable set of peptides.

So-called 'soft ionisation' techniques, such as ESI (Sec. 7.1.1.1.) or MALDI (Sec. 7.1.1.2.), tend to be employed as the ion sources in protein MS. These soft ionisation techniques are necessary because they induce very little, if any, fragmentation of the peptides; the intact peptides can therefore be observed. The resulting mass spectra have peaks representing the peptide ions of different *m/z* values (e.g. *m/z* vs. intensity). These MS spectra can be used to identify the protein present by 'fingerprint' identification (Henzel *et al.*, 1993; Pappin *et al.*, 1993; Yates *et al.*, 1993; James *et al.*, 1994). The MS mass lists can be compared to a database and statistically analysed to find the protein of best match. This technique affords very fast protein identification as it avoids time consuming *de novo* sequencing (e.g. Fig. 7.5). However, this tends to be limited to solutions containing a single protein. For the purposes of protein identification, MS fingerprinting is often sufficient, but, in a complex mixture where several proteins may be present (or samples with poor sequence coverage), this may not be enough to confirm a protein's identity. Mass redundancy may also be a problem, e.g. a peptide of 5 amino acid residues could have a

maximum of 120 possible sequences, all of which will have the same *m/z* value (de Hoffmann and Stroobant, 2007).

In order to elucidate the amino acid sequence of the individual peptides from the MS, the precursor ion (intact peptide ion) is isolated and then fragmented to create a set of product ions. Fragmentation in protein MS is usually achieved by collision induced dissociation (CID). This involves passing the precursor ion through a collision chamber containing an inert gas (usually nitrogen or argon), collisions with the gas convert kinetic energy to internal energy, which in turn cause fragmentation to create product ions (de Hoofman and Stroobant, 2007).

There are three possible points of bond cleavage along the peptide backbone (Fig. 7.3), resulting in a theoretical 6 ion series depending whether the positive charge is located at the N- or C-terminus. These series are called a, b and c when the positive charge is located on the N-terminus, and, x, y and z when the positive charge is located on the C-terminus (Roepstorff and Fohlman, 1984). The ions are then numbered starting from the N- and C-terminus, respectively. The mass differences between consecutive ions in a series allow identification of a residue. In addition, double cleavages can result in immonium ions. These contain a single amino acid side chain, appear in the low *m/z* range and can be used to identify likely amino acids within the peptide (i.e. amino acid composition), but not their position in the chain (Fig. 7.4). In CID, the y, b and a ion series, and immonium ions, are the most commonly observed species (Siedler *et al.,* 2010).

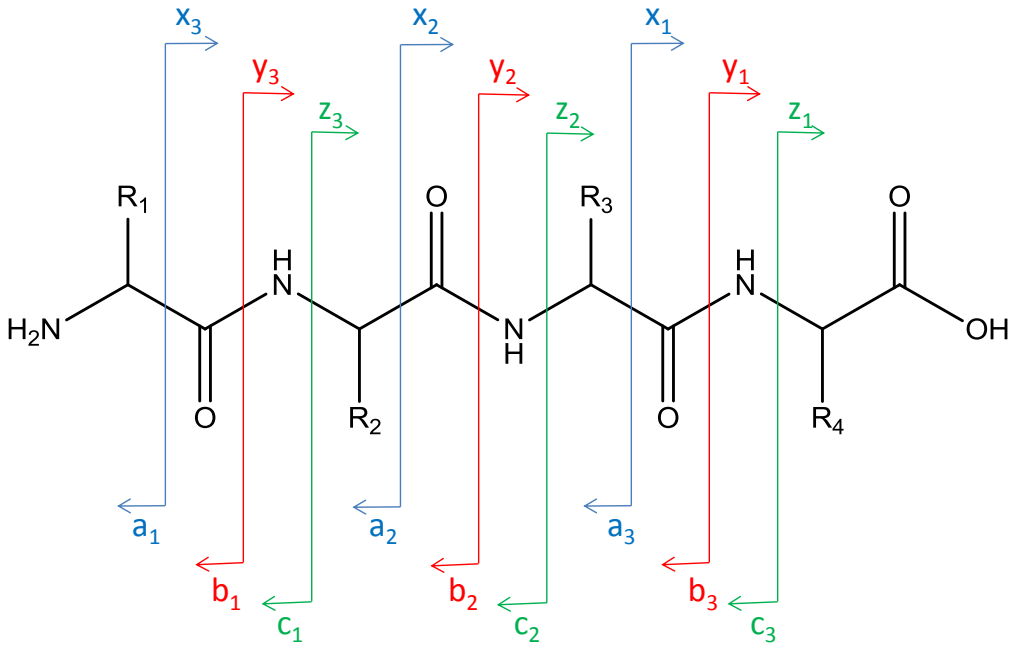

Figure7.3: Schematic showing fragmentation along a peptide chain during CID fragmentation

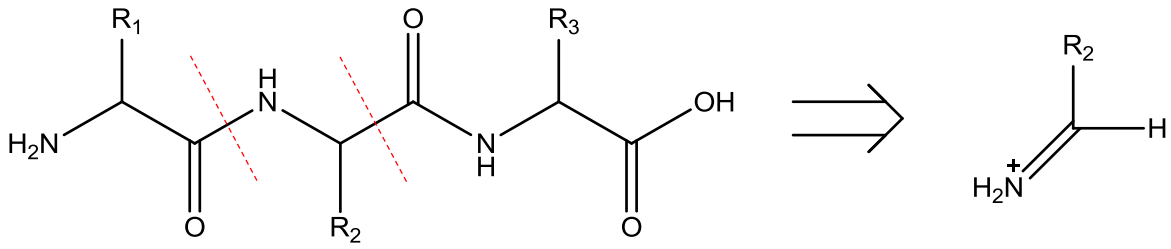

Figure 7.4: Immonium ion formation

Unfortunately, 'real' peptide mass spectra seldom have complete y, b and a ion series. This is because it is not equally likely for the positive ion to form on either side of the cleaved bond. The intensity of the *m/z* ions correlates to the stability of the ion in the gas phase, and not necessarily its concentration (e.g. Zhang, 2004; 2005). This is also the reason that quantitative MS analysis is difficult, as absence of an ion does not indicate absence of that peptide.

The general format of a protein MS and MS/MS experiment is summarised in Figure 7.5. Although there are many different MS and MS/MS set ups, with different ionisation and mass analyser technologies, for the purposes of this discussion the focus will be limited to those used by Cappellini *et al.* (unpublished data) in the preliminary MS study (Sec. 7.1.1.1.), and those employed in this study (Sec. 7.1.1.2.).

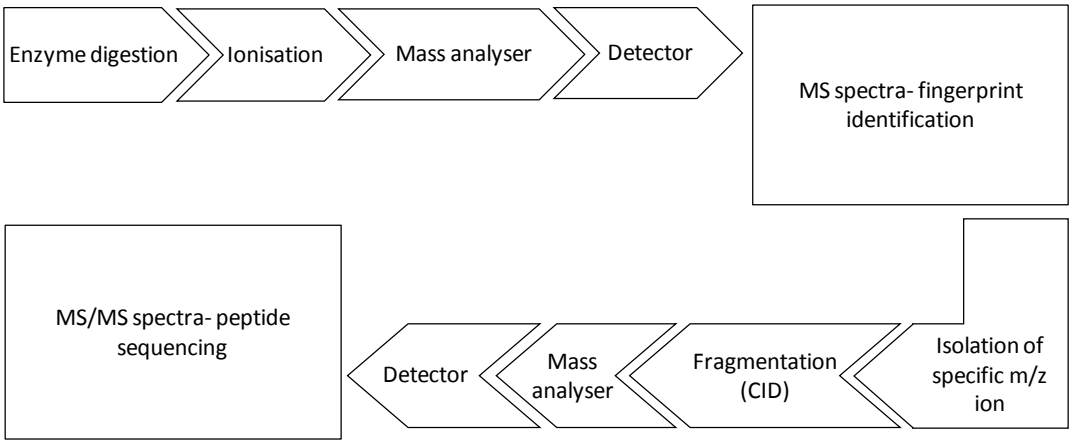

Figure 7.5: Generalised schematic of protein mass spectrometry

7.1.1.1. Liquid chromatography- electrospray ionisation MS (LC-ESI-MS)

Described in this section is the MS and MS/MS experimental set-up employed by Cappellini *et al.* (unpublished data) in the preliminary OES experiment.

ESI for the analysis of biological macromolecules was developed by Fenn and colleagues in 1989 (Fenn *et al.*, 1989). It was for this work that Fenn received a share of the Nobel Prize in Chemistry

in 2002. ESI works by passing the analyte in solution through an electrospray needle. There is a high potential difference between the tip of the needle and the counter electrode (Fig. 7.6). This forces the production of a spray of analyte/solvent droplets with the same polarity as that of the needle (positive in this instance). The droplets are attracted to the counter electrode, and as they travel the solvent evaporates, increasing the charge density. Eventually, the surface tension is not sufficient to hold the droplet together and it explodes via a 'Coulombic explosion' to form smaller droplets and 'naked' molecular ions, which may be singly or multiply charged. This process continues until all of the solvent has evaporated (Wilm and Mann, 1994). The presence of non-volatiles, or contaminants with less-volatility than the analyte (e.g. salts, ion paring agents, metabolites etc), can significantly interfere with droplet formation and/or evaporation of the solvent (King *et al.*, 2000; Annesley, 2003). For this reason, LC is often employed to clean a sample prior to ionization. LC is convenient because it can be easily coupled to ESI and it concentrates the analytes so that better S/N is achieved (de Hoffman and Stroobant, 2007).

The presence of multiply charged analytes tends to increase the complexity of the mass spectra, because a single peptide may result in several *m/z* peaks, e.g. a peptide of mass 60 Da may have an M^+ peak at 60 *m/z*, an M^{2+} peak at 30 *m/z* and an M^{3+} at 20 *m/z*. However, this does have the advantage of increasing the mass range that is detectable (see review, Griffiths *et al.*, 2001).

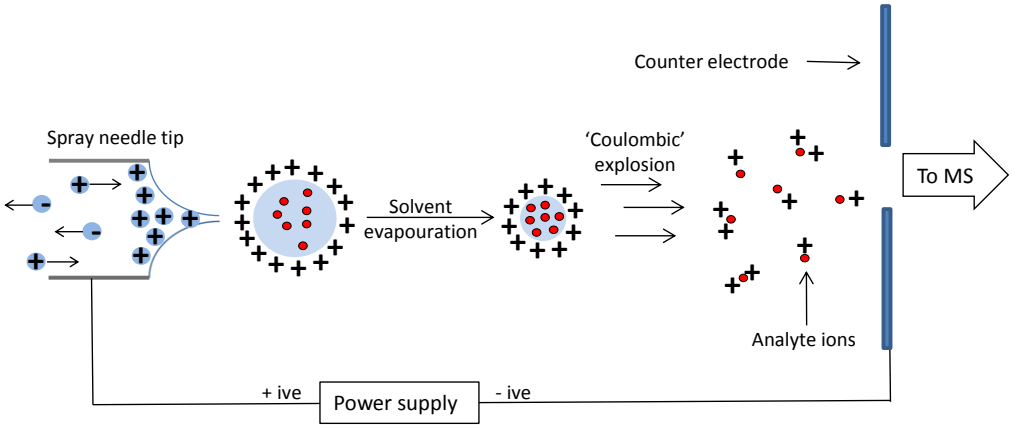

Figure 7.6: Schematic of electrospray ionisation (ESI)

Mass analysis was performed using a 3D ion trap, also called a Paul ion trap or a quadrupole ion trap (QIT). This technology was first developed by Paul in the 1950s (Paul and Steinwedel, 1953; Paul, 1990), and earned him a Nobel Prize in Physics in 1989.

A 3D ion trap consists of two hyperbolic electrodes facing each other (end caps in Fig. 7.7), with another hyperbolic ring electrode between them (Fig. 7.7). Combinations of alternating and constant voltages are applied to the electrodes such that when a molecular ion enters through the inlet, it becomes trapped in a figure of 8 configuration in the space between the electrodes.

The alternating voltage (AC) of the ring electrode can be altered to stabilise different *m/z* ions. Ions can be ejected from the trap by applying an AC current to the end caps and scanning the radio frequency amplitude of the ring electrode, thus destabilising the ions and ejecting them from the trap.

Tandem MS is achieved by the selection of a specific precursor ion by selective ejection of all other ions. The precursor ion can then be fragmented with CID. These isolation and fragmentation steps can be repeated a number of times.

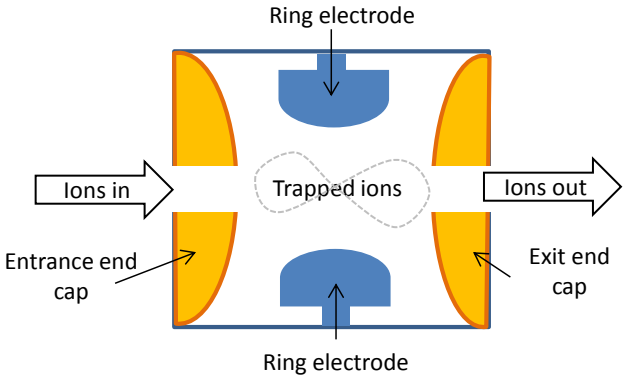

Figure 7.7: Schematic of a quadrupole ion trap mass analyser

7.1.1.2. Matrix assisted laser desorption ionisation (MALDI) MS

Described in this section are the techniques used in this study: MALDI MS and MALDI MS/MS.

MALDI is another soft ionisation technique which can be used as an alternative to ESI for the MS analysis of peptides. The use of MALDI for the ionisation of bio-molecules was pioneered by Tanaka *et al.*, (1988), and subsequently earned him a share of the 2002 Nobel Prize in Chemistry.

In MALDI the analyte is mixed with an excess of matrix solution and spotted onto a metal plate where the sample is allowed to dry, causing co-crystallisation of the matrix and analyte. There are a number of matrix compounds used, e.g. 3,5-dimethoxy-4-hydroxycinnamic acid (sinapinic acid), α-cyano-4-hydroxycinnamic acid (α-CHCA) and 2,5-dihydroxybenzoic acid, the choice of which depends on the sample in question (Cohen and Chait, 1996). The matrix has a strong absorbance at the laser wavelength, so that when a laser is fired it causes rapid heating and sublimation of the top layer of the analyte/matrix spot, which is subsequently released into the gas phase (Fig. 7.8). Charges from the matrix are transferred to the analyte to create $[M+H]^+$ charged species. In addition, often sodiated ($[M+Na]^+$) and potassiated ($[M+K]^+$) charged species are formed (Zenobi and Knochenmuss, 1998). The typical choice of lasers are a nitrogen laser (337 nm; used in this study) or a Nd:YAG lasers (355 nm and 266 nm).

Unlike ESI, MALDI does not require separation and concentration of the sample, therefore MALDI is often faster and cheaper as it does not require coupling to LC (de Hoffman and Stroobant, 2007).

Generally only singly charged species are created in MALDI, giving the advantage that analysis of the MS spectra are often simpler than ESI-MS spectra (El-Aneed *et al.,* 2009). This can also be a disadvantage however, as multiply charged analytes tend to give a better mass range, and often multiply charged analytes will 'fly' better when using time of flight (TOF) mass analysers, therefore sometimes giving a better sequence coverage (Griffiths *et al.*, 2001).

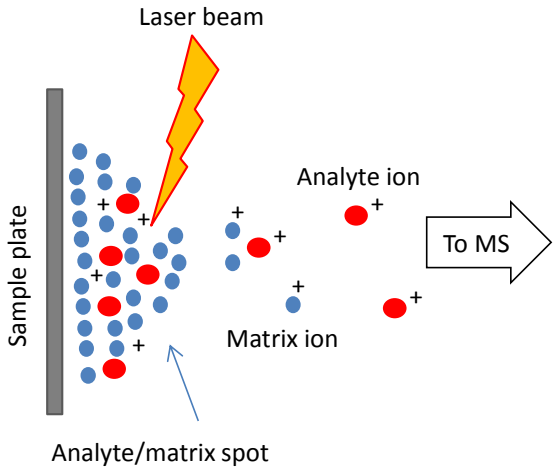

Figure 7.8: Schematic of ionisation using matrix assisted laser desorption/ionisation (MALDI)

MALDI methods tend to use TOF mass analysers, as they are well suited for the pulsed ion formation and they have a large *m/z* range (de Hoffman and Stroobant, 2007). Indeed, a TOF mass analyser was used in this study. TOF mass analysers work by accelerating ions with electric fields, and measuring the time it takes those ions to travel a certain distance. A low mass $[M+H]^+$ ion will reach the detector before a high mass $M+H^+$ ion, which will accelerate more slowly.

The ion current is then converted into electrical current using a micro channel plate (MCP) detector. The plate is made up of multiple, independent, glass walled channels containing a solid porous core coated with a semi-conducting layer (Fig. 7.9; Wiza, 1979). Each channel acts as an electron multiplier to make a detectable electrical signal.

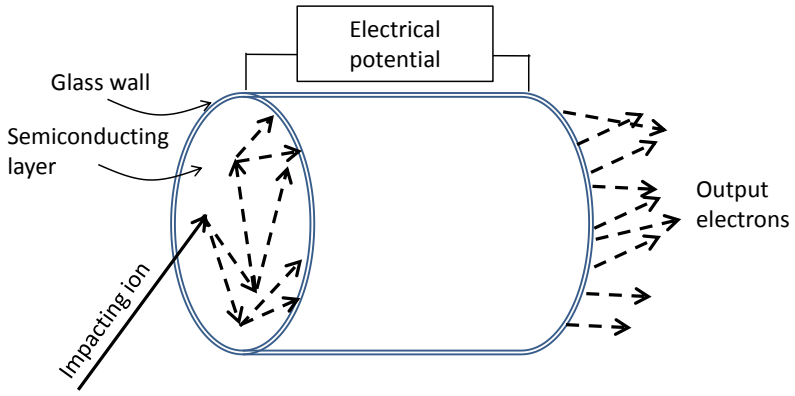

Figure 7.9: Schematic of a single micro channel from a micro channel plate detector

TOF mass analysers can be coupled together in order to perform MS/MS studies. Although there are a number of TOF/TOF configurations, the set-up employed by Bruker (and in this study) involves the following steps (Fig. 7.10; Suckau *et al.*, 2003; Cotter *et al.,* 2007):

- Precursor ions are separated by *m/z* in the first TOF by an applied field
- All ions then pass through a collision cell, where they are fragmented by CID. At this point, no electric potential is applied, therefore the product ions continue to travel at the same speed at which their precursor ion was travelling
- A mechanical mass selection gate can select the product ions of a specific precursor ion
- Once through the gate, the fragment ions pass through a 'LIFT cell' which reaccelerates the product ions according to their *m/z* values
- Ions are focused using a reflectron to give better mass resolution (de Hoffmann and Stroobant, 2007) before entering the detector
- Ions are detected by the MCP detector

In the MS mode the collision cell is a vacuum and the mass selection gate remains open.

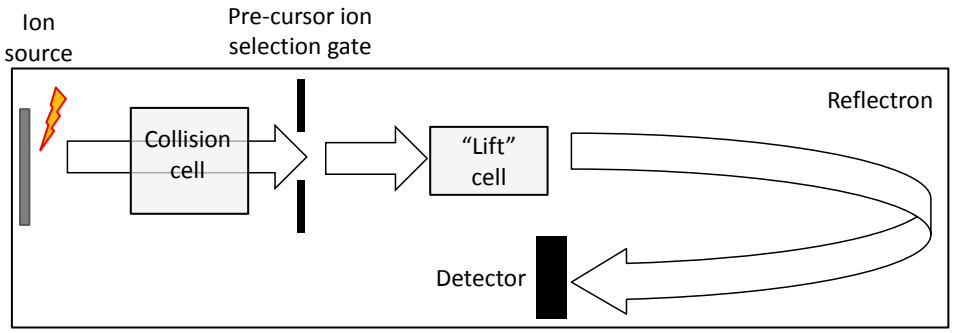

Figure 7.10: Simplified schematic of a Bruker TOF/TOF; Suckau et al., 2003

7.1.2. Study aims

This pilot study hopes to build on the preliminary findings by Cappellini *et al.* (unpublished data), and to establish whether MALDI MS and MALDI MS/MS can be used to observe peptide persistence in both sub-fossil and modern heated samples. MALDI was chosen over LC-ESI primarily because of its high-throughput capability and its reduced cost. It is hoped these MS data may be compared directly to the AAR data, in order to better comprehend the underlying degradation pathways in a complex, and largely poorly understood, system.

7.2. EXPERIMENTAL

7.2.1. OES samples

Modern unheated whole-shell and intra-crystalline samples were prepared in triplicate. A selection of samples from the 80 °C kinetic experiments using intra-crystalline modern OES samples (Sec. 4.2.1.) were also analysed. One sample was analysed from each of the following 80 °C time points: 24, 97, 120, 480, 720, 960, 1440, 2160, 4028 and 5880 h.

A selection of unheated sub-fossil samples, both intra-crystalline and whole-shell, were also analysed (Table 7.1).

Lot no.	Site	Age (ka)	No. of analyses	
			Intra-crystalline	Whole-shell
6887	EBC	MIS 1	0	6
6888	EBC	MIS 1	3	3
6889	EBC	MIS 1	3	6
6891	EBC	MIS 1	0	3
6893	EBC	MIS 1	3	3
6896	EBC	MIS 2	3	3
6899	EBC	MIS 2	3	3
6902	EBC	MIS 2	0	3
6907	EBC	MIS 2	6	3
4613	PP 5/6	48	6	6
4649	PP 5/6	69	6	6
4671	PP 5/6	72 – 70	6	6
4605	PP 5/6	72 – 70	6	6
4652	PP 5/6	79 – 76	6	6
4675	PP 5/6	86 – 79	6	6
4683	PP 30	151	6	6
4697	PP 30	151	6	6

Table 7.1: Summary of sub-fossil samples used in MS study

In addition, a set of whole-shell and intra-crystalline modern OES samples were isothermally heated at 140 °C for 20 and 40 min, as per the experimental detailed in Sec. 4.2.1. Each time point was performed in triplicate.

7.2.2. MS and MS/MS method details

The method used was developed by Demarchi *et al.*, (in press) and was based on that published by Cappellini *et al.*, (2012).

Approximately 10 mg of each powdered sample was weighed into low bind eppendorfs, and demineralised in approximately 800 µL 0.6 M HCl at 4 °C until the entire solid had dissolved. This usually took ~2 – 3 days. The acid was then removed by centrifugal evaporation.

A RapiGest buffer was purchased from Waters, UK, and used to aid the solubilisation of proteins and hence enhance enzymatic degradation. The Rapigest buffer solution was prepared as per the manufacturer's guidelines, by adding 1 mL of 50 mM ammonium bicarbonate to a vial of RapiGest (purchased from Waters). Samples were re-suspended in 100 µL of Rapigest buffer. The pH of the resulting sample solution was adjusted using ammonium bicarbonate solution and ammonium hydroxide solution to pH 7.0 – 7.5.

The samples were then reduced and alkylated using dithiothreitol (DTT) and iodoacetamide, respectively.

A DTT solution was prepared fresh by dissolving in water to a 1 M solution. 1 µL of DTT solution per 200 µL of the sample volume was added to each sample. This solution was then incubated at 60 °C for 1 h in order to reduce the peptides.

A 500 mM solution of iodoacetamide was prepared by dissolution in water. 1 µL of iodoacetamide solution was added per 33 µL of sample volume. The alkylation reaction was incubated at room temperature in the dark for 45 mins. The reaction was quenched by adjusting the pH to 7.4 – 7.6, using NH_4OH and 0.6 M HCl.

Acetonitrile (ACN) was added to each sample such that ~ 9 % was ACN v/v. 4 µL of 0.4 µg / µL of trypsin solution was added to each before incubation at 37 °C overnight. The following morning, an additional 2 µL of trypsin solution was added to each sample before incubation at 37 °C for a further 6 h. Digestion was stopped by adding 10 % TFA such that the pH < 2 (usually ~ 0.5 – 1 % v/v TFA).

The RapiGest buffer was removed by precipitation, this was aided by the acidification in the previous step, and completed with incubation at 37 °C for 45 min and centrifugation at 4 °C for 20 min. The supernatant was removed and collected in clean low bind eppendorfs.

The Lys residues were then converted into L-hArg to improve ionisation (Beardsley and Reilly, 2002). Volumes of 7 M NH_4OH and 1 g/mL of O-methylisourea hemisulphate solution were added as per Beardsley and Reilly's (2002) protocol. The resulting solutions were incubated at 65 °C for 5 min. Volumes of 10 % TFA solution were then added to quench the reaction.

Samples were then cleaned and de-salted using a solid phase (zip-tip) purification method. Equilibration and washing solutions were 0.1 % TFA in water, and wetting and elution solutions were 50 % ACN, 0.1 % TFA aqueous solution. 10 µL C18 zip-tips with 0.2 µL of chromatography media were purchased from Merke Millipore, USA, and were used as per the manufacturer's guidelines. The zip-tips were equilibrated by twice aspirating the wetting solution and dispensing to the waste, followed by twice aspirating the equilibration solution and dispensing into the waste. The sample was then aspirated and dispensed 10 times. The sample was washed by aspirating the wash solution and dispensing into the waste two times. To elute the sample, the elution solution was aspirated and dispensed into a clean low bind eppendorf, and finally this solution was then aspirated and dispensed 5 times to ensure elution of a maximum amount of sample.

Samples were dried in the centrifugal evaporator and re-suspended in 10 µL of 1 % TFA solution. 1 µL of the sample was then diluted again into 10 µL of 1 % TFA solution. 1 µL of sample and 1 µL of the matrix α-CHCA were spotted in triplicate onto a MALDI plate and allowed to dry prior to MS analysis.

A Bovine Serum Albumin (BSA) standard was prepared alongside the OES samples as an internal method check e.g. to check the effectiveness of the trypsin digestion (see example spectra in Appendix D).

Spots of external standard were spotted adjacent to every sample spot, and were used for calibration. These standards were des-Arg1-bradykinin ($M+H^+$ at *m/z* 904.7), angiotensin I (M+H+ at *m/z* 1296.7), Glu1-fibrinopeptide B ($M+H^+$ at *m/z* 1750.7), SCTH (1-17 clip) ($M+H^+$ at *m/z* 2093.1) ACTH (18-39 clip) ($M+H^+$ at *m/z* 2465.2) and SCTH (7-38 clip) ($M+H^+$ at *m/z* 3657.9).

Each experimental replicate was spotted in triplicate and analysed in the positive mode. A Bruker Ultraflex III, MALDI TOF/TOF was used in this study. MS spectra were acquired over the range of 500 – 4000 *m/z* using 800 – 1200 shots, 65 – 75 laser beam attenuation. MS/MS spectra were obtained automatically on the 10 most intense MS *m/z* ions. Precursor ions were fragmented

with CID (~ 3800 shots, laser focus of 29 – 50, laser refresh rate of 100 Hz). All ions, both precursor and product, with a S/N < 3 were excluded from all MS or MS/MS interpretations.

7.3. RESULTS

7.3.1. MS

It was found that intra-crystalline samples generally showed lower peak intensities and a corresponding decrease in S/N, compared to whole-shell samples; signal intensity was generally an order of magnitude lower for intra-crystalline samples (e.g. Fig. 7.11). It seems likely that the reduction in peak intensity is due to the reduction in amino acid concentration for intra-crystalline samples, typically up to ~50% for modern unheated OES samples (Chapter 3).

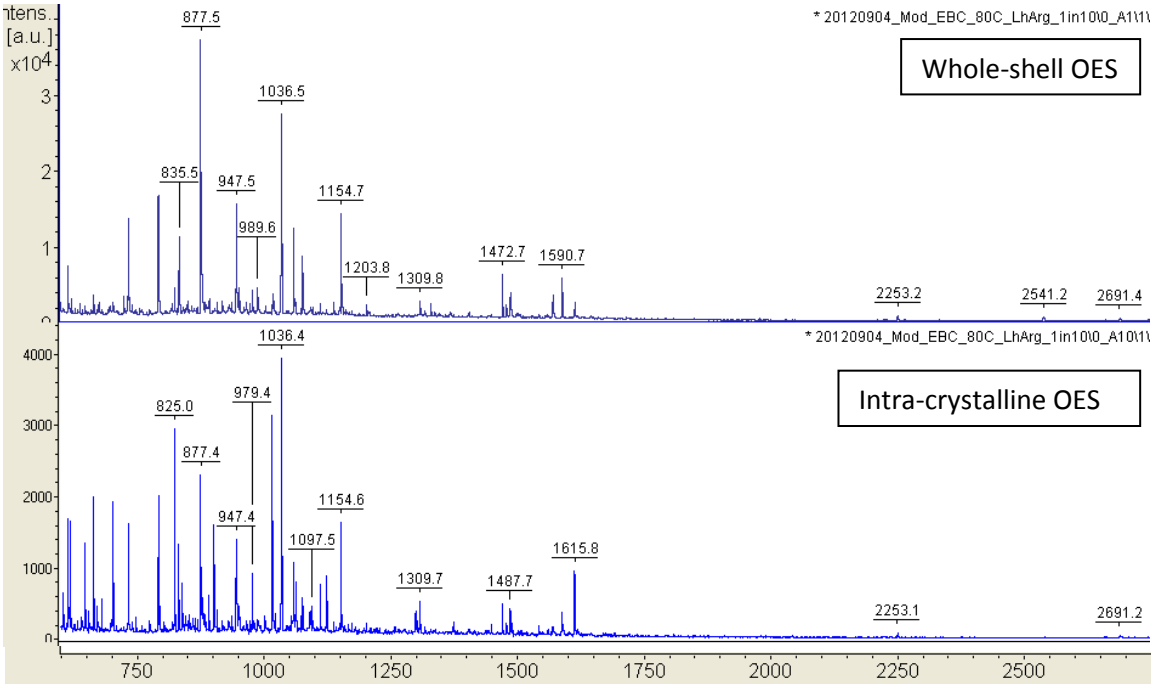

Figure 7.11: Example mass spectra of a modern whole-shell OES sample (top) and a modern intra-crystalline OES sample (Bottom).

There was a general trend in reduction in the number of MS peaks and peak intensities (and decrease in S/N) with heating of OES at both 80 °C (Fig. 7.12) and 140 °C (Fig. 7.13), as would be expected from the natural degradation of the peptides (Sec. 7.3.1.3.). For example, after 24 h at 80 °C, generally < 4 % hydrolysis was observed, this increased to < 6 % by 480 h and <50 % by 5760 h (see Sec. 4.3.2.; Appendix B).

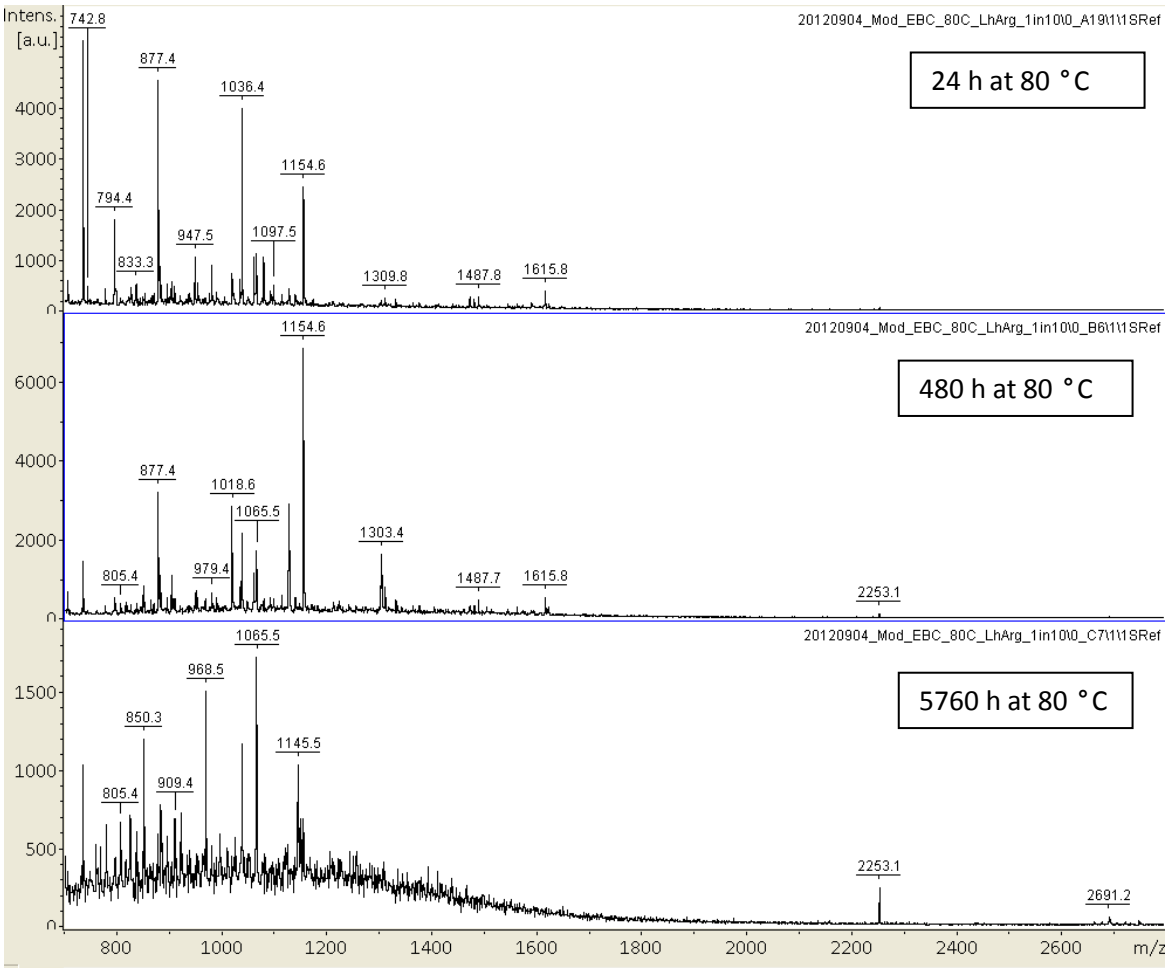

Figure 7.12: Example mass spectra of modern intra-crystalline samples heated isothermally under kinetic conditions at 80 °C; top = 24 h, middle = 480 h bottom = 5760 h

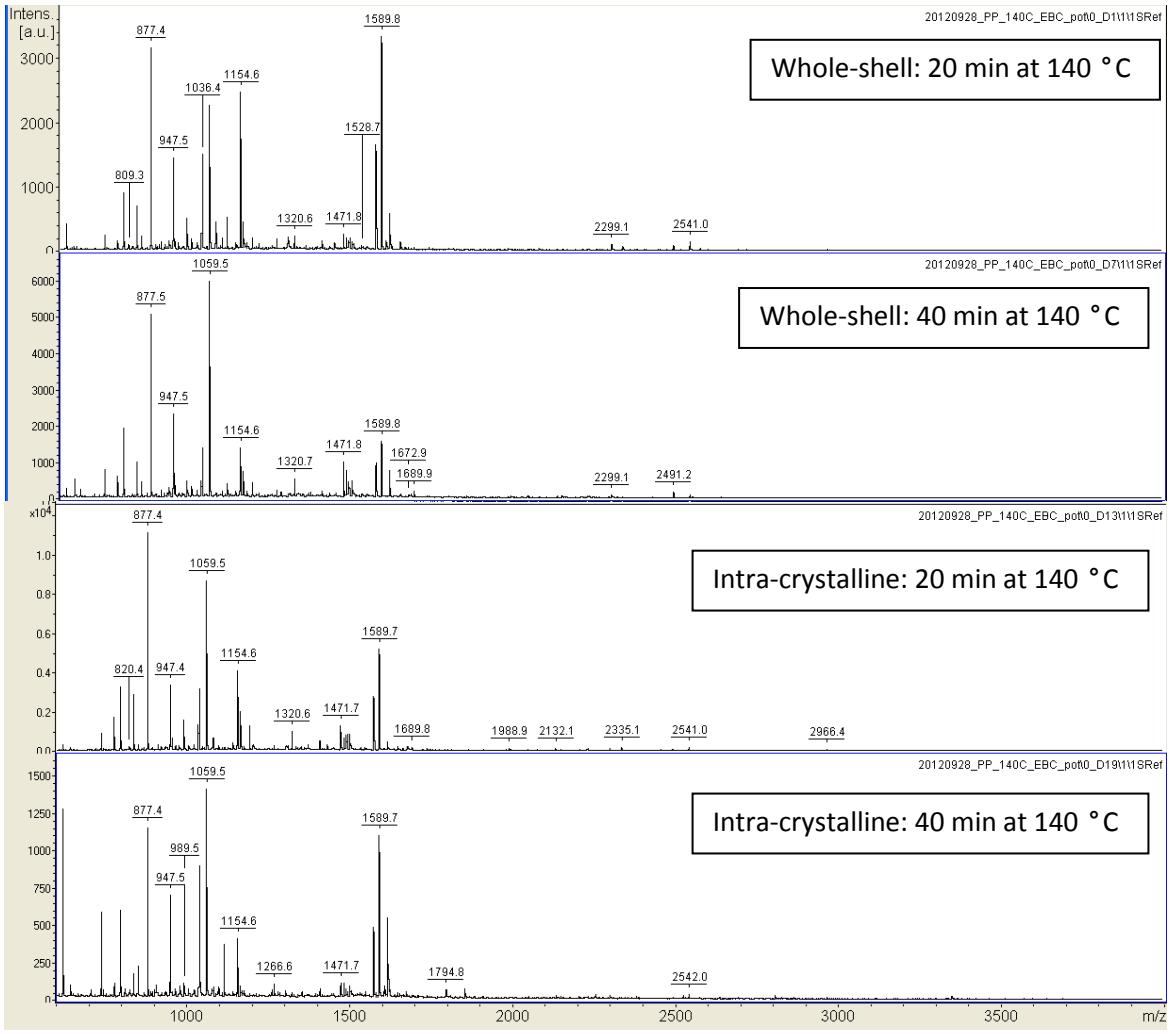

Figure 7.13: Example spectra of modern OES samples heated isothermally under kinetic conditions at 140 C; A: Whole-shell 20 min, B: Whole-shell 40 m, C: Intra-crystalline 20 m, D: Intra-crystalline 40 m

Lists of theoretical tryptic peptides for SCA-1 and SCA-2 were compiled. The list included all $[M + H]^+$ and $[M + Na]^+$ peptides up to 1 missed cleavage. A number of post translational modifications were also included, e.g. deamidation of Asn or Gln (Sec. 7.2.2.) and preparative modifications, e.g. modification of Cys to carbamidomethyl and conversion of Lys to L-hArg. Modifications can be characterised in two groups, the first are modifications which occur naturally when the protein degrades, e.g. deamidation, dehydration, hydrolysis, glycosylation etc. The second are modifications made either intentionally (e.g. conversion of Lys to L-hArg, reduction and alkylation of Cys (to form a carbamidomethyl); Sec. 7.2.2.), or as a consequence of sample preparation/sample analysis, (e.g. the different forms of charged species: $[M + H]^+$, $[M + Na]^+$, $[M + K]^+$, $[MH - NH_3]^+$, $[MH - H_2O]^+$).

By comparison of the mass lists from the mass spectra and the list of theoretical SCA-1 and SCA-2 peptides, a number of peptides can be tentatively identified (e.g. whole-shell unheated OES, Table

7.2), and it is clear that both SCA-1 and SCA-2 are likely to be present. However, the main purpose of this study was not to prove that SCA-1 or SCA-2 were present, but to show which parts of the proteins were preserved. Furthermore, this approach assumes both that the only peptides present are tryptic SCA-1 or SCA-2 peptides, and that they have not been modified in any other way than that stipulated above (e.g. it does not consider peptides created from the natural hydrolysis of the protein to form a peptide with a C-terminus residue other than R or K). Assuming tryptic peptides only, it seemed likely that the SCA-1 peptide (12-19) GNCYGYFR (N deamidated) was the source of the *m/z* 980 MS ion. However, there was an intense unexplained ion at *m/z* 865 present in the MS/MS spectrum (Fig. 7.14). This fragment ion could be explained if the peptide was actually (SCA-1: 13-19) NCYGYFR (N-deamidated (+1 Da), C-carbamidomethylated (+57 Da)), where G_{12} has been removed through natural hydrolysis, with a loss of 57 Da (Fig. 7.14). Indeed, the *m/z* 980 peptide is not present in modern unheated OES mass spectra, but it is present in samples heated at 80 °C (Table 7.5) and some sub-fossil samples (Table 7.5). There are a number of ions which do not appear to be as a result of the tryptic digest of SCA-1 or SCA-2 (Table 7.2), and identifying these ions may give additional SCA peptides which are preserved in the OES.

This shows that for the purposes of this study, analysis of MS spectra alone are not strong enough evidence to verify the preservation of all peptides in OES; ions need to be positively identified through MS/MS studies and *de novo* sequencing (Sec. 7.3.2.).

m/z	Possible source
835	SCA-1, YELPWK
877	SCA-1, YELPWK
979	SCA-1, GNCYGYFR
1033	SCA-1, YELPWKR
1036	SCA-1, GNCYGYFR
1037	SCA-1, GNCYGYFR
1480	SCA-1, HYSALDDDDYPK
1615	SCA-1, AGAHLASIHTSEEHR
2541	SCA-1, HCAVLDESSGFLSWDNDSCGER, or, HCAVLDESSGFLSWDNDSCGER
833	SCA-2, ERAGCAK
947	SCA-2, GWIPFDGR
1059	SCA-2, LDYGSWYR
1112	SCA-2, KPFICEYR
1154	SCA-2, KPFICEYR
1589	SCA-2, CYGFFPQELSWR
1590	SCA-2, CYGFFPQELSWR
825, 945, 953, 989, 1019, 1063, 1078, 1139, 1309, 1310, 1330, 1471, 1472, 1487, 1488, 1572, 1573, 2253, 2691	All ions which appeared with S/N > 5 but did not appear in the theoretical SCA-1 or SCA-2 tryptic digest mass lists

Table 7.2: MS of whole-shell unheated modern OES: assignments made purely on MS mass lists compared to theoretical tryptic SCA-1 and SCA-2 peptides

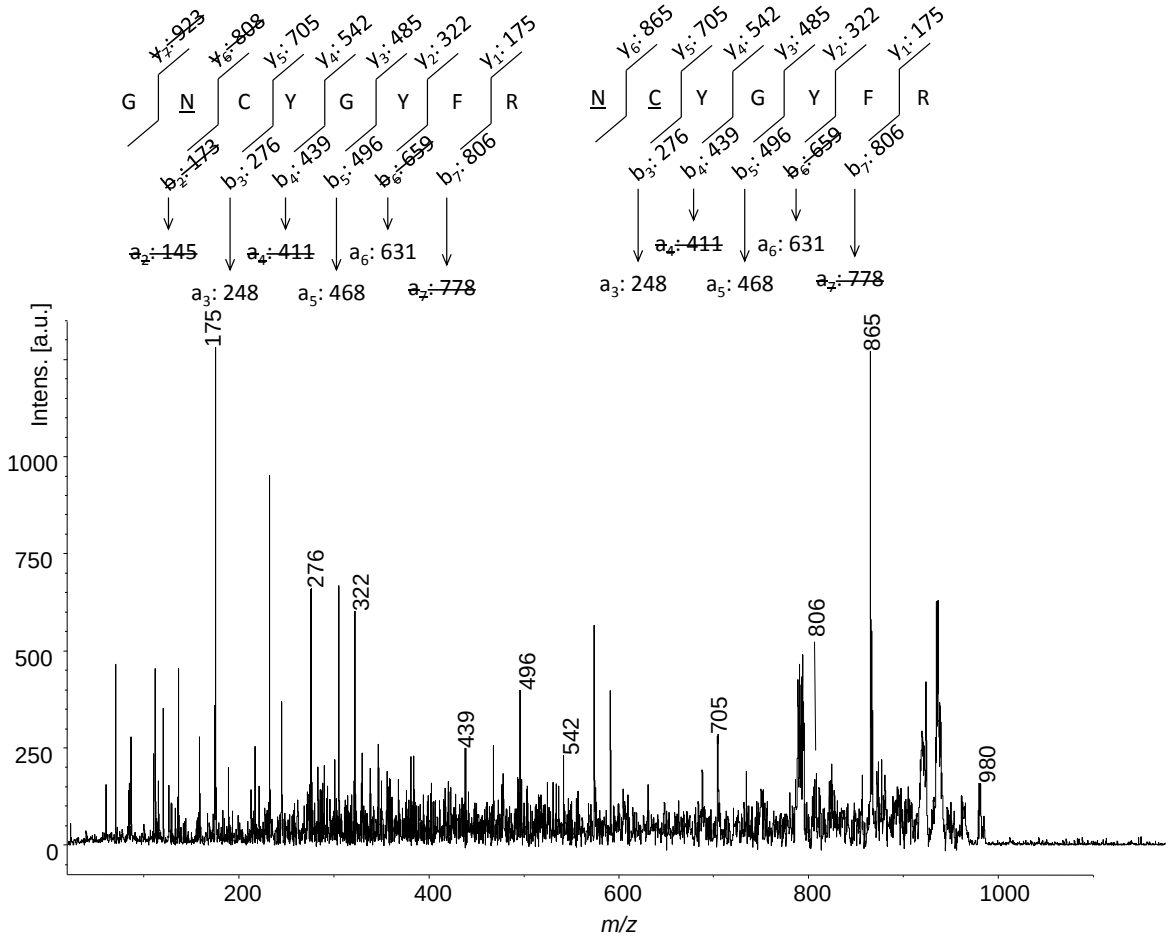

Figure 7.14: De novo sequencing of peptide ion m/z 980

7.3.2. Tandem MS

Manual *de novo* sequencing was attempted for all spectra obtained. An example of an SCA-2 sequenced peptide is given in Fig. 7.15. However, often the spectra were poor, due to low intensity of the precursor ion, or the precursor peak could not be isolated from ions of similar *m/z* values. Therefore, some ions could not be assigned to an amino acid sequence or an alternative source. The MS/MS ion search engine of MASCOT (www.matrixscience.com); was used to search the MS/MS ion peaks against a contaminants database in order to identify exogenous sources e.g. keratin, enzymes, BSA etc., although this did not identify any peaks.

Only MS ions which have been positively identified using MS/MS spectra will be discussed in this chapter. However, often MS/MS spectra for some peptides were not available in all samples. Therefore, it was assumed that peptides with the same MS *m/z* values have the same sequence. It is important at this stage to reiterate that the absence of an ion does not necessarily mean

absence of a peptide, and that the discussion is limited to only peptides which could be identified by *de novo* sequencing.

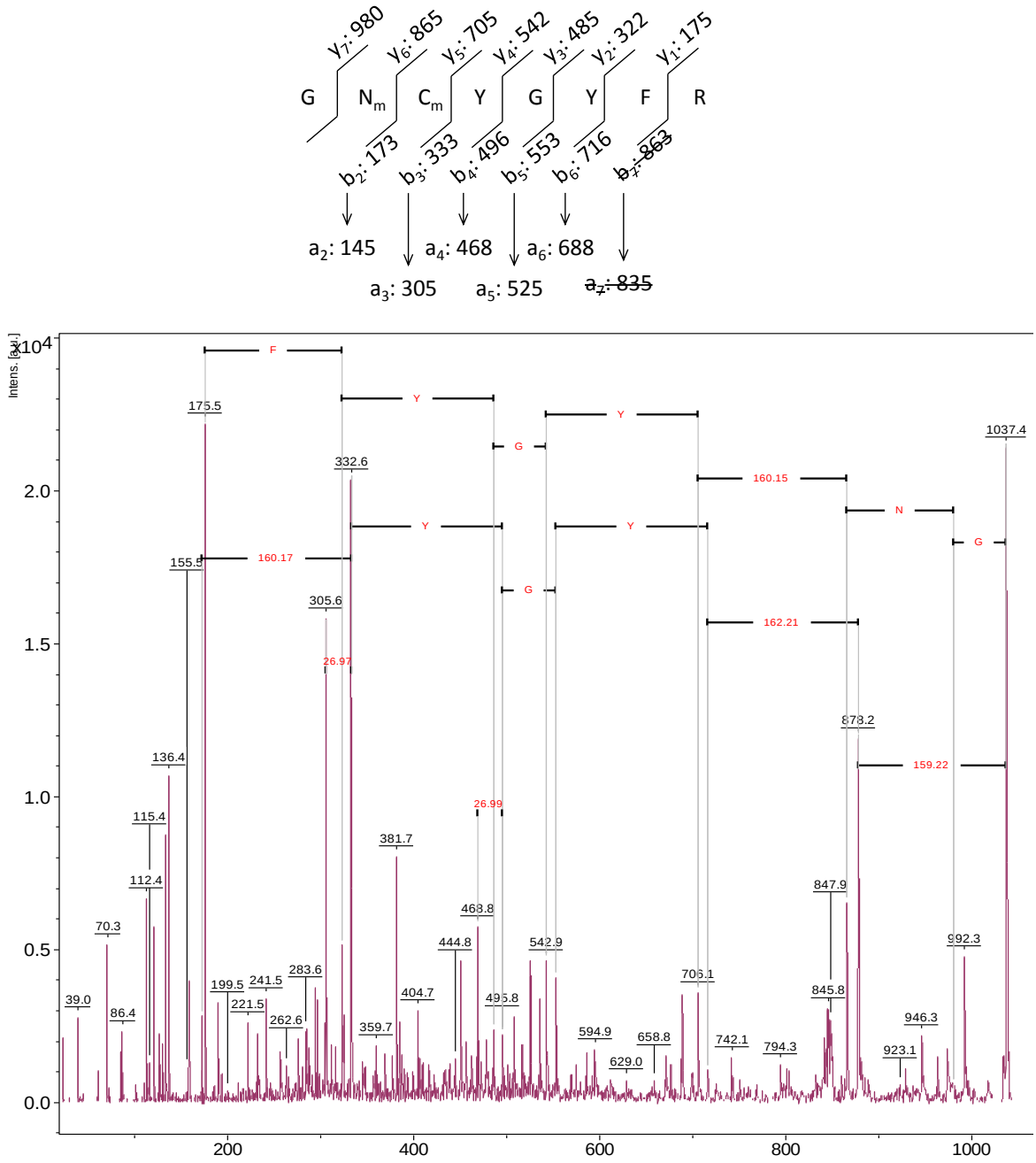

Figure 7.15: MS/MS of m/z 1037 with de novo sequencing (m = modified)

A summary of the peptides identified in this manner are given in Tables 7.3 and 7.4, along with the number of y and b ions which were present, the full MS/MS spectra with *m/z* ion identities are given in Appendix D.

m/z	y ions present	b ions present	Sequence (number given is the location of the first residue in the protein)
835	y_{1-6}	$b_{2, 4, 5}$	(6 – 11) GWLDFR (- 42, acylation)
877	y_{1-6}	b_{2-4}	(20-25) YELPW<u>K</u>
980	y_{1-5}	b_{3-6}	(13-19) <u>N</u>CYGYFR
1036	y_{1-7}	b_{3-6}	(12-19) GN<u>C</u>YGYFR
1037	y_{1-7}	b_{3-6}	(12-19) G<u>NC</u>YGYFR
1480	y_{1-7}	b_{2-11}	(88-99) HYSALDDDDYP<u>K</u>
1615	$y_{1-10, 14}$	b_{4-9}	(36-50) AGAHLASIHTSEEHR
2541	y_{1-16}	$b_{2-7, 10-13}$	(102-123) HCAVLDESSGFLSWDNDS<u>C</u>GER or H<u>C</u>AVLDESSGFLSWDNDSCGER

Table 7.3: De novo sequenced peptides from SCA-1; underlined residues have post-translational modifications (e.g. deamidation of Q or N), double underlined have other modifications (e.g. alkylation of Cys, or conversion of Lys to L-hArg).

m/z	y ions present	b ions present	Sequence (number given is the location of the first residue in the protein)
947	y_{1-6}	$b_{2, 3}$	(9-16) GWIPFDGR
1059	y_{1-7}	b_{2-6}	(97-104) LDYGSWYR
1112	y_{1-7}	b_{2-7}	(134-141) KPFI<u>C</u>EYR
1154	y_{1-8}	b_{2-7}	(134-141) <u>K</u>PFI<u>C</u>EYR
1164	y_{1-8}	b_{3-5}	(88-96) <u>N</u>WEWSDGT<u>K</u>
1589	$y_{1-5, 10, 11}$	b_{2-4}	(17-28) <u>C</u>YGFFPQELSWR

Table 7.4: De novo sequenced peptides from SCA-2; underlined residues have post-translational modifications (e.g. deamidation of Q or N), double underlined have other modifications (e.g. alkylation of Cys, or conversion of Lys to L-hArg).

7.3.2.1. Modern OES, whole-shell and intra-crystalline

Modern intra-crystalline and whole-shell OES samples were prepared in triplicate and spotted in triplicate. It was noted that peptides were not always present in all replicate samples; this was especially true for intra-crystalline samples (Table 7.5). This is potentially a consequence of low peak intensities, as was observed for the MS analysis of whole-shell vs. intra-crystalline samples, which was likely a result of reduced peptide concentrations (Sec. 7.3.1.).

m/z	SCA 1/2	Peptide	Whole-shell	Intra-crystalline
835	1	(6 – 11) GWLDFR (- 42, acylation)	9	**6**
877	1	(20) YELPWK	9	9
947	2	(9) GWIPFDGR	9	9
1036	1	(12) GNCYGYFR	9	9
1037	1	(12) GNCYGYFR	**5**	**4**
1059	2	(97) LDYGSWYR	9	9
1112	2	(134) KPFICEYR	9	9
1154	2	(134) KPFICEYR	9	9
1164	2	(88) NWEWSDGTK	**2**	0
1480	1	(88) HYSALDDDDYPK	9	7
1589	2	(17) CYGFFPQELSWR	9	9
1615	1	(36) AGAHLASIHTSEEHR	9	9
2541	1	(102) HCAVLDESSGFLSWDNDSCGER Or HCAVLDESSGFLSWDNDSCGER	9	**2**

Table 7.5: Summary table of sequenced peptides from modern intra-crystalline and whole-shell OES samples. The number indicates the number of samples the peptide in question was observed (total of 9: 3 spots for each triplicate sample)

For the purposes of this thesis, only peptides which have been positively identified will be discussed, as more work needs to be done to positively identify the remaining peptides. When peptides that were *de novo* sequenced were considered, both whole-shell and intra-crystalline OES samples showed an SCA-1 sequence coverage of 59 %. The whole-shell samples showed a slightly higher coverage for SCA-2 at 32 %, compared to 25 % for intra-crystalline samples (Fig. 7.16).

At this stage it is impossible to say whether the differences in sequence coverage for the whole-shell and intra-crystalline samples are due to higher protein concentrations in the whole-shell sample, or because there are genuine differences between the protein compositions in the whole-shell and the intra-crystalline fractions. However, no differences in amino acid compositions were observed from HPLC analysis of whole-shell and intra-crystalline samples (Sec.

3.3.3.), which suggests that the reduction in observed peptides in the MS analysis of intra-crystalline samples may indeed be due to a reduction in protein concentration.

SCA-1:

D K C P K G W L D F R **G N C Y G Y F R Y E L P W K R** A E A W C R S I R **A G A H L A S I H T S E E H R** A I A K F I S Q Y H H G E E E E D V W I G L F R W N S V W A W I D G S K K H **Y S A L D D D D Y P K** G K **H C A V L D E S S G F L S W D N D S C G E R** N A F I C K C T A

SCA-2:

R E R A G C A K **G W I P F D G R C Y G F F P Q E L S W R** R A E G F C Q R L G A R T H L A S I H S E E E H Q A I V S M L A S S Q P Y S D S E E E A G E E V W I G L H R P L G R R ***N W E W S D G T K*** **L D Y G S W Y R** D V F L R R R A C V A L E D T T D F A T W D V E L C S D R **K P F I C E Y R** T

Figure 7.16: Sequence coverage of modern whole-shell and intra-crystalline OES samples (Table 7.4). Peptides in bold were observed in both whole-shell and intra-crystalline samples; Italic and bold are peptides only seen in whole-shell samples; residues underlined indicate post-translational modification, e.g. deamidation of N or Q.

7.3.2.2. Kinetically heated samples

After just 24 h of heating at 80 °C the peptide (102-123) HCAVLDESSGFLSWDNDSCGER in SCA-1 is no longer present (Fig. 7.17), by 960 h a further two peptides from SCA-2 (17-28: CYGFFPQELSWR and 97-104: LDYGSWYR) have also disappeared (Fig. 7.17). After 1440 h heating (12-19) GNCYGYFR in SCA-1 is only observed in its deamidated form, and the peptides highlighted in green can no longer be detected by MS (Fig 7.17).

SCA-1:

D K C P K G W L D F R **G N C Y G Y F R Y E L P W K** R A E A W C R S I R A G A H L A S I H T S E E H R A I A K F I S Q Y H H G E E E E D V W I G L F R W N S V W A W I D G S K K **H Y S A L D D D D Y P K** G K H C A V L D E S S G F L S W D N D S C G E R N A F I C K C T A

SCA-2:

R E R A G C A K **G W I P F D G R** C Y G F F P Q E L S W R R A E G F C Q R L G A R T H L A S I H S E E E H Q A I V S M L A S S Q P Y S D S E E E A G E E V W I G L H R P L G R R N W E W S D G T K L D Y G S W Y R D V F L R R R A C V A L E D T T D F A T W D V E L C S D R **K P F I C E Y R** T

All peptides present in at least 2 out of 3 spots; red indicates a peptide no longer present at 24 h; peptides highlighted in blue have disappeared after 960 h heating (but are present at 24 h heating). Orange bold = peptides present up to 4000 h but not at 5760 h.

Figure 7.17: Summary of peptides present in 80 °C kinetics identified through MS/MS data

The same peptides are observed for the intra-crystalline OES samples as the whole-shell samples when heated at 140 °C for 20 or 40 min. After 20 min heating at 140 °C, OES samples still showed the same peptides as unheated OES samples, with the exception of an additional SCA-2 peptide (88-96: NWEWSDGTK), which was only previously seen in a small number of whole-shell unheated OES samples (highlighted in italics, Fig. 7.18). This suggests that the (SCA-2: 88-96) NWEWSDGTK peptide may be formed as a consequence of high temperature heating; indeed it is not observed in any sub-fossil samples either (Sec. 7.3.1.3.).

After 40 min of heating at 140 °C, both whole-shell and intra-crystalline samples showed a reduction in the number of *m/z* ions present in the MS spectra, but there was no observed change in the *m/z* ions which had been determined using MS/MS analysis.

SCA-1:

D K C P K G W L D F R **G N C Y G Y F R Y E L P W K R** A E A W C R S I R **A G A H L A S I H T S E E H R** A I A K F I S Q Y H H G E E E E D V W I G L F R W N S V W A W I D G S K K **H Y S A L D D D D Y P K** G K **H C A V L D E S S G F L S W D N D S C G E R** N A F I C K C T A

SCA-2:

R E R A G C A K **G W I P F D G R C Y G F F P Q E L S W R** R A E G F C Q R L G A R T H L A S I H S E E E H Q A I V S M L A S S Q P Y S D S E E E A G E E V W I G L H R P L G R R ***N W E W S D G T K*** **L D Y G S W Y R** D V F L R R R A C V A L E D T T D F A T W D V E L C S D R **K P F I C E Y R** T

Figure 7.18: Summary of peptides present in whole-shell OES heated at 140 °C for 20 m (highlighted in bold). Peptides in italics not observed in unheated or 80 °C samples.

7.3.2.3. Sub-fossil samples

The number of peptides detectable (and identifiable by MS/MS) was reduced for even the youngest sub-fossil samples (~300 yrs) compared to the number of peptides observed for modern samples (Fig. 7.19). The concentration of free amino acids within 250 yr old sub-fossil samples is generally low (determined using RP-HPLC; see Chapter 6), and for most amino acids the [FAA] / [THAA] is < 20 %, with the exception of Ser at 34 %. This may suggest that the peptides which are not present in the 300 yr old sample are more susceptible to degradation. However, this suggestion should be treated with caution, as it may be a consequence of the lower concentrations in sub-fossil samples, such that these peptides are present but not observed.

SCA-1:

D K C P K G W L D F R **G N C Y G Y F R Y E L P W K** R A E A W C R S I R **A G A H L A S I H T S E E H R** A I A K F I S Q Y H H G E E E E D V W I G L F R W N S V W A W I D G S K K **H Y S A L D D D D Y P K** G K H C A V L D E S S G F L S W D N D S C G E R N A F I C K C T A

SCA-2:

R E R A G C A K **G W I P F D G R** C Y G F F P Q E L S W R R A E G F C Q R L G A R T H L A S I H S E E E H Q A I V S M L A S S Q P Y S D S E E E A G E E V W I G L H R P L G R R N W E W S D G T K **L D Y G S W Y R** D V F L R R R A C V A L E D T T D F A T W D V E L C S D R **K P F I C E Y R** T

Figure 7.19: Coverage for a whole-shell sub-fossil sample independently dated by radiocarbon to 300 yrs. Peptides seen in modern samples but not in sub-fossil samples are highlighted in red.

There is a general trend towards a reduction in peptides observed with increased sample age. The oldest samples with SCA peptides present were 79 – 76 ka years for whole-shell samples (Fig. 7.20), and 72 – 70 ka for intra-crystalline samples (Fig. 7.21). Comparing this to the HPLC data it is clear that the majority of peptide bonds have been hydrolysed by these time points (Table 7.6), therefore we might not expect to see a lot of intact peptides in the MS or MS/MS analysis.

SCA-1:

D K C P K G W L D F R G N C Y G Y F R ***Y E L P W K*** R A E A W C R S I R A G A H L A S I H T S E E
H R A I A K F I S Q Y H H G E E E E D V W I G L F R W N S V W A W I D G S K K H Y S A L D D D D
Y P K G K H C A V L D E S S G F L S W D N D S C G E R N A F I C K C T A

SCA-2:

R E R A G C A K G W I P F D G R C Y G F F P Q E L S W R R A E G F C Q R L G A R T H L A S I H S E
E E H Q A I V S M L A S S Q P Y S D S E E E A G E E V W I G L H R P L G R R N W E W S D G T K L
D Y G S W Y R D V F L R R R A C V A L E D T T D F A T W D V E L C S D R **K P F I C E Y R** T

Figure 7.20: Peptides extracted from whole-shell samples of 72 – 70 ka highlighted in bold. Peptide extracted from whole-shell samples of 79 – 76 ka highlighted in italic bold text.

SCA-1:

D K C P K G W L D F R **G N C Y G Y F R Y E L P W K** R A E A W C R S I R A G A H L A S I H T S E E
H R A I A K F I S Q Y H H G E E E E D V W I G L F R W N S V W A W I D G S K K H Y S A L D D D D
Y P K G K H C A V L D E S S G F L S W D N D S C G E R N A F I C K C T A

SCA-2:

R E R A G C A K G W I P F D G R C Y G F F P Q E L S W R R A E G F C Q R L G A R T H L A S I H S E
E E H Q A I V S M L A S S Q P Y S D S E E E A G E E V W I G L H R P L G R R N W E W S D G T K **L**
D Y G S W Y R D V F L R R R A C V A L E D T T D F A T W D V E L C S D R **K P F I C E Y R** T

Figure 7.21: The oldest (72 – 70 ka) intra-crystalline sample which contained SCA peptides highlighted in bold, residues showing deamidation are underlined.

	Asx	Glx	Ser	Gly	Ala	Val	Phe	Ile
79 – 76 ka	59 %	9 %	59 %	61 %	72 %	47 %	45 %	45 %
72 – 70 ka	48 %	23 %	49 %	47 %	61 %	42 %	40 %	40 %

Table 7.6: [FAA] / [THAA] of oldest sub-fossil samples showing peptides in MS/MS analysis

7.3.3. Points of natural hydrolysis

Using the peptides identified in Sec. 7.3.1.1., the theoretical products of hydrolysis were considered, e.g. either loss of residues from the peptides, or previous loss of residues to form the

peptide in question. Some MS evidence was observed for possible sites of natural hydrolysis (Table 7.5). However, these peaks were not suitable for MS/MS analysis due to their poor S/N. Therefore, confirmation of natural hydrolysis could not be obtained. Nevertheless this data shows the potential for using this technique for mapping the peptide degradation and in some cases shows the sequential hydrolysis with time, e.g. *m/z* 947 (Table 7.7).

A potential point of natural hydrolysis was identified in SCA-1, which has previously not been seen (F_{18}; Table 7.7).

m/z	**Location of peptide within protein & samples which they are observed in**	**Possible hydrolysis related ion species**	**Observed possible hydrolysis products in MS spectra**
1154	SCA-2: (134) KPFICEYR • Observed in all modern OES samples : unheated (whole-shell and intra-crystalline), and all 140 °C & 80 °C heated samples • Observed in most whole-shell sub-fossil samples of < 15.5 ka	Additional R residue: *m/z* 1310: (133) RKPFICEYR	• Present in 80 °C 120 h and 480 h time points • Present in some whole-shell sub-fossil samples between 250 – 15000 yrs
		Additional DR residues: *m/z* 1425: (132) DRKPFICEYR	• Present in 80 °C 720 h only • Present in some whole-shell sub-fossil samples between 250 – 15000 yrs
1112	SCA-2: (134) KPFICEYR • As above	Loss of K residues: *m/z* 984: (135) PFICEYR	• Present in 80 °C 720 h and 1440 h
		Loss of KP residues: *m/z* 887: (136) FICEYR	• Present in 80 °C 720 h • Present in 140 °C intra-crystalline 20 m
980	SCA-1: (13) NCYGYFR • Observed in all modern	Loss of R residue: *m/z* 881: (13) NCYGYF	• Present in most 80 °C • Present in some 140 °C whole-shell 20 m

	OES samples heated at 80 °C for 480 h – 960 h • Observed in most whole-shell samples of < 15.5 ka and some intra-crystalline samples		• Present in most sub-fossil samples < 16 ka
947	SCA-2: (9) GWIPFDGR • Observed in all modern OES samples : unheated (whole-shell and intra-crystalline), and all 140 °C & 80 °C heated samples • Observed in most whole-shell samples of < 15.5 ka and some intra-crystalline samples	Loss of G residue: *m/z* 890: (10) WIPFDGR	• Present in 80 °C 720 h & 960 h • Present in 140 °C intra-crystalline 40 m
1154	SCA-2: (134) KPFICEYR • Observed in all modern OES samples : unheated (whole-shell and intra-crystalline), and all 140 °C & 80 °C heated samples • Observed in most sub-fossil samples < 71 ka	Loss of R residue: *m/z* 998: (134) KPFICEY	• Present in 80 °C 720 h • Present in some whole-shell samples < 250 yrs

Table 7.7: Summary of possible sites of natural hydrolysis using MS data only (peptide sequences not necessarily sequenced)

7.3.4. Deamidation

Both Asn and Gln can be deamidated during protein degradation, resulting in an increase of 1 mass unit (Sec. 1.3.1.1). Unheated modern OES samples generally showed little evidence for deamidation; the exceptions to this were N_{13} in SCA-1, which was deamidated in ~ 50 % of samples, and N_{88} in SCA-2, which was deamidated in a small number of whole-shell samples (Table 7.8). This may suggest that some deamidation occurs very rapidly, or that the sample preparation (e.g. acid demineralisation) facilitates this deamidation. Deamidation at other sites (e.g. N or Q residues) shows that the deamidation may increase with heating/time, e.g. N_{13} (row 2, Table 7.8) is present in a non-modified form in the majority of samples, but the deamidated form is only observed for 80 °C heated for > 480 h, indeed only the deamidated version is observed in sub-fossil samples >9 ka.

There is some evidence for deamidation at N_{86} (Table 7.8), which was previously not seen in the preliminary study by Cappellini *et al.*, (unpublished data).

Unmodified		Deamidated	Presence
Sequence	Mass	Sequence	
(12) GNCYCYFR *	1036	GNCYCYFR *	• 80 °C: deamidated in all samples; unmodified only in samples heated for ≤ 960 h • 140 °C: both forms in all samples • Sub-fossil samples: deamidated in most samples < 16 ka; unmodified peptide present for the majority of these samples • Present in a some whole-shell unheated modern samples
(13) NCYGYFR	979	NCYGYFR *	• 80 °C: unmodified version present in the majority of samples; deamidated version present only in 480 h, 720 h and 960 h samples. • 140 °C: deamidated version not present in any samples; unmodified version present in the majority of samples • Sub-fossil samples: both forms present only in some whole-shell young samples (< 1.5 ka); deamidated version alone is only present in whole-shell medium aged samples (9 – 16 ka)
(102) HCAVLDESSGFLSWDNDSCGER *	2541	HCAVLDESSGFLSWDNDSCGER	• Deamidated version not present in any samples • 140 °C: unmodified version present in most samples (whole-shell and intra-crystalline) • Unmodified version not present in any 80 °C or sub-fossil samples
(88) NWEWSDGTK	1163	NWEWSDGTK *	• 140 °C: deamidated version present in most samples; unmodified present only in some 20 m whole-shell samples • Neither version present in 80 °C samples or sub-fossil samples
(17) CYGFFPQELSWR (-H_2O)	1571	CYGFFPQELSWR (-H_2O) *	• 140 °C: deamidated version present in most samples; unmodified not present in any • Neither version present in 80 °C samples or sub-fossil samples
(17) CYGFFPQELSWR *	1589	CYGFFPQELSWR	• 80 °C: deamidated version not present; unmodified version present only in some 24 h and 96 h samples • 140 °C: unmodified version present in all samples; deamidated version present in none • Neither version present in sub-fossil samples
(75) WNSVWAWIDGSKK *	1660	WNSVWAWIDGSKK	• Neither version present in 80 or 140 °C heated samples • Sub-fossil samples

*Table 7.8: Summary of possible locations of deamidation; * = MS/MS sequenced*

7.4.1. Comparison with AAR data

A quantitative comparison of the MS data to the AAR data is not possible because the MS data is qualitative; interpretation of the absence of peaks in MS should be treated with caution, as it does not prove their absence within the sample. Nevertheless, a tentative comparison has been made between an intra-crystalline sub-fossil sample and two 80 °C heated intra-crystalline modern samples with similar levels of AAR (Table 7.9).

Sample	THAA D/L value				
	Asx	Glx	Ala	Val	Ile
Intra-crystalline sub-fossil (Lot no. 6888; MIS 1)	0.20	0.06	0.06	0.03	0.03
80 °C 24 h	0.20	0.08	0.08	0.03	0.02
80 °C 96 h	0.24	0.10	0.10	0.04	0.03

Table 7.9: Samples chosen with similar degrees of AAR for MS comparison (Fig. 7.14)

The overall sequence coverage is similar for each of the peptides detected in these three samples (Fig. 7.22), with the exception of an additional SCA-1 peptide (88- 99, HYSALDDDYPKGK) present in the 80 °C 24 h heated sample. Perhaps a more significant difference is that the sub-fossil sample only showed peaks for the deamidated form of the 'GNCYGYFR' SCA-1 peptide, whereas both 80 °C heated samples showed a mixture of deamidated and un-modified.

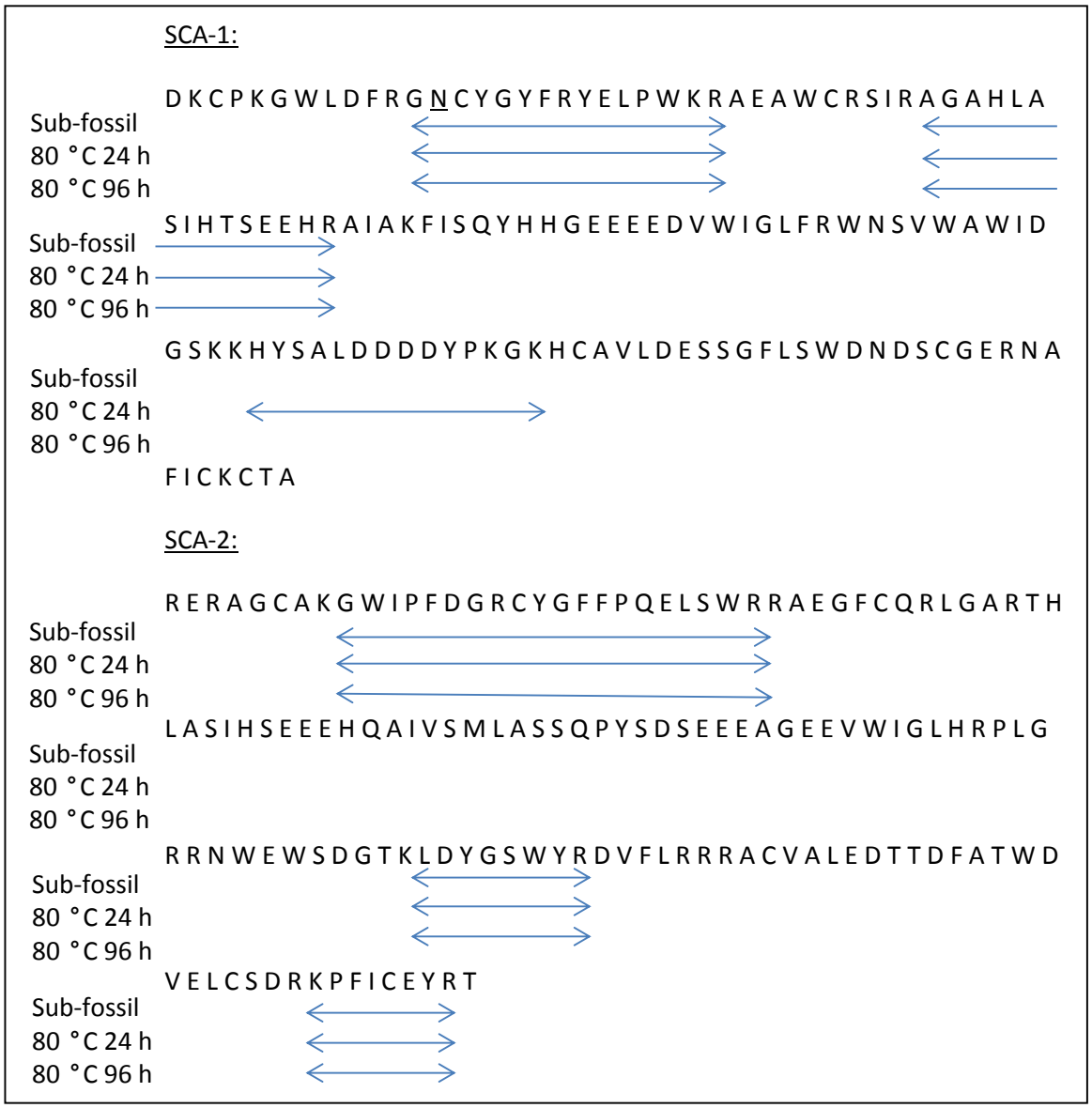

Figure 7.22: Comparison of sequence coverage of intra-crystalline OES samples (80 °C and sub-fossil), with similar levels of AAR.

A similar comparison was made for an older sub-fossil sample from MIS 2. As the previous example, two kinetic time points were used as it was not possible to find one time point which had similar extents of racemization over a range of amino acids. In this instance the 960 and 4028 h time points were chosen (Table 7.10).

Sample	THAA D/L value				
	Asx	Glx	Ala	Val	Ile
Intra-crystalline sub-fossil (Lot no. 6907; MIS 2)	0.47	0.12	0.19	0.09	0.12
80 °C 960 h	0.46	0.14	0.18	0.06	0.05
80 °C 4028 h	0.68	0.22	0.31	0.10	0.11

Table 7.10: Samples chosen with similar degrees of AAR for MS comparison (Fig. 7.15)

As with the previous comparison, the sequence coverage is similar for all samples (Fig. 23). The SCA-1 peptide, 'GNCYGYFR' was present in both the unmodified and deamidated version in the 960 h heated sample, but there was no evidence for the unmodified version in the sub-fossil or 80 °C 4028 h heated sample. This is similar to the previous comparison, where the sub-fossil sample suggested more deamidation had occurred than in kinetically heated samples of similar Asx and Glx D/L values.

Figure 7.23: Comparison of sequence coverage of intra-crystalline OES samples (80 °C and sub-fossil), with similar AAR. Dotted line indicates some evidence.

7.5. CONCLUSIONS

In order to unravel the complex degradation pathways of proteins within bio-minerals more details of the amino acid system, other than the THAA and FAA fractions, need to be studied. MS studies have been shown to have potential in opening the 'black box'.

Sequence coverage appeared to reduce with heating for kinetically heated modern OES samples, and with time for sub-fossil samples. Peptides from SCA-1 and SCA-2 were observed in modern OES samples with sequence coverage of 59 % and 32 %, respectively. The oldest sub-fossil samples with detectable and MS/MS sequenced SCA-1 or SCA-2 peptides present were 79 – 76 ka.

A number of potential sites of deamidation were located which have not been previously demonstrated. A number of potential natural hydrolysis sites were also located on both SCA-1 and SCA-2.

This study has given a glimpse into the 'black box' of protein degradation within bio-minerals. However, there were a number of issues that limit the utility of this study: i) This method is not quantitative and as such the absence of a peptide does not prove its absence from a sample, ii) Replicate samples often showed different amounts of sequence coverage, iii) A number of prominent peaks in the MS analyses, some of which have MS/MS spectra, were left un-identified as *de novo* sequencing was unsuccessful.

Further work to identify these unknown peptides may reveal additional points of hydrolysis, or diagenesis related modifications, and may increase sequence coverage. Further work should therefore focus on increasing the sensitivity and reproducibility of the MS method, perhaps by using LC-ESI MS/MS, or a combination of these two complementary techniques (e.g. Shevchenko *et al.*, 1996). Alternative enzymes, which cut the peptide at different locations (such as chymotrypsin), may liberate peptides which may show hydrolysis in different parts of the protein, and may allow the identification of natural hydrolysis peptides with C-terminal residues of K or L, which would otherwise be attributed to tryptic digests.

Despite the limitations highlighted here, this study was still a useful proof of concept and has taken some of the steps towards a better understanding of the complex diagenesis pathways in OES. Importantly, peptides have been recovered from samples as old as 72 – 70 ka, and some evidence for the natural hydrolysis and deamidation of SCA-1 and SCA-2 may have been identified.

CHAPTER 8: UHPLC METHOD FOR THE CHIRAL SEPARATION OF AMINO ACIDS

8.1. INTRODUCTION

The nature of amino acid enantiomeric pairs is such that their chemical behaviours are the same. However, some of their physical properties differ, e.g. their interaction with polarized light and their interactions with other enantiomeric compounds (e.g. Mason, 1991; Leffingwell, 2003). Separating enantiomeric pairs using chromatography requires either interaction or reaction with a chiral agent. This can be done by:

1. Formation of transient diastereomer complexes by:
    - Use of a chiral stationary phase (e.g. Meyer, 1991), or
    - Use of a chiral mobile phase (e.g. Hare and Gil-Av, 1979; Gil-Av *et al.*, 1980), or
2. Chemically altering the enantiomers by reaction with a chiral derivatising agent (CDA).

The diastereomers created by these interactions (either transient complexes (1), or covalently bonded (2)) are chemically discrete from one another, and therefore can be separated.

Some amino acids, e.g. Ile, have two asymmetric centres, and therefore can exist as two enantiomeric pairs as well as the corresponding diastereomeric pairs. Under geological conditions, L-Ile almost exclusively epimerises to form its diastereomeric isomer, a-Ile, it is for this reason that in the past many AAR studies have employed ion-exchange liquid chromatography (ILC), to focus solely on the separation of L-Ile and a-Ile, and not other amino acids (e.g. Hare and Mitterer, 1969; Miller and Hare, 1980; Hare *et al.*, 1985). However, there are advantages to studying several rates of racemization, e.g. temporal resolution (Chapter 6; Goodfriend, 1991) and in identifying compromised samples (Sec. 6.6.1., Brooks *et al.*, 1991).

There are a number of methods routinely used by AAR laboratories in order to separate the chiral forms of several amino acids, the most common being gas chromatography (GC) and reverse phase high pressure liquid chromatography (RP-HPLC).

8.1.1. Separation of chiral amino acids by gas chromatography

Sample preparation for GC analysis requires de-salting and derivatisation, to make analytes volatile and thermally stable, prior to injection onto the column (Kvenvolden *et al.*, 1973; Engel and Hare, 1985; Miller and Brigham-Grette 1989). Most GC methods use a chiral column (e.g.

Frank *et al.*, 1977), where an enantiomerically pure liquid stationary phase is bonded to the interior of the column. Although the detection methods are routinely flame ionised detection (FID) and nitrogen phosphorous detection (NPD), GC benefits from also being compatible with mass spectrometry (MS) detection (e.g. Liardony and Jost, 1981), which may allow identification of unidentified analytes. Routine GC methods with FID take approximately 110 min and typically resolve ~ 8 enantiomeric pairs for sub-fossil samples (Wehmiller and Miller, 2000; Wehmiller *et al.*, 2010).

Less commonly used GC methods use an additional pre-column derivatisation step with a chiral compound, such as (+)-2-butanol followed by acylation (e.g. with trifluoroacetic anhydride), prior to injection onto an achiral column (Engel and Hare, 1985; Kimber and Griffin, 1987). Although this method is capable of separating more analytes than alternative GC methods, the high cost of the derivitising agents currently prevents the routine use of this method (Wehmiller and Miller, 2000).

8.1.2. Current HPLC method

Chiral HPLC columns, required for the direct separation of enantiomers, tend to be very expensive compared to their achiral counterparts. Unlike GC, the HPLC CDAs tend to be cheaper, and readily available. Furthermore, the detection sensitivity of amino acids can be increased by the introduction of a fluorescent or chromophoric tag with the CDA (see review by Ilisz *et al.*, 2008). The sample size requirement for HPLC is therefore often less than typical GC sample size requirements (Wehmiller, 2013). Without introduction of a fluorescent or chromophoric tag, detection would be largely limited to MS, which is comparatively more expensive than fluorescence or UV detection. For these reasons AAR HPLC separation methods tend to favour the use of CDAs with a chromophoric tag.

Kaufman and Manley (1998) developed an indirect RP-HPLC method for the chiral separation of amino acids from bio-minerals based on a method by Brückner *et al.* (1991), and it is this method that is now routinely used for AAR HPLC analyses (Powell, 2012; Wehmiller, 2013; Powell, 2013).

The method benefits from an automated, online pre-column derivatisation with *o*-phthaldialdehyde (OPA) and *N*-iso-butyryl-L-cysteine (IBLC) (Brückner *et al.*, 1991; Kaufman and Manley, 1998), minimising lengthy pre-analysis preparative steps. OPA and IBLC react rapidly with primary amino groups to form the corresponding isoindole derivatives (Figure 8.1). IBLC is the CDA required to convert the enantiomers into diastereomers. OPA forms a fluorescent compound, enabling the use of fluorescence detection (FLD). However, secondary amino acids

(e.g. Pro) will not react, and therefore are not observed using this method (e.g. Brückner *et al.*, 1991).

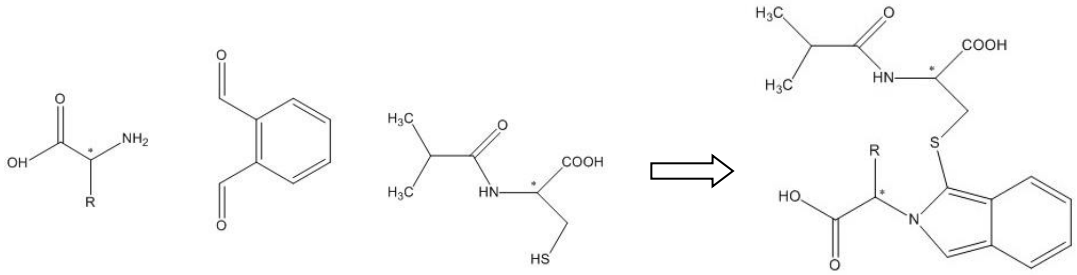

Figure 8.1: Schematic of OPA/IBLC derivitsation of a generic amino acid

A HyperSil base deactivated silicon (BDS) column (5 µm, 250 x 4 mm) was used, and is capable of routinely separating 9 amino acid pairs of analytes and an internal standard, L-hArg, in 90 min including flush time for sub-fossil mollusc samples (Kaufman and Manley, 1998), and 10 amino acid pairs, L-Thr and L-hArg in standard solutions. The method uses a tertiary gradient with sodium acetate buffer (pH 6.00), methanol (MeOH) and acetonitrile (ACN). The high concentration of sodium salts from the buffered mobile phase mean MS detection is not possible using this HPLC method. Although MS is more expensive than FLD, it may have been useful on occasion to identify unknown compounds, such as those observed in heated OES samples (Sec. 6.5.3.6.). Although other chiral amino acid HPLC methods using MS detection are available, they involve lengthy derivatisation steps which cannot be performed online (e.g. Min *et al.*, 2011).

The routine method used in the NeAAR laboratories at York is based on the Kaufman and Manley (1998) method. However, the solvent programme was extended as resolution of the later eluting analytes could not be replicated using the original method (Penkman, 2005). This method routinely separates 10 amino acid pairs and an internal standard, L-hArg (Fig. 8.2) in 115 min, inclusive of flush time, for both sub-fossil mollusc shell samples and standard solutions (Table 8.1) (Penkman, 2005). L- and D-Met were included in this method validation, however, L- and D-Tyr and L-Thr, can be separated but were not included in the method validation (Penkman, 2005).

Run time (min)	%A (sodium acetate buffer)	%C (methanol)	%D (acetonitrile)	Flow (mL / min)
0	95.0	5.0	0.0	0.56
31	76.6	23.0	0.4	0.60
95	46.2	48.8	5.0	0.60
95.9	0.0	95.0	5.0	0.60
99	0.0	95.0	5.0	0.60
100	95.0	5.0	0.0	0.60
115	95.0	5.0	0.0	0.56

Table 8.1: Solvent Gradient programme for RP-HPLC analysis (Penkman, 2005)

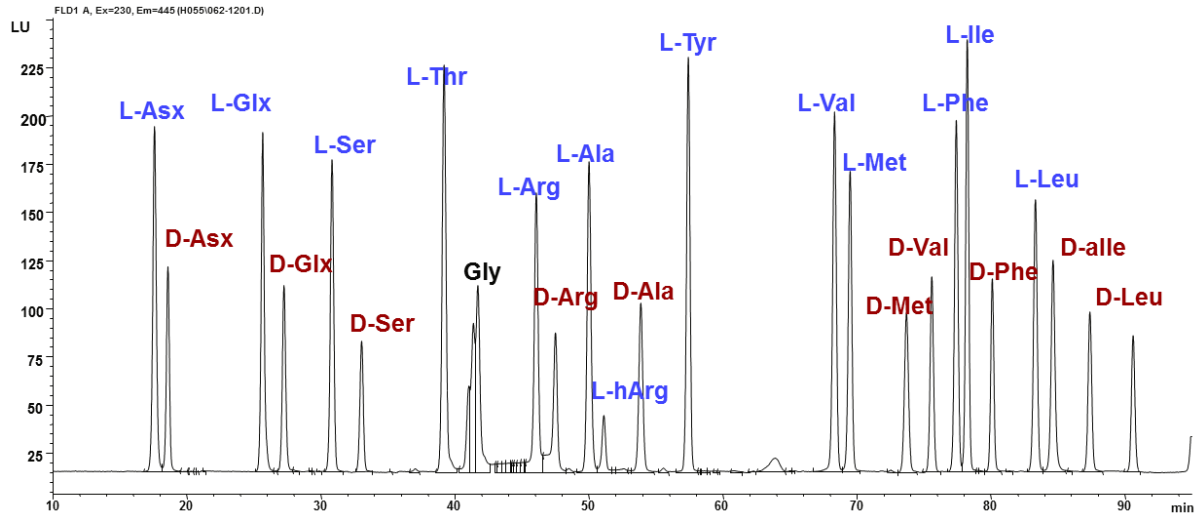

Figure 8.2: Typical HPLC chromatogram of an external standard solution

8.1.3. Ultra high pressure liquid chromatography (UHPLC)

Since the publication of Kaufman and Manley's (1998) method, there have been advances in chromatographic technology, notably the development of ultra-high pressure liquid chromatography (UHPLC), which can offer greater specificity with a reduction in run time (e.g. Swartz, 2005). This will allow a higher throughput of samples; at present only approximately 10 samples can be run per day using the current HPLC method. Separation of additional amino acids, previously not routinely included in HPLC AAR studies (e.g. His, Thr, Gly, Tyr), may benefit our understanding of the complex pathways of degradation within bio-minerals, they may be useful in

identifying heated or contaminated samples, species identification and/or may be valuable in respect to AAR dating.

UHPLC works on the same chemical principles as HPLC, that is to say that analytes are separated based on their affinities for the mobile and stationary phases. In RP-HPLC, where the stationary phase is non-polar and the mobile phase is polar, analytes elute in order of increasing hydrophobicity, i.e. hydrophobic analytes have a greater affinity to the stationary phase, therefore they will spend more time on the stationary phase and their retention times will be longer than for hydrophilic analytes. For a given HPLC method an analyte is identified based on its retention time. An efficient HPLC method will separate the analytes to a baseline resolution ($R_s \geq 1.5$) in the minimum amount of time. The resolution between two analytes is dependent on both their retention times and their peak width: $R_s = 2(t_{R2}-t_{R1}) / (W_1 + W_2)$, where t_R is the retention times of analyte 1 or 2, and W is the width of the peaks (a measure of time). Therefore, an efficient separation needs to minimise both the retention times and peak widths, and maximise analyte separation (e.g. Snyder *et al.*, 2012). Band broadening in LC is hypothesised to have three main sources:

A. Multiple flow paths

   The mobile phase can take different routes through the stationary phase, leading to differing velocity across the diameter of the column. This effect can be reduced by decreasing both the stationary phase particle size and the particle size distribution.

B. Analyte diffusion

   This describes how much the analyte diffuses in the longitudinal direction. This is affected by the column packing, and the choice of mobile phase, e.g. a gaseous mobile phase in GC will suffer from analyte diffusion more than the liquid mobile phase in LC. The effect of analyte diffusion can be reduced by increasing the mobile phase flow rate, as this encourages forward migration of the analytes.

C. Mass transfer

   Mass transfer describes the effect of absorption kinetics of the analytes onto the stationary phase. This can be affected by the physical properties of the stationary phase, e.g. pore size distribution, particle shape and particle size distribution. Anything that increases the length of the diffusion path will increase the time taken for transfer between the phases and therefore increase the band broadening. This effect is more complex than the previous two sources, however it can be decreased by both reducing the flow rate and by reducing the stationary phase particle size.

These three sources were described and combined by van Deemter *et al.*, (1956) to form the van Deemter equation (Eq. 8.1) which gives a value for 'theoretical plate height' (H). The plate model is used to describe column efficiency. A column can conceptually be divided into a series of separate layers (or theoretical plates). An analyte can be thought of as undergoing a series of equilibrations with each layer as it passes through the column. A column with very few theoretical plates will only be able to separate a small number of analytes. Increasing the number of theoretical plates increases the efficiency of a separation. This can be done by increasing the column length or ideally reducing the theoretical plate height, as H is inversely proportional to the efficiency.

$$H = A + B/u + Cu \qquad \textit{Equation 8.1}$$

where H = theoretical plate height, A = multiple paths parameter, B = diffusion co-efficient, u = linear velocity, C = mass transfer co-efficient (van Deemter *et al.*, 1956).

Reducing the stationary phase particle sizes will increase efficiency by reducing both the 'A' and 'C' terms. UHPLC uses stationary phase particles which are < 2 µm, compared to conventional HPLC which uses ~ 5 – 3.5 µm particle sizes. Therefore, the linear velocity can be increased without increasing the plate height and reducing the efficiency (Fig. 8.3). This allows UHPLC methods to use a faster flow rate, decreasing analysis time, but without compromising on efficiency.

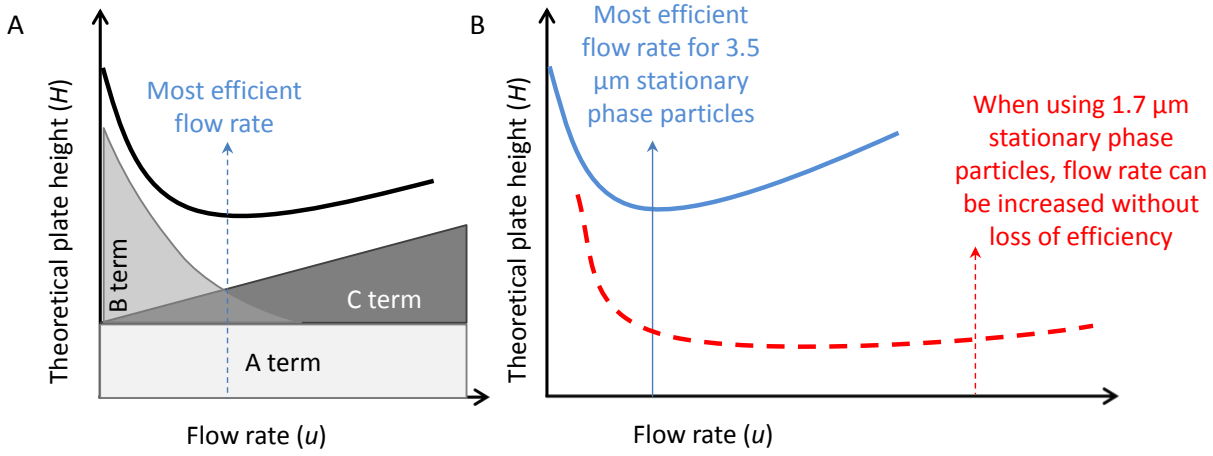

Figure 8.3: A: Schematic showing how the different band broadening effects from the van Deemter equation (Eq. 8.1) change with increasing flow rate and the resulting effect on the efficiency (efficiency α 1/ H). B: Schematic showing the effect of flow rate on efficiency for stationary phase particle sizes of different sizes

However, decreasing the stationary phase particle sizes increases the resistance to solvent flow, and therefore significantly increases the column generated back-pressure, as per Darcy's

equation, which shows that $\Delta p \propto 1 / d_p^2$, where Δp = pressure difference at the inlet and outlet of the column and d_p = stationary phase particle size (Cramers *et al.*, 1981; Nguyen *et al.,* 2006). Therefore, the introduction of commercially available UHPLCs required two main innovations:

1. The development of stationary phases with < 2 µm particle diameter. These needed to be manufactured such that they were stable under pressure, contained spherical particles and had a small particle size distribution.
2. The development of instruments capable of operating at high pressures, as UHPLC typically operate at up to 1000 bar, compared to HPLC systems which operate at < 400 bar.

8.1.3. HPLC to UHPLC method transfer

A successful HPLC to UHPLC method transfer must preserve the separation of the original method. In order to transfer an HPLC method to UHPLC a number of parameters should be altered (e.g. Guillarme *et al.,* 2007; 2008):

1. Column:

   A column of similar chemistry to the original HPLC column is usually chosen. The choice of column length depends on the method goals; a longer column would be chosen for complex separations (e.g. 150 mm), a shorter column chosen for simpler separations were a reduction in time is the primary objective (e.g. 50 mm).
2. Injection volume:

   This will depend on the choice of UHPLC column, although typically the UHPLC column will have a smaller internal volume. The injection volume needs to be geometrically scaled (Eq. 8.2) to prevent overloading of the column and the associated peak tailing.

$$Target\ inj.vol. = Original\ inj.vol. \times \frac{Target\ col.vol.}{Original\ col.vol.} \qquad \textit{Equation 8.2}$$

3. Solvent delivery:
   a. Flow rate:

   This can be scaled using the equation below (Eq. 8.3):

$$Target\ flow\ rate = Original\ flow\ rate \times \frac{d^2_{Target}}{d^2_{Original}} \qquad \textit{Equation 8.3}$$

   b. Adjust the gradient table:

   This is done such that the same number of solvent column volumes (cv) are maintained throughout the gradient table. Each gradient segment is expressed in units of cv (Eq. 8.4). This can then be used to calculate the new time per gradient segment (Eq. 8.5).

$$cv = (Flow\ rate \times Time) \,/\, (Column\ volume) \qquad \textit{Equation 8.4}$$

$$New\ segment\ time = cv \times target\ col.vol./target\ flow\ rate \qquad \textit{Equation 8.5}$$

4. Detection:

   The sampling rate may need to be increased due to the reduction in peak width.

Although this can all be done manually, there are a plethora of free online calculators which calculate the necessary changes in gradient table, e.g. Thermo Scientific (www.hplctransfer.com).

However, a straight method transfer will not take full advantage of UHPLC. Often retention times can be reduced further, whilst retaining the necessary resolution, by increasing the flow rate and/or optimising the gradient programme.

8.1.4. Method validation

Method validation is required as an assurance that a given method is suitable for its intended purpose, and it provides the limits to which the method is appropriate. The stringency of method validations will depend on the methods purpose, e.g. the guidelines set by the U.S. Food and Drug Administration (FDA) are designed to validate methods which may include the analysis of drugs for human trials, and therefore the limits are set very high. This level of validation may not always be appropriate, or possible. However, a thorough validation may reduce the time required to solve problems discovered at a later date. A typical method validation will tend to have the following components (e.g. Green, 1996; Snyder *et al.*, 2012):

1. Limits of detection and quantitation

   Limit of detection (LOD) is the lowest concentration of analytes that can be detected but not necessarily quantified. The limit of quantitation (LOQ) is the lowest concentration of an analyte which can be detected with the acceptable precision and accuracy (see below), as stated in the method details. The LOQ can either be determined experimentally or calculated based on a concentration which would give an acceptable signal to noise ratio (S/N; Green *et al.*, 1996). Although the FDA does not give specific guidelines on what levels of S/N are acceptable, the U.S. Pharmacopeial Convention (USP), suggests S/N levels for LOD and LOQ of 2-3 and 10, respectively.

2. Linearity

   A linearity study will provide analyte concentration limits where Beer's law is obeyed, e.g. the range in which the analyte response is linearly proportional to the analyte concentration. The FDA suggests a range of 120 % of nominal concentration, down to the LOQ, with a regression coefficient of ≥ 0.999. It is also suggested that a minimum of 3 different standard

concentrations are used, and each standard should be analysed in triplicate (Green *et al.*, 1996).

3. Precision

Precision tends to incorporate three elements: repeatability, intermediate precision and reproducibility (FDA, Reviewer Guidance, Validation of Chromatographic Methods, Nov 1994, CMC3).

a. Repeatability
    i. Injection repeatability: At least 5 injections with an RSD of ≤ 1%, although for low level impurities higher variations may be acceptable
    ii. Analysis repeatability: Consists of the several measurements of a sample by the same analyst
b. Intermediate precision
    i. Sometimes called 'ruggedness', this is the precision obtained when a method is performed by several analysts, on different days, using different machines, different columns and mobile phase preparations (Green *et al.*, 1996). This may help identify the primary sources of variability.
c. Reproducibility
    i. This normally includes an inter-laboratory comparison using homogeneous samples. The FDA suggests that this is not always necessary if an intermediate precision study has taken place. Indeed it was not appropriate within the scope of this study to include an inter-laboratory study.

4. Specificity

Specificity can be defined as "the ability of the method to accurately measure the analyte response in the presence of all potential sample components" (Green *et al.*, 1996, pp 306). This can be demonstrated in a number of ways depending on the nature of the method and/or analytes; for example forced degradation studies or spiking of the sample with impurities could be performed to demonstrate that baseline resolution was retained.

5. Accuracy

The accuracy of the method is defined by the closeness of a measured value to the true value. This can be assessed by calculating the concentration of a standard solution of known concentration, or by comparison of the calculated concentration to the calculated concentration from a previous, well established method. However, these methods are often not appropriate. Alternative approaches involve spiking of the sample matrix with a known amount of standard. The FDA recommends that these recovery studies should be performed

in triplicate at 3 different concentrations, for drug products they recommend 80, 100 and 120 % of the label claim. The mean indicates the accuracy of the method, whilst the standard deviation of the triplicate samples gives a measure of the sample analysis precision (Bullet point 3,a,ii). Where a blank matrix is not available, as is the case for this study, the accuracy can be assessed through standard additions. This method is similar to the spiking method above, but a real sample is used in-lieu of a blank matrix (Sec. 8.4.2.9.).

6. Analyte specific parameters

In addition to the components listed above there may be additional variables which need to be tested in order to fully define the method and its appropriate range, for example:

a. Response factors:

Where analyte concentrations are calculated relative to an internal standard, a response factor needs to be calculated such that the areas of the internal standard and analytes can be directly compared (Sec. 8.4.2.3.). This would usually be calculated using the linearity results.

b. Sample solution stability:

This should be tested in order to show that samples, mobile phases and any other reagents are stable under normal lab conditions for the time required to perform the analyses.

8.1.5. Scope of this study

This study aimed to transfer and optimise the current HPLC method to utilise the developments in UHPLC technology, with the following objectives:

1. To reduce analysis time
   - The current HPLC method can only run approximately 10 samples in 24 h.
2. To separate and validate additional analytes
   - The current method is unable to resolve D-His, L-His, D-Thr and Gly.
   - A small number of analytes appear to be separated using the current HPLC method, but were not included in the original method validation, e.g. L- and D-Tyr and L- and D-Lys.
   - The inclusion of previously unstudied amino acids and degradation products may help expand our understanding of protein degradation within bio-minerals (cf. Sec. 1.2.2.) and may allow, for example:
     - Alternative methods for identifying heated or compromised samples (cf. Chapter 6),

- Increased temporal resolution for AAR dating (cf. Chapter 6),
- Aid in species identification (e.g. Lajoie *et al.*, 1980; Miller et al., 2000)

3. To investigate the use of alternative buffers
    - Sodium acetate's effective buffering range is ~ 3.8 – 5.6 (Dawson *et al.*, 1986); therefore operating at pH 6.00 (as per Kaufman and Manley method) will reduce the effective buffering capacity. This may cause increased variability in the separation of analytes, especially for biological samples where analytes are often stable in different ionic states at different pHs (e.g. Asp in Fig. 8.6).
    - Sodium acetate buffer is not compatible with MS detection. Therefore other buffers, which are compatible, were considered.
4. To examine the applicability of the new method for AAR geochronology
    - Ideally the new UHPLC method will be applicable for the use of AAR geochronology; therefore it was tested using both modern and archaeological OES samples.

8.2. CHEMICAL AND SAMPLE PREPARATION

8.2.1. Chemicals and reagents

All amino acid standards were purchased from Sigma Aldrich, UK. The L-amino acid standard (AAS18) used contains L-Ala, ammonium chloride, L-Arg, L-Asp, L-Glu, Gly, L-His, L-Ile, L-Leu, L-Lys, L-Met, L-Phe, L-Pro, L-Ser, L-Thr, L-Tyr and L-Val all at 2.5 mmol dm^{-3}, and L-Cys at 1.25 mmol dm^{-3}. OPA and IBLC were purchased from Sigma Aldrich, UK.

An OPA/IBLC derivatising solution containing 260 mM IBLC and 170 mM OPA in 1 M potassium borate buffer was prepared and adjusted to pH 10.4 with potassium hydroxide pellets. OPA/IBLC solution is stable at room temperature for 3 days, after which sensitivity is reduced (Kaufman and Manley, 1998). Therefore, small aliquots of the solution, containing enough solution to run a sequence continuously for 3 days (200 µL), were stored in HPLC auto-sampler vials at – 4 °C and defrosted immediately prior to use. If any OPA/IBLC solution remains after > 3 days of being at room temperature, the solution was discarded.

HPLC-grade water was prepared using a Millipore Simplicity system. HPLC-grade ACN and MeOH were purchased from Fisher Scientific, UK.

Samples were solubilised in a rehydration solution consisting of 0.01 M HCl, 1.5 mM sodium azide and 0.01 mM, L-homo-arginine (L-hArg), a non-protein amino acid internal standard, L-hArg hydrochloride (Sigma-Aldrich; Product code: H1007).

The majority of glassware was sterilised by heating at 450 °C for at least 6 h. Volumetric flasks and Duran bottles used in the preparation and storage of the OPA/IBLC solution and the rehydration solution were sterilized by washing with concentrated nitric acid (as per Penkman, 2005).

Sodium acetate buffer (23 mM sodium acetate tri-hydrate, 1.5 mM sodium azide, 1.3 µM EDTA, adjusted to pH 6.00 ±0.01 with 10% acetic acid and sodium hydroxide) was prepared as per Sec. 2.3.2.

Ammonium acetate buffer was prepared by dissolving 9.22 g ammonium acetate (HPLC-grade, purchased from Fisher Scientific, UK) and 200 mg of sodium azide in 2 L of HPLC-grade water. The pH was adjusted to pH 5.80 using 10 % acetic acid solution.

The 'phosphate buffer' was prepared by dissolving 2.8 g Na_2HPO_4, 7.6 g $Na_2B_4O_7.10H_2O$ and 64 mg of sodium azide (all HPLC-grade, purchased from Fisher Scientific, UK), in 2 L of HPLC-grade water. The pH was then adjusted to pH 8.00 using 0.1 M HCl solution.

8.2.2. Preparation of standard solutions

Individual D-amino acid standards were prepared by dissolution of the single amino acid standards in HPLC-grade water (Table 8.2). A bulk concentrated racemate standard was prepared by mixing volumes of the single D-amino acids and 800 µL of the L-amino acid standard solution, such that D/L values were approximately 1 (Table 8.2). The resulting bulk concentrated standard solution was then diluted 1/20 with rehydration fluid to make the final standard solutions (Table 8.2).

Analyte	D-enantiomers*		Final standard solution (with 1/20 dilution with rehydration fluid)		
	Concentration of single amino acid standard (mM)	Volume added to the bulk concentrated standard solution (µL)	D/L	D-isomer (µM)	L-isomer (µM)
Asp	36.1	55	1.01	40.5	40.8
Glu	37.8	54	1.01	40.5	40.8
Ser	36.0	56	0.99	41.1	40.8
Thr	40.3	50	0.99	41.1	40.8
His	40.3	50	0.99	41.1	40.8
Met	35.8	56	1.00	40.9	40.8
Val	44.4	45	1.00	40.8	40.8
Phe	35.3	57	0.99	41.1	40.8
Tyr	1.98	1000	1.01	40.4	40.8
*Ile	37.4	53	1.01	40.5	40.8
Leu	47.4	42	1.01	40.6	40.8
Arg	36.6	55	0.99	41.1	40.8
Ala	25.4	79	1.00	41.0	40.8
L-hArg	NA	NA	NA	NA	9.5

*Table 8.2: Volumes used in the preparation of concentrated and bulk solution of external amino acid standard. * all D- isomers with the exception of Ile where it is D-aIle.*

8.2.3. Preparation of ostrich eggshell samples

The OES fragments were artificially aged by heating at 140 °C for 8 h, and then powdered with an agate pestle and mortar to < 200 µm. Samples were then submerged in 50 µL of 12% (w/v) NaOCl per mg of OES for 48 h in order to remove exogenous contamination. The OES was then washed five times in HPLC-grade water, with a sixth wash with HPLC-grade methanol to reduce any leftover bleach, before air-drying overnight. Note that this OES preparation was done prior to the bleaching experiment, which showed 72 h bleaching was necessary to isolate the closed system proteins (Chapter 3). However, as the OES sample was prepared in a single batch if inter-

crystalline proteins were present, they would be homogeneous in the sample. Furthermore, the amino acid composition in the inter- and intra-crystalline fractions have been shown to be very similar (Chapter 3), therefore it is not expected that using 48 h bleached OES, opposed to 72 h, will pose a problem for this study.

FAA and THAA analyses were undertaken as outlined in Chapter 2.

8.2.4. Method transfer

The purpose of this study was to transfer and optimise the HPLC method for UHPLC use. An Agilent 1200 series Rapid Resolution system fitted with a binary pump, column thermostat, solvent degasser and fluorescence detector was used. In order to transfer the method, a number of parameters were changed, and some were kept the same. Parameters where no change was necessary include:

- Derivitsation procedure and injector programme (Sec. 2.3.2.):

  Samples are derivatised using an automated injector program in the same way as the HPLC method: 1.1 µL of OPA/IBLC solution is drawn into the sample loop followed by 2 µL of sample and then a further 1.1 µL of OPA/IBLC solution, the resulting solution is mixed 13 times within the needle seat (approximately 5 min) prior to injection onto the column.
- Detection method, other than increasing the FLD sampling rate from every 0.25 s to 0.054 s (Sec. 2.3.2.):

  The fluorescence detector uses a Xenon-arc flash lamp at a frequency of 55 Hz, with a 280 nm cut-off filter and an excitation wavelength of 230 nm and emission wavelength of 445 nm (as per the HPLC method; Kaufman and Manley, 1998; Penkman, 2005).

Parameters which were changed included the choice of column, mobile phase compositions, solvent gradient, flow rates and column temperature.

8.2.4.1. Mobile phase composition

The original Kaufman and Manley (1998) method used a quaternary pump, but the Agilent 1200 series Rapid Res UHPLC system available for this study has a binary pump. Therefore, the organic mobile phases, ACN and MeOH, were combined into one mobile phase for the UHPLC method. The mixture of ACN/MeOH was tested between 0 and 15 % with respect to ACN.

The HPLC method uses a sodium acetate buffer at pH 6.00. As already discussed, this is outside the effective buffering range of sodium acetate buffer. Therefore, alternative buffer compositions were trialled, including:

1. A sodium acetate buffer with increased concentration (as this will increase the buffering capacity)
2. A phosphate buffer (10 mM Na_2HPO_4 : 10 mM $Na_2B_4O_7$); effective buffering range of 5.8 – 8.0 pH (Dawson *et al.*, 1986)

In addition, an ammonium acetate buffer at pH 5.8 was trialled (effective buffering ranges of pH 3.8 – 5.8 and 8.2 – 10.2; www.chem.agilent.com/cag/cabu/buffersel.htm) to assess whether it offered suitable separation. Ammonium acetate buffer benefits from being MS compatible, whereas sodium acetate and the phosphate buffer are not.

8.2.4.2. Solvent gradient & flow rates

An initial direct transfer of solvent gradient and flow rates was performed (Sec. 8.1.3.), and then optimised to further reduce the run times, and increase resolution of previously unresolved analytes. Altering the composition of the mobile phase changes an analyte's affinity to the mobile phase and as such its retention times. In order to increase the separation of two analytes the solvent gradient may be reduced, exaggerating the difference in time the different analytes spend in the mobile phase. However, reducing the gradient too much may result in band broadening and a corresponding reduction in resolution, due to increased time spent on the column and increased influence of mass transfer. Increasing the flow rate reduces analysis time and the contribution from analyte diffusion; however, it can also cause a reduction in resolution due to increased band broadening from mass transfer. The maximum flow rate is also limited by the pressure limitations of the machine; in the case of the Rapid Res 1200 series, this upper limit is 600 bar. The gradient programme and flow rates were therefore altered in order to try to resolve the necessary analytes, in the minimum amount of time.

8.2.4.3. Column temperature

Controlling the column temperature is important to ensure that fluctuating room temperatures do not affect the reproducibility of separations. Furthermore, increasing the column temperature does a number of positive things: i) it reduces solvent viscosity which reduces the back-pressure, therefore allowing faster flow rates without topping out the pressure, ii) it reduces the contribution of mass transfer to the band broadening, therefore increasing resolution, and iii) it reduces retention times.

However, increasing the column temperature can decrease the column life-time, and the stability of the analytes at increased temperatures should also be considered. The original HPLC method used a column temperature of 25 °C (Kaufman and Manley, 1998), therefore the temperature range tested was kept to a modest 25 – 40 °C, although the column manufacturer (Agilent; Sec. 8.3.1.1.) guidelines suggest the column is stable to 60 °C.

8.3. RESULTS AND DISCUSSION

8.3.1. Transfer and optimisation of UHPLC sodium acetate buffer method

The initial transfer and optimisation was done keeping the composition of mobile phase A (sodium acetate buffer), derivatisation procedure and detection methods the same as with the Kaufman and Manley (1998) method.

Parameters which were changed included the column (Sec, 8.3.1.1.), the mobile phase gradients and flow rates (Sec. 8.3.1.2.), and the column thermostat temperature (Sec. 8.3.1.3.).

8.3.1.1. Column choice

Initial method development was done using an Agilent ZORBAX Eclipse C18 column (100 x 4.6 mm, 1.8 µm). However, this was later changed to the ZORBAX Eclipse C18 Plus (100 x 4.6 mm, 1.8 µm) column, which offered better between column batch reproducibility, with respect to retention times and resolution.

8.3.1.2. Mobile phase B

Reduction in ACN concentration to below 5 % caused a loss of resolution for later eluting analytes, whilst increasing to over 10 % offered little improvement to the chromatography. As acetonitrile is a more expensive and a more toxic solvent than MeOH, keeping the ACN content low was preferable. The optimal mix was found to be a mobile phase B composition of acetonitrile/methanol of 7.5/92.5, v/v.

8.3.1.3. Gradient table and flow rate

The optimised gradient is given in Table 8.3; where, Mobile phase A: sodium acetate buffer at pH 6.00 (23 mM sodium acetate tri-hydrate, 1.5 mM sodium azide, 1.3 µM EDTA, adjusted to pH 6.00 ±0.01 with 10% acetic acid and sodium hydroxide), mobile phase B: acetonitrile/methanol (7.5/92.5 %, v/v).

Time (min)	% B	Flow rate (mL / min)
0	7.7	1.25
8.8	16.2	1.25
11	18	1.25
23	21.7	1.25
25	21.7	1.25
30	24.8	1.25
31.5	26	1.25
33	35	1.25
49	50	1.3
55	98	1.3
60	5	1.25

Table 8.3: UHPLC method pump timetable

8.3.1.4. Column thermostat

The column thermostat employed a small temperature gradient, just above room temperature in order to reduce variability. Although generally it is observed that increasing temperature increases resolution, Fitznar *et al.* (1999) noted this was not the case for a chiral amino acid HPLC method using OPA/NBC derivatisation. Furthermore, operating at increased temperatures can decrease column lifespan, therefore temperature increases were kept to a minimum (Table 8.4).

Time (min)	Temp(°C)
0	25
10	28
40	28
50	25

Table 8.4: UHPLC method column thermostat timetable

The optimised UHPLC method takes 60 min per sample (including flush time), and routinely separates 28 components within standard samples with baseline resolution, including 13 enantiomeric pairs, Gly and L-hArg. A typical standard chromatogram is shown in Figure 8.4.

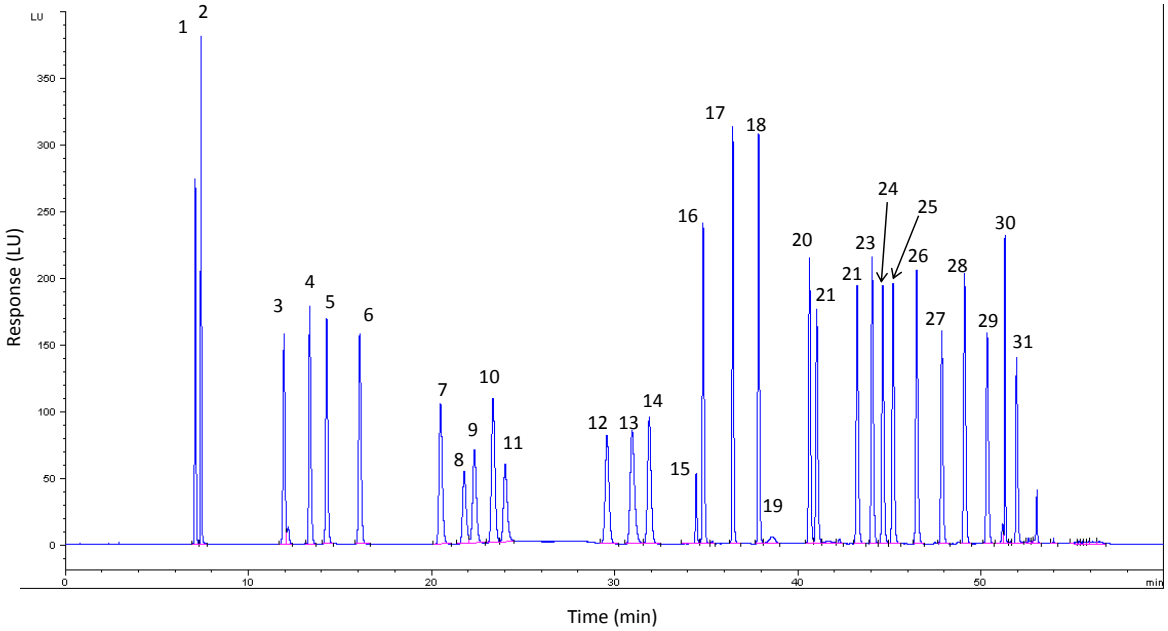

Figure 8.4: Typical UHPLC chromatogram (sodium acetate method) of an external standard solution. 1. L-Asp, 2. D-Asp, 3. L-Glu, 4. D-Glu, 5. L-Ser, 6. D-Ser, 7. L-Thr, 8. L-His, 9. Gly, 10. D-Thr, 11. D-His, 12. L-Arg, 13. L-Ala, 14. D-Arg, 15. L-hArg, 16. D-Ala, 17. L-Tyr, 18. D-Tyr, 19. Gly (secondary peak), 20. L-Val, 21. L-Met, 22. D-Met, 23. D-Val, 24. L-Phe, 25. L-Ile, 26. D-Phe, 27. L-Leu, 28. D-alle, 29. D-Leu, 30. L-Lys, 31. L-Lys (secondary).

8.3.1.5. Secondary analyte peaks

It is known that when using OPA and *N*-acetyl-L-cysteine (NAC), the derivatives of Gly, Lys and Ala are more susceptible to degradation to the thermodynamically favourable di-substituted derivative than other amino acids (Molnar-Perl and Vasanits, 1999). IBLC differs from NAC by replacement of a methyl group by methyl ethyl (Fig. 8.5, highlighted in red). Indeed, it has been observed that the OPA/IBLC derivatives of Lys and Gly degrade more readily than other amino acids (Brückner *et al.*, 1994). It is likely that degradation is the cause of a small secondary peak for Gly observed in both the HPLC (~ 64 min; Fig 8.2) and UHPLC (~ 38 min; Fig 8.4) methods. Two peaks, of similar intensities, are also routinely observed for L-Lys (D-Lys is not included in the standard solution) in the UHPLC method (at ~ 52 and 53 min; Fig 8.4). Indeed, Lys is well documented as forming unstable OPA/IBLC derivatives (Brückner *et al.*, 1994; Fitznar *et al.*, 1999), especially at lower pHs, and thus often has degraded by the time it elutes from the column at the end of the run (Umagat and Kucera, 1982; Fitznar *et al.*,1999). Therefore, it is likely that the secondary Lys peaks are also due to degradation of the derivatised amino acid. It is not known

whether L-Lys also forms two peaks in the HPLC method, as Lys typically elutes in the flush time (e.g. R_t > 90 min), however, it is speculated that it would.

No secondary peaks are observed associated with Ala in either the HPLC or the UHPLC method.

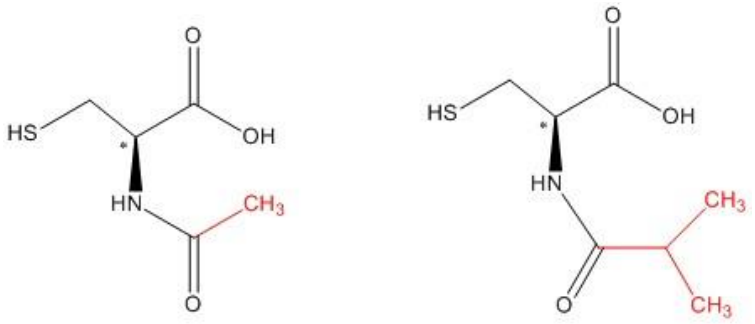

Figure 8.5: Left, NAC; right, IBLC. Differences are highlighted in red

Additional peaks are also commonly observed in the UHPLC method, which are associated with Asp (e.g. Fig. 8.6), and to a lesser degree Glu. The Asp secondary peaks were often more significant when analysing OES samples compared to standard solutions. Fitznar *et al.* (1999) observed splitting of Asp peaks with column aging, and suggested this may be due to the dissociated vs. un-dissociated forms (i.e. a small amount of the zwitterion form of Asp may be present, Fig. 8.7). Sodium acetate's effective buffering limit is pH 5.60, therefore operating at pH 6.00 will result in reduced buffering efficiency. This may yield greater variability in the ratio of different ionic forms of the analyte. An alternative hypothesis is that the secondary peaks are down to the presence of both protonated and sodiated Asp.

A sodium acetate buffer with increased concentration (~ 120 % of routine concentration), therefore increasing the buffering strength, was tested. However, this failed to prevent or reduce the peak splitting. Therefore, a phosphate buffer with an effective buffering range of pH 5.8 – 8.0 (Sec. 8.3.2.1.) and a sodium free buffer, ammonium acetate buffer, were also tested (Sec. 8.3.2.2.).

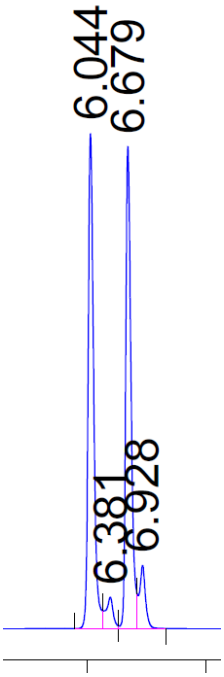

Figure 8.6: Example of secondary Asx peaks from a standard sample

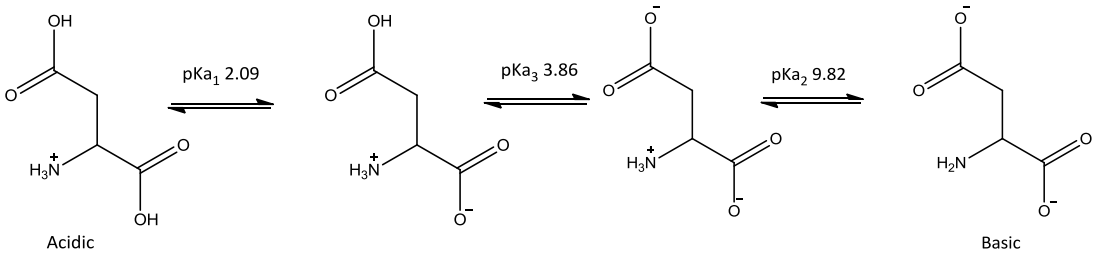

Figure 8.7: Ionised forms of aspartic acid: left, acidic conditions (< pH 2) and right, basic conditions (pH > 10) (Campbell and Farrell, 2011)

8.3.2. Alternative buffers

8.3.2.1. Phosphate buffer

The phosphate buffer method used was based on an achiral HPLC method from Agilent (Agilent application note, 2010; Table 8.5), which used the same ZORBAX Eclipse plus column already in use. The derivatisation method uses OPA, which derivatises amino acids with primary amine groups, and 9-fluorenyl-methyl chloroformate (FMOC), which derivatises amino acids with secondary amine groups, such as Pro.

Time (min)	%B	Method details
0	2	Flow = 1.5 ml/min
0.35	2	Column Temp = 40 °C
13.4	57	Mobile Phase A: 10 mM Na_2HPO_4 : 10 mM $Na_2B_4O_7$, pH 8.2: 5 mM NaN_3
13.5	100	Mobile Phase B: 45:45:10, ACN:MeOH:H_2O
15.7	100	Derivatisation: OPA and FMOC
15.8	2	
16	End	

Table 8.5: Agilent achiral amino acid UHPLC method (Agilent application note, 2010)

The method was adapted by decreasing the gradient, decreasing the flow rate, increasing the run time, reducing the pH of mobile phase A to pH 8.00 and introducing IBLC, such that it could separate chiral amino acids (Table 8.6). The method developed is outlined in Table 8.6.

Time (min)	%B	Method details
0	2	Flow = 1.2 mL / min
2	5	Column Temp = 40 °C
6	17	Mobile Phase A: 10 mM Na_2HPO_4 : 10 mM $Na_2B_4O_7$, pH 8.0: 5 mM NaN_3
10	18	Mobile Phase B: 45:45:10, ACN:MeOH:H_2O
16	21	Derivatisation: same as sodium acetate UHPLC method (Sec. 8.3.1.)
30	45	Detection: as sodium acetate UHPLC method (Sec. 8.3.1.)
33	100	
35	2	

Table 8.6: Modified chiral amino acid UHPLC method using phosphate buffer

The phosphate buffer has an effective buffering range of 5.8 – 8.0 pH (Dawson *et al.*, 1986), higher than that of the sodium acetate buffer. Using a buffer within its effective buffering range should minimise the presence of different protonated forms of analytes. Running at pH 8.00 may also have benefits for His, which should be ~ 99 % ionised at pH 8, opposed to only 44 % at pH 6.00 (Table 8.7), assuming that the pK_a's of the derivatised analytes are similar to those of the analytes.

Residue	Side Chain pKa	% Ionised	
		pH 6.0	pH 8.0
Asp	3.86	99%	100%
Glu	4.07	99%	100%
His	6.10	44%	99%
Arg	12.48	0%	0%
Lys	10.53	0%	0%
Tyr	10.07	0%	1%

Table 8.7: Expected percentage of ionised amino acids at different pHs, calculated based on their pK_a's at room temperature.

The resulting method separated ~28 components, the majority to baseline separation, within ~ 31 min run time (Fig. 8.8). The standard solution contains 28 analytes, however, Lys is split into 2 peaks using the sodium acetate method, and therefore > 28 peaks are expected suggesting the co-elution of 2 components. The secondary Asx peaks persist even at a higher pH, with a stronger buffer. Therefore, it seems unlikely that the peaks are due to the persistence of non-ionised analytes.

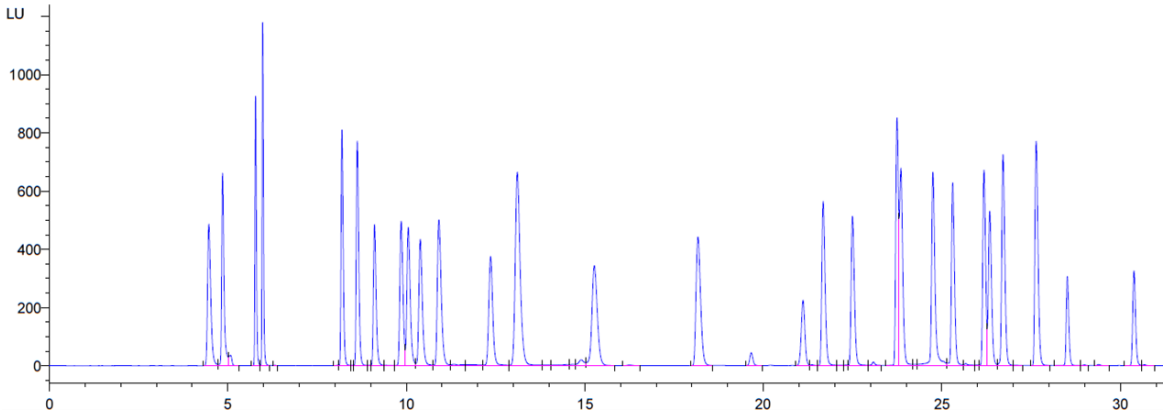

Figure 8.8: Example of separation of an external standard solution using an un-optimised phosphate buffer UHPLC method

This method shows great promise in reducing the analysis time even more so than the sodium acetate buffer method (Sec. 8.3.1.). Unfortunately, there was not enough time within this study to include the optimisation and validation of this method in addition to the sodium acetate method.

8.3.2.2. Ammonium acetate buffer

To test the hypothesis of sodiated vs. pronated analytes, a sodium free buffer, ammonium acetate buffer, was tested. Ammonium acetate's effective buffering ranges are 3.8 – 5.8 & 8.2 – 10.2 (www.chem.agilent.com/cag/cabu/buffersel.htm), so like sodium acetate, it will have a

reduced buffering capacity at pH 6. However, it has the added benefit that it is compatible with MS analysis.

Unfortunately, the secondary peaks were still present (Fig. 8.9). Furthermore, the second half of the separation was dominated by a very large peak and a raised baseline, which made quantitation of many analytes impossible (Fig. 8.9). It was suspected that this was due to ammonia reacting with the OPA/IBLC, as it is known that ammonia reacts with OPA (Kulla and Zuman, 2008). This was confirmed by injection of a derivatised water sample, which was also shown to have the additional peaks (Fig. 8.9). The ammonium acetate buffer neither removes the secondary peaks nor gives good resolution of the analytes, and was therefore not tested further. This may suggest that the cause of the secondary peaks is not related to a sodium based buffer. However, there are other sources of sodium in the method, such as the glass the samples are prepared and stored in, so this cause of secondary Asp peaks cannot be ruled out completely.

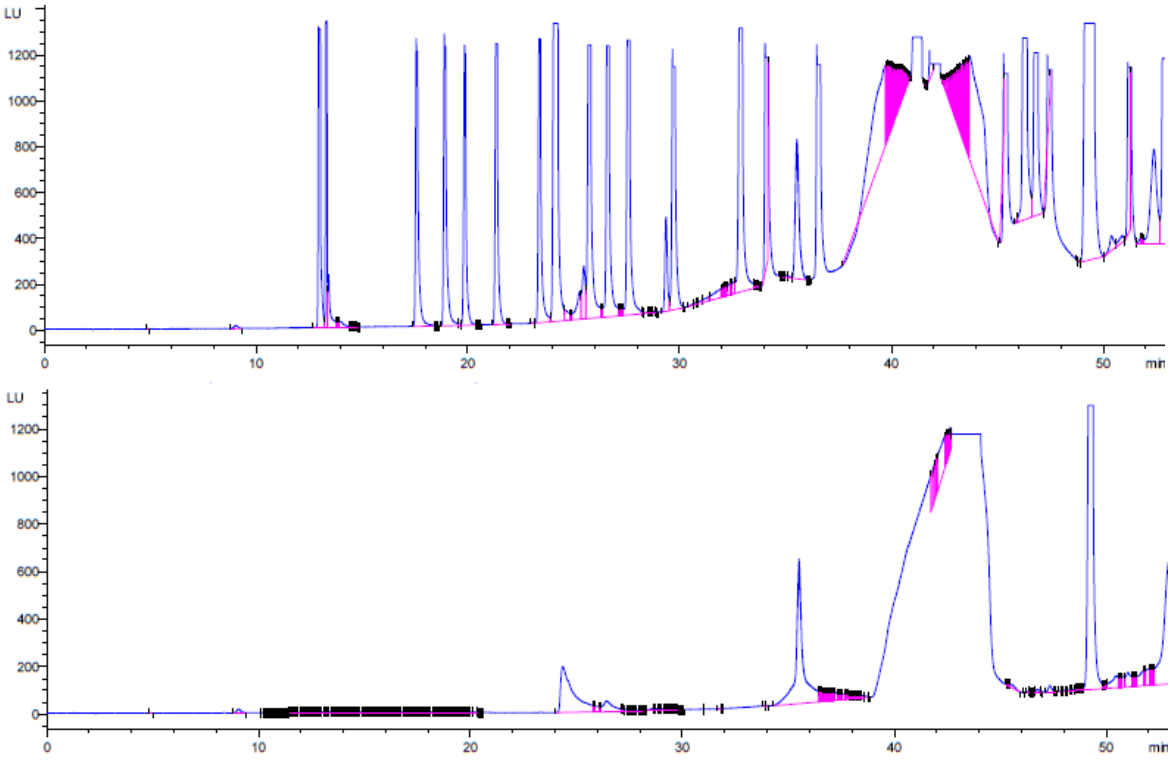

Figure 8.9: Example of separation of external standard solution using ammonium acetate buffer. Top: standard solution; Bottom: water.

8.3.3. Method Validation of UHPLC method with sodium acetate buffer

Unfortunately, within the time constraints of this study, it was not possible to optimise and validate the phosphate buffer method in addition to the sodium acetate method. Presented in

this section is the validation of the sodium acetate buffer method. The linearity, precision, limit of detection (LOD), limit of quantification (LOQ) and specificity of the method were tested using a standard solution prepared as per Table 8.2. To examine the applicability of this method for AAR geochronology, the method was then tested using both modern and archaeological OES samples (Sec. 8.3.3.7 - 8.3.3.11.).

8.3.3.1. Treatment of secondary peaks

It is unclear what is responsible for the secondary Asp and Glu peaks: presence of sodiated analytes, secondary OPA/IBLC/amino acid derivatives or degradation of the analytes are some possibilities. Identification of the compounds responsible for these peaks was not possible during the course of this study, as this would need to be done by LC-MS. The Asp secondary peaks were often large, so the secondary peaks of Asp were summed with the primary peaks for the validation of this method. Shoulders on the Asp peaks are often observed in the HPLC method, but the peaks are very rarely separated, and therefore treatment of these additional peaks has not been considered in previous HPLC methods (e.g. Kaufman and Manley, 1998; Penkman, 2005)

The Glu secondary peaks were not commonly observed, and where generally unresolved. Within a set of samples containing standards and OES samples ~ 50 % of samples showed a secondary Asp peak compared to ~ 13 % showing secondary Glu peaks. Therefore the secondary Glu peaks were not included in the UHPLC method validation.

The secondary Gly peak was previously observed in the HPLC method, yet not included in any previous method validation (Kaufman and Manley *et al.*, 1998; Penkman, 2005); therefore it was not included in the UHPLC method validation either.

The secondary L-Lys peak is often poorly resolved, especially for OES samples (e.g. Fig. 8.11), for this reason it was not included in the method validation (Sec. 8.4.2.).

8.3.3.2. LOD/LOQ

The LOD was defined as the lowest concentration where the S/N > 3. The LOQ was defined as the lowest concentration with S/N > 10 and where the %RSD of 6 repeat injections was < 20 %. The LOQ and LOD were determined experimentally by injection of diluted standard solutions. In addition, a theoretical LOQ was calculated from the experimental data in order to find the lowest concentration where the S/N = 10. Noise levels were calculated using ChemStation software, using the ASTM noise determination (this method is based on the standards set by the American Society for Testing and Materials).

The LOD for most analytes was found to be ~0.2 % of nominal (~ 0.08 µM), which equates to ~0.16 pmol per injection. The LOQ was found experimentally to be ~0.6 % of nominal (approximately 0.2 µM; ~4 pmol) for most analytes using 6 repeat injections (Table 8.8). The exceptions to this were L-His, D-His, D-Leu and L-Lys, which showed high variability between their repeat injections (> 20%). L- and D-His also showed a lower than required S/N at ~0.6 % concentration, and it was observed that both L- and D-His became increasingly degraded during the six injections, such that they were not detectable in the final two injections. In addition, a theoretical LOQ, where the S/N = 10, was calculated based on the noise levels and signal intensities from the 0.6 % standards (Table 8.8).

The calculated LOQ's are in the same order of magnitude as that of the Kaufman and Manley (1998) method (although a value of ~ 0.1 pM is quoted, it is suspected that their LOQ is actually ~ 0.1 pmol, as these units appear to be used interchangeably in the paper). These LOQs are two orders of magnitude lower than the LOQs quoted by alternative chiral amino acid UHPLC papers using different detection methods, e.g. Eto *et al.*, (2011) who quote LODs of ~5 – 23 pmol using UV detection or 11 – 64 pmol when using circular dichroism (CD) detection methods. Higher sensitivities have been reported for chiral amino acid separations using MS detection, with LODs as low as 5 – 300 fmol (Min *et al.*, 2011). However, this method requires time-consuming off-line derivatisation steps prior to analysis.

Analyte	Experimental data (~0.6 % of nominal)			Theoretical LOQ (µM)	
	Average S/N	%RSD of area	Concentration (µM)	Concentration (µM)	Amount (pmol)
L Asx	12.1	4.24	0.22	0.18	0.36
D Asx	14.7	2.43	0.22	0.15	0.30
L Glx	13.2	5.90	0.22	0.17	0.34
D Glx	30.1	1.89	0.22	0.07	0.14
L Ser	18.7	14.91	0.22	0.12	0.24
D Ser	14.2	11.98	0.22	0.16	0.32
L Thr	7.7	19.33	0.22	0.28	0.56
L His	7.5	43.28	0.22	0.29	0.58
Gly	20.8	14.70	0.22	0.11	0.22
D Thr	9.2	14.64	0.22	0.24	0.48
D His	6.6	25.18	0.22	0.33	0.66
L Arg	12.2	5.36	0.22	0.18	0.36
L Ala	9.6	4.44	0.22	0.23	0.46
D Ala	13.3	10.45	0.22	0.17	0.34
D Arg	42.0	5.07	0.22	0.05	0.10
L Tyr	49.5	1.03	0.22	0.04	0.08
D Tyr	49.1	1.90	0.22	0.04	0.08
L Val	34.6	3.17	0.22	0.06	0.12
L Met	26.4	3.10	0.22	0.08	0.16
D Met	29.4	3.72	0.22	0.08	0.16
D Val	34.6	1.28	0.22	0.06	0.12
L Phe	30.0	2.65	0.22	0.07	0.14
L Ile	32.8	6.61	0.22	0.06	0.12
D Phe	31.8	9.04	0.22	0.06	0.12
L Leu	26.5	9.86	0.22	0.08	0.16
D alle	33.7	19.94	0.22	0.06	0.12
D Leu	11.9	26.49	0.22	0.18	0.36
L Lys (1°)	128.9	22.54	0.22	0.02	0.04

Table 8.8: Summary of LOQ data: average S/N data calculated from 6 repeat injections, % relative standard deviation (RSD) of the peaks (< 20% is considered unacceptable, highlighted in bold). A theoretical LOQ was calculated based on the noise levels observed in the 0.625% standard sample.

8.3.3.3. External standard linearity

A standard stock solution was diluted with HPLC-grade water to give 8 concentrations between 130 % and the LOD (0.2 %) of the standard nominal concentration (~40 µM; Table 8.2). The samples were run using OPA/IBLC solution which had been defrosted for between 9 and 35 hours, therefore minimising the effects of degradation of OPA/IBLC solution (Sec. 8.2.1.). The responses

are reported as absolute areas, not normalised to L-hArg. The concentrations presented are those of the standard solutions prepared prior to mixing with OPA/IBLC solution.

The fluorescence signal for the analytes is linear within the range of approximately 0.08 – 53 µM (~ 0.16 – 106 pmol; Table 8.9). Unfortunately, in this study the concentrations were not tested high enough to find the upper limit of the linearity range.

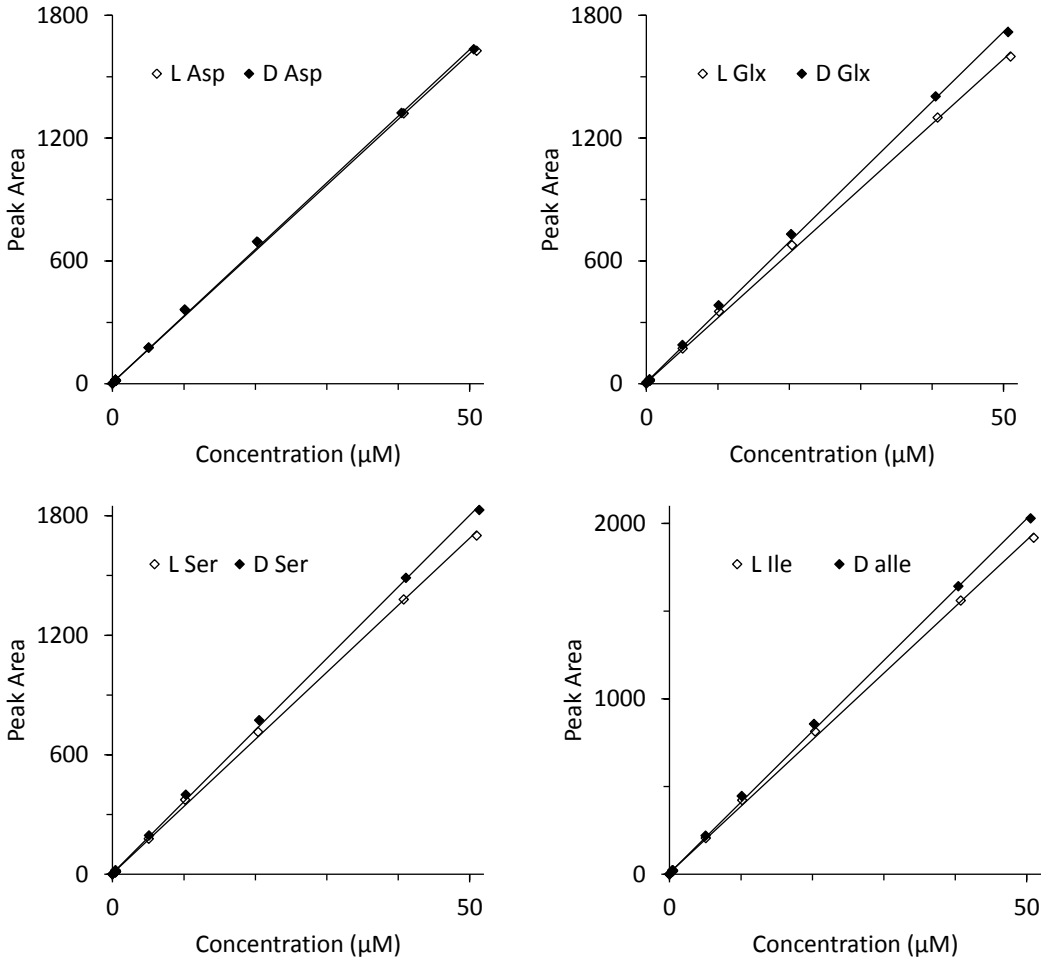

Figure 8.10: Linearity plots for Asp, Glx, Ser and Ile (see also Table 8.9 and Appendix F)

	Concentration (µM)		Linearity		
Analyte	Low	High	Gradient	Intercept	R^2
	0.2%	130%			
L-Asx	0.08	53.0	32.13	6.61	0.9995
D-Asx	0.08	52.6	32.52	6.75	0.9994
L-Glx	0.08	53.0	31.61	5.95	0.9995
D-Glx	0.08	52.7	34.22	8.26	0.9994
L-Ser	0.08	53.0	33.67	3.78	0.9995
D-Ser	0.08	53.4	35.96	4.79	0.9995
L-Thr	0.08	53.0	31.76	2.37	0.9995
L-His	0.08	53.0	16.63	-1.66	0.9995
Gly	0.08	53.0	26.19	8.96	0.9996
D-Thr	0.08	53.4	35.19	2.69	0.9997
D-His	0.08	53.4	20.96	-4.83	0.9993
L-Arg	0.08	53.0	29.34	4.35	0.9997
L-Ala	0.08	53.0	35.26	6.62	0.9996
D-Arg	0.08	53.4	31.56	3.37	0.9997
D-Ala	0.08	53.3	40.94	8.25	0.9996
L-Tyr	0.08	53.0	43.60	7.66	0.9996
D-Tyr	0.08	52.6	46.80	8.88	0.9995
L-Val	0.08	53.0	38.64	6.93	0.9996
L-Met	0.08	53.0	33.79	4.82	0.9996
D-Met	0.08	53.2	37.25	7.08	0.9995
D-Val	0.08	53.0	42.26	7.74	0.9995
L-Phe	0.08	53.0	36.18	6.36	0.9995
L-Ile	0.08	53.0	37.93	7.97	0.9995
D-Phe	0.08	53.4	38.83	6.92	0.9996
L-Leu	0.08	53.0	31.24	5.24	0.9995
a-Ile	0.08	52.6	40.38	7.49	0.9995
D-Leu	0.08	52.7	32.17	7.43	0.9994
L-Lys (1°)	0.08	53.0	22.54	48.34	0.9971
L-hArg	0.02	98.1	33.25	17.83	0.9996

Table 8.9: Summary of linearity data

8.3.3.4. Response factors

Response factors were calculated relative to L-hArg over the range of the linearity (Table 8.10; Fig. 8.10). As previous studies found, generally the D-isomers were found to fluoresce more than the corresponding L-isomers (Brückner *et al.*, 1991; Kaufman and Manley, 1998).

The response factors are also reported as D/L correction factors, so that they can be compared to the Kaufman and Manley (1998) method (Table 8.10). Generally there is good agreement between the factors calculated using the different methods, with the notable exception of Ile.

Analyte	Response relative to L-hArg	D/L correction factors		
		Analyte	UHPLC	Kaufman and Manley (1998)
L-Asx	1.03	Asx	1.01	0.96
D-Asx	1.02			
L-Glx	1.05	Glx	1.08	1.08
D-Glx	0.97			
L-Ser	0.99	Ser	1.07	1.12
D-Ser	0.92			
L-Thr	1.04	Thr	1.11	
L-His	1.99			
Gly	1.27	His	1.26	
D-Thr	0.94			
D-His	1.58	Arg	1.08	1.22
L-Arg	1.13			
L-Ala	0.94	Ala	1.16	1.10
D-Arg	1.05			
D-Ala	0.81	Tyr	1.07	1.06
L-Tyr	0.76			
D-Tyr	0.71	Val	1.09	1.02
L-Val	0.86			
L-Met	0.98	Met	1.10	
D-Met	0.89			
D-Val	0.79	Phe	1.07	1.10
L-Phe	0.92			
L-Ile	0.87	Ile	1.06	1.26
D-Phe	0.85			
L-Leu	1.06	Leu	1.03	
a-Ile	0.82			
D-Leu	1.03			
L-Lys (1°)	1.47			

Table 8.10: Response factors reported as both relative to the internal standard (L-hArg) and as a D/L correction factor.

8.3.3.5. Precision

The overall variability of standards were analysed over a period of 2 months, using 2 different columns, a variety of standard ages (up to 5 days), and varying OPA/IBLC ages (up to 3 days). Sodium acetate buffer was prepared fresh at least every 5 days within the following concentration ranges: sodium acetate trihydrate 23 mM +/- 0.01%, sodium azide 1.5 mM +/- 0.03% and EDTA 1.3 µM +/- 0.19%. The buffer was adjusted to pH 6 using a pH probe re-calibrated prior to every use to within 5% calibration error (as per manufacturer's guidelines).

No other UHPLC machines and/or modules were available for comparison.

Variability in retention times was small (< 1% relative standard deviation (RSD)) for all analytes, except L- & D-Asp and L- & D-Glu, all of which showed higher %RSD (< 4 %). Variability in relative peak areas were generally below 5 %, with the exceptions of L-His, D-His, Gly, L-Leu and D-Leu which were all below 10%, and L-Lys which was 11.5%. Variability in relative D/L peak areas were generally < 1%, with the exceptions of Glu and Arg (both <4%), and Leu and His (~ 7%).

The variability between D/L values were typically < 1 % for all but Asx (2 %), Glx (4 %) and Arg (3 %). This variability is of similar magnitude to that quoted for the HPLC method (Kaufman and Manley, 1998).

8.3.3.6. Specificity

Standard samples were heated at 110 °C for up to 1440 min in duplicate. Half width resolution remained at > 1.75 for all analytes during the forced degradation, with the exception of L-Ala whose resolution dropped to 1.69 for one of the 1440 min duplicate samples. The high temperatures caused degradation of some amino acids, especially Glu, Arg and Met. A number of additional peaks developed during the study, the most significant of which were one peak eluting at ~ 3 min, and 2 peaks within the Thr/His/Gly cluster of peaks at ~ 20 – 25 min (Fig. 8.11). The identities of these are unknown and they do not correspond to any of the single amino acid standards that were analysed. A forced degradation of single amino acids suggested that peaks eluting within the 20 – 25 min window may be a result of His, Arg and/or Met degradation products. All of these peaks have been observed in heated modern OES samples, although they are usually small (e.g. Fig. 8.12).

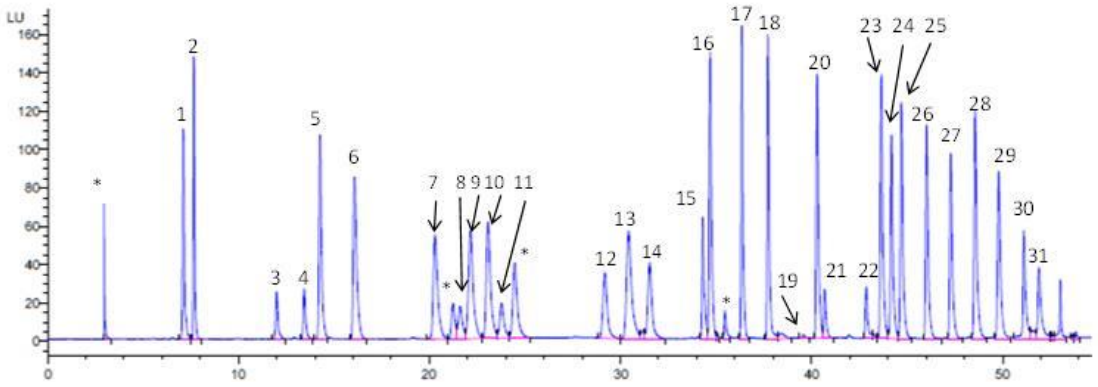

*Figure 8.11: Standard sample heated at 110 °C for 1440 min prior to analysis. Unknown degradation compounds marked with a *. 1. L-Asp, 2. D-Asp, 3. L-Glu, 4. D-Glu, 5. L-Ser, 6. D-Ser, 7. L-Thr, 8. L-His, 9. Gly, 10. D-Thr, 11. D-His, 12. L-Arg, 13. L-Ala, 14. D-Arg, 15. L-hArg, 16. D-Ala, 17. L-Tyr, 18. D-Tyr, 19. Gly (secondary peak), 20. L-Val, 21. L-Met, 22. D-Met, 23. D-Val, 24. L-Phe, 25. L-Ile, 26. D-Phe, 27. L-Leu, 28. D-alle, 29. D-Leu, 30. L-Lys, 31. L-Lys (secondary).*

8.3.3.7. Ostrich eggshell samples

AAR geochronology uses bio-minerals which contain many compounds other than those found within the standard solution; for example eggshells contain calcium, polysaccharides (Baker and Balch, 1962), phospholipids (Simkiss, 1958) and protein complexed with acid-mucopolysaccharides (Simkiss and Tyler, 1957). The method was validated using OES in order to assess its applicability for separation of amino acids in bio-minerals. An example of a UHPLC chromatogram for the THAA of an artificially-aged modern OES sample is shown in Figure 8.12.

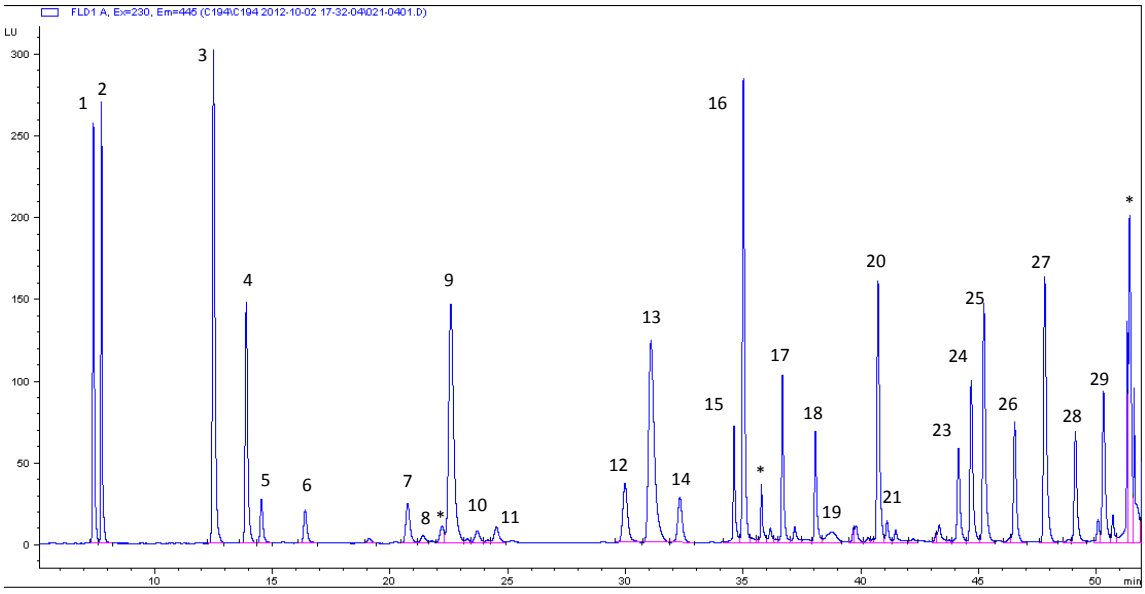

*Figure 8.12: Chromatogram of THAA fraction of a modern OES sample artificially aged by heating at 110 °C for 720 h. Standard amino acid assignments: 1. L-Asp, 2. D-Asp, 3. L-Glu, 4. D-Glu, 5. L-Ser, 6. D-Ser, 7. L-Thr, 8. L-His, 9. Gly, 10. D-Thr, 11. D-His, 12. L-Arg, 13. L-Ala, 14. D-Arg, 15. L-hArg, 16. D-Ala, 17. L-Tyr, 18. D-Tyr, 19. Gly (secondary peak), 20. L-Val, 21. L-Met, (22. D-Met, not present), 23. D-Val, 24. L-Phe, 25. L-Ile, 26. D-Phe, 27. L-Leu, 28. D-alle, 29. D-Leu (L-Lys unresolved). * = unidentified compounds*

8.3.3.8. Sample size requirement

Routinely a mass of 1 – 2 mg of bio-mineral per sample is used for ease of handling. THAA OES samples are rehydrated in 60 µL of rehydration fluid per mg of bio-mineral, FAA OES samples are rehydrated with 20 µL / mg, which usually puts all amino acids within the validated concentration range (0.1 – 106 pmol; Table 8.9). Only 2 µL of sample is used per injection, therefore the mass requirement could easily be reduced without a reduction in fluorescence response. L-His is the

analyte of the smallest peak area for a modern OES sample (Fig. 8.12). Theoretically, the dilution of a modern OES sample can be increased from 60 to 360 µL / mg whilst maintaining a S/N > 10 for the analyte of smallest peak area, L-His in this example (Fig. 8.12). Assuming a required volume of 2 µL, a theoretical minimum mass for this THAA sample could be as little as 0.6 µg. Typically, FAA analyses require ~6 times the mass of THAA samples, due to lower concentrations of free amino acids, although this is very dependent on the sample's history. However, working with such small masses will likely introduce error in the calculation of absolute concentrations, although this will cancel out in the calculation of D/L values.

Kaufman and Manley quoted a minimum mass for bivalves of 1 µg. The concentrations of amino acids in OES are typically much higher than in mollusc shells (Brooks *et al.*, 1990), therefore the minimum working masses for real samples are probably comparable in the HPLC and UHPLC methods.

8.3.3.9. Precision

Five samples of 20 µL of standard solution were dried in the centrifugal evaporator and subsequently rehydrated in 20 µL of rehydration fluid. In addition five samples of FAA and THAA OES samples were prepared as per the method detailed in Sec. 8.3.2.6. Areas are reported relative to the area of L-hArg.

The errors associated with the analytical method (i.e. the standard samples) are shown to be small (< 5%). Larger errors are observed for D-His and L- Lys. Fitznar *et al.* (1999) also observed higher variability for His and Lys OPA/IBLC derivatised analytes, and attributed this to the instability of these derivatised analytes. However, this may not fully explain our results, as it might be expected that L-His would be similarly unstable as D-His. Thr has two asymmetric carbons (like Ile), and therefore has 4 isomers, which likely elute at similar retention times as L- and D-Thr. Therefore, it may be that one of these compounds is causing increased variability in the D-His peak areas.

The variability observed for OES samples is higher than for standard samples. The errors observed for the FAA samples are generally higher than those from the THAA samples, and may be a consequence of an increased influence from compounds other than amino acids within the samples. Indeed the baseline is generally noisier for FAA samples than for THAA samples.

D-Arg and D-Met (and to a lesser extent L-Tyr, D-Tyr and L-Met) show a much higher variability in THAA samples than other amino acids, which are generally < 4 % (Table 8.11). It has previously been noted that mollusc shells commonly have a co-eluting peak with D-Arg, which results in a higher variability for Arg D/L values (Penkman, 2005), so perhaps there is a similar co-eluting

compound in OES, although no shoulders are observed on the peak. It seems likely that the variability is due to the nature of the bio-mineral, given that the variability shown in the standards are all very low.

Analyte	OES				Standard	
	FAA		THAA			
	Average	%RSD	Average	%RSD	Average	%RSD
	Relative area		Relative area		Relative area	
L-Asx	63	4.7%	4915	0.6%	22.85	1.5%
D-Asx	8	13.0%	675	0.6%	22.82	1.5%
L-Glx	42	6.4%	5352	0.8%	20.72	1.6%
D-Glx			413	0.4%	24.08	1.5%
L-Ser	42	4.5%	3368	0.6%	23.45	1.5%
D-Ser	16	9.2%	466	1.5%	25.37	1.5%
L-Thr	26	8.3%	1875	2.1%	22.36	1.6%
L-His			794	1.9%	12.46	1.7%
Gly	98	5.8%	3538	2.5%	17.59	2.0%
D-Thr	25	11.1%	399	3.2%	25.07	2.3%
D-His			186	3.2%	15.03	3.7%
L-Arg			2682	0.8%	20.52	2.4%
L-Ala	35	4.5%	4725	0.6%	24.77	1.6%
D-Arg			341	38.1%	22.06	1.5%
D-Ala	16	26.9%	317	1.9%	28.81	1.7%
L-Tyr			1130	13.9%	30.72	1.5%
D-Tyr			54	13.8%	32.72	1.6%
L-Val	14	18.6%	2867	1.5%	27.56	1.4%
L-Met	14	23.6%	622	13.7%	23.35	1.3%
D-Met			51	30.4%	26.17	1.3%
D-Val			109	5.8%	29.99	1.7%
L-Phe			2535	0.6%	25.55	1.7%
L-Ile			3137	0.6%	26.91	1.5%
D-Phe			144	6.3%	27.67	1.6%
L-Leu	25	18.1%	3670	0.5%	21.93	1.6%
D-alle			91.06	1.4%	28.41	1.7%
D-Leu			166	1.7%	22.69	1.7%
L-Lys (1°)			1224	1.7%	1.50	4.1%

Table 8.11: Precision data for repeat preparations of 5 standards, 5 FAA OES and 5 THAA OES samples. Areas reported are relative to the internal L-hArg standard.

8.3.3.10. Accuracy: Standard additions

No blank matrix is available due to the nature of the samples. Therefore, a standard addition technique was used to assess the effect of the matrix on the analytes' observed responses. An

FAA and a THAA solution of OES sample were spiked with known concentrations of standard mixture (25%, 50% and 75% v/v of sample to standard solution) and the observed responses compared with the calculated responses. Each sample was prepared in triplicate. The areas reported for this experiment are absolute areas, not relative to the internal standard. An effort was made to run all samples with OPA/IBLC solution of the same age to minimise the errors associated with absolute areas.

For an assay method the required accuracy may be as high as 100 % ±2 % (Green, 1996). It is observed that the majority of amino acids in this study have errors < 10% between calculated and observed concentrations (Table 8.12). Higher errors are seen for His, Gly and Thr, this is likely due to reduced resolution. D-Arg also shows higher error due to a co-eluting peak, which is also seen in other bio-minerals when using the HPLC method (e.g. Penkman, 2005). L-Lys also shows high variability, probably due to the instability of its OPA/IBLC derivative (Sec. 8.3.1.). Although these errors are higher than that required for an assay method, they are acceptable for this type of study.

There are a number of unidentified peaks within the chromatogram for the OES samples, including a peak eluting after L-Met (peak 21 in Fig. 8.12), causing some reduction in resolution (half width resolution to ~ 1). This peak does not appear to be present in OES samples analysed using the RP-HPLC method, and may therefore not be resolved from either the L-Met or L-Val peak using the original method.

It appears that the sample matrix does not significantly affect the observed responses of the analytes. Therefore, this study shows that the method is accurate for real samples, as well as standard samples.

Analyte	FAA			THAA		
	25% standard	50% standard	75% standard	25% standard	50% standard	75% standard
L-Asp	2%	2%	1%	2%	5%	2%
D-Asp	3%	2%	1%	4%	5%	2%
L-Glx	2%	3%	3%	2%	5%	2%
D-Glx	3%	2%	2%	4%	5%	2%
L-Ser	2%	3%	2%	2%	4%	1%
D-Ser	3%	2%	2%	4%	5%	2%
L-Thr	2%	3%	2%	2%	5%	2%
L-His	7%	10%	9%	12%	10%	6%
Gly	16%	7%	7%	4%	6%	5%
D-Thr	6%	5%	2%	3%	6%	2%
D-His	7%	9%	5%	9%	11%	7%
L-Arg	6%	7%	3%	2%	4%	2%
L-Ala	4%	2%	2%	2%	4%	2%
D-Arg	4%	6%	3%	14%	6%	2%
D-Ala	3%	2%	1%	4%	6%	3%
L-Tyr	5%	2%	3%	3%	5%	2%
D-Tyr	3%	3%	3%	3%	5%	2%
L-Val	5%	2%	2%	2%	5%	2%
L-Met	14%	4%	19%	7%	5%	3%
D-Met	7%	3%	18%	9%	4%	3%
D-Val	4%	6%	3%	3%	6%	2%
L-Phe	7%	3%	6%	3%	5%	4%
L-Ile	6%	4%	3%	2%	4%	2%
D-Phe	2%	3%	3%	4%	5%	2%
L-Leu	6%	3%	6%	2%	5%	4%
D-alle	4%	8%	5%	3%	7%	4%
D-Leu	6%	3%	6%	9%	7%	8%
L-Lys (1°)	31%	35%	6%	7%	7%	8%

Table 8.12: Relative standard deviations (%) between calculated concentrations and observed concentrations of OES FAA and THAA samples with 25%, 50% and 75% standard additions (v/v). Data presented are averages of triplicate samples

8.3.3.11. Specificity

A number of forced degradation OES samples and standard addition samples were analysed. Half width resolution was calculated for the standard addition samples and forced degradation OES

samples with baseline resolution considered > 1.5. Baseline resolution was present for all analytes in the standard addition study, and in the forced degradation with the exception of L-Met in the standard solution, which was degraded for 1440 m. This was due to the presence of additional peaks reducing the resolution.

A number of single amino acid standards and possible degradation products/contaminants, which were not included in the combined racemic standard solution, were also run. Comparison of the retention times to the peaks observed in OES samples (e.g. Fig. 8.11) allows us to tentatively identify possible sources of some unidentified peaks (Table 8.13). However, additional work needs to be carried out to positively identify whether these compounds are responsible for these peaks.

Possible peak identity	Position in chromatogram	Probable source
Diaminopimelic acid	Approximately the same retention as the unknown peak eluting after L-Met (peak 21, Fig. 8.8)	A derivative of Lys and is found in some bacterial cell walls, so may be an indication of a compromised sample (Ghuysen and Hakenbeck, 1994).
α-amino-n-butyric acid	Elutes between L- and D-Tyr (peaks 17 & 18 Fig. 8.8)	Formed from the dehydration of Thr (Bada et al., 1978)
y-amino-n-butyric acid	Elutes between D-Ala and L-Tyr (peaks 16 and 17, Fig. 8.8).	Formed from the decarboxylation of Glu (Bada, 1991)

Table 8.13: Degradation products possibly observed in OES samples

8.4. CONCLUSIONS

A modified RP-HPLC method (Penkman, 2005; 20 components and an internal standard, in 115 min total run time) based on the original method by Kaufman and Manley (1998), has been transferred to UHPLC. It has been optimised in order to resolve and characterise additional analytes and reduce the run time (Table 8.14). The UHPLC method can routinely separate 28 components (and an internal standard) in 60 min total run time. However, L-Lys should be treated with caution due to the instability of its isoindol derivative and its propensity for forming

two HPLC-peaks. The utility of the additional analytes, separated using UHPLC (Table 8.14), to AAR geochronology is open to debate. For example, Gly is a thermally stable amino acid (Vallentyne, 1964), therefore its concentration may be a useful variable when analysing very old sub-fossil samples. The rates of racemization of His, Thr and Tyr may also be useful in offering greater temporal resolution, however, an analysis of a suite of sub-fossil samples and artificially degraded modern samples would be required to ascertain how useful these analytes are to AAR geochronology.

The UHPLC method has been shown to be applicable for use with complex bio-mineral samples, such as OES, indicating that the matrix does not interfere with the specificity. This was tested through the use of standard additions (Sec. 8.4.2.9.), which has not been used in previous AAR RP-HPLC method validations.

A number of additional peaks observed in the OES samples, but not in the standard solution, have been tentatively identified using retention times (Sec. 8.4.2.10; Table 8.13). However, more work needs to be done in order to prove, i) the analyte's identity, e.g. through standard addition studies, and ii) the analyte's utility, if any, to AAR, e.g. through analysis of a suite of sub-fossil and heated modern OES samples. Asn and Gln were not included in the standard solution, as it is very unlikely either would be preserved within fossil samples (Hill, 1965), but single amino acid analysis show that they would be resolved, unlike the original HPLC method where Asn co-eluted with Ser and D-Gln co-eluted with L-Gln (Kaufman and Manley, 1998).

There is however still room for refinement. Inclusion of 9-fluorenylmethoxycarbonyl (FMOC) to the derivitising solution may allow characterisation of secondary amino acids such as Pro and hydroxyl-proline (e.g. Brückner *et al.*, 1991). A further reduction in analysis time may be achieved by using a phosphate buffered mobile phase (Sec. 8.3.1.1.), which showed great promise as an alternative to the sodium acetate buffered method. This method may also benefit from running at a higher pH which has been shown to stabilise the Lys/OPA/IBLC derivatives (Umagat *et al.*, 1982; Fitznar *et al.*, 1999). In addition, the run time for the sodium acetate method may be reduced further by increasing the column thermostat temperature. This was originally not increased as previous studies had suggested that this may result in reduced resolution (Fitznar *et al.,* 1999), and it was thought that higher temperatures may affect the stability of the derivatised analytes (Sec. 8.3.1.4.). However, the phosphate method was run at 40 °C without seemingly causing degradation of the analytes, therefore increasing column temperature may reduce analysis time of the sodium acetate method further.

	Kaufman and Manley (1998) HPLC	**Modified HPLC method (Penkman, 2005)**	**UHPLC**
Machine	Hewlett-Packard HP1100 HPLC	Agilent 1100 series HPLC	Agilent Rapid Res 1200 series UHPLC
Column	HyperSil BDS (5 µm, 250 x 4 mm)	HyperSil BDS (5 µm, 250 x 4 mm)	Agilent ZORBAX Eclipse Plus ^{18}C (1.8 µm, 100 x 4.6 mm)
Derivatisation	Fully automated injection programme. Amino acids derivatised using OPA/IBLC		
Detection	The fluorescence detector uses a Xenon-arc flash lamp at a frequency of 55 Hz, with a 280 nm cut-off filter and an excitation wavelength of 230 nm and emission wavelength of 445 nm		
Run time, including wash/equilibrium time	90 min	115 min	60 min
Components separated[#]	– L & D: Asx, Glx, Ser, Tyr, Arg, Ala, Val, Phe & Leu (D-Leu is unresolved in sub-fossil mollusc samples). – A & I Ile – Internal standard, L-hArg – L-Thr (not included in method validation)	– L & D: Asx, Glx, Ser, Arg, Ala, Val, Met, Phe & Leu (D-Leu is poorly resolved in sub-fossil OES samples; Sec 2.3.2.). – A & I Ile – L-hArg – L-Thr, L-Tyr & D-Tyr (not included in method validation)	– L & D: Asx, Glx, Ser, **Thr, His, Tyr**, Arg, Ala, Val, Met, Phe & **Leu**. – A & I Ile – **Gly** – L-hArg – Unvalidated amino acids: **L-Asn, D-Asn & L-Lys**
LOQ	~ 0.1 pmol	~ 0.1 – 0.7 pmol	
Linearity range	~ 20 – 170 pmol	~ 0.1 – 106 pmol	
Solvent details	Tertiary gradient: Sodium acetate buffer (pH 6.00), MeOH and ACN	Binary gradient: Sodium acetate buffer (pH 6.00) and MeOH/ACN (92.7:7.5 v/v)	
Minimum bio-mineral sample size	~ 1 µg for bivalves; ~0.6 µg for OES*		

*Table 8.14: Summary of original RP-HPLC methods and new UHPLC method. * Assumed that the sample size requirement would be similar for each method as LOQs are similar. [#]Analytes separated in UHPLC method and not the modified HPLC method (Penkman, 2005) are highlighted in **bold***

CHAPTER 9: CONCLUSIONS

9.1. OVERALL CONCLUSIONS

Previous studies have shown the utility of OES for AAR geochronology and suggested that its success may be due to its closed system behaviour with regard to protein degradation (Brooks *et al.*, 1990; Miller *et al.*, 2000). These studies did not use an oxidative pre-treatment to isolate a fraction of so called 'intra-crystalline' proteins, which in other bio-minerals has been shown to reduce variability (e.g. Towe and Thompson, 1972; Sykes *et al.*, 1995; Penkman *et al.*, 1998; Penkman *et al.*, 2011; Demarchi *et al.*, 2013a). This thesis has demonstrated that oxidative pre-treatment of OES for 72 h with 12 % (w/v) NaOCl isolates a fraction of proteins, operationally defined as the 'intra-crystalline fraction', through the removal of inter-crystalline and exogenous amino acids (of up to 50 % of the concentration) (Sec. 3.7.). Closed system behaviour of the intra-crystalline fraction was evidenced through high temperature studies at pH values of 4, 7 and 9, and at temperatures of 80 – 140 °C (Sec. 3.3.5.2.). These studies demonstrated that the intra-crystalline fraction was both resistant to leaching and unaffected by the pH environment, between pH 4 – 9. The intra-crystalline fraction leached < 1 % of its amino acids after 24 h heating at 140 °C, which is comparable to that of the 'stable amino acid fraction' reported by Brooks *et al.* (1990). In addition, the closed system behaviour of the intra-crystalline fraction has been demonstrated for sub-fossil samples up to at least 151 ka (Sec. 6.5.7.).

It was also observed that for modern samples heated in controlled environments, the trends in protein degradation are different for whole-shell and for intra-crystalline amino acids (3.3.6.). Indeed, bleach treatment reduces variability for a small number of sub-fossil samples, where uncertainty may be introduced through variable leaching rates, different ground water conditions and potentially exogenous contamination (Sec. 6.5.6.).

This thesis therefore indicates that OES approximates a closed system with regard to protein degradation. It is argued that the intra-crystalline fraction offers a sample where uncertainties introduced from the burial environment can be minimised. Furthermore, because the intra-crystalline degradation products are contained within an effectively-closed system, other degradation reactions (e.g. hydrolysis, decomposition and racemization of the FAA fraction) may all potentially be used for the purpose of amino acid geochronology.

Kinetic studies of the intra-crystalline fraction in OES show that Ile, Phe, Val, Ala, Asx, Glx and Ser give predictable trends of both hydrolysis and racemization, in both the FAA and THAA fractions,

and therefore show potential for estimating relative ages of OES samples from archaeological and geological contexts (Chapter 4).

The trends in degradation reactions at increased temperatures were compared to the observed trends in diagenetic reactions of sub-fossil samples, in order to assess the applicability of using high temperature kinetic studies to extrapolate to lower temperatures, over geological time spans. These comparisons showed that the relationships between competing and/or related degradation reactions is often complex, and that these reactions are dependent on the temperature a sample is exposed to. The principal source of FAA is through hydrolysis, therefore FAA concentrations were compared to THAA D/L values for samples heated at different temperatures. These comparisons suggest that the activation energies for hydrolysis were generally lower than for racemization reactions. As hydrolysis and racemization are intrinsically linked, this suggests using high temperature kinetic studies to extrapolate to low temperatures is flawed in this case, as the relative rates of racemization are unlikely to be equivalent at increased temperatures (Chapter 4; 5). Previously, it was suggested that similar trends of FAA A/I vs. THAA A/I at different temperatures in the *Dromaius* emu eggshell may provide some evidence that the activation energies for hydrolysis and epimerization of Ile were similar (Miller *et al.*, 2000). This study has shown that plots of FAA D/L vs. THAA D/L plots provide insufficient evidence to reach this conclusion for the intra-crystalline fraction of OES (Sec. 4.4.1.). High temperature studies still have an important role in helping to elucidate the trends in the diagenesis of proteins within bio-minerals, but caution should be taken as the relative rates of reaction may not be the same at all temperatures. The use of low-temperature data to constrain the observed rates is therefore necessary.

The epimerization of Ile in ratite eggshells has previously been shown to approximate reversible first order kinetics (RFOK) (Brooks *et al.*, 1990; Johnson *et al.*, 1997; Miller *et al.*, 1999, 2000). This can now be extended for the intra-crystalline fraction of OES to include Phe, Val and Ala (and epimerization of Ile), all of which have regions where they appear to follow RFOKa within limited DL ranges (Chapter 5). However, it is very unlikely that the amino acids within a bio-mineral truly follow RFOK (e.g. Wehmiller and Hare, 1971; Wehmiller, 1980; Mitterer and Kriausakul, 1989; Collins and Riley, 2000; Clarke and Murray-Wallace, 2006). Therefore, RFOK loses its chemical rationale, and is instead a mathematical transformation used to describe the data, in the same way the constrained power kinetic (CPK) transformation and the scaling method do.

Addition of low temperature data to the kinetic models generally caused an increase in the estimated activation energies, for both hydrolysis and racemization, for the majority of amino acids (Sec. 5.3.). The different methods of estimating activation energies often give different, and equally plausible, results. The differences observed highlight the problem of assigning activation

energies from a single observed overall rate constant without considering the underlying mechanisms and the contributing rate constants. It is therefore argued that in this case, activation energies calculated in this manner cannot be used to calculated accurate absolute sub-fossil ages. Therefore, a chronological framework for South Africa was built by AAR analysis of a suite of OES samples with calibration from independent dating methods (OSL and radiocarbon), up to 151 ka (6.5.7.). A sample of unknown age, from the same region as PP and EBC may therefore be given an approximate age.

OES is ubiquitous to archaeological sites in Africa and therefore may be useful to provide geochronological information for many sites. Unfortunately, human activity at archaeological sites results in many OES samples being exposed to anthropogenic fire, artificially increasing the extent of protein degradation. In these cases, it is likely a large number of OES samples would need to be analysed in order to identify the least-degraded samples. However, as OES AAR analysis is both relatively rapid and inexpensive, this does not pose a major problem. The exclusion of these artificially old samples from AAR age models will decrease the error associated with OES AAR. However, independent identification of heating markers would make the technique more robust. Through extensive artificial heating studies on modern OES samples, a checklist has been developed to identify samples exposed to high temperatures. It seems there is not a single key indicator for identifying heated samples, as these markers will vary depending on the degree of heating and the age of the sample. However, a series of 6 markers have been identified (Sec. 6.5.4.1.). It is prudent to use several markers so as to not remove samples of 'genuine' AAR age without just cause.

Using OES AAR, samples from MIS 1, 2, 3/4, 5 and 6 could be successfully differentiated. The utility of analysing several amino acids has also been demonstrated, e.g. faster racemizing amino acids, such as Asx, give better age resolution for younger samples (i.e. MIS 2 – 3). Slower racemizing amino acids, such as Ile, give better resolution for the older samples (e.g. between samples from MIS 5 and 6). It has been shown that OES AAR offers a useful additional relative dating technique for archaeological and palaeontological sites in Africa up to at least 151 ka (Sec. 6.5.7.). The upper limits of this technique were not tested in this study; samples of 151 ka showed Ile A/I values of ~ 0.6, i.e. ~half way to equilibrium. This therefore demonstrates the utility of OES AAR geochronology for South African samples far older than 151 ka.

A preliminary study using MALDI MS has shown the utility of using MS to observe the degradation of peptides within OES. Indeed, peptides from samples as old as ~ 71 ka could be characterised, this is believed to be the oldest example of protein extracted from eggshells (Chapter 7). In addition, it has been possible to identify potential sites of natural hydrolysis and deamidation in both modern heated and sub-fossil samples.

A new UHPLC method was developed and validated, allowing analysis in approximately half the time of the HPLC method used, and separating additional amino acids (Chapter 8). Due to difficulties in separation, these amino acid have not previously been available in AAR studies, and therefore may offer further insight into protein degradation within bio-minerals.

9.2. FUTURE WORK

The overall aims of this project were met (e.g. Sec. 1.4). However, this project raised interesting questions as to the true nature of the inter- and intra-crystalline fractions in bio-minerals, e.g. their location and their behaviour when heated (Sec. 9.2.2.). It is also clear that the progression of OES AAR requires analysis of older samples (Sec 9.2.1.), and further analysis in order to open the 'black box' of protein breakdown (Sec. 9.2.3.). The new UHPLC method was successful in reducing analysis time by 50 % and increasing the number of analytes, however there is still room for improvement (Sec. 9.2.4.).

9.2.1. Extending the chronological framework

This work has shown the potential for the limit of OES AAR in South Africa to extend well beyond 151 ka (the oldest samples analysed in this study). Therefore, older samples from other well stratified sites need to be analysed in order to extend the chronological framework beyond 151 ka, and to test the limits of OES AAR in South Africa.

9.2.2. The nature of the intra-crystalline fraction

Pre-heat and post-heat oxidative treatments do not isolate the same fraction of proteins in OES. This is in contrast to coral (Tomiak *et al.*, 2013) and some bivalve mollusc shells (*Margaritifera* and *Corbicula*; Penkman *et al.*, 2008). These observations raise interesting questions about the intra- and inter-crystalline fractions in OES, and how they differ from other bio-minerals. This could be investigated initially through an imaging study using samples exposed to varying amounts of heat and different oxidative treatments. For example, a study by Gries and colleagues (2009) used a combination of transmission electron microscopy, Z-contrast, electron tomography, energy-dispersive X-ray analysis and electron energy-loss spectroscopy to analyse voids in aragonite layers in mollusc shells. The study revealed the locations and estimations of the sizes of these voids, and crucially, in addition, they showed that these voids are likely to contain organic material. It would be very interesting to see whether this was also the case for OES, and whether any changes with heat and/or oxidative treatment could be observed. Further analysis of the organics would also be useful in order to identify for example whether melanoidin compounds

may be formed (Sec. 3.3.7.; Collins and Riley, 2000), which may explain the additional bleach resistant fraction created from heating whole-shell samples .

In a small study of whole-shell sub-fossil samples it was found that for the majority of sub-fossil samples oxidative pre-treatment made little difference to the AAR results, in respect to racemization and amino acid concentration (Sec. 6.5.6). It is presumed that this is the case because the majority of inter-crystalline amino acids have leached from the system by the time of sampling. However, a small number of sub-fossil samples showed significantly higher concentrations of amino acids in the whole-shell samples. To assess the statistical significance of oxidative pre-treatment on OES AAR results a larger study of whole-shell and pre-treated sub-fossil samples is required. In addition, analysis of sub-fossil OES samples from different sites, e.g. open air sites or sites with variable water conditions, may show whether oxidative treatment results in a reduction in AAR variability compared to whole-shell samples.

9.2.3. Opening the 'black box'

A significant step forward in the reliability of AAR geochronology was the realisation of a potentially closed system fraction of proteins provided by the intra-crystalline fraction. Limiting AAR analysis to this fraction has been shown to give more reliable dating information (Towe, 1980; Sykes *et al.*, 1995; Penkman *et al.*, 2008). However, the intra-crystalline fraction itself contains many different amino acid fractions which change in relative concentrations as degradation progresses. Unravelling the different trends of degradation in these fractions may increase the reliability of AAR dating further. Indeed, eventually it may even be possible to use activation energies of specific reactions to give accurate absolute dates and thermal histories simultaneously. However, significant work needs to be done before this point may be reached. Further work therefore should focus on increasing our understanding of protein degradation within bio-minerals and its relationship to temperature.

Initial steps have already been made in this respect, e.g. Chapter 7, where the potential of using MS for this application has been demonstrated. However, the method needs to be improved, such that more peptides are observed and characterized. In addition, on-going work within this group has included the study of simpler systems, e.g. model peptides (Demarchi, *et al.*, in press) and the isolated SCA-1 and SCA-2 proteins (Woodman, 2012).

In recent years there has been growing use of quantitative MS proteomic methods; this would be a logical progression. Most of these methods employ an isotopic tag, using the assumption that isomers will have the same size, charge, hydrophobicity and other physical properties, which would affect the peak intensity (e.g. Bantscheff *et al.*, 2007). Therefore, the relative peak

intensities can be quantitatively compared. The quantitative analysis of the protein degradation in bio-minerals would be a useful next step to this study. One suitable method could include iTRAQ (Isobaric Tags for Relative and Absolute Quantification), which works by introducing a different isobaric tag to the primary amine groups of up to 8 different samples. The samples are combined and then analysed and the relative heights of each peptide can be compared. However, only 8 samples can be compared at any one time, and the MS spectra are likely to be very complex due to the presence of multiple peptides. This kind of study would be labour intensive and expensive. However, it may offer an unrivalled insight into protein degradation within bio-minerals, and is necessary for the continued development of AAR dating.

9.2.4. Further UHPLC method development

The HPLC to UHPLC method transfer was successful in reducing analysis time and increasing the number of analytes (Chapter 8). The phosphate buffer method showed promise at reducing this analysis time by a further 50 %, therefore it would be worthwhile to complete this method development and validation. In addition, the sodium acetate buffer method may be improved by increasing the column temperature. This was originally not increased as previous studies had suggested that this may result in reduced resolution (Fitznar *et al.,* 1999), and it was thought that higher temperatures may affect the stability of the derivatised analytes (Sec. 8.3.1.4.). However, the phosphate method was run at 40 °C without seemingly causing degradation of the analytes, therefore increasing column temperature may reduce analysis time of the sodium acetate method further.

APPENDIX

Appendices are attached in electronic form on a CD.

Appendix A: Bleaching and leaching data
Appendix B: Kinetic experiments and calcs
Appendix C: Sub-fossil data and artificial heating identification
Appendix D: MS data

LIST OF ABBREVIATIONS

AA	Amino acid
AAR	Amino acid racemization
AC	Alternating current
α-CHCA	α-cyano-4-hydroxy-cinnamic acid
ACN	Acetonitrile
BDS	Base deactivated silicon
BSA	Bovine Serum Albumin
CD	Circular dichroism
CDA	chiral derivitising agent
CPK	Constrained power kinetic
DKP	diketopiperazines
D/L	D-amino acid / L-amino acid
EA	Activation energy
EBC	Elands Bay Cave
EDTA	Ethylenediaminetetraacetic acid
ESR	Electron spin resonance
ESI	Electron spray ionisation
FAA	Free amino acids
FAAw	Free amino acids in supernatant
FDA	Food and Drug Administration
FID	Flame ionisation detector
Fig.	Figure
FLD	Fluorescence detector
FMOC	9-fluorenyl-methyl chloroformate
FPD	Flame photometric detector
GC	Gas chromatography
HPLC	High pressure liquid chromatography
IBLC	*N*-iso-butyryl-L-cysteine
IFOK	Irreversible first order kinetics
IFOKa	Apparent irreversible first order kinetics
ILC	Ion exchange chromatography
ka	Thousand years old
k	Rate constant
LC	Liquid chromatography
LOD	Limit of detection
LOQ	Limit of quantification

Ma	Million years ago
MALDI	Matrix assisted laser desorption ionisation
MCP	Micro channel plate
MeOH	Methanol
MS	Mass spectrometry
MSA	Middle stone age
MIS	Marine isotope stage
m/z	Mass to charge ratio
NaAc	Sodium acetate
NPD	Nitrogen phosphorous detection
OES	Ostrich eggshell
OPA	*o*-phthaldialdehyde
OSL	Optically stimulated luminescence
PP	Pinnacle Point
RFOKa	Apparent reversible first order kinetics
RFOK	Reversible first order kinetics
RP-HPLC	Reverse phase HPLC
RSD	Relative standard deviation
R^2	Coefficient of determination
SCA-1	Struthiocalcin-1
SCA-2	Struthiocalcin-2
Sec.	Section
SEM	Scanning electron microscope
S/N	Signal to noise ratio
TFA	Trifluoroacetic acid
THAA	Total hydrolysable amino acids
THAAw	Total hydrolysable amino acids in supernatant
TL	Thermoluminescence
TOF	Time-of-flight
UHPLC	Ultra high pressure liquid chromatography
U-series	Uranium series dating
USP	U.S. Pharmacopeial Convention
UV	Ultra-violet
v/v	Volume/volume
w/v	Weight/volume
w/w	Weight/weight
XRD	X-ray diffraction
Yrs	Years old

REFERENCES

Abelson, P.H. 1954. Amino acids in fossils. *Science* 119, 576

Abelson, P.H. 1955. Organic constituents of fossils. *Carnegie Institute of Washington Year Book* 54, 107-9

Abeyratne, M., Spooner, N., Grün, R., Head, J. 1997. Multidating studies of Batadomba Cave, Sri Lanka. *Quaternary Science Reviews* 16:243-55

Adams, J.M., Faure, H. 1997. (eds.), QEN members. Review and atlas of palaeovegetation: Preliminary land ecosystem maps of the world since the Last Glacial Maximum. Oak Ridge National Laboratory, TN, USA. http://www.esd.ornl.gov/ern/qen/adams1.html

Addadi, L., Weiner, S. 1992. Control and design principles in biological mineralization. *Angewandte Chemie International Edition in English* 31, 153-169

Agilent application note, 2010. Improved amino acid methods using Agilent ZORBAX Eclipse Plus C18 columns for a variety of Agilent LC instrumentation and separation goals. 5990-4547EN_5989_5672.qxd

Aitken, M.J. 1985. Thermoluminescence dating. London: Academic press

Aitken, M.J. 1990. Science-based dating in archaeology. Longman Archaeology Series

Aitken, M.J. 1998. An introduction to optical dating. Oxford University Press, UK

Akiyama, M. 1980. Diagenetic decomposition of peptide linked serine residues in the fossil scallop shells. In *Biogeochemistry of amino acids*, ed. PE Hare, TC Hoering, K King. pp. 115 - 20. New York: Wiley

Ambrose, S. 1998. Chronology of the Later Stone Age and food production in East Africa. *Journal of Archaeological Science* 25 (4): 377–392.

Annesley, T.M. 2003. Ion suppression in mass spectrometry. *Clinical chemistry* 49(7): 1041-1044

Anslyn, E.V., Dougherty, D.A. 2005. Modern physical organic chemistry. University Science Books, U.S.

Anton, S. C. 2003. Natural history of Homo erectus. *American Journal of Physical Anthropology* S37, 126-70

Arias, J.L., Fink D.J., Xiao, S., Heuer, A.H., and Caplan, A.I. 1993. Biomineralization and eggshells: Cell-mediated acellular compartments of mineralized extracellular matrix. *Int. Rev. Cytol*. 145:217–250.

Bada, J.L. 1971. Non-equilibrium systems in natural water chemistry. *Advances in chemistry series* (Ed. Hem, J.D. & Gould, R.F.) American Chemical Society, Washington D.C. 106, 309

Bada, J.L. 1972a. The dating of fossil bones using the racemization of isoleucine. *Earth and Planetary Science* 15, 223

Bada, J.L. 1972b. Kinetics of racemization of amino acids as a function of pH. *Journal of the American Chemical Society* 94 (4): 1371–1373.

Bada, J.L., Schroeder, R.A. 1972. Racemization of isoleucine in calcareous marine sediments: Kinetics and mechanism. *Earth and Planetary Science Letters* 15: 1–11.

Bada, J.L., and Schroeder, R.A., 1975. Amino acid racemization reactions and their geochemical implications. Die Naturwissenschaften 62 (2): 71-79.

Bada, J.L., Shou, M.Y., Man, E.H., and Schroeder, R.A. 1978. Decomposition of hydroxy amino acids in foraminiferal tests: Kinetics, mechanism and geochronological implications. *Earth Planetary Science Letters* 41 (1): 67 – 76.

Bada, J.L., Man, E.H. 1980. Amino acid analysis in deep sea drilling project cores: Kinetics and mechanisms of some reactions and their applications in geochronology and in palaeotemperature and heat flow determinations. *Earth Science Reviews* 16:21-55

Bada, J.L. 1984. Racemization of Amino Acids. In *Chemistry and Biochemistry of the Amino Acids*, ed. H Slavkin, P Price, pp. 399 - 415. London.: Chapman & HallBurk and Stuivier (1981)

Bada, J.L. 1985. Racemization of Amino Acids. In *Chemistry and Biochemistry of the Amino Acids*, ed. GC Barrett, 399–414. Chapman & Hall.

Bada, J.L., Zhao, M.X., Steinberg, S., Ruth, E. 1986. Isoleucine stereoisomers on the Earth. *Nature* 319 (6051), 314-316

Bada, J.L., 1991. Amino-acid cosmogeochemistry*. Philosophical Transactions Of The Royal Society Of London Series B-biological Sciences* 333:349-58

Bailey, G. 2004. World Prehistory from the margins: The role of coastlines in human evolution. *Journal of Interdisciplinary Studies in History and Archaeology* 1(1) 39-50

Baker, J.R., Balch, D.A. 1962. A study of the organic material of hen's eggshell. *The Biochemical Journal* 82 (1956): 352–61.

Beardsley, R.L., Reilly, J.P. 2002. Optimization of guanidination procedures for MALDI mass mapping. *Analytical Chemistry* 74(8): 1884-1890

Berger, G.W. 1988. Dating Quaternary events by luminescence, in D.J. Easterbrook (ed.) *Dating Quaternary sediments.* Geochronological Society of America, Special paper 227: 13-50

Bhattacharyya, S.K., Banerjee, A.B. 1974. D-amino acids in the cell pool of bacteria. *Folia Microbiol.* 19: 43-50

Bird, M.I., Fifield, L.K., Santos, G.M., Beaumont, P.B., Zhou, Y., di Tada, M.L., Hausladen, P.A. 2003. Radiocarbon dating from 40 to 60 ka BP at Border Cave, South Africa. *Quaternary Science Reviews* 22:943-7

Blumenschine, R.J., Peters, C.R., Masao, F.T., Clarke, R.J., Deino, A.L., Hay, R.L., Swisher, C.C., Stanistreet, I.G., Ashley, G.M., McHenry, L.J., Sikes, N.E., Van Der Merwe, N.J., Tactikos, J.C., Cushing, A.E., Deocampo, D.M., Njau, J.K., Ebert, J.I. 2003. Late Pliocene Homo and hominid land use from Western Olduvai Gorge, Tanzania. *Science* 299, 1217-12121

Boaz, N.T. 1979. Hominid evolution in Eastern Africa during the Pliocene and Early Pleistocene. *Annual Review of Anthropology* 8: 71-85

Brennan, T.V., Clarke, S. 1993. Spontaneous degradation of polypeptides at aspartyl and asparaginyl residues: Effects of the solvent dielectric. *Protein Science : a Publication of the Protein Society* 2 (3): 331–8.

Bright, J., Kaufman, D.S. 2011a. Amino acid racemization in lacustrine ostracodes, Part I: Effect of oxidizing pre-treatments on amino acid composition. *Quaternary Geochronology* 6 (2): 154–173.

Bright, J., Kaufman, D.S. 2011b. Amino acids in lacustrine ostracodes, Part III: Effects of pH and taxonomy on racemization and leaching. *Quaternary Geochronology* 6 (6): 574–597.

Brinton, K., Bada, J.L. 1995. Comment on 'Aspartic Acid Racemization and Protein Diagenesis in Corals over the Last 350 Years' by G. A. Goodfriend, P. E. Hare, and E. R. M. Druffel. *Geochimica Et Cosmochimica Acta* 59 (2): 415–416.

Brooks, A.S, Hare, P.E., Kokis, J.E., Miller, G.H., Ernst, R.D., Wendorf, F. 1990. Dating Pleistocene archaeological sites by protein diagenesis in ostrich eggshell. *Science (New York, N.Y.)* 248 (4951): 60–4.

Brooks, A.S., Hare, P.E., Kokis, J.E., Durana, K. 1991. A burning question: differences between laboratory-induced and natural diagenesis in ostrich eggshell proteins. *Carnegie Institute of Washington Year Book*:176-9

Brown, F.H., Lajoie, K.R. 1971. Radiometric age determinations on Pliocene/Pleistocene formations in the Lower Omo Basin, southern Ethiopia. *Nature* 229: 483-85

Brown, K.S., Marean, C.W., Herries, A.I.R., Jacobs, Z., Tribolo, C., Braun, D., Roberts, D.L., Meyer, M.C., Bernatchez, J. 2009. Fire as an engineering tool of early modern humans. *Science (New York, N.Y.)* 325 (5942): 859–62.

Brown, K.S., Marean, C.W., Jacobs, Z., Schoville, B.J., Oestmo, S., Fisher, E.C., Bernatchez, J., Karkanas, P.,Matthews, T. 2012. An early and enduring advanced technology originating 71 ,000 years ago in South Africa. *Nature* 491 (7425): 590–593.

Brückner, H., Wittner, R., Godel, H. 1991. Fully Automated High-performance Liquid Chromatographic separation of DL-amino acids derivatized with o-phthaldialdehyde together with N-isobutyryl-cysteine. Application to food samples. *Chromatographia* 32 (7-8): 383–388.

Brückner, H., Haasmann, S., Langer, M., Westhauser, T., Wittner, R. 1994. Liquid chromatographic determination of D- and L-amino acids by derivatisation with *o*-phthaldialdehyde and chiral

thiols: Applications with reference to biosciences. *Journal of Chromatography A* 666(1-2): 259-273

Burk, R.L., Stuivier, M. 1981. Oxygen isotope ratios in trees reflect mean annual temperature and humidity. *Science*, 211, 1417 - 1419

Butzer, K.W., Fock, G.J., Scott, L., Stuckenrath, R., 1979. Dating and context of rock engravings in southern Africa. *Science* 203 (4386), 1201–1214

Campbell, M.K., Farrell S.O. 2011. Biochemistry, Ed. 7. Cengage Learning

Cann, R.L., Stoneking, M., Wilson, A.C. 1987. Mitochondrial DNA and human evolution. *Nature* 325: 31-36

Cappellini, E., Jensen, L.J., Szklarczyk, D., Ginolhac, A., da Fonseca, R.A., Stafford, T.W., Holen, S.R., Collins, M.J., Orlando, L., Willersley, E., Gilbert, M.T., Olsen, J.V. 2012. Proteomic analysis of a Pleistocene mammoth femur reveals more than one hundred ancient bone proteins. *Journal of Proteome Research* 11(2): 917-26.

Child, A.M., Gillard, R.D., Pollard, A.M. 1993 Microbially induced promotion of amino acid racemization in bone: isolation of the micro-organisms and detection of their enzymes. *Journal of Archaeological Science*, 20, 159-168.

Clarke, S.J. 2005. Isoleucine epimerisation and stable isotope ratio studies of cassowary, megapode and aepyornis eggshells: biogeochemical and palaeonenvironmental implications. PhD thesis, School of Earth and Environmental Sciences, University of Wollongong.

Clarke, S., Murray-Wallace, C.V. 2006. Mathematical expressions used in amino acid racemisation geochronology - A review. *Quaternary Geochronology* 1 (4): 261–278.

Clarke, S.J., Miller, G.H., Fogel, M.L., Chivas, A.R., Murray-Wallace, C.V. 2006. The amino acid and stable isotope biogeochemistry of elephant bird (*Aepyornis*) eggshells from Southern Madagascar. *Quaternary Science Reviews* 25 (17-18): 2343–2356.

Cohen, S.L., Chait, B.T. 1996. Influence of matrix solution conditions on the MALDI-MS analysis of peptides and proteins. *Analytical Chemistry* 68(1): 31–7.

Cohen, K.M., Gibbard, P. 2011. Global chronostratigraphical correlation table for the last 2.7 million years. Subcommission on Quaternary stratigraphy (International Commission on Stratigraphy), Cambridge, England.

Collins, M.J., Waite, E.R., van Duin, C. 1999. Predicting protein decomposition: The case of aspartic-acid racemization kinetics. *Philosophical Transactions of the Royal Society of London. Series B, Biological Sciences* 354(1379): 51–64.

Collins, M.J., Riley, M., 2000. Amino acid racemization in biominerals, the impact of protein degradation and loss. In *Perspectives in Amino Acid and Protein Geochemistry*, ed. Goodfriend, G.A., Collins, M.J., Fogel, M.L., Macko, S.A., Wehmiller, J.F., pp. 120-41. New York: Oxford University Press

Compton, J.S. 2011. Pleistocene Sea-level fluctuations and human evolution on the Southern Coastal Plain of South Africa. *Quaternary Science Reviews* 30 (5-6): 506–527.

Coplen, T.B. 1994. Reporting of stable hydrogen, carbon, and oxygen isotopic abundances (Technical report). *International Union of Pure and Applied Chemistry* 66(2) 273 - 276

Cotter, R.J., Griffith, W., Jelinek, C. 2007. Tandem time-of-flight (TOF/TOF) mass spectrometry and the curved-field reflectron. *Journal of Chromatography B* 855(1): 2-13

Cramers, C. A., Rijks, J. A., & Schutjes, C. P. M. (1981). Factors determining flow rate in chromatographic columns. *Chromatographia*, *14*(7), 439-444.

Crisp, M., Demarchi, B., Collins, M., Morgan-Williams, M., Pilgrim, E., Penkman, K. 2012. Isolation of the intra-crystalline proteins and kinetic studies in *Struthio Camelus* (ostrich) eggshell for amino acid geochronology. *Quaternary Geochronology* 16: 110-128

Davis, J.O., 1978. Quaternary Tephrochronology of the Lake Lahontan area, Nevada and California. Nevada Archaeological Survey Paper 7. University of Nevada, Reno, NV, 137

Dawson, R. M. C., Elliot, D. C., Elliot, W. H., Jones, K. M. 1986. Data for biochemical research. 3rd ed., Oxford Science Publ.

de Hoffmann, E., Stroobant, V. 2007. Mass Spectrometry: Principles and applications. 3rd edition. John Willey and Sons, UK.

Deacon, H.J. 1978. Changing patterns in the late Pleistocene/early Holocene prehistory of southern Africa as seen from the Nelson Bay Cave stone artefact sequence. *Quaternary Research*, *10*(1), 84-111.

Deacon, H.J, Deacon, J. 1999. Human beginnings in South Africa: Uncovering the secrets of the stone age. Rowman Altamira. 214pp

DeGiorgio, M., Jakobsson, M. and Rosenberg, N., 2009. Explaining worldwide patterns of human genetic variation using a coalescent-based serial founder model of migration outward from Africa. *PNAS* 106 (38) 16057 – 16062

Demarchi, B., Williams, M.G., Milner, N., Russell, N., Bailey, G., Penkman, K. 2011. Amino acid racemization dating of marine shells: A mound of possibilities. *Quaternary International : the Journal of the International Union for Quaternary Research* 239 (1-2): 114–124

Demarchi, B., 2009. Geochronology of coastal prehistoric environments : a new closed system approach using amino acid racemization. PhD Thesis, Department of Archaeology, University of York, York, UK.

Demarchi, B., Rogers, K., Fa, D.A., Finlayson, C.J., Milner, N., Penkman, K.E.H., 2013a, Intra-crystallline protein diagenesis (IcPD) in *Patella vulgata,* Part I: Isolation and testing of the closed system. Quaternary Geochronology; 16: 144-157

Demarchi, B., Collins, M.J., Tomiak, P.J., Davies, B.J., Penkman, K.E.H., 2013b, Intra-crystalline protein diagenesis (IcPD) in Patella vulgate. Part II: Breakdown and temperature sensitivity. Quaternary Geochronology. 16: 158-172

Demarchi, B., Collins, M., Bergström, E., Dowle, A., Penkman, K., Thomas-Oates, J., Wilson, J. In press. New experimental evidence for in-chain amino acid racemization of serine in a model peptide. *Analytical Chemistry* doi: 10.1021/ac4005869

D'Errico, F., Stringer, C.B. 2011. Evolution, revolution or saltation scenario for the emergence of modern cultures? *Philosophical Transactions of the Royal Society of London. Series B, Biological Sciences* 366(1567) 1060-1069

Dlamini, T.C., Hayne, R.J., 2004 Influence of agricultural land use on the size and composition of earthworm communities in northern KwaZulu-Natal, South Africa. *Applied Soil Ecology* 27: 77–88

Duller, G.A.T. 2004. Luminescence dating of Quaternary sediments: recent advances. *Journal of Quaternary Science* 19: 183-92

Duller, G.A.T. 2008a. Luminescence Dating: guidelines on using luminescence dating in archaeology. Swindon: English Heritage

Duller, G.A.T. 2008b. Single-grain optical dating of Quaternary sediments: why aliquot size matters in luminescence dating. *Boreas* 37: 589-612

Duller, G.A.T., Wintle, A.G. 2012. A review of the thermally transferred optically stimulated luminescence signal from quartz for dating sediments. *Quaternary Geochronology* 7: 6-20

Eby, G.N., 2004. Principles of environmental geochemistry. Brooks/Cole- Thomson Learning, Pacific Grove, CA, 514 pp.

Eggins, S.M., Grün, R., McCulloch, M.T., Pike, A.W.G., Chappell, J., Kinsley, L., Mortimer, G. 2005. In situ U-series dating by laser-ablation multi-collector ICPMS: New prospects for Quaternary geochronology. *Quaternary Science Reviews* 24 (23-24): 2523–2538.

El-Aneed, A., Cohen, A., Banoub, J. 2009. Mass spectrometry, review of the basics: Electronspray, MALDI, and commonly used mass analyzers. *Applied Spectroscopy Reviews* 44(3): 210-230

Emiliani, C. 1955. Pleistocene temperatures. *Journal of Geology* 63:585-99

Emiliani, C. 1966. Palaeotemperature analysis of Caribbean cores P 6304-8 and P 6304-9 and a generalised temperature curve for the last 425,000 years. *Journal of Geology* 74:109-26

Engel, M.H., Hare, P.E., 1985, Gas liquid chromatographic separation of amino acids and their derivatives, in Garrett, G.C.,ed. Chemistry and Biochemistry of Amino Acids: London/New York, Chapman and Hall, p. 462-479

Engel, M.H., Goodfriend, G.A., Qian, Y.R., Macko, S.A., 1994. Indigeneity of organic-matter in fossils-a test using stable-isotopes analysis of amino-acid enantiomers in Quaternary mollusc

shells. *Proceedings of the National Academy of Sciences of the United States of America.* 91, 10475-10478

Eto, S., Yamaguchi, M., Bounoshita, M., Mizukoshi, T., Miyano, H. 2011. High-throughput comprehensive analysis of d-and l-amino acids using ultra-high performance liquid chromatography with a circular dichroism (CD) detector and its application to food samples. *Journal of Chromatography B*, *879*(29): 3317-3325.

Falini, G., Weiner, S., Addadi, L., 2003. Chitin-silk fibroin interactions: Relevance to calcium carbonate formation in invertebrates. *Calcified Tissue International* 72, 548–554

FDA, Reviewer Guidance, Validation of Chromatographic Methods, Nov 1994, CMC3

Feng, Q.L., Zhu, X., Li, H.D., Kim, T.N. 2001. Crystal orientation regulation in ostrich eggshells. *Journal of Crystal Growth* 233: 548–554.

Fenn, J. B., Mann, M., Meng, C. K., Wong, S. F., Whitehouse, C. M. 1989. Electrospray ionization for mass spectrometry of large biomolecules. *Science* 246(4926): 64–71.

Fitznar, H.P., Lobbes, J.M., Kattner, G. 1999. Determination of enantiomeric amino acids with high-performance liquid chromatography and pre-column derivatisation with o-phthaldialdehyde and N-isobutyrylcysteine in seawater and fossil samples (mollusks). *Journal of Chromatography A* 832(1-2): 123-132

Frank, H., Nicholson, G. J., and Bayer, E., 1977. Rapid gas chromatographic separation of amino acid enantiomers with a novel chiral stationary phase. *Journal of Chromatographic Science*, 15, 174-176

Frank, H., Woiwode, W., Nicholson, G., Bayer, E. 1981. Determination of the Rate of Acidic Catalyzed Racemization of Protein Amino Acids. *Liebigs Annalen Der Chemie* 1981 (3): 354–365.

Friedman, M., Liardon, R., 1985. Racemization kinetics of amino acid residues in alkali-treated soybean proteins. Journal of Agricultural and Food Chemistry 33, 666-672.

Gascoyne, M., Schwarcz, H., Ford, D. 1983. Uranium-Series Ages of Speleothem from Northwest England: Correlation with Quaternary Climate. *Philosophical Transactions of the Royal Society of London. Series B, Biological Sciences* 301:143-64

Gebauer, D., Völkel, A., Cölfen, H. 2008. Prenucleation calcium carbonate clusters. *Science (New York, N.Y.)* 322 (5909): 1819–22.

Geiger, T., Clarke, S. 1987. Deamidation, isomerization, and racemization at Asparaginyl and Aspartyl residues in peptides. *The Journal of Biological Chemistry* 262(2): 785-794

Gibbard, P.L., Head, M.J., Walker, M.J.C. 2010. Formal ratification of the Quaternary System / Period and the Pleistocene Series / Epoch with a Base at 2 .58 Ma. *Journal of Quaternary Science* 25(2): 96–102.

Ghuysen, J-M., Hakenbeck, R. 1994. New comprehensive Biochemistry, Vol 27: Bacterial Cell Wall. Elsevier. Pp 581

Gil-Av, E., Tishbee, A., Hare, P.E., 1980. Resolution of underivatized amino acids by Reverse-Phase-Chromatography. *Journal of the American Chemical Society* 102(15): 5115-5117

Goodfriend, G., Hare, P., Druffel, E. 1992. Aspartic acid racemization and protein diagenesis in corals over the Last 350 Years. *Geochimica Et Cosmochimica Acta* 56 (10): 3847–3850.

Green, J.M. 1996. A practical guide to analytical method validation. *Analytical Chemistry* 68(9): 305A-309A

Grossman, E.L., Ku, T.L., Oxygen and carbon isotope fractionation in biogenic aragonite: Temperature effects, *Chemical Geology: Isotope Geoscience section*, 59:59-74

Gries, K., Kroger, R., Kubel, C., Fritz, M., Rosenauer, A. 2003. Investigations of voids in the aragonite platelets of nacre. *Acta Biomaterialia* 5: 3038-3044.

Griffiths, W.J, Jonsson, A.P., Liu, S., Rai, D.K., Wang, Y. 2001. Electrospray and tandem mass spectrometry in biochemistry. *The Biochemical Journal* 355(3): 545–61.

Grün, R. 1989. Electron spin resonance (ESR) dating. *Quaternary International* 1: 65-109.

Grün, R. 1993. Electron spin resonance dating in palaeoanthropology. *Evolutionary Anthropology: Issues, News, and Reviews* 2:172-81.

Grün, R., Beaumont, P. 2001. Border Cave Revisited: a Revised ESR chronology. *Journal of Human Evolution* 40 (6): 467–82.

Godwin, H. 1962. Half-life of radiocarbon. *Nature* 195: 984-984

Goodfriend, G.A. 1987. Evaluation of amino-acid racemization/epimerization dating using radiocarbon-dated fossil land snails. *Geology* 15: 698-700

Goodfriend, G.A., 1991. Patterns of racemization and epimerization of amino-acids in land snail shells over the course of the Holocene. *Geochimica et Cosmochimica Acta* 55:293-302

Goodfriend, G.A., Meyer, V.R., 1991. A comparative study of the kinetics of amino acid racemization /epimerization in fossil and modern mollusk shells. *Geochimica et Cosmochimica Acta* 55 (11): 3355-3367

Goodfriend, G.A., Hare, P.E. 1995. Reply to comment by K.L.F. Brinton and J. L. Bada on Aspartic acid racemization and protein diagenesis in corals over the last 350 years. *Geochimica et Cosmochimica Acta* 59:417-8

Guillarme, D., Nguyen, D. T. T., Rudaz, S., & Veuthey, J. L. (2007). Method transfer for fast liquid chromatography in pharmaceutical analysis: application to short columns packed with small particle. Part I: isocratic separation. *European journal of pharmaceutics and biopharmaceutics*, *66*(3), 475-482

Guillarme, D., Nguyen, D. T., Rudaz, S., & Veuthey, J. L. (2008). Method transfer for fast liquid chromatography in pharmaceutical analysis: Application to short columns packed with

small particle. Part II: Gradient experiments. *European Journal of Pharmaceutics and Biopharmaceutics*, *68*(2), 430-440.

Hare, P.E., Mitterer, R.M. 1967. Non-protein amino acids in fossil shells. *Yearbook of the Carnegie Institute of Washington* 73: 576–581.

Hare, P.E., 1969 Geochemistry of proteins, peptides, and amino acids. *Organic Geochemistry* (Eds Eglinton, G. and Murphy, M.T.J.), Springer- Verlag, Berlin 438-463

Hare, P.E., Mitterer, R.M. 1969. Laboratory simulation of amino acid diagenesis in fossils. *Carnegie Institute Washington Year Book* 67: 205 – 208.

Hare, P.E., 1971. Effect of hydrolysis on the racemization rate of amino acids. *Carnegie Institute of Washington Yearboo*k 70:256-8

Hare, P.E. 1974. Amino acid dating of bone - the influence of water. *Carnegie Institute of Washington Year Book* 73:576-81

Hare, P.E., Gil-Av, E. 1979. Separation of D and L amino acids by liquid chromatography: use of chiral eluants. *Science* 204, 1226-1228

Hare, P.E., St John, P.A., Engel, M.H. 1985. Ion-exchange separation of amino acids. *Chemistry and Biochemistry of the Amino Acids* (Ed. Barrett, G.C.), Chapman and Hall, London 415-425

Hays, J.D., Imbrie, J., Shackleton, N.J. 1976. Variations in the Earth's Orbit: Pacemaker of the Ice Ages. *Science* 194:1121-32

Head, M.J., Gibbard, P.L., Salvador, A. 2008. The Quaternary: its character and definition. Episodes 31: 234–238.

Hendy, E.J., Tomiak, P.J., Collins, M.J., Hellstrom, J., Tudhope, A.W., Lough, J.M., Penkman, K.E.H., 2012. Assessing amino acid racemization variability in coral intra-crystalline protein for geochronological applications. *Geochimica et Cosmochimica Acta*, 86, 338-353

Henning, G.R., Grün, R. 1983. ESR dating in Quaternary geology. *Quaternary Science Reviews* 2(2-3): 157-238

Henshilwood, C. S., Sealy, J. C., Yates, R., Cruz-Uribe, K., Goldberg, P., Grine, F. E., Watts, I. 2001. Blombos Cave, southern Cape, South Africa: preliminary report on the 1992–1999 excavations of the Middle Stone Age levels. *Journal of Archaeological Science*, *28*(4), 421-448.

Henshilwood, C., d'Errico, F., Vanhaeren, M., van Niekerk, K., Jacobs, Z. 2004. Middle Stone Age shell beads from South Africa. *Science (New York, N.Y.)* 304 (5669): 404.

Henshilwood, C.S., d'Errico, F., Yates, R., Jacobs, Z., Tribolo, C., Duller, G.A.T. , Mercier, N. 2002. Emergence of modern human behaviour: Middle Stone Age engravings from South Africa. *Science (New York, N.Y.)* 295 (5558): 1278–80.

Henshilwood, C.S., Marean, C.W. 2003. The origin of modern human behaviour. *Current Anthropology* 44 (5): 627–51.

Henzel, W.J., Billeci, T.M., Stults, J.T., Wong, S.C., Grimley, C., Watanabe, C. 1993. Identifying proteins from two-dimensional gels by molecular mass searching of peptide fragments in protein sequence databases. *Proceedings of the National Academy of Sciences of the United States of America* 90(11): 5011–5.

Heredia, A. 2005. Microstructure and thermal change of texture of calcite crystals in ostrich eggshell *Struthio Camelus*. *Materials Science and Engineering: C* 25 (1): 1–9.

Hilgen F. 1991. Astronomical calibration of Gauss to Matuyama sapropels in the Mediterranean and implication for the Geomagnetic Polarity Time Scale. *Earth and Planetary Science Letters* 104:226-44

Hill, R.L., 1965. Hydrolysis of proteins. *Advances in Protein Chemistry* 20:37-107

Hincke, M.T., Nys, Y., Gautron, H. 2010. The role of matrix proteins in eggshell formation. *Journal of Poultry Science* 47:208-219

Hincke, M.T., Tsang, C.P.W., Courtney, M., Hill, V. and Narbaitz, R., 1995. Purification and immunochemistry of a soluble matrix protein of chicken eggshell (ovocleidin-17). *Calcif. Tiss. Intl.* 56 578-583

Hoang, C.T., Taviani, M. 1991. Stratigraphic and tectonic implications of uranium-series- dated coral reefs from uplifted Red Sea islands. *Quaternary Research* 35(2): 264-273

Hoering, T.C., 1980. The organic constituent of fossil mollusc shells. In: *Biogeochemistry of amino acids.* eds. Hare, P. E., Hoering, T. C., King, K. J., Wiley, New York, pp. 193-201

Huntley, D.J., Godfrey-Smith, D.I., Thewalt, M.L.W. 1985. Optical dating of sediments. *Nature* 313:105-107

Ilisz, I., Berkecz, R., Peter, A. 2008. Application of chiral derivatizing agents in the high-performance liquid chromatographic separation of amino acid enantiomers: A review. *Journal of Pharmaceutical and Biomedical Analysis* 47(1): 1-15

Imbrie, J., Hays, J.D., Martinson, D.G., McIntyre, A., Mix, A.C. 1984. The orbital theory of Pleistocene climate: support from a revised chronology of the marine δ18 O record. Milankovitch and Climate: Understanding the Response to Astronomical Forcing, *Proceedings of the NATO Advanced Research Workshop* Palisades, NY: Dordrecht: D. Reidel Publishing

Imbrie, J., Boyle, E.A., Clemens, S.C., Duffy, A., Howard, W.R., Kukla, G., Kutzbach, J., Martinson, D.G., McNtyre, A., Mix, A.C., Molfino, B., Morley, J.J., Peterson, L.C., Pisias, N.G., Prell, W.L., Raymo, M.E., Shackleton, N.J., Toggweiler, J.R. 1992 On the structure and origin of major glaciation cycles 1. Linear responses to Milankovitch forcing. *Paleoceanography* 7, 701-738

Ingalls, A.E., Lee, C., Druffel, E.R.M. 2003. Preservation of organic matter in mound-forming coral skeletons. *Geochimica Et Cosmochimica Acta* 67 (15): 2827–2841.

Jacobs, Z., Duller, G.A.T., Wintle, A.G., Henshilwood, C.S. 2006. Extending the chronology of deposits at Blombos Cave, South Africa, back to 140 ka using opticaldating of single and multiple grains of quartz. *Journal of Human Evolution* 51: 255-273

Jacobs, Z., Roberts, R.G., Lachlan, T.J., Karkanas, P., Marean, C.W., Roberts, D.L. 2011. Development of the SAR TT-OSL Procedure for dating Middle Pleistocene dune and shallow marine deposits along the Southern Cape Coast of South Africa. *Quaternary Geochronology* 6 (5): 491–513.

Jacobs, Z., Hayes, E.H., Roberts, R.G., Galbraith, R.F., Henshilwood, C.S. 2013. An improved OSL chronology for the Still Bay Layers at Blombos Cave, South Africa: Further tests of single-grain dating procedures and a re-evaluation of the timing of the Still Bay Industryacross Southern Africa. *Journal of Archaeological Science* 40 (1): 579–594.

James, P., Quadroni, M., Carafoli, E., Gonnet, G. 1994. Protein identification in DNA databases by peptide mass fingerprinting. *Protein Science* 3(8): 1347-1350

Janz, L., Elston, R.G., Burr, G.S. 2009. Dating North Asian surface assemblages with ostrich eggshell: Implications for paleoecology and extirpation. *Journal of Archaeological Science* 36 (9): 1982–1989.

Jarvis, M.J.F., Jarvis, C., Keffen, R.H. 1985. Breeding seasons and laying patterns of the southern African Ostrich *Struthio camelus*. *Ibis* 127(4): 442–449

Johnson, B.J., Miller, G.F., Fogel, M.L., Beaumont, P.B. 1997. The determination of Late Quaternary paleoenvironments at Equus Cave, South Africa, using stable isotopes and amino acid racemization in ostrich eggshell. *Palaeogeography, Palaeoclimatology, Palaeoecology* 136 (1-4): 121–137.

Jouzel, J., Alley, R.B., Cuffey, K.M., Dansgaard, W., Grootes, P., Hoffman, G., Koster, R.D., Peel, D., Shuman, M., Stievenard, M., Stuiver, M., White, J. 1997. Validity of the temperature reconstruction from water isotopes in ice cores. *Journal of Geophysical Research* 102 (C12): 26471 – 26487.

Kandel, A.W. 2004. Modification of ostrich eggs by carnivores and its bearing on the interpretation of archaeological and paleontological finds. *Journal of Archaeological Science* 31 (4): 377–391.

Kandel, A.W., Conrad, N.J., 2005. Production sequences of ostrich eggshell beads and settlement dynamics in the Geelbek Dunes of the Western Cape, South Africa. *Journal of Archaeological Science* 32: 1711–1721

Karkanas, P., Bar-Yosef, O., Goldberg, P., Weiner, S. 2000. Diagenesis in prehistoric caves: the use of minerals that form *in situ* to assess the completeness of the archaeological record. *Journal of Archaeological Science* 27(10): 915-929

Kaufman, D.S., Miller, G.H. 1992. Overview of amino acid geochronology. *Comparative Biochemistry and Physiology Part B: Comparative Biochemistry* 102(2): 199-204

Kaufman, D.S., Manley, W.F. 1998. A new procedure for determining DL amino acid ratios in fossils using reverse phase liquid chromatography. *Quaternary Science Reviews* 17 (11): 987–1000.

Kaufman, D.S., Miller, G.H. 1995. Isoleucine epimerization and amino acid composition in molecular-weight separations of pleistocene genyornis eggshell. *Geochimica Et Cosmochimica Acta* 59: 2757–2765.

Kaufman, D.S., 2000. Amino acid racemization in ostracodes. In *Perspectives in Amino Acid and Protein Geochemistry,* ed. Goodfriend, G.A., Collins, M.J.,Fogel, M.L., Macko, S.A., Wehmiller, J.F. pp. 145-60. New York: Oxford University Press

Kaufman, D.S., 2006. Temperature sensitivity of aspartic and glutamic acid racemization in the foraminifera *Pulleniatina*. *Quaternary Geochronology* 1 (3), 188-207

Kimbel, W.H., Johanson, D.C., Rak, Y. 1997. Systematic assessment of a maxilla of Homo from Hadar, Ethiopia. *American Journal of Physical Anthropology* 103: 235-262

Kimber, R.W.L., Griffin, C.V. 1987. Further evidence of the complexity of the racemization process in fossil shells with implications for amino acid racemization dating. *Geochimica et Cosmochimica Acta*, 51: 839-846

King, R., Bonfiglio, R., Fernandez-metzler, C., Miller-stein, C., Olah, T. 2000. Mechanistic investigation of ionization suppression in electrospray ionization. *Journal Am. Soc. Mass Spectrom* 11: 943-950

Klein, R.G. 1995. Anatomy, behaviour, and modern human origins. *Journal of World Prehistory* 9 (2) (June): 167–198.

Kriausakul, N., Mitterer, R.M. 1978. Isoleucine epimerization in peptides and proteins: kinetic factors and application to fossil proteins. *Science* 201 (4360): 1011–1014.

Kriausakul, N., Mitterer, R.M. 1980a. Comparison of isoleucine epimerization in a model dipeptide and fossil protein. *Geochimica Et Cosmochimica Acta* 44 (5): 753–758.

Kriausakul, N., Mitterer, R.M. 1980b. Some factors affecting the epimerization of isoleucine in peptides and proteins. In *Biogeochemistry of Amino Acids*, ed. P E Hare, T C Hoering, and K King JR, 283 296. Wiley, New York.

Kriausakul, N., Mitterer, R.M.1983. Epimerization of COOH-terminal isoleucine in fossil dipeptides. *Geochimica et Cosmochimica Acta* 47, 963-966

Kromer, B., Spurk, M. 1998. Revision and tentative extension of the tree-ring based ^{14}C calibration, 9200 – 11 855 cal BP. *Radiocarbon* 40: 1117-1125

Kulla, E., Zuman, P. 2008. Reactions of orthophthaladehyde with ammonia and 2-aminoethanol. *Organic and Biomolecular Chemistry*. 6: 3771-3780

Kvenvolden, K.A., Peterson, E., Wehmiller, J.F., Hare, P.E. 1973. Racemization of amino acids in marine sediments by gas chromatography. *Geochimica et Cosmochimica Acta* 37 (10): 2215-2225

Lahr, M.M., Foley, R. 1994. Multiple dispersals and modern human origins. *Evolutionary Anthropology* 3: 48-60

Laidler, K.J. 1984. The development of the Arrhenius equation. *Journal of Chemical Education* 61, 494-498

Lajoie, K.R., Wehmiller, J.F., Kennedy, G.L., 1980. Inter- and intra-generic trends in apparent racemization kinetics of amino acids in Quaternary mollusks. In *Biogeochemistry of amino acids*, ed. PE Hare, TC Hoering, KJ King, pp. 305- 40. New York: Wiley

Lakshminarayanan, R., Kini, R.M., and Valiyaveettil, S., 2002. Investigation of the role of ansocalcin in the biomineralization in goose eggshell matrix. *Proc. Natl. Acad. Sci. U. S. A.*, 99: 5155–5159

Lakshminarayanan, R., Valiyaveettil, S., Rao, V.S., and Kini, K.M. 2003. Purification, characterization, and in vitro mineralization studies of a novel goose eggshell matrix protein, ansocalcin. *Journal of Biological Chemistry* 278: 2928–2936

Lammie, D., Bain, M.M., Wess, T.J. 2005. Microfocus X-ray scattering investigations of eggshell nanostructure. *Journal of Synchrotron Radiation* 12: 721-726

Leakey, L.S.B., Tobias, P.V., Napier, J.R., 1964. A new species of the genus Homo from Olduvai Gorge. *Nature* 202, 7-9.

Leakey, M.D., Hay, R.L., Curtis, G.H., Drake, R.E., Jackes, M.K., White, T.D. 1976. Fossil hominids from the Laetoli Beds. *Nature* 262:460-6

Leffingwell 2003. Chirality and Bioactivity I: Pharmacology. *Leffingwell Reports* 3(1) 1-27

Lewin, R., Foley, R. 2003. Principles of human evolution. 2nd ed., Oxford Blackwell Pub. Co.

Li, B., Borchardt, R.T., Topp, R.M., VanderVelde, D., Schowen, R.L. 2003. Racemization of an asparagine residue during peptide deamidation. *Journal of the American Chemical Society* 125 (38): 11486–7.

Lian, O.B., Roberts, R.G. 2006. Dating the Quaternary: progress in luminescence dating of sediments. *Quaternary Science Reviews* 25:2449-68

Liardony, R., Jost, R. 1981. Racemization of free and protein-bound amino acids in strong mineral acid. *International Journal of Peptide and Protein Research* 18(5): 500-505

Liardon, R., Ledermann, S. 1986. Racemization kinetics of free and protein-bound amino acids under moderate alkaline treatment. *Journal of Agricultural and Food Chemistry* 34 (3): 557–565.

Libby, W.F. 1955. Radiocarbon dating. Chicago: University of Chicago Press

Lombard, M. 2005. The Howiesons Poort of South Africa: what we know, what we think we know, what we need to know. *Southern African Humanities*, *17*, 33-55.

Lowe, J.J., Walker, M.J.C. 1997. Reconstructing Quaternary environments. Harlow: Addison Wesley Longman. pp.446

Madsen, A.T., Murray, A.S. 2009. Optically stimulated luminescence dating of young sediments: A review. *Geomorphology* 109: 3-16

Maillard, L.C. 1912. Action of amino acids on sugars. Formation of melanoidins in a methodical way. *Compt. Rend.* 154: 66

Manley, W.F., Miller, G.H., Czywczynski, J., 2000. Kinetics of aspartic acid racemization in *Mya* and *Hiatella*: modelling age and paleotemperature of high-latitude quaternary molluscs. In *Perspectives in Amino Acid and Protein Geochemistry*, ed. GA Goodfriend, MJ Collins, ML Fogel, SA Macko, JF Wehmiller, pp. 120-41. N.Y.: Oxford University Press

Mann, K., Siedler, F., 1999. The amino acid sequence of ovocleidin-17, a major protein of the avian eggshell calcified layer. *Biochem. Mol. Biol. Int.,* 47, 997–1007.

Mann, K., Seidler, F. 2004. Ostrich (*Struthio Camelus*) eggshell matrix contains two different C-type lectin-like proteins. Isolation, amino acid sequence, and post-translational modifications. *Biochimica Et Biophysica Acta (BBA) - Proteins & Proteomics* 1696 (1): 41–50.

Marean, C.W., Nilssen, P. J., Brown, K., Jerardino, A., Stynder, D. 2004. Paleoanthropological investigations of Middle Stone Age sites at Pinnacle Point, Mossel Bay (South Africa): archaeology and hominid remains from the 2000 field season. *Palaeoanthropology*, *2*, 14-83.

Marean, C.W. 2010. Pinnacle Point Cave 13B (Western Cape Province, South Africa) in context: The Cape Floral Kingdom, Shellfish, and Modern Human Origins. *Journal of Human Evolution* 59 (3-4): 425–43.

Marean, C.W, Bar-Matthews, M., Bernatchez, J., Fisher, E., Goldberg, P., Herries, A.I.R., Jacobs, Z. 2007. Early human use of marine resources and pigment in South Africa during the Middle Pleistocene. *Nature* 449 (7164) (October 18): 905–8.

Marean, C.W., Bar-Matthews, M., Fisher, E., Goldberg, P., Herries, A., Karkanas, P., Nilssen, P.J., Thompson, E. 2010. The stratigraphy of the Middle Stone Age sediments at Pinnacle Point Cave 13B (Mossel Bay, Western Cape Province, South Africa). *Journal of Human Evolution* 59 (3-4): 234–55.

Marin, F., Luquet, G. 2005. Molluscan biomineralization: The proteinaceous shell constituents of *Pinna nobilis* L. *Materials Science and Engineering C* 25 (2): 105–111.

Marin, F., Luquet, G., Marie, B., Medakovic, D., 2007. Molluscan shell proteins: primary structure, origin and evolution. *Current topics in developmental biology* 80:209-76

Mason, S.F. 1991. Prebiotic sources of bimolecular handedness. *Chirality* 3: 223-226

Matsuo, H., Kawazoe, Y., Sato, M., Ohnishi, M. & Tatsuno, T. 1967 Studies on racemization of amino acids and their derivatives 1. On Deuterium-Hydrogen exchange reaction of amino acids derivatives in basic media. C*hemical & Pharmaceutical Bulletin* 15 (4), 391

McBrearty, S., Brooks, A.S. 2000. The revolution that wasn't: A new interpretation of the origin of modern human behaviour. *Journal of Human Evolution* 39 (5): 453–563.

McDougall I., Brown, F.H., Fleagle, J.G. 2005. Stratigraphic placement and age of modern humans from Kibish, Ethiopia. *Nature* 433:733-6

McDougall I., Brown, F.H., Fleagle, J.G. 2006. Earliest known modern humans from Kibish, Ethiopia. *Geochimica et Cosmochimica Acta* 70:A409-A

Meldrum, F.C., Sear, R.P. 2008. Now you see them. *Science* 322 1802-1803

Mellars, P. 2006. Why did modern human populations disperse from Africa ca. 60,000 years ago? A new model . *PNAS* 103(25): 9381–9387.

Meyer, V.R. 1991. Amino acid racemization- A tool for dating. *ACS Sym* 471: 217-227

Millard, A.R. 2008. A critique of the chronometric evidence for hominid fossils: I. Africa and the Near East 500-50 Ka. *Journal of Human Evolution* 54 (6): 848–74.

Miller, G.H., Hollin, J.T., Andrews, J.T. 1979. Aminostratigraphy of UK Pleistocene deposits. *Nature* 281:539-43

Miller, G.H., Hare, P.E., 1980. Amino Acid Geochronology: integrity of the carbonate matrix and potential of mollusc shells. In *Biogeochemistry of amino acids*, ed. PE Hare, TC Hoering, KJ King, pp. 415-43. New York: Wiley

Miller, G.H., Brigham-Grette, J. 1989. Amino acid geochronology: resolution and precision in carbonate fossils. *Quaternary International* 1:111-28

Miller, G.H., Wendorf, F., Ernst, R., Schild, R., Close, A.E., 1991. Dating lacustrine episodes in the eastern Sahara by the epimerization of isoleucine in ostrich eggshells. *Palaeogeography, Palaeoclimatology, Palaeoecology* 84:175- 89

Miller, G.H., Beaumont, P.B., Jull, A.J., Johnson, B. 1992. Pleistocene geochronology and palaeothermometry from protein diagenesis in ostrich eggshells: Implications for the evolution of modern humans. *Philosophical Transactions of the Royal Society of London. Series B, Biological Sciences* 337 (1280): 149–57.

Miller, G.H., Hart, C.P., Roark, E.B., Johnson, B.J. 2000. Isoleucine epimerization in eggshells of the flightless Australian birds *Genyornis* and *Dromaius*. In *Perspectives in Amino Acid and Protein Geochemistry*, ed. G A Goodfriend, M J Collins, M L Fogel, S A Macko, and J F Wehmiller, 161–181. Oxford University Press.

Miller, G.H., Beaumont, P.B., Deacon, H.J., Brooks, A.S., Hare, P.E., Jull, A.J.T. 1999. Earliest modern humans in Southern Africa dated by isoleucine epimerization in ostrich eggshell. *Quaternary Science Reviews* 18 (13): 1537–1548.

Min, J.Z., Hatanaka, S., Yu, H., Higashi, T., Inagaki, S., Toyo'oka, T. 2011. Determination of DL-amino acids, derivatized with R(-)-4-(3-isothiocyanatopyrrolidin-1-yl)-7-(N,N-dimethylaminosulfonyl)-2,1,3-benzoxadiazole, in nail of diabetic patients by UPLC-ESI-TOF-MS. *Journal of Chromatography. B, Analytical Technologies in the Biomedical and Life Sciences* 879(29): 3220–8.

Mitterer, R.M., Kriausakul, N. 1984. Comparison of rates and degrees of isoleucine epimerization in dipeptides and tripeptides. *Organic Geochemistry* 7 (1): 91–98.

Mitterer, R.M., Kriausakul, N. 1989. Calculation of amino acid racemization ages based on apparent parabolic kinetics. *Quaternary Science Reviews* 8 (4): 353–357.

Moir, M.E., Crawford, R.J. 1988. Model studies of competing hydrolysis and epimerization of some tetrapeptides of interest in amino acid racemization studies in geochronology. *Canadian Journal of Chemistry* 66 (11): 2903–2913.

Molnar-Perl, I., Vasanits, A. 1999, Stability and characteristics of the o-phthaldialdehyde/3-mercaptopropionic acid and o-phthaldialdehyde/N-acetyl-l-cysteine reagents and their amino acid derivatives measured by high-performance liquid chromatography. *Journal of Chromatography A* 835(1-2): 73-91

Murray-Wallace, C.V., Bourman, R.B., Prescott, J.R., Williams, F., Price, D.M., Belperio, A.P. 2010. Aminostratigraphy and thermoluminescence dating of coastal aeolianites and the Later Quaternary history of a failed delta: The River Murray Mouth region, South Australia. *Quaternary Geochronology* 5 (1): 28–49.

Neuberger, A. 1948. Stereochemistry of amino acids. *Advances in Protein Chemistry* 4: 297–383.

Nguyen, D. T. T., Guillarme, D., Rudaz, S., & Veuthey, J. L. (2006). Fast analysis in liquid chromatography using small particle size and high pressure. *Journal of separation science*, *29*(12), 1836-1848.

Nimiki, M. 1988. Chemistry of Maillard Reactions: Recent studies on the Browning mechanism and the development of antioxidants and mutagens. *Advances in Food Research*. 32, 115-184

Nowell, A. 2010. Defining behavioral modernity in the context of Neandertal and anatomically modern human populations. *Annual Review of Anthropology* 39,437-452

Nys, Y., Hincke, M.T., Arias, J.L., Garcia-Ruiz, J.M., Solomon, S.E. 1999. Avian eggshell mineralization. *Poultry and Avian Biology Reviews* 10:143-66

Ohtani, S. 1995. Estimation of age from dentin by utilizing the racemization of aspartic acid: Influence of pH. *Forensic Science International* 75: 181–187.

Orem, C.A., Kaufman, D.S. 2010. Effects of basic pH on Amino Acid Racemization and leaching in freshwater mollusk shell. *Quaternary Geochronology* 6, 233-245.

Orton, J., 2008. Later Stone Age ostrich eggshell bead manufacture in the Northern Cape, South Africa. *Journal of Archaeological Science* 35, 1765–1775.

Ortiz, J. E., Torres, T., Yanes, Y., Castillo, C., De La Nuez, J., Ibáñez, M., Alonso, M.R. 2006. Climatic cycles inferred from the aminostratigraphy and aminochronology of Quaternary dunes and palaeosols from the Eastern Islands of the Canary Archipelago. *Journal of Quaternary Science* 21 (3) (March): 287–306

Oviatt, C.G., 1989. Quaternary geology of part of the Sevier Desert, Millard County,Utah. *Utah Geological and Mineral Survey Special Studies 70*.

Pappin, C., Hojrupt, P., Bleasbyl, A.J. 1993. Rapid identification of proteins by peptide-mass fingerprinting. *Current biology*.3(6): 327-332

Parkington, J. E. 1992. Making sense of sequence at the Elands Bay cave, western Cape, South Africa. *Guide to archaeological sites in the south-western Cape*, *6*, 12.

Patnaik, R., Sahni, A., Cameron, D., Pillans, B., Chatrath, P., Simons, E., Williams, M., Bibi, F. 2009. Ostrich-like eggshells from a 10.1 million-yr-old Miocene ape locality, Haritalyangar, Himachal Pradesh, India. *Current Science* 96(11) 1485-1495

Paul, W., Steinwedel, H.1953. *Zeitschrift für Naturforschung*, 8A; p448.

Paul, W. 1990. Agewandte Chemie - International Edition, 29, p739.

Penkman, K.E.H., 2005, Amino Acid Geochronology: a closed system approach to test and refine the UK model. Unpublished PhD Thesis, University of Newcastle-upon-Tyne, UK.

Penkman, K.E.H., Kaufman, D.S., Maddy, D., Collins, M.J. 2008. Closed-system behaviour of the intra-crystalline fraction of amino acids in mollusc shells. *Quaternary Geochronology* 3 (1-2): 2–25.

Penkman, K.E.H., Preece, R.C., Keen, D.H., Maddy, D., Schreve, D.C., Collins, M.J. 2007. Testing the aminostratigraphy of fluvial archives: The evidence from intra-crystalline proteins within freshwater shells. *Quaternary Science Reviews* 26 (22-24): 2958–2969.

Penkman, K.E.H., Preece, R.C., Bridgland, D.R., Keen, D.H., Meijer, T., Parfitt, S.A., White, T.S., Collins, M.J. 2011. A chronological framework for the British Quaternary Based on *Bithynia* opercula. *Nature* 476 (7361): 446–9.

Petraglia, M.D., Haslam, M., Fukker, D.Q., Boivin, N., Clarkson, C. 2010. Out of Africa: new hypotheses and evidence for the dispersal of Homo sapiens along the Indian Ocean rim. *Annals of Human Biology* 37(3) 288-311

Pickett, J.W., Ku, T.L., Thompson, C.H., Roman, D., Kelley, R.A., Huang, Y.P., 1989. A review of age determinations on Pleistocene corals in eastern Australia. *Quaternary Research* 31(3), 392-395.

Pontzer, H. 2012. Overview of Hominin Evolution. *Nature Education Knowledge* 3(10):8

Powell, J., 2012 Amino Acid Racemization Proficiency Study, Report III: Ostrich eggshell (A). NeAAR, University of York, UK.

Powell, J. 2013. Determination of measurement uncertainty in aminostratigraphy: Towards a new chronology. Unpublished PhD thesis, University of York.

Preece, R.C., Penkman, K.E.H., 2005. Molluscan assemblages and amino acid dating of the Lower Palaeolithic site at East Farm, Barnham, Suffolk. *Proceedings of the Geologists' Association* 116: 363-377

Radkiewicz, J.L., Zipse, H., Clarke, S., Houk, K.N. 1996. Accelerated racemization of aspartic acid and asparagine residues via succinimide intermediates: An ab initio theoretical exploration of mechanism. *Journal of the American Chemical Society* 118 (38): 9148–9155.

Rector, A.L., Reed, K.E., 2010. Middle and late Pleistocene faunas of Pinnacle Point and their paleoecological implications. *Journal of Human Evolution* 59 (3-4), 340 - 357

Reimer, P.J., Reimer, R.W. 2006. A marine reservoir correction database and on-line interface. *Radiocarbon* 43(2A), 461-463

Reimer, P.J., Baillie, M.G.L., Bard, E., Bayliss, A., Beck, J.W., Blackwell, P.G., Ramsey, C.B., Buck, C.E., Burr, G.S., Edwards, R.L., Friedrich, M., Grootes, P.M., Guilderson, T.P., Hajdas, I., Heaton, T.J., Hogg, A.G., Hughen, K.A., Kaiser, K.F., Kromer, B., McCormac, F.G., Manning, S.W., Reimer, R.W., Richards, D.A., Southon, J.R., Talamo, S., Turney, C.S.M., van der Plicht, J., Weyhenmeyer, C.E. 2009. IntCal09 and Marine09 radiocarbon age calibration curves, 0 – 50,000 years cal BP. *Radiocarbon*, 51(4) 1111-1150

Renfrew, C., Clarke, R.M. 1974. Problems of the radiocarbon calendar and its calibration. *Archaeometry* 16(1) 5-18.

Reyes-Grajeda, J.P., Marín-García, L., Stojanoff, V., Moreno, A. 2007. Purification, crystallization and preliminary X-ray analysis of Struthiocalcin-1 from ostrich (*Struthio Camelus*) eggshell. *Acta Crystallographica. Section F, Structural Biology and Crystallization Communications* 63(11): 987–9.

Rightmire, G.P., 1998. Human evolution in the Middle Pleistocene: the role of Homo heidelbergensis. *Evolutionary Anthropology* 6, 218-227

Rightmire, G. P. 2009. Middle and later Pleistocene hominins in Africa and Southwest Asia. *PNAS* 106 (38) 16046-16050

Rink, W J. 1998. Electron spin resonance (ESR) dating and ESR applications in Quaternary science and archaeometry. *Radiation Measurements* 27 (5-6): 975-1025.

Roepstorff, P., Fohlman, J. 1984. Letter to editors. *Biological Mass Spectrometry* 11(11): 601

Roof, S. 1997. Comparison of isoleucine epimerization and leaching potential in the molluskan genera Astarte, Macoma, and Mya. *Geochimica Et Cosmochimica Acta* 61:5325-33

Schellmann, G., Radtke, U. 1999. Problems encountered in the determination of dose and dose rate in ESR dating of mollusc shells. *Quaternary Science Reviews* 18:1515-27

Shackleton, N.J., Opdyke, N.D. 1973. Oxygen isotope and paleomagnetic stratigraphy of equatorial Pacific core V28-238: Oxygen isotope temperature and ice volumes on a 10^5 year and 10^6 year time scale. *Quaternary Research* 3:39-55

Shackleton, N.J. 1987. Oxygen isotopes, ice volumes and sea level. *Quaternary Science Reviews* 6:183-90

Shackleton, N.J., Duplessy, J-C., Arnold, M., Maurice, P., Hall, M.A., Cartlidge, J. 1988. Radiocarbon age of last glacial Pacific deep water. *Nature* 335: 708-711

Shevchenko, A., Jensen, O.N., Alexandre V. Podtelejnikov, A.V., Sagliocco, F., Wilm, M., Vorm, O., Mortensen, P., Shevchenko, A., Boucherie, H., Mann, M. Linking genome and proteome by mass spectrometry: Large-scale identification of yeast proteins from two dimensional gels. *Proceedings of the National Academy of Sciences of the United States of America* 96(25): 14440-14445

Siedler, J., Zinn, N., Boehm, M.E., Lehmann, W.D. 2010. *De novo* sequencing of peptides by MS/MS. *Proteomics* 10(4): 634-649

Simkiss, K. and Tyler, C., 1957. A histochemical study of the organic matrix of hen eggshells. *Quart. J. Micr. Sci* 98, 10

Simkiss, K. 1958. Reactions between eggshell matrix and metallic cations. *Quart. J. Micr. Sci.* 99, 5

Simkiss, K., 1986. The process of biomineralization in lower plants and animals- an overview. In *Biomineralization in Lower Plants and Animals* (Edited by Leadbeater BSC and Riding R) pp 19-37. The Systematics Association Special Publication, 30. Clarendon, Oxford.

Smart, P.L. 1991, Uranium series dating, in PL Smart, PD Frances (eds), Quaternary Dating Methods- A user's guide. Technical Guide 4, *Quaternary Research Association*, Cambridge, 45-83

Smith, G. G., Williams, K.M., Wonnacott, D.M. 1978. Factors affecting the rate of racemization of amino acids and their significance to geochronology. *The Journal of Organic Chemistry* 43 (1): 1–5.

Smith, G.G., De Sol, B.S. 1980. Racemization of amino acids in dipeptides shows COOH > NH_2 for non-sterically hindered residues. *Science (New York, N.Y.)* 207 (4432): 765–7.

Smith, G.G., Evans, 1980. The effect of structure and conditions on the rate of racemization of free and bound amino acids biochemistry of amino acids (Ed. Hare, P.E., Hoering, T.C. and King, K.Jr.), Wiley, New York 257-282

Smith, G.G., Reddy, G.V. 1989. Effect of the side-chain on the racemization of amino acids in aqueous solution. *Journal of Organic Chemistry* 54:4529-35

Snow, N.H., Slack, G.C. 2002. Head-space analysis in modern gas chromatography. *TrAC Trends in Analytical Chemistry* 21(9-10): 608-617

Snyder, L.R., Kirkland, J.J., Glajch, J.L. 2012. Practical HPLC method development. 2nd Ed. John Wiley and Sons.

Sohn, Ho., Ho, C-T. 1995. Ammonia generation during thermal degradation of amino acids. *Journal of Agricultural and Food Chemistry* 43(12): 3301-3003

Steinberg, S., Bada. 1981. Diketopiperazine formation during investigations of amino acid racemization in dipeptides. *Science (New York, N.Y.)* 213 (4507) (July 31): 544–5.

Stephenson, R.C., Clarke, S. 1989. Succinimide formation from aspartyl and asparaginyl peptides as a model for the spontaneous degradation of proteins. *The Journal of Biological Chemistry* 264 (11): 6164–70.

Stringer, C.B. 2000. Palaeoanthropology: Coasting out of Africa. *Nature* 405 (6782):24-7

Stringer, C.B. 2003. Human evolution: Out of Ethiopia. *Nature* 423: 692-695

Stuiver, M., Grootes, P.M., Brajunas, T.F. 1995. The GISP2 $\delta^{18}O$ climate record of the past 16,500 years and the role of the sun, ocean and volcanoes. *Quaternary Research* 44: 341-354

Stuiver, M., Heusser, C.J., Yang, C. 1978. North American glacial history extended to 75,000 years ago. *Science* 200: 16-21

Stuiver, M., Brazunias, T.F., Becker, B and Kromer, B. 1991. Climatic solar, oceanic and geomagnetic influences on Late-Glacial and Holocene atmospheric $^{14}C/^{12}C$ change. *Quaternary Research* 34: 1-24

Stuiver, M., Reimer, P.J., Bard, E., Beck, J.W., Burr, G.S., Hughen, K.A., Kromer, B., McCormac, G., van der Plicht, M., Spurk, M. 1998. INTCAL98 radiocarbon calibration, 24,000-0 cal BP. *Radiocarbon* 40: 1041-1084

Suckau, D., Resemann, A., Schuerenberg, M., Hufnagel, P., Franzen, J., Holle, A. 2003. A novel MALDI LIFT-TOF/TOF mass spectrometer for proteomics. *Anal Bioanal Chem* 376: 952-965

Swartz, M. 2005. UPLC™: An introduction and review. *Journal of Liquid Chromatography & Related Technologies* 28(7): 1253–1263.

Sykes, G. 1995. The significance of a geochemically isolated intra-crystalline organic fraction within biominerals. *Organic Geochemistry* 23 (11-12) (November): 1059–1065.

Takahashi, O., Kobayashi, K.,Oda, A. 2010. Modelling the enolization of succinimide derivatives, a key step of racemization of aspartic acid residues: Importance of a two-H_2O mechanism. *Chemistry & Biodiversity* 7 (6): 1349–56.

Tanaka, K., Waki, H., Ido, Y., Akita, S., Yoshida, Y., Yoshida, T. 1988. Protein and polymer analyses up to m/z 100,000 by laser ionization time-of-flight mass spectrometry. *Rapid Commun Mass Spectrom* 2(20): 151–3.

Texier, P.J., Porraz, G., Parkington, J., Rigaud, J.P., Poggenpoel, C., Miller, C., Tribolo, C., Cartwright, C., Coudenneau, A., Klein, R., Steele, T., Verna, C. 2010. A Howiesons Poort Tradition of Engraving Ostrich Eggshell Containers Dated to 60,000 Years Ago at Diepkloof Rock Shelter, South Africa. *Proceedings of the National Academy of Sciences of the United States of America* 107(14): 6180–5.

Tomiak, P.J., Hendy, E.J., Collins, M.J., Demarchi, B., Murrells, S., McCullagh, P., Davis, S.A., Penkman, K.E.H., 2013 Protein degradation kinetics in artificially and 'naturally aged' coral skeletons, *Quaternary Geochronology* 16: 87-109

Towe, K.M., Thompson, G.R. 1972. The structure of some bivalve shell carbonates prepared by ion-beam thinning. A comparison study. *Calcified Tissue Research* 10 (1): 38–48.

Towe, K.M. 1980. Preserved organic ultrastructure: An unreliable indicator for paleozoic amino acid biogeochemistry. In *The Biogeochemistry of Amino Acids*, ed. PE Hare, TC Hoering, and K King JR, 65–74. Wiley, New York.

Umagat H., Kucera, P. 1982. Total amino acid analysis using pre-column fluorescence derivatisation. *Journal of Chromatography A* 239: 463-474

Vallentyne, J. R., 1964. Biogeochemistry of organic matter II: Thermal reaction kinetics and transformation products of amino compounds. *Geochimica et Cosmochimica Acta.* 28: 157-88

Van Deemter, J.J., Zuiderweg, F.J., Klinkenberg, A. 1956. Longitudinal diffusion and resistance to mass transfer as causes of non-ideality in chromatography. *Chemical Engineering Science*, *5*(6): 271-289.

van der Plicht, J. 2002. Calibration of the ^{14}C timescale: towards the complete dating range. *Netherlands Journal of Geosciences* 84: 85-96

Vogel, J.C., Beaumont, P.B., 1972. Revised radiocarbon chronology for the Stone Age in South Africa. *Nature* 237, 50-51

Vogel, J.C., Visser, E., Fuls, A. 2001. Suitability of ostrich eggshell for radiocarbon dating. *Radiocarbon* 43 (1): 133-137

Walker, M. 2005. Quaternary dating methods. Chichester: John Wiley & sons

Walker, M., Johnsen, S., Rasmussen, S.O., Popp, T., Steffensen, J., Cwynar, L.E.S.C., Hughen, K. 2009. Formal definition and dating of the GSSP (Global Stratotype Section and Point) for the base of the Holocene using the Greenland NGRIP ice core , and selected auxiliary Records. *Journal of Quaternary Science* 24(1): 3-17

Walton, D. 1998. Degradation of intra-crystalline proteins and amino acids in fossil brachiopods. *Organic Geochemistry* 28 (6): 389–410.

Wang, X.L., Lu, Y.C., Wintle, A.G. 2006. Recuperated OSL dating of fine-grained quartz in Chinese loess. *Quaternary Geochronology* 1:89-100

Wang, H-Y., Qian, H., Yao, W-R. 2011. Melanoidins produced by the Maillard reaction: Structure and biological activity. *Food Chemistry* 128(3): 573-584

Wehmiller, J.F., Hare, P.E. 1971. Racemization of amino acids in marine sediments. *Science* 173: 907-911

Wehmiller, J.F. 1980. Intergeneric differences in apparent racemization kinetics in mollusks and foraminifera: Implications for models of diagenetic racemization. In *Biogeochemistry of Amino Acids*, ed. P E Hare, T C Hoering, and K King JR, 341–356. John Wiley and Sons.

Wehmiller, J.F. 1993. Applications of organic geochemistry for quaternary research: aminostratigraphy and aminochronology. In *Organic Geochemistry*, ed. MH Engel and SA Macko, pp 755–783. New York.

Wehmiller, J.F. 1982. A review of amino acid racemization studies in Quaternary mollusks: Stratigraphic and chronologic applications in coastal and interglacial sites, Pacific and Atlantic Coasts, United States, United Kingdom, Baffin Island, and Tropical Islands. *Quaternary Science Reviews* 1 (2): 83–120.

Wehmiller, J.F. 2013. Interlaboratory comparison of amino acid enantiomeric ratios in Pleistocene fossils. *Quaternary Geochronology* 16: 173-182

White, T.D., Asfaw, B., DeGusta, D., Gilbert, H., Richards, G.D., Suwa, G., Howell, F.C. 2003. Pleistocene *homo sapiens* from Middle Awash, Ethiopia. *Nature* 423 (6941): 742–7.

Wilm, M.S., Mann, M. 1994. Electrospray and Taylor-Cone Theory, Dole's beam of macromolecules at last. *International Journal of Mass Spectrometry and Ion Processess* 136: 167-180

Wilson, H., Cannon, R. K. 1937. The glutamic acid-pyrrolidone carboxylic acid system. *The Journal of Biological Chemistry* 119, 309-331

Wiza, J.L. 1979. Microchannel plate detectors. *Nuclear Instruments and Methods* 162: 587-601

Woodman, F. 2012. Purification and kinetic investigation of struthiocalcin from *Struthio camelus* (ostrich) eggshell. Unpublished MChem Thesis, University of York, UK.

Wynn, T. & Coolidge, F. L. 2011. The implications of the working memory model for the evolution of modern cognition. *International Journal of Evolutionary Biology* 2011, Article ID 741357 doi:10.4061/2011/741357

Yates, J.R., Speicher, S., Griffin, P.R., Hunkapiller, T. 1993. Peptide mass maps: a highly informative approach to protein identification. *Analytical Biochemistry* 214: 397-408

Zenobi, R., Knochenmuss, R. 1998. Ion formation in MALDI mass spectrometry. *Mass Spectrometry reviews* 17: 337-366

Zhang, Z. 2004. Prediction of Low-energy collision-induced dissociation spectra of peptides. *Analytical Chemistry* 76(14): 3908-3922

Zhang, Z. 2005. Prediction of low-energy collision-induced dissociation spectra of peptides. With three or more charges. *Analytical Chemistry* 79(19): 6364-6373

Zink, A.J.C., Susino, G.J., Porto, E., Huffman, T.N. 2012. Direct OSL dating of Iron Age pottery from South Africa – Preliminary dosimetry investigations. *Quaternary Geochronology* 8: 1-9